HAYLEY LEES

HERTFORD COLLEGE

Molecular mechanisms of premature ageing in a worm model of human Werner syndrome

Submitted for examination for the degree of D.Phil. in Biochemistry

University of Oxford

Trinity Term 2014

Molecular mechanisms of premature ageing in a worm model of human Werner syndrome

Hayley Lees

Hertford College

D.Phil. in Biochemistry

Trinity Term 2014

Abstract

Investigating the biological basis of ageing is both fascinating and medically relevant, as we strive to understand both how organisms age, and how our knowledge might be put to good use in an increasingly long-lived human population. Despite the complexity of ageing biology, it is very striking that longevity, in a wide variety of organisms, can be modified by manipulating single genes. In this thesis, I investigate phenotypes associated with mutations in *C. elegans* homologues of human *WRN*, the gene mutated in the progeroid Werner syndrome (WS).

Mutant phenotypes in the worm recapitulate aspects of the pathophysiology observed in WS patients, including premature ageing, genomic instability, and sensitivity to DNA damaging agents. *wrn-1* overexpression, on the other hand, appears to enhance longevity, suggesting that *wrn-1* acts as a *bona fide* anti-gerontogene. The combination of *wrn-1* mutations with mutation in the worm p53 homologue, *cep-1*, unexpectedly triggers a novel and very striking enhanced lifespan and healthspan phenotype, termed synthetic super-viability

(SSV). The SSV phenotype is modulated by various environmental inputs such as temperature stress.

The data presented here can be incorporated into a model in which stress **sensing** (involving p53) is the crucial determinant of longevity outcomes. Several theories of ageing incorporate the idea that ‘that which does not kill us, makes us stronger’ – encapsulated in a biological sense in the idea of hormesis, a physiological shift in response to stress. Here, this hypothesis is expanded to include the notion that intrinsic **responses** to stress may themselves act to limit lifespan - too much of a good thing can be bad.

Thesis supervisors: Dr. Alison Woollard and Dr. Lynne Cox

Acknowledgements

Words cannot express how grateful I am to have been given the opportunity to not only undertake a D.Phil. project in the first place, but to have done one that I am truly passionate about, and most of all, to do it in such a fantastic environment. The members of the Woollard lab, Cox lab, and Genetics Unit – past and present – have made this experience an unforgettable one. They have taught me so much – not only about science and research, but also about life and its ups and downs. I have been extremely privileged to work with such fantastic colleagues, who are not only my friends, but also feel like an extended family. My two supervisors, Alison and Lynne, both deserve huge praise for putting up with me and for all of the help they have given to me. I doubt I will ever be able to repay them for all the kindness and patience they have shown me. I would also like to thank both of them for making the decision to explore a new avenue of research, and for securing funding from AgeUK (formerly Research into Ageing). A special mention must go to Karolina and Lea - thank you for being by my side through thick and thin. I couldn't have done it without you. I must also thank Tim, for enduring my long, unsociable working hours and for giving me his support.

Thank you to my loving family, for giving me the confidence and support to pursue something I loved, and for always reminding me of what is really important in life – I dedicate this work to you.

Table of Abbreviations

Abbreviation	Full name
4-NQO	4-Nitroquinoline 1-oxide
53BP1	p53-binding protein 1
ARMS-PCR	Amplification Refractory Mutation System Polymerase Chain Reaction
BLASTP	Basic Local Alignment Search Tool (Protein)
BS	Bloom syndrome
C. elegans	*Caenorhabditis elegans*
CGC	Caenorhabditis Genetics Center
CGC	Caenorhabditis Genetics Center
CPT	Camptothecin
DAPI	4',6-diamidino-2-phenylindole
DDR	DNA damage response
DMSO	Dimethyl sulfoxide
DNA	Deoxyribonucleic acid
Dpy	Dumpy
DR	Dietary restriction
FITC	Fluorescein Isothiocyanate
FOXO	Forkhead box O
FUdR	5-fluoro-2'-deoxyuridine
Gamma-H2AX	Phosphorylation of histone variant H2AX at Ser 139
GFP	Green fluorescent protein
Gy	Gray
HRDC	Helicase-and-Ribonuclease D/C-terminal
HU	Hydroxyurea
IGF	insulin-like growth factor
IIS	Insulin/IGF (insulin-like growth factor)-like signalling
IR	Ionizing radiation
L1…4	Laval stage 1…4
M9	*C. elegans* buffer
mTOR	mammalian target of rapamycin
NGM	Nematode Growth Medium
NLS	Nuclear Localisation Sequence
NTS	Nuclear Translocation Signal
OP50	*E. coli* uracil auxotroph whose growth is limited on NGM plates.
PI	Propidium Iodide
PI3K	Phosphatidylinositol-4,5-bisphosphate 3-kinase
PTEN	Phosphatase and tensin homolog
RNAi	RNA interference
RQC	RecQ C-terminal
RTS	Rothmund-Thomson syndrome
SEM	Standard Error of the Mean
SSV	Synthetic super-viability

TUNEL	Terminal deoxynucleotidyl transferase dUTP nick end labeling
Unc	Uncoordinated
UV	Ultra Violet
WS	Werner syndrome
WT	Wild-type

Table of Contents

Chapter 1 - Introduction

1.1 Research into the biology of ageing

One of the fundamental aims of research into the biology of ageing is to reveal the series of events which lead to the degenerative changes associated with the ageing process. Another key aim is to identify genetic and environmental factors that influence these changes.

Ageing is no longer considered a passive, entropic process of deterioration, but one that is influenced by many different genetic and environmental factors (Gems & Partridge, 2013; Guarente & Kenyon, 2000; Kenyon, 2010b; Partridge & Slack, 2013). The genetic basis of ageing is potentially very broad, possibly involving thousands of genes in the case of humans (Martin, 1982). Given the polygenic nature of ageing, as well as the influence that various lifestyle choices has on this process, it is understandable to view ageing as an extremely complex process – one so complex that even understanding how it happens, let alone developing drugs and other treatment modalities to counter it would seem far beyond our reach. It has been demonstrated that the ageing process is accompanied by many different changes that happen from the level of molecules, right the way through from organelles, to cells, and to tissues, which consequently leads to changes at the organismal level (Lopez-Otin et al, 2013). All these changes appear to occur simultaneously, and distinguishing cause from effect is a difficult challenge (Gems & Partridge, 2013).

Though understanding the ageing process for sheer scientific curiosity is reason enough to pursue these aims, the field of biogerontology aims to apply

the knowledge gained from research in these areas to develop interventions - or anti-ageing treatments - that could ‘treat’ ageing, just like we would aim to develop interventions to treate other diseases (Kenyon, 2010b).

This has been met with some objections – some of which are borne out of reasonable fears and others which are just plain baffling. An example of the latter is the argument that ageing is natural and therefore we should not treat it. By that same token we should not treat cancer, or cystic fibrosis. A more reasonable argument is the fear that anti-ageing interventions will see us all living forever.

Mainstream biogerontology research, however, is aimed at helping people to live healthier lives for longer (Olshansky et al, 2007). Ageing, after all, is the biggest risk factor for age-related diseases, therefore tackling the ageing process itself offers the chance to postpone or even avoid many age-related diseases all at once (Fontana et al, 2010; Kenyon, 2010b; Niccoli & Partridge, 2012).

Despite the profound complexity of both the causes and manifestations of ageing, pioneering work in the simple nematode worm, *C. elegans*, (and later, work in other model organisms (Fontana et al; Guarente & Kenyon, 2000; Kenyon, 2010b; Partridge, 2010; Tissenbaum & Guarente, 2002)) demonstrated that, actually, understanding the biology of ageing is not quite as inaccessible as it may first seem.

1.2 Ageing can be manipulated with single interventions

A striking discovery was made in the model organism, *Caenorhabditis elegans* that mutation in just a single gene can extend the lifespan of the worm by 2-fold (Kenyon et al, 1993). This illustrated the crucial point that altering the rate of ageing was surprisingly straightforward despite the apparent complexity of the pathways involved. Later studies in the nematode and other model organisms revealed that conserved mechanisms dictate the pace of ageing and lifespan, reviewed in (Barbieri et al, 2003; Fontana et al; Gems & Partridge, 2013{Hekimi, 2001 #521; Guarente & Kenyon, 2000; Kenyon, 2010b; Partridge, 2010), suggesting that research in model organisms would be widely applicable.

Though Klass was the first to isolate long-lived *C. elegans* strains (Klass, 1983), the first two long-lived mutants to be identified were *age-1* and *daf-2* (Friedman & Johnson, 1988a; Friedman & Johnson, 1988b; Kenyon et al, 1993). These mutants demonstrated that longevity is a) plastic and b) under genetic control (to at least some degree) (Kenyon, 2005). A further single gene mutation in the *daf-16* gene revealed that the increased longevity of *age-1* and *daf-2* mutants was dependent on functional *daf-16* (Kenyon et al, 1993; Larsen et al, 1995). *daf-16* single mutants were found to have a decreased lifespan (Lin et al, 2001). When the genetic lesions in these mutants were identified, it became clear that insulin signalling was at the heart of the regulation of lifespan. *daf-2* turned out to encode an insulin-like receptor, and *daf-16* a FOXO transcription factor acting downstream (Dorman et al, 1995; Kenyon et al, 1993; Kimura et al, 1997; Larsen et al, 1995; Lin et al, 1997; Ogg et al, 1997). In addition to *daf-*

16, the longevity of *age-1* and *daf-2* mutants was also found to be dependent on *daf-18* (Dorman et al, 1995; Larsen et al, 1995) encoding a homologue of the PTEN phosphatase, which is a negative regulator of PI3K signaling in wild-type worms under conditions of abundant food (Ogg & Ruvkun, 1998; Rouault et al, 1999). These results had profound consequences: not only did they implicate insulin/IGF-1 signalling (IIS, figure 1.0) (reviewed in (Kaletsky & Murphy, 2010), a pathway previously found to be linked to growth and metabolism in mammals (Butler & LeRoith, 2001; Hietakangas & Cohen, 2009), to ageing in worms (and eventually across taxa (Bartke, 2008; Bluher et al, 2003; Clancy et al, 2001; Gems & Partridge, 2001; Guarente & Kenyon, 2000; Holzenberger et al, 2003; Tatar et al, 2003)), but they also defined an epistasis pathway for this process and established a successful approach for further ageing research in *C. elegans* – i.e. identifying genes which when mutated could alter lifespan (Guarente & Kenyon, 2000). In addition, finding genes which extend lifespan when over-expressed is another approach (Murakami & Johnson, 1998).

These discoveries also opened up the idea that certain conserved 'pathways' regulate the ageing process, since newly identified longevity strains carry mutations that affected the same cellular processes (Guarente & Kenyon, 2000; Hekimi et al, 2001). Furthermore, the discoveries made in simple model organisms could be applied to mammalian ageing (Barbieri et al, 2003; Smith et al, 2008b; Tissenbaum & Guarente, 2002).

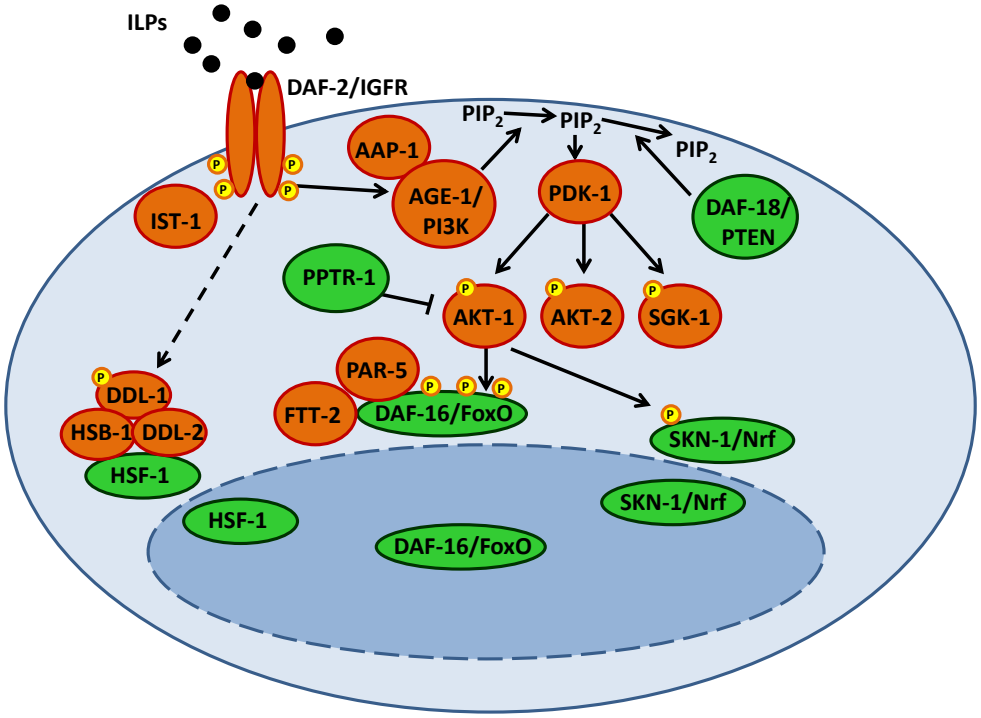

Figure 1.0: Schematic of *C. elegans* IIS. The labs of Klass and Johnson isolated and characterized the first long-lived *C. elegans* mutant, *age-1.* Subsequently, other components of the IIS pathway were also identified. Active IIS promotes the phosphorylation of the transcription factors DAF-16/FoxO, HSF-1, and SKN-1/Nrf, causing them to be sequestered in the cytoplasm. In the diagram above, the insulin/IGF-1 receptor ortholog DAF-2 and other pathway components that promote IIS are coloured orange, and molecules that either antagonize IIS or are antagonized by IIS are coloured green. Insulin-like peptides (ILPs), which may either promote or antagonize DAF-2 activity, are coloured black. PIP_2, = phosphatidylinositol 4,5-bisphosphate; PIP_3 = phosphatidylinositol 3,4,5-trisphosphate.

Subsequently many long-lived mutants have been discovered to be dependent on *daf-16,* and testing for dependence or independence on this gene has become a standard approach for classifying newly identified longevity genes (Landis & Murphy, 2010). Initially, genes which when mutated resulted in increased lifespan (in a *daf-16*-dependent manner) were believed to act within the IIS pathway, by mechanisms that are similar to reduced *daf-2* signalling. However, it is now clear that many factors are able to modulate DAF-16 activity

by mechanisms independent from reduced IIS (Kenyon, 2010b). An example is germline signalling, which limits longevity in a *daf-16* and *daf-12* (a nuclear hormone receptor) dependent manner, and also requires undifferentiated germ line stem cells (Hsin & Kenyon, 1999). Both IIS and germline activity regulate *daf-16* accumulation in the nuclei, but the nuclear localisation patterns are different (Lin, 2001), indicating complexity in the DAF-16-dependent pathways that regulate aging.

1.3 Why does *C. elegans* make such a good model system for ageing research?

C. elegans has all the advantages of genetic tractability, coupled with a completely sequenced and highly annotated genome. This makes it, in common with other model organisms, an excellent system in which to study a huge array of biological problems. The advantageous features of *C. elegans* are tabulated below (table 1.1).

Advantage	Reference	Explanation
Completely sequenced genome.	(The *C. elegans* sequencing consortium, (1998)	Wide range of genetic techniques are facilitated by information being easily available online at www.wormbase.co.uk.
Invariant cell lineage. Every somatic cell fate mapped (959 cells in hermaphrodites).	(Sulston & Horvitz, 1977)	Allows links to be drawn between genotype and phenotype when mutation alters cell fate, with analysis possible at single cell resolution.
RNAi mediated gene knockdown allows gene function to be	(Fire, 2007)	Gene function can easily be studied by RNAi feeding, producing a 'targeted' forward genetics

easily studied.		approach.
C. elegans is a eukaryote	Wormbook (http://www.wormbook.org/)	Cellular and molecular structures (membrane bound organelles; DNA complexed into chromatin and organized into discrete chromosomes, etc.) and control pathways are conserved with higher organisms.
Is a multicellular organism – with a complex developmental process (includes embryogenesis; morphogenesis; growth to adulthood)	Wormbook (http://www.wormbook.org/)	Biological information from *C. elegans* may be directly applicable to humans.
>45% of genes have identifiable orthologues in humans.	(Rubin et al, 2000)	*C. elegans* can be used as a model system to study human genetic disease.
Presence of both males and hermaphrodites (0.5% and 99.5% respectively).	(Brenner, 1974)	Allows both selfing and crossing. Self-fertilization leads to homozygosity of alleles. Strains are easily maintained.
Small and easy to maintain, with a rapid and convenient life cycle.	(Brenner, 1974)	Large numbers of worms can easily be grown allowing experiments to easily be performed on large numbers of worms including life-span studies.
Transparent body	(Brenner, 1974)	Amenable to microscopy.

Table 1.1: Advantages of *C. elegans* as a model organism. *C. elegans* is a useful model organism for a variety of reasons particularly pertinent to my project.

With respect to understanding the biology of ageing, there are several features that set *C. elegans* apart from other model systems. Most obviously, worms have an easily assayed lifespan of about 3 weeks, which is plastic (i.e. sensitive

to experimental manipulation), and a life cycle of 3 days (figure 1.1). Thus experimentation is straightforward and efficient.

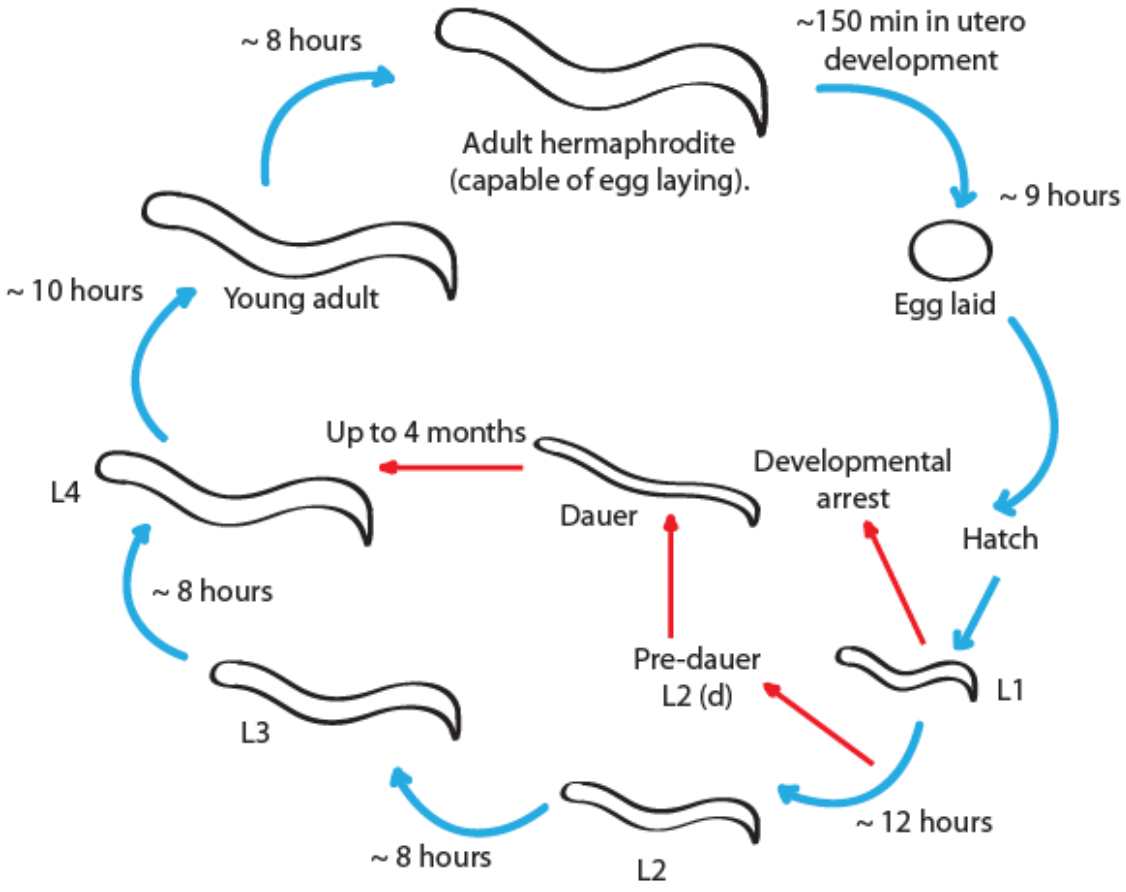

Figure 1.1 : Representation of the life cycle of *C. elegans* at 20^{0}C. Adapted from Wormatlas©.

An important read-out of ageing in model organisms is the survival curve (Sutphin & Kaeberlein, 2009), and for many years assessing and altering the trajectory of this has been the primary focus of biogerontology studies. However, the quality of ageing or rather, how well the health of an organism is maintained is arguably more important, since there is no point in living longer if the period of morbidity is simply increased. Therefore, ageing research is now

looking to focus on improving the healthspan, rather than simply the lifespan of an organism (Herndon et al, 2002; Niccoli & Partridge, 2012). Indications of improved healthspan in *C. elegans* can include:

- prolonged maintenance of locomotive capabilities, particularly moving across a petri dish in search for food or by the high thrashing rates observed when dropped into liquid
- continued ingestion of food, as measured by pharyngeal pumping rate.
- maintained tissue integrity and morphology
- a general, overall youthful appearance (i.e. one reminiscent of that of chronologically younger worms), with delayed late-life shrinkage.

In addition, a particular survival curve trajectory is indicative of prolonged health span – specifically, one in which the onset of mortality is delayed, resulting in the majority of the population living a longer life, followed by a sharp drop-off of survival following this period (i.e., a curve which starts with an extended plateau and then declines rapidly – curve C, figure 1.1b). In this instance, the period of morbidity is reduced, so that the majority of animals experience a long, healthy life, with a narrow period of morbidity (otherwise known as ‘compression of morbidity’) (Fries, 1992; Fries, 2005).

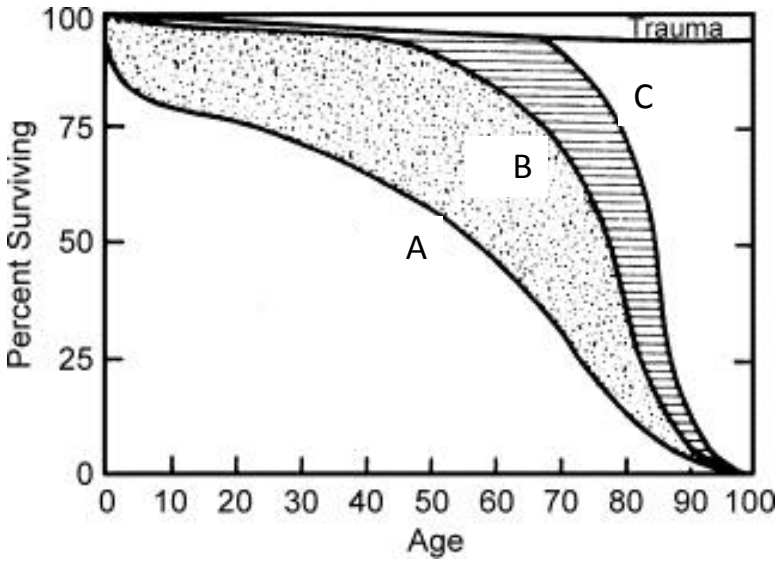

Figure 1.1b: Schematic of various survivorship curves. Out of curves A, B, and C, curve C represents the most ideal survivorship curve. In this instance, the onset of mortality is delayed and is followed by a sharp drop-off of survival following the onset of mortality. Although the maximal lifespan of all three curves is the same, mortality begins at earlier ages in curves A and B compared to curve C, with concomitant increase in the period of morbidity. The compression of morbidity (as seen in curve C) is the desired outcome of research into the biology of ageing. Note that trauma can cause death at any age. Adapted from J.F. Fries and L.M. Crapo, *Vitality and Aging* (San Francisco: W.H. Freeman, 1981).

Nematodes display several age-related changes reminiscent of those seen in other organisms. For instance, movement in later life is uncoordinated and less frequent until worms eventually stop moving, whether this be crawling across a petri dish or thrashing in liquid. Concomitantly, muscle tissue degenerates with age and is thought to contribute to the reduction in motility. As well as general locomotion, other muscle-related phenotypes have been described, such as the decrease in pumping rate of the pharynx (Epstein et al, 1972; Garigan et al, 2002; Herndon et al, 2002; Klass, 1977).

The mix of autofluorescent pigments collectively known as lipofuscin accumulates with age in worms and in many other organisms (Garigan et al,

2002; Klass, 1977; Russell & Seppa, 1987) and has often been used as a read-out for biological age (Hosokawa et al, 1994). Tissue integrity also decreases as worms age and the appearance of vacuole-like structures can often been seen (Herndon et al, 2002). The levels of oxidised proteins also increases with ageing (Adachi et al, 1998; Goudeau & Aguilaniu, 2010), and gene expression profiles also changes with age, with some genes being up-regulated in later life, while down-regulation of others is associated with ageing (Golden & Melov, 2004; Hill et al, 2000; Lund et al, 2002). In the germline, endoreduplication of oocyte DNA results in large chromatin masses (sometimes referred to as 'germline tumours'), which can swell up inside the uterus until they eventually fill the entire mid body of the worm (McGee et al, 2012). Recently, studies have revealed features of the ageing nervous system of the worm, which include synapse deterioration and accumulation of outgrowths from specific neurones, such as branching from the main dendrite or new growth from stomata, which is referred to as neurite sprouting (Toth et al, 2012), as well as a reduced ability to regenerate axons in later life (Gabel et al, 2008; Hammarlund et al, 2009; Nix et al, 2011; Wu et al, 2007).

The relevance of worm ageing to higher organism ageing has been questioned, because of the primary role of the IIS pathway in regulating dauer formation. However, dauer formation can be treated as a response to stress (in this case, starvation and over-crowding) which has pro-longevity phenotypes. Despite the fact that on a gross level, dauer state does not reflect the biology of higher organisms, at a cellular/genetic/metabolic level, there are many similarities. Furthermore, the IIS pathway is conserved from worms to humans, and studies in mice have confirmed the importance of IIS in ageing in mammals (Barbieri et

al, 2003; Bartke, 2008; Barzilai et al, 2012; Gems & Partridge, 2013; Kaletsky & Murphy, 2010; Kenyon, 2010b). Perhaps the existence of the dauer state contributes to the malleability of lifespan in *C. elegans*.

1.4 'Pathways' of ageing

There is much ambiguity in the literature over the definition of the word 'pathway' in the context of ageing-regulation, since it can refer to both genetic pathways and to biochemical and physiological ones, as well as biological processes. With regards to insulin signalling, this represents a defined, biochemical signalling cascade. For other longevity pathways, the definition is not so clear, and multiple 'cross-pathway' interactions complicate the picture further.

1.4.1 The insulin/IGF-1 signalling (IIS) pathway

The IIS pathway is probably best understood in *C. elegans*. In the presence of insulin-like peptides (Li et al, 2003; Pierce et al, 2001), the insulin/IGF-1 receptor tyrosine kinase, DAF-2, is activated and triggers a PI3(AGE-1)/AKT/SGK kinase cascade. The result of this cascade induction is the phosphorylation of the FOXO transcription factor, DAF-16 (Henderson & Johnson, 2001; Hertweck et al, 2004; Lee et al, 2001; Lin et al, 2001; Ogg & Ruvkun, 1998; Paradis et al, 1999; Paradis & Ruvkun, 1998). Hyperphosphorylated DAF-16 is consequently retained in the cytoplasm, resulting in worms living a WT life span.

If insulin signalling is reduced (Henderson & Johnson, 2001; Lee et al, 2001; Lin et al, 2001), stress (including starvation, heat and oxidative) increased (Henderson & Johnson, 2001), or if the major negative regulator of AGE-1/PI3 Kinase, DAF-18/PTEN phosphatase, is activated (Mihaylova et al, 1999; Ogg & Ruvkun, 1998), then DAF-16/FOXO will no longer be hyperphosphorylated and will translocate to the nucleus. Here, the transcription factor turns on survival genes which include (but are not limited to) those responsible for managing the response to heat shock, oxidative stress, metabolism, innate immunity, autophagy, and xenobiotic response (Honda & Honda, 1999; Lee et al, 2003a; McElwee et al, 2004; Melendez et al, 2003; Murphy et al, 2003).

1.4.2 Other nutrient sensing pathways

In addition to IIS, other nutrient sensing pathways have also been linked to longevity in model organisms and in humans (Barzilai et al, 2012; Fontana et al, 2010; Kenyon, 2010b), and illustrate the importance of bioenergetics pathways in determining the rate of ageing. While IIS senses glucose (Lee et al, 2009), a pathway converging on mTOR senses high amino acid concentrations (see review, (Stanfel et al, 2009)). Both of these signal for nutrient abundance and promote anabolism, and are major accelerators of ageing. Limiting signalling of either of these pathways increases healthy ageing (in a variety of organisms) (Johnson et al, 2013; Laplante & Sabatini, 2012; Selman et al, 2009). Conversely, the AMPK- and sirtuin-related pathways sense low energy states by detecting high AMP levels and high NAD+ levels (see reviews by (Hardie, 2007), and (Houtkooper et al, 2010a; Houtkooper et al, 2010b)), respectively,

and therefore signal for nutrient scarcity low energy states and catabolism (Price et al, 2012). When these pathways are activated, then this can also lead to an increase in healthy ageing. For instance, AMPK activation can shut off mTORC1 (Alers et al, 2012), and may also mediate the lifespan extending effects of metformin, at least in mice and worms (Anisimov et al, 2011; Mair et al, 2011; Onken & Driscoll, 2010).

1.4.3 The 'mitochondrial pathway' of ageing

Genome-wide RNAi screens in *C. elegans* revealed that mutations in various components of the mitochondrial electron transport chain (ETC) could extend life span (Dillin et al, 2002; Lee et al, 2003b). Knock down of *nuo-2, cyc-1, cco-1* and *atp-3* were found to have the most robust effect on life span and encode subunits of complex I, III, IV and V, respectively. The reduced mitochondrial respiration caused by knock down of these genes could also extend lifespan of both *daf-16* and *daf-2* mutants. Interestingly, mitochondrial RNAi clones such as *F13G3.7* (a mitochondrial carrier gene) and *F57B10.3* (a phosphoglycerate mutase gene) actually extended life in a DAF-16-dependent manner, implying that there is interplay between mitochondrial function and IIS with respect to the control of longevity (Dillin et al, 2002).

Subsequent work using mutations or RNAi knockdown of mitochondrial ETC components revealed that the resulting life span extending effects acted through two different mechanisms. One of these involves the activation of the mitochondrial unfolded protein response (UPR^{mt}) (Durieux et al, 2011; Hamilton

et al, 2005; Yoneda et al, 2004), and the other works through the stabilisation of the hypoxia-inducible transcription factor, HIF-1 (Lee et al, 2010b).

1.4.4 Hypoxia and ageing

The response to hypoxia has also been shown to regulate ageing (Kaeberlein & Kapahi, 2009; Leiser & Kaeberlein, 2010). Hypoxic conditions in *C. elegans* lead to the inhibition of VHL-1-dependent ubiquitination of HIF-1, which in turn results in the stabilisation of HIF-1 and the extension of lifespan. Unexpectedly, the deletion of *hif-1* affects lifespan in a temperature dependent manner (Chen et al, 2009; Leiser et al, 2011; Leiser & Kaeberlein, 2010). When *hif-1* mutants are grown at 25°C, life span is extended, but at 20°C or 15°C lifespan is similar to that of WT at these temperatures. Under some conditions, this temperature-dependent effect on lifespan by deletion of *hif-1* is dependent on DAF-16, whilst under other conditions it is dependent on TOR signalling. Once again, this illustrates the point that although pathways which regulate longevity have been defined, these do not act alone and there is a great deal of interplay between these pathways. Furthermore, longevity outcomes are context dependent – lifespan may be increased or decreased depending on the genetic background and/or by environmental conditions.

1.4.5 The dietary restriction pathway and ageing

Yet another conserved lifespan-determining pathway is the dietary restriction (DR) pathway - described as nutrient restriction without malnutrition. The lifespan extending effects of DR have been reported in many different species,

including yeast, nematodes, fruit flies, and mice, and also in rats, dogs, fish, spiders and monkeys (Anderson & Weindruch, 2010; Colman et al, 2009; Fontana et al, 2010; Kennedy et al, 2007; Masoro, 2005; Mattison et al, 2007). DR is believed to act via the inhibition of TOR activity, consequently reducing protein translation and promoting autophagy. Unsurprisingly, there is cross talk between TOR signalling and components of other signalling pathways, including but not limited to interactions with HIF-1 or DAF-16 (in *C. elegans*, for instance (Chen et al, 2009; Robida-Stubbs et al, 2012)).

The TOR pathway modulates metabolic processes as well as ageing. Yeast studies involving rapamycin identified components of TOR signalling, including TOR complex 1 (TORC1) (Heitman et al, 1991; Kunz et al, 1993). Rapamycin specifically inhibits TORC1 (which is a multimeric protein complex consisting of TOR kinase partnered with a protein called Raptor, PRAS40 (proline-rich AKT substrate 40 kDa), and a G β L protein) by first forming a complex with FKBP12 (Abraham & Wiederrecht, 1996), which then binds and inhibits TOR kinase and extends lifespan. The mechanism by which lifespan is extended is believed to involve decreased protein translation via reduced phosphorylation of S6 kinase or activation of 4E-binding protein (4EBP), which is an inhibitor of eukaryotic translation initiation factor 4E (eIF4E). Inhibition of the TOR pathway increases lifespan in many species, and causes a physiological shift towards tissue maintenance (Cox, 2009; Cox & Mattison, 2009; Harrison et al, 2009; Jia et al, 2004; Kaeberlein et al, 2005; Kapahi et al, 2004; Vellai et al, 2003).

Different DR methods extend lifespan by both independent and overlapping genetic pathways (Greer & Brunet, 2009; Mair et al, 2009). IIS mediates part of the beneficial effects on DR on longevity in worms and flies (Fontana et al,

2010) through the FOXO transcription factor (Kenyon et al, 1993; Slack et al). In worms, at least part of the *daf-16*-dependency of DR is via sensory perception, implying that longevity is partially regulated by environmental cues, including the sensing of food (Alcedo & Kenyon, 2004; Apfeld & Kenyon, 1999; Smith et al, 2008a).

1.4.6 Signals from the reproductive system that influence ageing

Germline signalling has been established as having an important role in the influence of lifespan. Mutations which prevent the development of germ cells, such as those in *mes-1* or *glp-1*, cause lifespan extension in *C. elegans* (Arantes-Oliveira et al, 2002; Broue et al, 2007; Hsin & Kenyon, 1999; Kenyon, 2005; Kenyon, 2010a; Kenyon, 2010b; Yamawaki et al, 2008; Yamawaki et al, 2010). Though this lifespan extension is dependent on DAF-16, it is also dependent on the hormone receptor, DAF-12, and a growing body of research is focusing on the crosstalk between the germline and the soma in terms of how and why this signalling takes place, and the consequences it has on post-mitotic lifespan. Though a similar system in mammals has yet to be identified, studies have shown that the mammalian reproductive system can affect lifespan. If ovaries from young mice are transplanted into old recipients, the lifespans of the recipients are extended (Cargill et al, 2003; Mason et al, 2009).

1.4.7 Sensory perception pathways and ageing

In addition, defects in *C. elegans* sensory perception caused by mutations in genes such as *daf-19*, *che-2* and *daf-10*, result in lifespan extension which is *daf-16* dependent (Apfeld & Kenyon, 1999). Furthermore, laser ablation of specific sensory neurones can also extend life span, suggesting that longevity is partially regulated by environmental cues (Alcedo & Kenyon, 2004). Lifespan extension caused by DR has been shown to involve food sensing in a *daf-16* independent manner, indicating that sensory perception is probably able to alter lifespan via multiple mechanisms.

1.4.8 Telomeres, senescence, and ageing

Cells in culture and *in vivo* have been demonstrated to undergo cellular senescence – a state of essentially irreversibly arrested proliferation and altered differentiated function (Campisi, 1996; Campisi et al, 1996; Hayflick, 1965; Hayflick & Moorhead, 1961; Stanulis-Praeger, 1987) – and the number of senescent cells increases with age (Collado et al, 2007). The accumulation of senescent cells is thought to contribute to ageing via various mechanisms, such as compromising tissue renewal (e.g. by limiting the number of stem cell progenitors), impairing tissue function and integrity, and producing a pro-inflammatory secreteome or 'senescence-associated secretory phenotype' (Kuilman et al, 2010; Rodier & Campisi, 2011; Salminen et al, 2012).

The first type of cellular senescence to be documented was replicative senescence: the progressive decline in proliferative potential as a consequence of repeated cell divisions (Hayflick & Moorhead, 1961), and evidence suggest that this is caused by telomere shortening (Levy et al, 1992). With each round

of cell division, 50-200 bp of 3' telomeric DNA is left unreplicated (and consequently ~100-200 bp will be deleted), since DNA polymerase requires a primer to initiate 5'-3' synthesis. Some cells, such as stem cells, can circumvent this incomplete end-replication problem by expressing telomerase – however, most mammalian somatic tissues do not express telomerase. Telomere shortening is known to occur during normal ageing in both humans and mice (Blasco, 2007; Harley et al, 1990), and cells undergo replicative senescence when they acquire one or more critically short telomeres (Levy et al, 1992; Olovnikov, 1973). Furthermore, the premature ageing disorder, Werner syndrome (see section 1.6.1), is characterised by *in vitro* premature replicative senescence of patient fibroblasts, caused by telomere attrition (Chang et al, 2004; Crabbe et al, 2007; Crabbe et al, 2004; Damerla et al, 2012; Ishikawa et al, 2011).

In addition to critically short telomeres, cellular senescence can be induced by a variety of stimuli, including: DNA damage (Chen et al, 1995; Di Leonardo et al, 1994; Robles & Adami, 1998), chromatin remodelling (Ogryzko et al, 1996), oncogenic (Serrano et al, 1997; Zhu et al, 1998) and mitogenic stimuli (Lin et al, 1998), and tumour suppressor activity (Dimri et al, 2000; Ferbeyre et al, 2000; McConnell et al, 1998; Pearson et al, 2000).

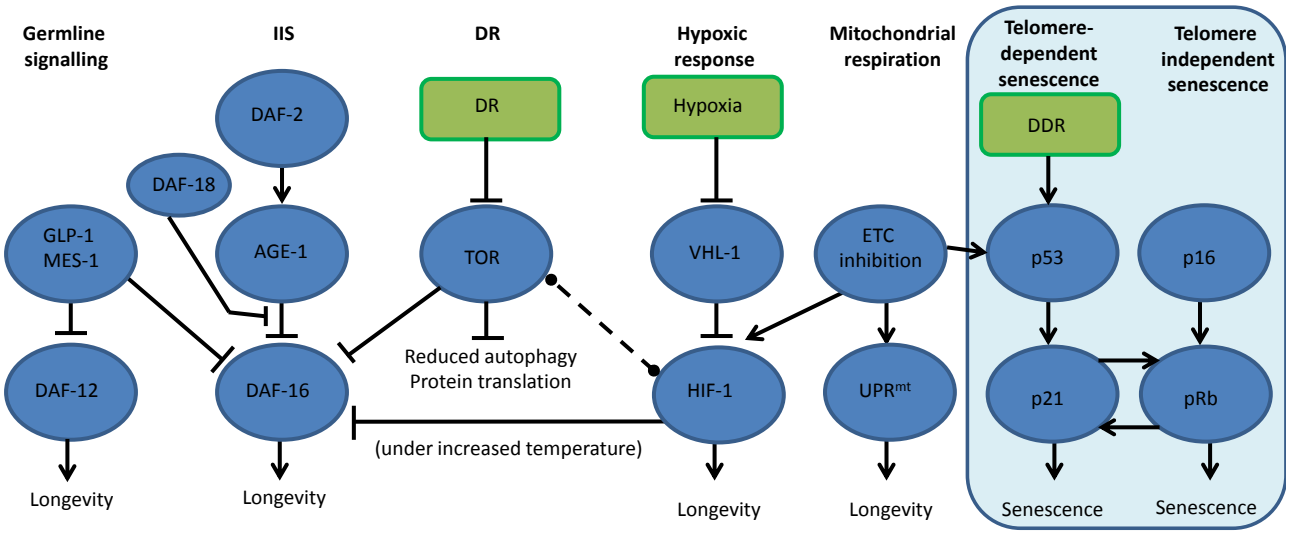

Figure 1.2: Simplified representation of some of the major pathways that have been shown to influence lifespan in *C. elegans*, and two senescence-promoting pathways shown to operate in mammals. The light blue box indicates pathways which have yet to be linked to ageing in worms but are known to influence ageing in mammals. Genetic factors are represented by ovals and environmental factors by rectangles. As well as forming part of the hypoxic response, HIF-1 also interacts with TOR/Raptor and the DR pathway, but in a complex manner dependent on additional experimental variables that are currently unknown (represented by dashed lines).

In conclusion, diverse types of gene products (such as those involved in signal transduction, nutrient sensing, silencing and transcription factors, telomere maintenance, and mitochondrial enzymes) can affect lifespan of not only *C. elegans*, but other organisms too. Genetic analysis suggests that these activities converge on a handful of 'pathways' that influence ageing in *C. elegans* (see figure 1.2) as well as in other species. Although the precise molecular details vary, the common thread between them is that these pathways act as nutrient and stress sensors, and can mediate lifespan in response to many different environmental and physiological signals. Perhaps they are part of the trade-off mechanisms that maintains other aspects of the organism's physiology in good order. A balance must be achieved between

activation and inhibition of these pathways, since too little or too much function or activity can be detrimental to the organism. This helps to explain the observation that both delayed and accelerated ageing share common longevity assurance mechanisms (Schumacher et al, 2008b). Some of the pathways covered in section 1.4 are given as examples of major pathways which regulate longevity in *C. elegans*, but do not represent a complete review of all pathways which are known to influence ageing.

1.5 Stress and ageing

30 years on from the discovery that insulin/IGF-1 signalling regulates lifespan, a myriad of conserved, interconnected signalling pathways that influence ageing have been identified, as discussed above (Gems & Partridge, 2013; Kenyon, 2010b). Notably, these pathways share a common denominator – they are mechanisms which sense and respond to signals that reflect the level of biological stress.

The most widely studied longevity intervention, dietary restriction (DR), is an example of one of these 'stress signals' and increases lifespan or healthspan in all investigated eukaryotic species (including non-human primates) (as discussed in section 1.4.5 (Anderson & Weindruch, 2010; Colman et al, 2009; Fontana et al, 2010; Kennedy et al, 2007; Mattison et al, 2012).

Since the discovery of the link between DR and longevity, many other stress signals have been identified which can also extended lifespan and/or healthspan in a variety of organisms, including: elevated temperature (Apfeld et al, 2004; Hercus et al, 2003; Lithgow et al, 1995; Shama et al, 1998), oxidative

stress (Heidler et al, 2009), thermosensory signals (Lee & Kenyon, 2009), chemosensory signals (Maier et al, 2010), signals from the reproductive system (Arantes-Oliveira et al, 2002; Cargill et al, 2003; Hsin & Kenyon, 1999; Libina et al, 2003; Lin et al, 2001; Sgro & Partridge, 1999), reduced rates of respiration (Copeland et al, 2009; Dell'agnello et al, 2007; Kenyon, 2005), decreased translation (Garigan et al, 2002; Hamilton et al, 2005; Hansen et al, 2007; Pan et al, 2007), infection (Jakobsen et al, 2013), and DNA damage (Lans et al, 2013).

The response in each case is controlled by regulatory proteins which often control longevity in response to more than one stress. These regulatory proteins are part of the aforementioned signalling pathways (section 1.4), and perturbations in such pathways in one tissue can affect lifespan by influencing cells other than those in which the perturbation was initially made. In other words they can act cell non-automously to establish a new homeostasis (Bishop & Guarente, 2007; Kenyon, 2005; Murphy et al, 2007). It has become clear that it is not simply the fact that signalling pathways are perturbed, but it is the precise nature of these perturbations which is important in dictating longevity outcomes, since all of these pathways are essential to the animal and both their complete loss or, conversely, their over-activation can have detrimental effects. For instance, while IIS downregulation reflects a defensive response which aims to minimise metabolism and cell growth and thus minimise damage, and consequently can result in longer survival, there is also the risk that this response actually aggravates ageing (Lopez-Otin et al, 2013; Marino et al, 2010; Schumacher et al, 2008b).

Overall, then, stress signals can causes global physiological shifts, intended to protect animals from the negative effects of stress, which have the effect of extending lifespan. A little bit of stress can be beneficial, or in the words of Friedrich Nietzsche, 'that which does not kill us, makes us stronger' (Gems & Partridge, 2008).

1.6 Using human progeroid syndromes as another approach to studying ageing

Though the IIS pathway and its influence on ageing was first discovered in a model organism, there exist single gene disorders in humans which have also been instrumental in understanding the biology of ageing at a fundamental level. Segmental progeroid or 'accelerated ageing' syndromes are heritable genetic syndromes which present some, but not all, of the features seen in normal human ageing (Kipling et al, 2004; Kipling & Faragher, 1997; Martin, 1985; Moser et al, 1999; Pereira et al, 2008). The age-related phenotypes observed in patients with such syndromes present prematurely compared to 'normal' individuals. A great advantage of using such genetic syndromes to elucidate potential mechanisms of ageing is that they are monogenic, allowing us to test hypotheses regarding the role of that gene in a given process and may indicate the contribution of a given mechanism to normal ageing (Kipling et al, 2004). Although progeroid syndromes are considered partial phenocopies of normal ageing as opposed to the real thing, they appear to overlap mechanistically and pathologically with normal ageing (Cox & Faragher, 2007).

Consequently they are considered valuable models for studying ageing (Cox & Faragher, 2007; Ghosh & Zhou, 2014; Kipling & Faragher, 1997).

Despite this, there is still some debate as to whether such syndromes genuinely represent premature ageing rather than novel pathology. The gold standard for demonstrating that a gene has anti-ageing functions is to show that its over-expression extends life span. Conversely, a gene product which promotes ageing may be shown to accumulate in biologically older tissues, for example. While the latter has been demonstrated in the case of Progerin (see Dreesen & Stewart, 2011), a direct link between increased longevity and over expression of WRN (see below) has yet to be shown. However, genome wide association studies have revealed SNPs in *WRN* are linked to exceptional human longevity (Sebastiani, 2012).

There are several human syndromes in which pathology associated with normal ageing seems to accumulate at an accelerated rate. Two of these, Werner syndrome and Hutchinson-Gilford progeria syndrome (HGPS, caused by *LMNA* mutation, (Cao & Hegele, 2003; Eriksson et al, 2003; Pollex & Hegele, 2004)), particularly stand out because in these diseases, many tissues show age-related phenotypes. However, they are both segmental in nature, as only a subset of tissues seems to age prematurely (Martin & Oshima, 2000). Nevertheless, knowledge of the molecular pathology of these diseases could also provide insight into normal ageing (Brown et al, 1985; Goto, 1997).

1.6.1 Werner's syndrome – a canonical segmental progeroid syndrome

Werner's syndrome (WS) is an autosomal recessive disease and is classified as a segmental progeroid syndrome which prematurely displays an extensive, though incomplete, range of ageing-specific phenotypes across multiple tissues and organ systems (Epstein et al, 1966; Goto, 1997; Martin et al, 1999; Salk, 1982). WS is well understood with regards to the pathology of the disease, and more closely mimics normal ageing than any other segmental progeroid syndrome (see figure.1.3) reviewed in (Brown et al, 1985; Cox & Faragher, 2007; Nehlin et al, 2000).

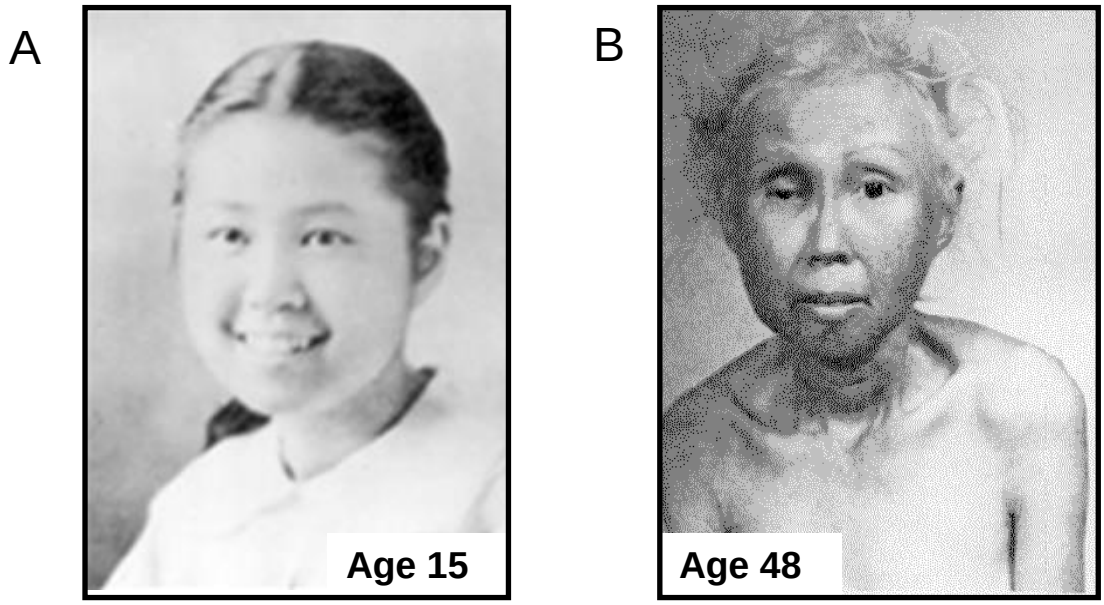

Figure 1.3: Premature ageing in a Werner syndrome patient. (A) shows a 15 year old Japanese girl with WS, who appears phenotypically normal. (B) is of the same patient but at 48 years of age. The woman looks remarkably older than her chronological age – WS mimics normal ageing but in a greatly accelerated manner. Adapted from (Epstein et al, 1966).

WS is caused by a mutation in the WRN gene which is located on chromosome 8p12-p11.2 (Yu et al, 1996). WS patients prematurely develop a wide range of

features and similar clinical symptoms to those that are observed in the normal elderly, as outlined in table 1.2 (Goto & Miller, 2001). They also have a greatly increased risk of developing certain types of cancer, particularly thyroid cancer, melanoma, soft tissue sarcoma, and osteosarcoma (Goto & Miller, 2001; Goto et al, 1996). The most common causes of death are cardiovascular disease and cancer (Goto & Miller, 2001). Thus, the two biggest causes of death amongst Werner syndrome patients (cancer and heart disease) are the same as for the general population (Goto & Miller, 2001; Statistics, 2012).

Features of Werner syndrome	
grey hair	Alopecia
short stature	excretion of hyaluronic acid
skin abnormalities leading to ulceration	type II diabetes
bilateral cataracts	Osteoporosis
immunodeficiency due to T cell atrophy	Arteriosclerosis
hoarse or high-pitched voice	Atherosclerosis
	calcification of soft tissue

Table 1.2: The features and clinical symptoms displayed by WS patients, which are similar to those seen in normally aged individuals. The median lifespan of Japanese WS patients has improved from 48 years in 1992 to 57 at present years, due to improved clinical recognition and better cancer treatment.

cDNA microarray analysis (Kyng et al, 2003) revealed that young WS cells display similar gene expression patterns to cells taken from normally aged individuals, emphasising the usefulness of WS as a model system for normal ageing. Somatic cells of WS patients present several other striking features. The majority of WS fibroblasts in culture have a replicative potential of fewer than 20 population doublings before they become senescent, compared with 40-60 for normal fibroblasts (Martin et al, 1970; Salk, 1982; Tollefsbol & Cohen, 1984). The observed premature replicative senescence phenotype is hypothesised to account for premature ageing in WS patients, and also ageing of normal tissue (Campisi, 2005; Cox & Faragher, 2007; Davis et al, 2003; Kipling et al, 2004). However, WS fibroblasts also display a mutator phenotype which leads to genomic instability that is characterised by extensive chromosomal deletions and rearrangements (Ariyoshi et al, 2007; Fukuchi et al, 1989; Shen & Loeb, 2000).Furthermore, mutation of WRN induces a metabolic shift and causes oxidative stress (Kashino et al, 2003; Li et al, 2014; Massip et al, 2009; Pagano et al, 2005; Pallardo et al, 2010). It is unclear which of these phenotypes is the primary cause of premature ageing in WS.

1.6.2 The WRN gene

The *WRN* gene encodes a 1432 amino acid protein, with several conserved domains (figure 1.4). WRN is a member of RecQ family of helicases, which are conserved in all three domains of life (Hartung et al, 2000; Hickson, 2003; Opresko et al, 2003). Humans possess five RecQ family members, which function in maintaining genomic integrity (Hickson, 2003). Null mutations in

three out of five of these RecQ helicases cause known genetic instability diseases (Shen & Loeb, 2000): Bloom syndrome (BS), Rothmund-Thomson syndrome (RTS) and WS. Genetic instability is manifested differently in each of these. Unlike WS where reciprocal chromosomal translocations and extensive genomic deletions are the characteristic hallmarks, increased sister chromatid exchange and chromosomal rearrangements that result in somatic mosaicism are indicative of BS and RTS, respectively (Hickson, 2003). Knowing the molecular mechanisms leading to genetic aberrations characteristic of deficiencies in RecQ helicases such as WRN will help to explain the role played by the helicase in maintaining integrity of the human genome.

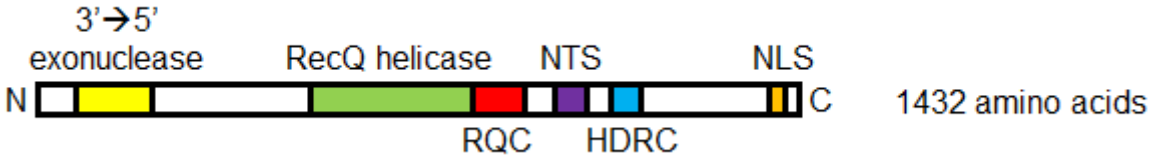

Figure 1.4: Cartoon representation of human WRN and its principle domains. The exonuclease domain (yellow) and the helicase domain (green) are shown, along with the RQC (RecQ C-terminal, red), the NTS (nuclear translocation signal, purple), the HDRC, Helicase-and-Ribonuclease D/C-terminal, blue), and the NLS (nuclear localisation sequence, orange). WRN also has a nucleolar localisation sequence at the C terminus, within the NLS.

WRN has been shown to be involved in many different aspects of DNA metabolism (see figure 1.5). Hyper-recombination in some WS cells has been proposed to account for the characteristic genomic instability (Cox et al, 2007; Fukuchi et al, 1989; Salk et al, 1981; Scappaticci et al, 1982; Yamagata et al, 1998), and is supported by the hyper-recombination phenotype seen in

Saccharomyces cerevisiae, *Schizosaccharomyces pombe*, and *Escherichia coli*, in which the WRN helicase homologue in each case is mutated (Cox & Faragher, 2007). WS cells are also hypersensitive to certain DNA-damaging agents, such as camptothecin (Lowe et al, 2004; Pichierri et al, 2000; Poot et al, 1999), 4-NQO and DNA cross-linking agents (Poot et al, 2001; Prince et al, 1999; Rodriguez-Lopez et al, 2007), but insensitive to UV and γ-radiation (Dhillon et al, 2007), suggesting a role for WRN in DNA repair. This DNA damage hypersensitivity also suggests a role for WRN in homologous recombination (Saintigny et al, 2002). Other defects at the cellular level include an extended S-phase and reduced RNA transcription (Balajee et al, 1999; Gray et al, 1998). In addition to roles in DNA repair and recombination (figure 1.5), WRN is also important for DNA replication and this is supported by the co-purification of WRN with PCNA in a large replication complex (Lebel et al, 1999; Rodriguez-Lopez et al, 2003) accumulation of aberrant replication forks in WS fibroblasts (Rodriguez-Lopez et al, 2002), and the hypersensitivity of WS fibroblasts to camptothecin (Poot et al, 1999). Camptothecin treatment induces single strand breaks by inhibiting topoisomerase I, and attempts to replicate over these breaks are thought to lead to replication fork collapse (Squires et al, 1991).

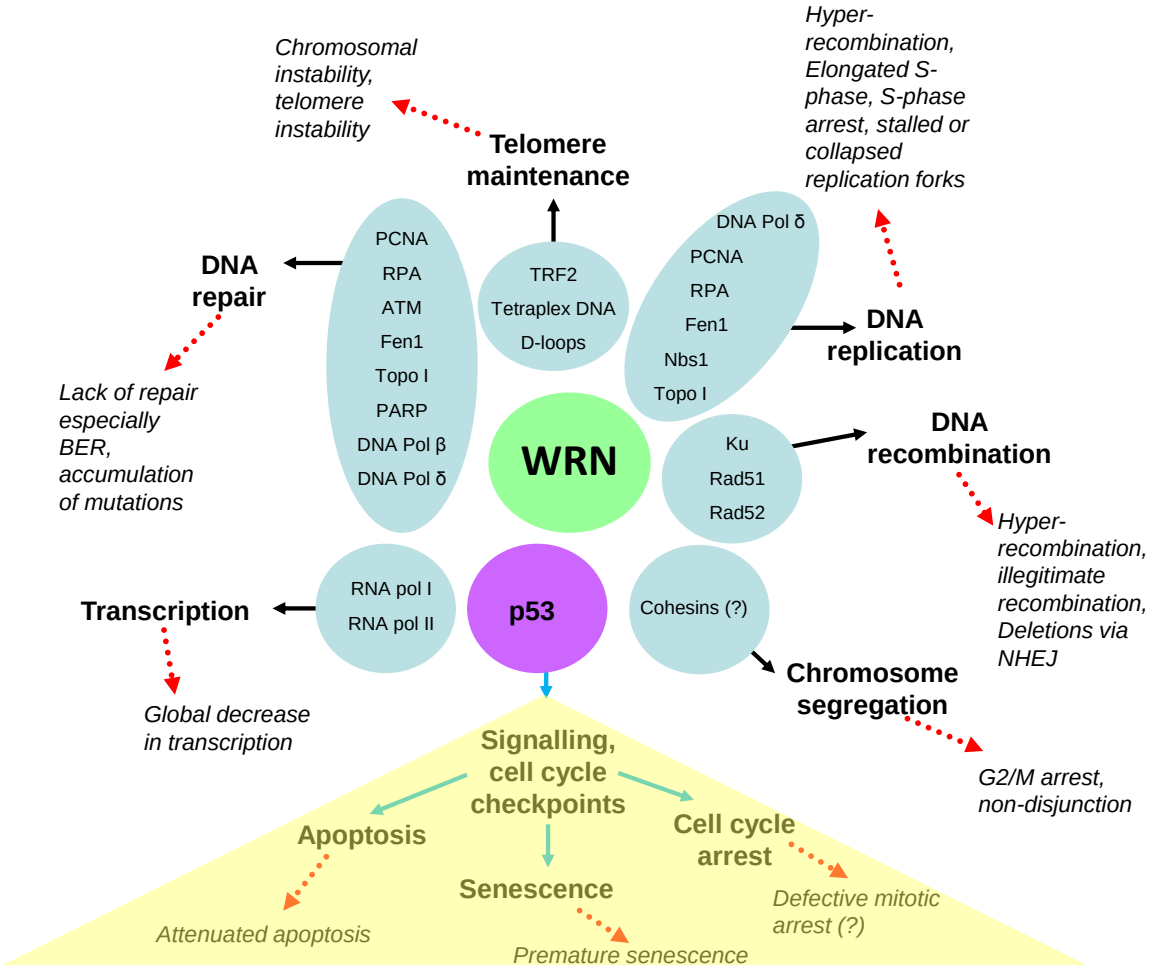

Figure 1.5: Involvement of WRN in key aspects of DNA metabolism. WRN can either directly (through its helicase and exonuclease activities) or indirectly (via multiple protein-protein interactions – blue ovals) affect major aspects of DNA metabolism (bold text). Absence of WRN causes inappropriate execution of these processes, leading to various molecular outcomes (red arrows). Note that the interacting proteins shown in this figure are only a subset of all known interacting proteins, and there is substantial overlap between WRN activity in various DNA metabolic processes. The involvement of WRN in various aspects of DNA metabolism has also been inferred through its in vitro substrate specificity (see table 4.1). Though not strictly DNA metabolism, some of the emerging roles of WRN which are performed in concert with the WRN interacting protein, p53 (purple oval), are also shown.

In addition to the RecQ helicase domain (Gray et al, 1997), WRN also contains an exonuclease domain at its N-terminus which exhibits a 3' → 5' exonucleolytic activity (figure 1.4), thus making it enzymatically unique amongst the RecQ family (Huang et al, 1998; Shen et al, 1998a). The C-terminal

nucleolar and nuclear localization sequences cause WRN to be sequestered in the nucleolus of G1 in the cell cycle (Marciniak et al, 1998). Other domains include the HRDC and RQC domains which aid DNA binding and recruitment of various proteins (Kitano et al, 2007; Lee et al, 2005; Tadokoro et al, 2012). The large number of identified protein partners, along with the presence of a variety of functional domains, may explain the pleiotropic activity of WRN in major aspects of DNA metabolism (see figure1.5) (Lee et al, 2005).

In vitro studies have determined the biochemical activities of human WRN helicase and exonuclease (Gray et al, 1997; Huang et al, 1998), along with a number of *in vitro* substrates for both activities (Cheng et al, 2007; Shen et al, 1998b). Furthermore, a considerable number of proteins which functionally and physically interact with WRN have been identified (see Fig.1.5) (Lee et al, 2005). Despite this, only limited knowledge has been obtained regarding *in vivo* substrates of WRN and the mechanisms that may co-ordinate the helicase and exonuclease activities (Opresko et al, 2001), owing to difficulties in dissociating the two key enzyme activities *in vivo* (Shen et al, 1998a).

The relative importance of the helicase and exonuclease activities to ageing is still unclear, despite extensive studies (Cox et al, 2007; Cox & Faragher, 2007; Crabbe et al, 2004; Dhillon et al, 2007; Kamath-Loeb et al, 2004; Kashino et al, 2005; Machwe et al, 2007; Rodriguez-Lopez et al, 2002; Rodriguez-Lopez et al, 2007; Sidorova, 2008). Dissection of the relative contributions of the helicase and exonuclease domains to genome stability and ageing is thus critical for a proper molecular understanding of the biology of WS, and in the search for drugs to treat age-related diseases (Cox & Faragher, 2007).

1.6.3 Limitations of WS models

Studies of human WS are limited by shortage of patient-derived cells and cell lines, and an inability to study WRN's effects on whole organism biology. Furthermore, assessing the biological impact of loss of enzymatic function of either the helicase or the exonuclease activities is challenging due to the fact that both are found on the same polypeptide (Shen et al, 1998a). Various mouse models of Werner syndrome are available (Lebel, 2002; Massip et al, 2006) (Chang, 2005; Chang et al, 2004), although their utility is limited since, like human *WRN,* murine *WRN* encodes both helicase and exonuclease activities on the same polypeptide. In addition, telomeres of inbred laboratory mice are substantially longer than human telomeres (~50 Kb compared to ~15 Kb, respectively (Gomes et al, 2011; Wright & Shay, 2000)) – consequently, the telomeres of $WRN^{-/-}$ mice need to be made artificially short before WS phenotypes are observed, by knocking out *Terc* (encoding the telomerase RNA component (Chang et al, 2004; Du et al, 2004)). Phenotypes of premature ageing are only seen in the $Wrn^{-/-}$ $terc^{-/-}$ mice 5-6 generations after loss of Terc. Hence there is a need for other model organisms that permit full 'birth-to-death' studies of ageing, particularly those with short life spans, to facilitate rapid knowledge acquisition. Model organisms which also allow for the separate genetic manipulation of the exonuclease and helicase activities would be highly informative.

Unlike in mammals, invertebrate WRN-like genes do not encode both a RecQ helicase and exonuclease as these activities are encoded at distinct genetic loci (reviewed (Plchova et al, 2003). The *Drosophila* homologue of the hWRN exonuclease has been identified (Boubriak et al, 2009; Cox et al, 2007;

Saunders et al, 2008), and flies mutant for this exonuclease exhibit some of the key phenotypes of human WS cells (Boubriak et al, 2009; Cox et al, 2007; Saunders et al, 2008), specifically hypersensitivity to CPT, and highly elevated levels of mitotic DNA recombination. However, it has yet to be established which of the three possible RecQ helicases is the WRN helicase orthologue in flies, making this a limited model for the study of WS (Cox & Faragher, 2007). *C. elegans* is an obvious model for the study of WS and ageing, containing as it does, homologues of both the WRN helicase and WRN exonuclease, and this is the starting point of the work described in this thesis (Ketting et al, 1999; Lee et al, 2004).

1.7 An emerging role for the Janus-faced p53 in senescence and ageing

The nuclear phosphoprotein, p53, is a sequence-specific transcription factor and a key tumour suppressor. Under physiological conditions, p53 is present at low levels and performs important housekeeping roles especially in regulating energy metabolism (Bensaad et al, 2006; Corcoran et al, 2006; Madan et al, 2012; Vousden & Lane, 2007), but a variety of stresses can lead to rapid induction of p53 levels and activity (see figure 1.6) (Vousden & Lane, 2007). In multicellular organisms, the induction of p53 in response to genomic damage serves to ensure that cells are prevented from dividing whilst the damage remains, by regulating target genes involved in processes such as cell cycle arrest, DNA repair, senescence or apoptosis (reviewed by (Vousden & Lane,

2007)). Thus, the activation of p53 in response to genomic instability is a critical countermeasure to carcinogenesis.

Recent studies in transgenic mice have demonstrated that p53 is also important for development, metabolism, reproduction and, interestingly, ageing. On the one hand, p53 promotes organismal survival through cancer suppression (hence increasing life expectancy), but on the other hand it can actively shorten lifespan. This has led to p53 being termed as a 'two-faced (or Janus faced) protein' (Rodier et al, 2007).

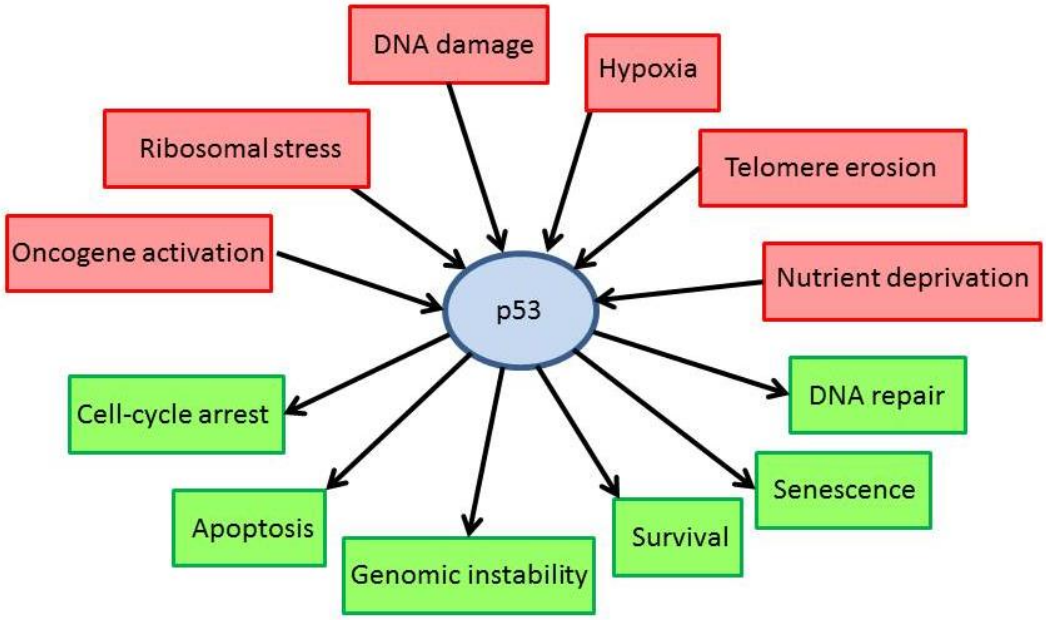

Figure 1.6: Activators and responses of p53. Activation of p53 by a variety of stresses can result in a number of cellular responses. Which cellular response is induced is in part determined by activation of target-gene expression. The role of p53 in ageing is likely to depend on which cellular response is activated and the context in which the activation occurs.

1.7.1 p53 activity drives ageing

While p53 (and its transcriptional target p21) have been known for some time to be important in driving both telomere-dependent and –independent cellular senescence (Cox & Faragher, 2007; Davis et al, 2006; Davis et al, 2003; Evans et al, 2003; Herbig et al, 2004; Sitte et al, 1998; Smith & Kipling, 2004), the role of p53 in organismal ageing first came to light in a transgenic mouse model in which the p53 gene was mutated, producing a constitutively active N-terminally truncated protein (Tyner et al, 2002). The resultant mice had very reduced lifespans and displayed a plethora of age-related phenotypes, including greying and loss of fur, kyphosis and osteoporosis, organ atrophy, and reduced tolerance to stress. In a subsequent study, mice which overexpressed a naturally occurring short variants of p53 (Delta40p53 (p44) were found to have hyperactive IGF-signalling (through both increased expression and increased signalling activity of IGF-R), together with a reduced lifespan and accelerated ageing (Maier et al, 2004). Moreover, such mice showed premature neurodegeneration when a humanised form of amyloid precursor protein was introduced (Pehar et al, 2010). Hence p53, and naturally occurring variant forms, regulate longevity and ageing phenotypes. The mechanism by which an excess of functional p53 shortens lifespan is currently unclear, but it is provocative to suppose that hyperactivity of IGF signalling may be an important component.

An alternative method for activating p53 *in vivo* is to generate mutants which mimic constitutive phosphorylation of transcription-associated residues (T21D and S23D); yet again, the premature appearance of characteristic features of ageing were observed in mice transgenic for this mutant p53, together with

marked stem cell loss (Liu et al, 2010). Depletion of the p53-transcriptional target and pro-apoptotic gene PUMA by RNAi rescued the stem cell loss and ageing phenotype in the T21D/S23D mice (Liu et al, 2010), suggesting that widespread apoptosis of stem cells, which presumably limits tissue self-renewal, could explain the ageing phenotypes mediated by p53. These findings together suggest that overactive p53 compromises healthy ageing.

While constitutive activation or overexpression of p53 can promote ageing, the story is far from clear. Increased expression of both p53 and the tumour suppressor p19 Arf (an inhibitor of MDM2 – which is itself an inhibitor of p53) in the super-arf/p53 transgenic mouse model actually slows the rate of age-related health decline and resulted in extended lifespan (Matheu et al, 2007). Both genes in this model were present in increased copy number, thus leading to increased expression whilst maintaining endogenous post-transcriptional regulation. Hence overexpression of p53 *per se* is not sufficient to drive ageing (at least in an arf-overexpressing background) and indeed can have the opposite effect of enhancing longevity. However, transgenic mice with one or two extra copies of genomic p53 along with flanking regulatory sequences, showed an enhanced p53 response and were resistant to both spontaneous and carcinogen-induced tumours, but had a normal lifespan (and no signs of premature ageing) (Garcia-Cao et al, 2002; Mendrysa et al, 2006; Mendrysa & Perry, 2006), suggesting that when properly regulated, the enhanced p53 activity increases tumour resistance and does not promote ageing in mice. Therefore, the role of p53 in ageing is complex and context dependent.

1.7.2 Loss of p53 function can lead to premature ageing

The next logical question to ask would be whether reduced or complete lack of p53 activity impacts on longevity. However, as anticipated given p53's vital role as a potent tumour suppressor, mice null for p53 developed cancer with very high incidence and at early ages (74% develop tumours by 6 months) (Donehower et al, 1992), thwarting initial attempts to study possible anti-ageing impacts of p53 loss. However, despite initial obstacles, mice with various loss-of-function p53 mutations have been developed. One of these was a knock-in mouse in which Serine 18 was replaced with alanine and thus could no longer be phosphorylated by ATM in response to DNA damage (Armata et al, 2007). Perhaps unexpectedly, given that mice with p53 phosphomimics age prematurely, the non-phosphorylatable form of p53 also led to accelerated ageing (Armata et al, 2007). Notably, S18 (S15 in humans) is important not only for activation in response to DNA damage but also for p53 protein stabilisation and prevention of degradation by MDM2 (Shieh et al, 1997). Hence the ageing observed in S18A mice may be a consequence of DNA damage that remains unrepaired since a key component in the DNA damage response pathway, i.e. p53, is dysfunctional. It has been widely reported that old cells show high levels of intrinsic DNA damage (for instance, surrogate markers gamma H2AX and 53BP1 are chronically elevated); since the DDR results in p53 activation, it will result in turn in the onset and maintenance of the senescent state driven by overactive p53. Premature ageing is also a feature of DNA repair syndromes such as Xeroderma Pigmentosum or Werner syndrome, again supporting the assertion that ongoing signalling of DNA damage (or the inability to respond appropriately) can drive ageing (Coppede & Migliore, 2010; Thoms et al, 2007).

Together, these findings from mice models suggest that both loss-of-function, or certain gain-of-function mutations in p53 cause organismal ageing, while physiological p53 activity is protective against cancer and is necessary for normal survival. Hence in normal cells with wild type p53, p53 may only act as a gerontogene (i.e. promoting ageing) when it is chronically activated, for example in response to ongoing or unrepaired DNA damage. This emphasises the fact that optimal health is about maintaining balance in function of regulatory processes.

1.7.3 WRN and p53

p53 and WRN have been shown to functionally interact in cultured mammalian cells . For instance, p53-mediated apoptosis is attenuated in WS cells (Blander et al, 2000; Spillare et al, 1999); WRN over-expression results in enhanced p53-dependent transcriptional activity (Blander et al, 1999); transcription of the *WRN* gene is modulated by p53 (Yamabe et al, 1998); and WRN knockout mice display accelerated mortality in a p53-null background (Lombard et al, 2000). Physical interaction between the two proteins has also been demonstrated *in vitro* (Blander et al, 1999; Spillare et al, 1999), as well as functional biochemical interaction – specifically, inhibition of both the exonuclease and helicase activity of WRN by p53 (Brosh et al, 2001; Sommers et al, 2005). Since these assays are *in vitro*, often relying on purified recombinant proteins with oligonucleotide DNA substrates, their physiological relevance is unclear. Because of the high tumour incidence in p53 null mice (Attardi & Jacks, 1999), which is further exacerbated by loss of WRN (Lombard et al, 2000), it has not been possible to

study the impact of WRN-p53 interactions on organismal ageing. To analyse ageing effects of WRN and p53 independently of cancer impact, it is therefore necessary to look in an organism that is not susceptible to the life-limiting effects of metastatic cancer. Since *C. elegans* is short lived and adult somatic cells of worms are entirely post-mitotic, they do not develop somatic cancers. In this thesis, therefore, I use *C. elegans* to explore the relationship between p53 and WRN in ageing.

1.8 Aims of this thesis

The work described in this thesis sets out to:

1) set up a *C. elegans* model of WS (chapter 3).

2) analyse the phenotypes of worms carrying mutations in WS homologues (chapters 3 and 4).

3) investigate the effect of genetic context on WS mutant phenotypes, particularly with respect to p53 function (chapter 5).

4) asses the physiological basis of WRN/p53 interactions, especially with respect to altered stress responses (chapter 6).

Chapter 2 - Materials and Methods

2.1 DNA methods

2.1.1 PCR amplification of DNA

For PCR reactions, DNA template was obtained from either lysed single nematodes, plasmids, or fosmids. Primers were synthesised by MWG (for sequences, see Table 2.1). PCR reactions were performed using Taq polymerase (NEB). A typical Taq reaction mix of 25µl contained 2.5µl template DNA, 2.5 µl 10x ThermoPol buffer (final concentration10mM Tris.HCl, 50mM KCl, 1.5mM $MgCl_2$, pH 8.3), 4 µl dNTP mix (final concentration 0.4mM of each of dATP, dCTP, dGTP and dTTP), 2.5 µl forward primer (0.4 µM final), 2.5 µl reverse primer (0.4 µM final), 1 µl enzyme (at 5U/µl ie 5U in the final reaction) and 10 µl ultrapure water (ddH_2O). All PCR mixes were overlaid with approximately 30 µl of mineral oil and placed in a Biometra TRIO Thermoblock thermocycler.

Standard cycling parameters were as follows: A single denaturation step at 95°C for 2 minutes was followed by 30 cycles of denaturation (30 seconds 95^oC), annealing (30 seconds at the melting temperature of the primer minus 5°C) and extension at 68°C. The extension time depended on the length of the desired PCR product and equated to approximately 1min/kb. A final extension step at 68°C for 10 minutes allowed completion of synthesis, and was followed by a hold step at 4°C.

2.1.2 Agarose gel electrophoresis

DNA fragments were separated by 0.5-2% agarose gel electrophoresis, depending on the size of desired fragment, in TBE buffer (45 mM Tris-borate, 1 mM EDTA), Ethidium bromide (final concentration 0.5µg/ml) was added to gel mix cooled to 50°C prior to pouring into a 10x10cm gel tank; gels were allowed to set at room temperature. DNA samples were mixed with loading dyes (10mM Tris.Hcl pH7.4, 1mM EDTA, 10% glycerol, 0.1% w/v xylene cyanol or bromophenol blue). Gels were run in TBE buffer at 70V for 30-60 minutes. Ethidium-stained DNA was visualised by exposure to UV light and images collected using AlphaImager software linked to a transilluminator camera. According to expected product size, one of three different types of molecular weight markers were used: 10kb ladder, 1kb ladder, and Low Molecular Weight (LMW) ladders (all from NEB).

2.1.3 BfaI restriction enzyme digest

BfaI digestion of DNA was used as part of the genotyping method outlined in section 2.3.13. DNA was digested according to the manufacturer's conditions (NEB). PCR products were purified using Qiagen spin columns according to manufacturer's instructions, then 8µl of this post-genotyping PCR product (Section 2.3.13) was digested with 1µl of BfaI in Buffer 3 (final concentration 100mM NaCl, 50mM Tris-HCl, 10mM $MgCl_2$, 1mM DTT, pH 7.9, NEB) at 37° for 2 hours. The products of digestion were then analysed by electrophoresis on a 2% agarose gel (see Section 2.1.2).

2.1.4 Gel extraction

Gel bands representing DNA fragments of the required size (e.g. following Bfa1 digestion) were excised from the gel using a clean razor blade under long wavelength UV transillumination. DNA was purified from the agarose gel bands using Qiaquick Gel Extraction Kit (Qiagen) according to manufacturer's instructions (Qiagen).

2.1.5 DNA Sequencing

All DNA sequencing of linear PCR products and plasmid DNA was conducted by Geneservice using either standard primers or specific primers (which were supplied to Geneservice at 3.2µM). Sequence analysis used the alignment function of ApE software (A Plasmid Editor, version v2.0.47, http://biologylabs.utah.edu/jorgensen/wayned/ape/).

2.1.6 Sequence alignments

BLASP alignment and sequence identity searches were conducted with the reference protein sequence of human *WRN* (GI:110735439) against the translated *C. elegans* genome (release WS245), using default parameters (http://www.wormbase.org/db/searches/blast_blat and https://blast.ncbi.nlm.nih.gov) WRN-1, MUT-7 and ZK1098.3 FASTA sequences were obtained from Wormbase (http://www.wormbase.org), the SIB Bioinformatics Resource Portal (www.expasy.org) or UniProtKB (http://www.uniprot.org).

2.1.7 Fosmid rescue

Rescue experiments (Chapter 3) were performed using fosmid WRM0638bB07 from the *C. elegans* fosmid library produced by Don Moerman (see http://www.lifesciences.sourcebioscience.com/clone-products/non-mammalian/c-elegans/c-elegans-fosmid-library/), which contains the entire *wrn-1* operon as part of a ~40kB genomic DNA fragment (see Table 2.0) in the fosmid vector pCC1FOS (Epicentre – see Figure 2.0). Fosmids in this library are usually maintained at low copy number; in order to obtain sufficient fosmid DNA for injection into worms, induction to obtain high copy number was carried out by inoculating a single bacterial colony bearing the fosmid into LB medium supplemented with 12.5 µg/ml chloramphenicol, in a 15ml Falcon tube; cultures were grown overnight at 37^{o}C with shaking at 220 rpm. The overnight culture was then inoculated into a larger volume of LB-chloramphenicol together with CopyControl induction solution (Epicentre), ensuring adequate aeration during bacterial growth. Cells were centrifuged and DNA purified by standard methods using a Qiagen miniprep kit optimised for large plasmids.

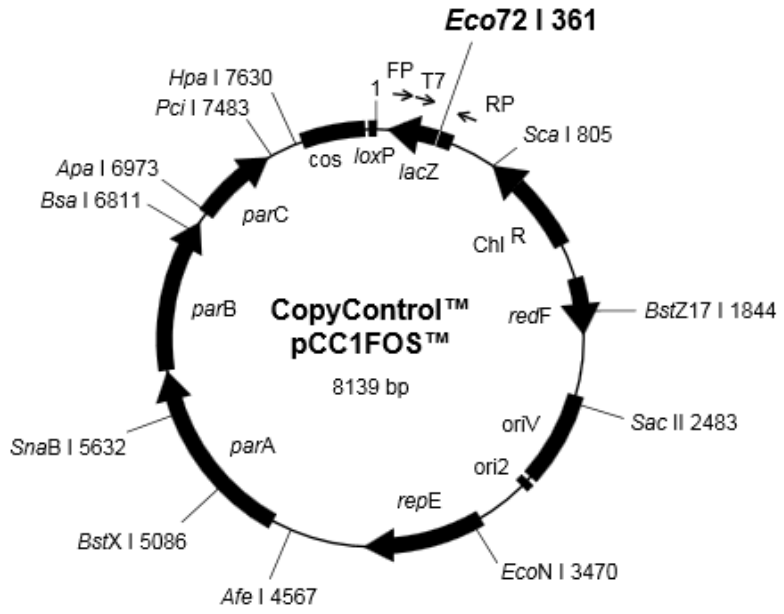

Note: Not all restriction enzymes that cut only once are indicated above.
See Appendix E for complete restriction information.
Primers are not drawn to scale.

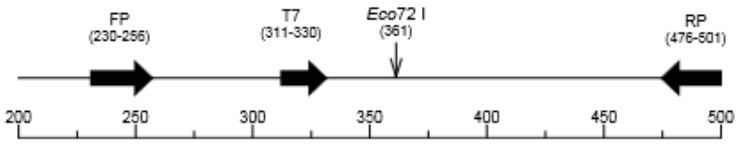

FP = pCC1™/pEpiFOS™ Foward Sequencing Primer	5' GGATGTGCTGCAAGGCGATTAAGTTGG 3'
RP = pCC1™/pEpiFOS™ Reverse Sequencing Primer	5' CTCGTATGTTGTGTGGAATTGTGAGC 3'
T7 = T7 Promoter Primer	5' TAATACGACTCACTATAGGG 3'

Figure 2.0: pCC1FOS™ Vector Map. The fosmid map was provided by http://www.epibio.com.

Gene name	Protein coding	non-coding RNA
F18C5.10	√	
wrn-1	√	
tag-184	√	
C56E6.10		√
iron-15	√	
C56E6.9	√	
abcx-1	√	
C56E6.13		√
C56E6.15		√
abch-1	√	
C56E6.4	√	
C56E6.12		√
*C56E6.2**	√	

Table 2.0: Genes carried by fosmid WRM0638bB07. * = partial coverage by fosmid.

2.1.8 Primer design

Software programmes ApE ('A plasmid Editor' version 1.17) and Primer3 (http://bioinfo.ut.ee/primer3-0.4.0/) were used to design primers (except those used in TETRA-primer ARMS PCR procedure for *mut-7* genotyping (see section 2.3.13), which were designed essentially according to (Ye et al, 2001). Oligonucleotide primers were purchased from Eurofins (MWG) and stored at 400 µM in 10mM Tris.HCl pH7.4 1mM EDTA (TE) at -20^{o}C. All primer sequences with annealing temperature and extension time are shown in Table 2.1 – other conditions are as for standard PCR reactions (Section 2.1.1).

Primer	Sequence 5' --> 3'	Genotyping of	Annealing temperature	Extension time
HL001	AGCGATGAAGCGTCGAGCTG	*wrn-1(gk99)*	58°C	40 sec
HL002	TCTCCTTGATCGGAATCATCCGAAG	*wrn-1(gk99)*		
HL003	CCTCGCTATTGATGAAGCTCATTGTG	*wrn-1(tm764)*	58°C	40 sec
HL004	ATACCAAATGCAACTGTCGCAACG	*wrn-1(tm764)*		
HL005	CATCGTAATCCTACGAGATCACC	*mut-7(pk204)*	58°C	60 sec
HL006	GATTGATATGAAGCATACGATGCC	*mut-7(pk204)*		
HL007	TGGAAATTTATTTTTACTTATAGAATGTTA	*mut-7(pk204)*		
HL008	TCTCCACACACATAGAAGCTGAG	*mut-7(pk204)*		
HL009	GCG GAA ACC ATG CCA AAC	*ZK1098.3(tm2546)*	57°C	30 sec
HL010	TCC AAG TTC AGA CAA CAG AAT TTC C	*ZK1098.3(tm2546)*		
HL011	GCGGTCAACATGGAAATTTATTTTTACTTAT AGAATGCT	*mut-7(pk204)* (alternative)	56°C	30 sec
HL012	CGCGACATTTCCACTTTTACTCCGTC	*mut-7(pk204)* (alternative)		
HL013	ACATTTTCAGTTTGTGAAATACGAC	*cep-1(gk138)*	54°C	120 sec
HL014	TGCGTTGAGAAAATAATTGAATG	*cep-1(gk138)*		
HL015	GCCGCCCGTAGAAGTAAATC	*him-6(ok412)*	55°C	150 sec
HL016	ACGCCAGTCGTAGTGTTTCC	*him-6(ok412)*		

Table 2.1 Oligonucleotides used in this study.

2.2 Bacterial methods

2.2.1 Bacterial strains

Two bacterial strains were used as feeder cultures for nematode growth. OP50 is a uracil-deficient strain of *E. coli* (Brenner, 1974), which prevents overgrowth of the bacterial lawn when seeded onto NGM plates. HT115 (DE3) is an *E. coli* strain containing a tetracycline-selectable transposon disrupting the RNase III gene (a gift from the Fire lab) which was used in all RNAi experiments. The DE3 prophage provides phage T7 RNA polymerase required for expression from the T7 promoters flanking RNAi-coding constructs in RNAi plasmids.

2.2.2 Culture and maintenance of bacterial strains

Bacterial strains were streaked onto 2YT plates, or individual colonies were inoculated into liquid 2YT media and grown at 37^{o}C. Plate and liquid media were supplemented with appropriate antibiotics where appropriate (15µg/ml chloramphenicol, or 50µg/ml ampicillin in or kanamycin). Glycerol stocks of bacteria for long terms storage were prepared by mixing 500µl of an overnight bacterial culture grown from a single colony with 80% autoclaved glycerol, and frozen at -80°C.

2.3 Nematode methods

2.3.1 *C. elegans* strains

Sydney Brenner in 1974 pioneered the use of Bristol N2 as a common laboratory strain of *C. elegans* (Brenner, 1974). Consequently, the Bristol N2 wild type strain was used as a control in all experiments in this thesis. All other strains used were derived from the N2 strain.

Strain	Genotype
AW0579	*wrn-1(gk99)II;mut-7(pk204)III*
AW0580	*wrn-1(tm764)II;mut-7(pk204)III*
AW0869	*unc-119(ed3)IIIouEx723[unc-119+]*
AW0898	*wrn-1(tm764)II;unc-119(ed3)IIIouEx743[unc-119+]*
AW0928	*cep-1(gk138)I;wrn-1(gk99)II/mIn1[dpy-10(e128)mIs14]II*
AW0929	*cep-1(gk138)I;wrn-1(tm764)II/mIn1[dpy-10(e128)mIs14]II*
AW0930	*wrn-(tm764)II;unc-32(e189) dpy-18(e499)III*
AW0931	*wrn-1(tm764)II;unc-119(ed3)IIIouEx768[unc-119++fosmid]*
AW0933	*cep-1(gk138)I;him-6(ok412)IV*
AW0976	*cep-1(gk138)I;zIs356[daf-16p::daf-16a/b::GFP+rol-6]IV*
AW0977	*wrn-1(gk99)II;zIs356[daf-16p::daf-16a/b::GFP+rol-6]IV*
AW0978	*wrn-1(tm764)II;zIs356[daf-16p::daf-16a/b::GFP+rol-6]IV*
AW1006	*cep-1(gk138)I;wrn-1(gk99)II;zIs356[daf-16p::daf-16a/b::GFP+rol-6]IV*
AW1007	*cep-1(gk138)I;wrn-1(tm764)II:zIs356[daf-16p::daf-16a/b::GFP+rol-6]IV*
DR2078	*mIn1[dpy-10(e128) mIs14]/bli-2(e768) unc-4(e120)II.*
JK2739	*lin-6(e1466) dpy-5(e61) I/hT2 [bli-4(e937) let-?(q782) qIs48] I;III*
MD0701	*bcIs39[(lim-7)ced-1p::GFP+lin-15(+)]V*
NL917	*mut-7(pk204)III*
TJ1	*cep-1(gk138)I*
TJ356	*zIs356 [daf-16p::daf-16a/b::GFP+rol-6]IV*
TM2546	*ZK1098.3(tm2546)III*
TM764	*wrn-1(tm764)II*
VC174	*wrn-1(gk99)II*
VC193	*him-6(ok412)IV*
CB4867	*unc-32(e189) dpy-18(e499)III*

Table 2.2: Strains used in this thesis. Shaded boxes indicate strains I generated during the course of the work described here. Strains AW869 and AW898 were generated by Dr Samantha Hughes (Department of Biochemistry, University of Oxford). Remaining strains were obtained from the *Caenorhabditis* Genetics Center (CGC) or the National Bioresource Project. Fosmid= WRM0638bB07.

2.3.2 Culture and maintenance of *C. elegans* strains

C. elegans strains were cultured by standard techniques (Brenner, 1974; Sulston & Hodgkin, 1988). OP50 bacteria from an overnight liquid culture were streaked onto 35mm NGM plates and allowed to dry. Worms were propagated by manual picking using a flamed platinum wire, or by excising a portion of NGM plate. Strains were usually maintained at 20°C (though some experiments required incubation at 25^{o}C – see individual figures for details). For longer term maintenance e.g. over holiday periods, worms were placed at 15^{o}C. Stocks were also frozen in liquid nitrogen.

2.3.3 Generation of males

Male nematodes are required for use in out-crossing and genetic crosses. To generate males from hermaphrodite stocks, five L4 stage hermaphrodites were picked onto an NGM plate seeded with OP50 bacteria and heat shocked at 30°C for 5.5, 6, or 6.5 hours before being transferred back to 20°C. Following reproduction and hatching, male offspring were selected and isolated. In order to maintain a male N2 stock, three L4 stage hermaphrodites were picked onto a seeded OP50 plate along with five males to allow for sexual reproduction and maintenance of males at a ratio of 1:1 males:hermaphrodites.

2.3.4 Outcrossing *C. elegans* strains and generation of double mutants

Newly obtained strains from CGC were outcrossed at least 4 times to remove background mutations. Briefly, three N2 males were placed on an NGM agar

plate (seeded with OP50) together with a single mutant L4 hermaphrodite of the chosen strain and left until eggs were produced. The original males were removed from the plate at this point to avoid confusion with male progeny. Male offspring were selected and a new cross set up using three males and one N2 hermaphrodite. Hermaphrodite progeny were individually picked onto separate plates, allowed to self-fertilise and produce progeny; the adults were then genotyped (as described in section 2.3.11) to identify heterozygous mutants. Progeny of heterozygotes were themselves picked to individual plates, allowed to self, genotyped, and homozygous mutants were selected and maintained.

To generate double mutant strains, genetic crosses were performed essentially as previously described (Sulston & Hodgkin, 1988; Sulston & Horvitz, 1977) though this was modified for generation of *wrn-1;mut-7* double mutants (shown in figure 2.1).

2.3.5 Generation of balanced strains

Due to reasons outlined in Chapter 4, *wrn-1* and *mut-7* single mutant strains were maintained as balanced heterozygotes. Crosses were performed to generate the following balanced strains: *wrn-1(gk99)II/mIn1[dpy-10(e128)mIs14]II; wrn-1(tm764)II/mIn1[dpy-10(e128)mIs14]II;* and *mut-7(pk204)(III)/ hT2 [bli-4(e937) let-?(q782) qIs48]I;III.* The strains were maintained at 20°C by picking heterozygotes (marked by pharyngeal GFP expressed from the balancer – non-GFP-expressing worms are homozygous for the *wrn-1* or *mut-7* mutations, as homozygous balancer is lethal). Strains were regularly assessed for correct segregation of progeny and lack of exceptional segregants and recombinational events.

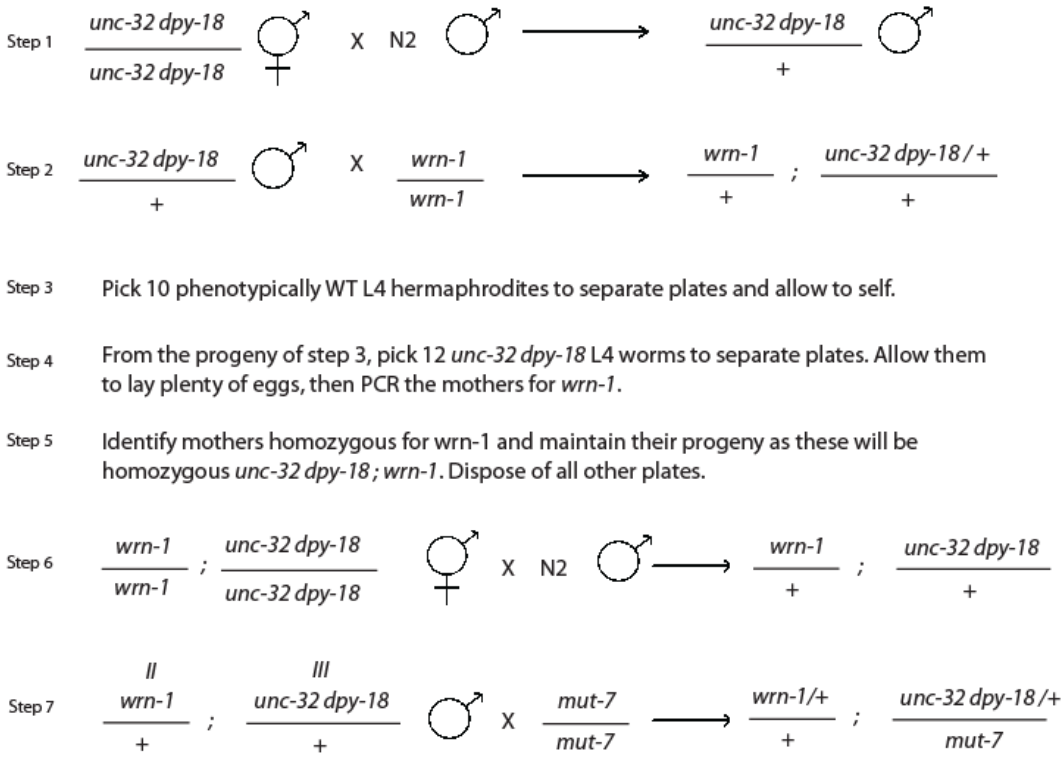

Figure 2.1. Crossing strategy for generation of *wrn-1; mut-7* mutants. Mutation of *wrn-1* and *mut-7* was confirmed by genotyping PCR and verified by sequencing.

2.3.6 Light microscopy

A low power Leica dissection microscope (either 1x or 10x objective) was used during routine worm maintenance and when assessing gross morphological phenotypes, brood sizes or for motility assays. Detailed morphological analysis was carried out using a Zeiss Axiophot microscope fitted with differential interference contrast (DIC) and fluorescence optics. Worms were anaesthetised on 2% agarose pads as previously described using 0.2% phenoxypropanol (Sulston & Hodgkin, 1988) or by picking into 20µl of 10µM muscimol (Sigma-Aldrich) and then mounting on 2% agar. A coverslip was then slowly lowered on top of the worm. An Axiocam camera with Axiovision software (release 4.5) was used for acquisition of digital photographs. A Zeiss 63x oil immersion objective was used for tissue and germline analysis, and a 40x Zeiss oil immersion objective was used for whole worm microscopy.

For live fluorescence imaging of worms (e.g. for analysis of the overall appearance ageing worms, for visualising DAF-16::GFP, and for maintaining worm stocks balanced with GFP-labelled markers), a Leica MZIII dissection microscope was used (either 1x or 10x objective). An attached Hamamatsu camera and HCImage Live (V3.0) imaging software was used for image acquisition (stills and movies).

2.3.7 Confocal microscopy

Images were taken using a Leica TCS SP5 II confocal microscope under standardised scanning conditions, using a 64X objective, excitation wavelength 488 nm, 35% full power laser on acquisition setting with argon laser selected and set to 30%, with peak emission spectrum set for FITC and centred around

520 nm. All worms were photographed on the same day to avoid effects of light source variation on apparent fluorescence intensity. A standardised capture method was used for every photo whereby the plane with the most intense autofluorescence was focused on. Photos were taken as quickly as possible to minimise the effect of bleaching.

2.3.8 Quantification of autofluorescence

LAS AF® software was used to quantifiy autofluorescence intensity, combining the amount (in pixels) and intensity of autofluoresence for each photomicrograph examined. The same area of worm was analysed in each case (region of interest (ROI): width=50 µm, height=210 µm), covering approximately the entirety of the gut. Background autofluorescence for the same ROI corresponding to an area of the slide where the worm was not present was also quantified and subtracted from the autofluorescence value obtained for each worm, in order to minimise noise. Statistical analysis was performed using one-way and two-way ANOVA with post-hoc contrasts.

2.3.9 Assessment of tissue integrity and youthfulness

The distal gonad and the head region of *C. elegans* were photographed under fluorescence and Nomarski optics. Heads were blindly scored on a scale of 1-5: 5 referring to animals so deteriorated as to be nearly unrecognisable; 1 representing a youthful appearance; and 2, 3, and 4 representing animals that fall in between these two extremes. A representative image for each score was provided to aid the assessor. The scoring system did not represent a strict quantitative relationship in that animals with a score of 2 did not have twice as much damage as animals scored with a value of 1). The gonad and the tissue

surrounding it were also rated on a 1 - 5 scale, using the same criteria. Youthfulness was also scored on a 1- 5 scale, using images of entire worms. Statistical analysis was performed using one-way and two-way ANOVA with post-hoc contrasts.

2.3.10 Construction of transgenic worms

Injections of fosmid DNA were performed as described previously (Mello and Fire, 1995). Constructs were injected (by myself and Dr Samantha Hughes) into the germlines of young adult worms with the *unc-119(ed3) allele* (with or without other mutant alleles*)* at a concentration of 10-20 ng/µl DNA. The rescuing *unc-119*$^{+}$ *(pDP#MM016β)* plasmid was used as a co-injection marker (Maduro and Pilgrim, 1995). Rescued progeny (i.e phenotypically wild type, lacking the parental uncoordinated phenotype) in the first generation were picked and stable lines selected for analysis. The presence of the fosmid in transformed worms was confirmed by genotyping PCR against *wrn-1* (see 2.3.11) and by sequencing of *wrn-1.*

2.3.11 RNAi by feeding

Feeding clones of HT115 (DE3) bacteria containing L4440 plasmids encoding appropriate dsRNA were selected from a genome-wide library (Kamath & Ahringer, 2003). The sequence of the inserts was confirmed by sequencing (Source Bioscience) using primers against the T7 promoters that flank the RNAi cassette.

Bacteria were streaked from frozen glycerol stocks onto 2YT plates containing ampicillin and used to inoculate 2ml liquid 2YT culture containing 50µg/ml each

of ampicillin and tetracycline. The culture was incubated at 37°C, with shaking, overnight. Plates containing NGM agar, 25µg/ml carbenicillin and 1mM IPTG were seeded with 100µl of the bacteria and allowed to dry overnight (to create the RNAi feeder plates). Two days later, 3 stage L4 hermaphrodites were transferred to each seeded plate and maintained at 20°C. Their progeny, at L4 stage, were picked onto fresh RNAi feeder plates, also at 20°C. For lifespan analysis, an initial n value of 60 worms per strain was used, with 1 worm per plate. *pop-1* (embryonic lethal) was used as a positive control for RNAi uptake and empty vector as a negative control for all RNAi experiments.

2.3.12 Single worm lysis

PCR from single worms was performed as follows. Briefly, individual worms were picked into 2.5µl of lysis buffer (50µM KCl, 2.5µM $MgCl_2$, 10µM Tris.HCl pH 8.3, 0.45% NP40, 0.45% Tween 20, 0.01% gelatine, 0.1 mg/ml proteinase K) in the lid of a thin-walled 0.5ml Eppendorf tube; tubes were closed and the mix briefly centrifuged to ensure the lysis mix transferred to the base of the tube. Tubes were subsequently frozen at -80°C for 1 hour, and then incubated for 1 hour at 60°C, followed by 15 minutes at 95°C. PCR was then performed using 2.5µl of lysis mix as the DNA template (see section 2.1.1).

2.3.13 Genotyping

Where it was not possible to follow mutant alleles phenotypically, PCR was used for genotyping. In the case of deletion alleles, PCR primers were designed to anneal to a region either side of the deletion, resulting in a single PCR product in WT animals, a single smaller PCR product in individuals homozygous for the deletion, and two differently-sized products in

heterozygotes (see Figure 3.3 for position of *wrn-1* genotyping primers). Unless otherwise specified, PCR was performed using Taq polymerase (NEB) as described in section 2.1.1 and Table 2.1.

2.3.14 Genotyping of the *mut-7(pk204)* allele

Genotyping of the point mutation *mut-7(pk204)* required the use of tetra-primer ARMS PCR (Figure 2.2), since this allele is a point mutation that cannot be detected simply on the basis of size difference in standard PCR. This method employs two pairs of primers which generate two allele-specific amplicons (Figure 2.2B). One primer pair (HL005 and HL006, Table 2.1) was designed to produce a PCR product which corresponds to the WT allele (shown in pink and red in Figure 2.2), while the other pair (HL007 and HL008, Table 2.1) was designed to produce a PCR product specific to the mutant allele (light and dark blue in Figure 2.2). One inner primer of both primer pairs was designed to include a 3'-terminal match to the allele in question (Ye et al, 2001). Since allelic specificity is conferred almost completely by the 3'-terminal match (or, indeed, mismatch), this PCR method requires considerable optimisation to achieve successful genotyping. I developed conditions whereby tetra-primer ARMS PCR-based genotyping of *mut-7(pk204)* could distinguish between the *pk204* allele and the WT allele (Table 2.1). Genotyping N2 worms by this method produced a strong band at 607bp expected for worms homozygous for the WT *mut-7* allele. While this band could not be detected in *mut-7(pk204)* worms, the predicted 312bp band could be detected instead (data not shown).

2.3.15 An alternative method for genotyping *mut-7(pk204).*

Genotyping by tetra-ARMS PCR became increasingly unreliable for later generations of balanced heterozygous and homozygous *mut-7(pk204)* worms, sometimes detecting only a non-specific band of ~900bp generated by amplification using the two outermost primers and hence observed for both wild type and *mut-7(pk204)* strains (see Figure 2.2).

This led to the need to develop an alternative approach to genotyping *mut-7(pk204)*. In this method (Figure 2.2) primers were designed to introduce a Bfa-1 restriction site into the final PCR product from *mut-7(pk204)* worms but not from worms with WT *mut-7*. Two primers were used: a standard forward primer (HL011, purple), and a reverse primer (HL012, blue) of which the 3'-terminal nucleotide was complementary to the base immediately adjacent to the *pk204* base. The reverse primer included a single base mismatch (red C) which was not specific to either allele (C or T) - therefore a PCR product would be amplified by the primer pair regardless of genotype. However, if the PCR product contained the *pk204* allele (T), a BfaI restriction site (C^TAG) would be present in this amplicon, but not in the WT PCR product (since sequence at this locus would be CCAG).

The mismatched base was introduced in order to ensure a restriction site could be generated in the PCR product when the *pk204* allele had been amplified (and not when WT had been amplified) – without this base change, no restriction site would have been present in the PCR product for either allele. PCR products were then purified (Qiagen PCR Cleanup) and incubated with BfaI (NEB) at 37°C for two hours. Digestion products were separated by

agarose gel electrophoresis. Since a BfaI site would only be present following amplification of the mutant *pk204* allele, two bands 62 and 38 bp would be expected from *mut-7(pk204)* homozygotes and only one band of 100 bp from WT worms (Figure 2.2). This method was validated by genotyping *mut-7(pk204)* homozygotes which had recently been out-crossed; it could successfully distinguish between the WT and mutant allele of *mut-7*.

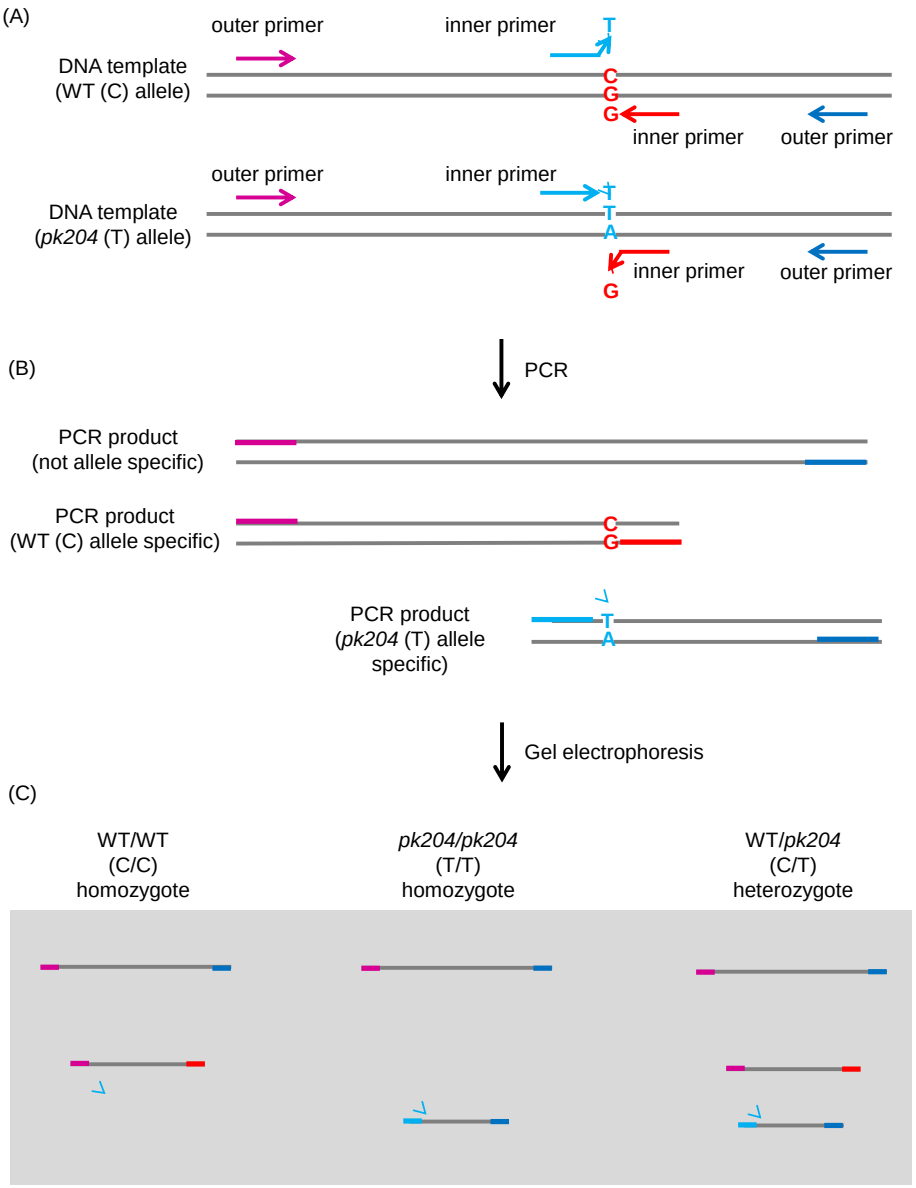

Figure 2.2: **Schematic presentation of the tetra-primer ARMS-PCR method used to genotype *mut-7* alleles**. Diagram is adapted from (Ye et al, 2001). The *pk204* mutation is a C → T substitution. Using two primer pairs (A), two allele-specific PCR products are produced (B). One primer pair (pink and red) will produce a PCR product specific to the WT (C) allele, while the second primer pair (light and dark blue) will produce a PCR product specific to the *pk204* (T) allele. The two outer primers (pink and dark blue) are positioned at different distances from the SNP (A) so that the two allele-specific PCR products differ in length (B). These PCR products can them be discriminated by gel electrophoresis (C). Note that regardless of genotype, a non-allele specific band is always generated (the upper most band in section C) – this is produced by amplification from the two outer primers (pink and blue).

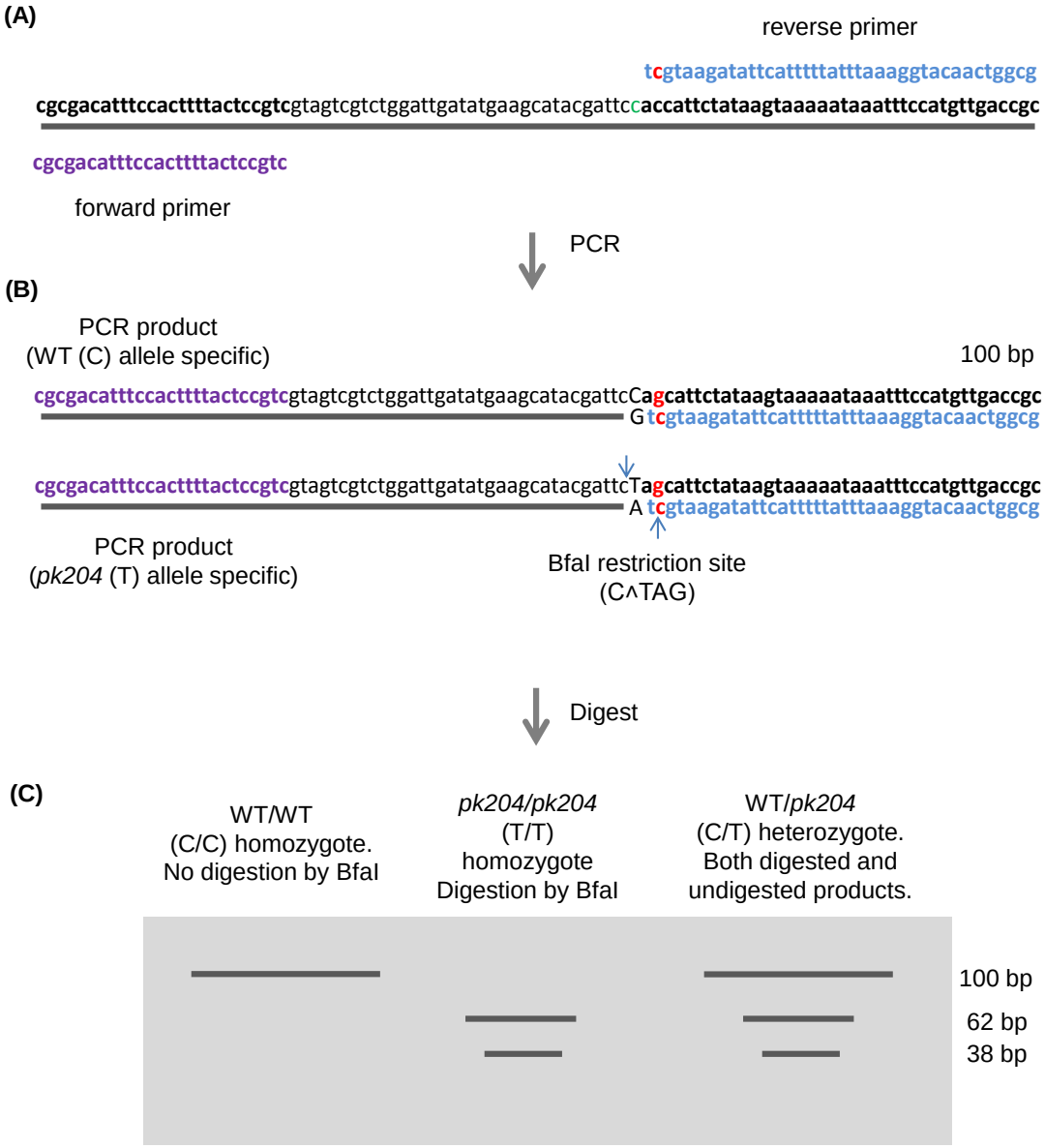

Figure 2.3: **Schematic representation of an alternative method for genotyping *mut-7* alleles.** A pair of primers (A) are used to amplify a 100bp region containing the *mut-7* allele (B) - either WT C or *pk204* T. The combination of the *pk204* allele (T), and the mismatched cytosine (red) introduced by the reverse primer (blue) in the PCR product creates a BfaI restriction site which is absent in WT PCR products but present in *mut-7(pk204)*-derived PCR products (B). Purification followed by incubation of the PCR products with BfaI results in allele-specific restriction patterns when visualised by gel electrophoresis (C).

2.3.16 Lifespan analysis

Lifespan analysis was performed on 55mm NGM-agar plates, with one worm per plate (to minimise the tendency of worms to crawl off the plate, and because reports suggest that having multiple worms on one plate can alter life span). Plates were seeded with OP50, and incubated at 20˚C. Where appropriate, OP50 bacteria were mixed with 4.9 mM FUdR prior to seeding the plates (see Chapter 3, Figure 3.6). Hermaphrodite worms were picked onto the plates at L4 stage (day 0 of the analysis) and picked onto new plates every day during egg laying to separate them from progeny. Worms were assessed daily and scored as dead when unresponsive to three light taps with a platinum wire. On average, each experiment was set up using 72 worms per strain, per condition. This allowed for a final n of ~60 worms after accounting for loss of worms due to crawling off the plate or bagging (see individual figures for n values for specific experiments).

2.3.17 Brood size analysis

Brood sizes were measured using ≥20 synchronised L4 worms of each strain, which were picked individually onto 55 mm NGM plates seeded with OP50 (i.e. one worm per plate), and moved to fresh plates every day until egg laying had stopped. Plates were seeded the day before worms were added to ensure the bacterial lawn was thin, thus making eggs easier to score. Furthermore, the bacterial lawn was seeded in a thing line across the plate to facilitate counting of progeny. Counting of unhatched eggs and live worms was performed on plates from which the original L4 worm had been transferred on the previous day. Dead eggs were counted 24 hours after the mother was removed, since all

viable eggs would have hatched within this time. Counting of larvae was facilitated by storing plates at 4°C for half an hour before scoring, in order to minimise worm movement. All plates were scored in triplicate, and the mean and standard deviation was calculated for each.

2.3.18 Thrashing assay

To assess motility of worms, individual adult worms at the age of interest were picked directly into ~20µl M9 buffer (42 mM Na_2HPO_4, 22 mM KH_2PO_4, 86 mM NaCl, 1mM $MgSO_4$) that had been pipetted onto an unseeded NGM plate. Worms were allowed to acclimatise to the liquid for ~1 minute. Using a timer and a counter, the number of sigmoidal thrashes made by the worm in a 30 second period was then recorded. 10 worms per strain per age were analysed.

2.4 Genomic instability assays

2.4.1 DAPI staining of dissected gonads

DAPI staining of germlines allows for the detection of a variety of morphological features including nuclear size, shape, distribution together with chromosomal structure and spatial organisation. Though DAPI staining of whole worms is possible and preferred in some instances (for visualising germline tumours, for example), the more technically challenging approach of dissecting intact gonads for DAPI staining allows for more detailed and higher resolution analysis.

Clean worms were picked individually into 180 µl 1x PBS containing 25mM levamisole and 10mM EDTA in a watch glass and decapitated using round

edge scalpel blades.19 µl 37% formaldehyde (i.e. final concentration 3.7%) was added to the watch glass, and fixation was allowed to proceed for 60 minutes at room temperature in a humidified chamber. Most of the liquid was then removed by careful pipetting under a microscope. 500 µl 100% methanol (prechilled to −20°C) was added, and incubated at room temperature for a further 5 minutes. Approximately 250 µl of the solution was then removed, followed by three washes with 1 ml PBS each time. DAPI was then added to a final concentration of 100 ng/ml of DAPI and samples incubated for 10 minutes, washed a further three times in 1 ml PBS each time and mounted for observation on an agar pad. 10 µl VECTASHIELD anti-fade mounting medium (Vector Laboratories, H-1000) was immediately added to the pad and covered with a cover slip.

2.4.2 Visualisation of apoptotic corpses by TUNEL

Dissected gonads were prepared as in section 2.4.1). After the third PBS wash, most of the liquid was removed, leaving about 20 µl. For the labelling of corpses in dissected gonads the *In Situ Cell Death Detection Kit, Fluorescein* (Roche) was used according to manufacturer's instructions. Briefly, 5 µl of Enzyme Solution was mixed with 45 µl of Label Solution and added to samples which were then incubated in this mix for 1 hour in the dark at 37°C and then washed twice with PBS. DAPI was added as above (Section 2.4.1) and dissected gonads were mounted on agar pads for microscopy (as described in section 2.4.1 above). Label Solution only was used as a negative control.

2.4.3 Propidium iodide (PI) staining of chromosomes

Worms at 1 day post-L4 were picked onto unseeded NGM plates, allowed to crawl around for ~15 minutes, picked into a watch glass containing 2ml 0.5% phenoxypropanol (PP), left for ~10 minutes until movement had stopped, and then decapitated using a round edge blade. Most of the liquid was removed, and three washes with PBS-Tween (1%) were performed. The sample was incubated for 1 hour at 37°C with RNase A (1µl taken from 200 µg/ml solution). Liquid was removed and samples were incubated with 400 µl of 1µg/ml PI for 10 minutes and then washed three times with 1ml PBS each time. Samples were mounted on microscope slides as before (section 2.4.1).

2.4.4 DAPI staining of whole worms

Worms of the desired age were picked into a watch glass containing 10µl M9 buffer. 200µl of 150nM DAPI dissolved in 100% ethanol was added, followed by incubation in a dark chamber for 2 hours. Worms were washed three times in 2 ml M9 each time, the left to soak on a further 2ml M9 overnight at 4°C in a humid chamber. Microscopy was performed the following day as outlined for dissected gonads (Section 2.4.1).

2.4.5 Hydroxyurea treatment

A lawn of OP50 was spread onto 55mm NGM plates so that most of the plate was covered, and was allowed to dry overnight. Two days later, plates were overlaid with 250µl hydroxyurea (HU) solution in M9 to a final HU concentration

of 25mM and incubated overnight. The following day, at least 50 adult worms at 1 day post-L4 of a given genotype were picked to a single HU plate, and two plates per strain were set up (total of 100 HU-treated worms per genotype). This was repeated for negative control plates lacking HU but otherwise treated identically, giving 100 untreated worms per genotype in each control. 24 hours later, the germlines of treated and untreated worms were dissected and stained with DAPI (see Section 2.4.1) for analysis by DIC and fluorescence microscopy. Mitotic nuclei of WT worms undergo a transient cell cycle arrest at the G2/M checkpoint: G2-arrested germ cells are easily recognised on the basis of their relatively large size.

2.4.6 IR sensitivity assays

All IR assays were conducted with a caesium-137 source. In order to determine IR dosage to animals on plates, the decay time (in seconds) for 30 Gy at the time of exposure (specifically, 547.14 seconds) was used to calculate the number of minutes of exposure to achieve a dose of 60 Gy (18.24 minutes). At least 20 worms per genotype were then irradiated with 60 Gy at the late L4 stage. Negative controls were mock treated but not irradiated. For microscopic analysis for assessment of G2 cell cycle arrest, the gonads of irradiated and non-irradiated control worms of the same age were dissected 12 hours after treatment, and analysed by DIC and fluorescence microscopy. Apoptosis was assessed by TUNEL staining (see Section 2.4.2) in at least 15 dissected germlines per strain at either 12 or 48 hours post-irradiation.

2.4.7 Scoring for radiation sensitivity

Mutations resulting in defective checkpoint or repair pathways can render the germline of worms hypersensitive to IR, which causes a severe decrease in the production of viable progeny (number of zygotes and/or fractional viability of zygote). Brood size analyses were therefore conducted (see also Section 2.3.15) to assess radiation sensitivity.

Late L4 stage worms were irradiated with 60 Gy then incubated at 20°C for 24 hours. Five worms per strain per treatment were picked onto each of 8 plates (i.e. a total of 40 worms per condition, per genotype) which had a freshly seeded bacterial lawn approximately 1cm in diameter. 12 hours later the adult worms were removed from the plate and the total number of eggs laid was counted. Dead eggs (i.e. any unhatched eggs) were counted 24 hours after the initial count, to obtain percentage embryonic lethality and percentage survival/viability. It should be noted that this assay specifically determines damage sensitivity of meiotic pachytene cells.

2.4.8 Chromosome fragmentation assay

Observing chromosome fragmentation confirms whether DNA damage sensitivity directly correlates with increased DNA double-strand breaks (DSBs) (Craig et al, 2012; Gartner et al, 2004). Chromosomal fragmentation can be studied directly by DAPI staining meiotic chromosomes of late-stage oocytes. L4 worms were treated with a DSB-inducing agent (for example, IR or CPT), dissected 48 hours later, and intact germlines were then fixed and stained with DAPI (see Section 2.4.1). High resolution microscopy was used to observe the germlines. The appearance of diakinesis chromosomes and/or chromosome

fragments in at least 20 nuclei for each treatment and each genotype was noted and photographed.

2.4.9 Camptothecin sensitivity assay

The procedure to assess sensitivity to camptothecin (CPT) was adapted from (Nakamura et al, 2007). ≥20 L4 worms were transferred to 0.2 ml tubes containing 100 µl M9 buffer containing 0.5% dimethyl sulfoxide (DMSO) in the presence or absence of 0.15 mM camptothecin. Worms were incubated at 20°C for 2 hours, dispensed onto bacteria-free NGM plates, allowed to recover for 30 minutes, then transferred onto separate plates seeded with OP50 (one worm per plate). Subsequently, either brood size assays were conducted (see Section 2.3.15) or germline dissection and staining was performed 12 hours later (for assessment of pre-meiotic cell cycle arrest and apoptosis) or 48 hours later (for assessment of diakinesis chromosomes and apoptosis).

2.4.10 Germline mortality assay

C. elegans mortal germline mutants (Mrt mutants) are classified based on a decrease in fecundity over successive generations until they reach sterility. The method outlined here was established by (Ahmed & Hodgkin, 2000). The experiment was conducted at 25°C, with a parallel experiment at 20°C. Five L4 hermaphrodites were picked onto petri dishes seeded with OP50 and allowed to lay for 3 days at 25°C, or 4 days at 20°C). After this point, five L4 worms from the next generation (i.e. the offspring of the worms which had initially been picked to the plate) were picked onto fresh OP50 plates, and the cycle started again. Each time that L4s were picked, the generation and approximate brood size was recorded until the strain became sterile (in which case only the five

infertile hermaphrodites would be left on a plate). Five plates (A-E) were set up for each strain at each temperature (20°C and 25°C). The scoring system used is outlined in Figure 4.12.

2.5 Stress assays

2.5.1 Lifespan analysis at 25°C.

Survival analysis was performed in exactly the same way as that at 20°C (see section 2.3.13) but worms were maintained at 25°C throughout the experiment.

2.5.2 UV sensitivity

Worms 5 days post L4 were picked to unseeded NGM plates and irradiated with ultraviolet light (UV-C) using a XL-1000 Stratalinker UV-C light source, at a dose of 10J/m^2. Individual worms were then picked to separate 55mm NGM plates and were assayed for survival every day. Worms that left the plate or died due to bagging were censored.

2.5.3 Thermotolerance assay – chronic heat stress

Worms at 5 days post-L4 were transferred to NGM plates (10 worms per plate) which had been pre-warmed to the stress temperature (35°C) and then incubated at 35°C for the remainder of the experiment. Survival was assayed every 30-60 minutes. All plates were removed from the incubator simultaneously, and for ~15 minutes for each survival analysis. Once survival analysis at a given time point was complete, all plates were returned to the stress temperature. Worms that left the plate or died due to bagging were censored.

2.5.4 Thermotolerance assay – acute heat stress

L4 worms on individual plates were incubated at 33°C for 2 hours, then removed and maintained at 20°C for the rest of the survival analysis.

2.6 Statistical analysis

2.6.1 Lifespan analysis

Statistical analysis of lifespans was performed using the online resource OASIS (see Appendix for details). Mean and median lifespan, including 95% confidence intervals and standard error was calculated and significance was tested using a variety of statistical tests. These included: Log Rank/Mantel-Cox test with Chi square, P-value, and Bonferroni P-value calculations; Fisher's Exact Test, to test different survival functions at specific time points instead of overall lifespan; and Normalised Chow test, to verify the difference in the lifespan variations. Cumulative Hazard plots were also generated by the OASIS programme and formed part of the Normalised Chow test assessment. Microsoft Excel 2010 was used to process and store the large quantity of data generated by OASIS. The results of the statistical analysis of lifespan data (and n-values for each experiment) can be found in section I of the Appendix.

2.6.2 Statistical analysis of brood size

Brood sizes (and all other statistical tests hereon in) were analysed using the statistical software package provided by Microsoft Excel 2010. One-way/Single Factor ANOVA was used to test the null hypothesis that the means of several populations (i.e. the mean brood size of several strains) are all equal. The

statistical analysis package calculates an F value and an F crit value generated from the entire data set of a given experiment. If the F value is greater than the F crit value, then the null hypothesis can be rejected, since the mean brood sizes tested are not equal.

Since a significant ANOVA test does not indicate where the differences in brood sizes lie, post hoc contrasts were performed. These included Student T-Test (Two-Sample Assuming Equal Variances), and Bonferroni corrections. The Bonferroni correction counteracts the problem of multiple comparisons and is considered the most conservative method to control the familywise error rate (the probability of making one or more false discoveries or type I errors). The results of the statistical analysis (and n-values for each experiment) can be found in section II of the Appendix.

2.6.3 Assessing the effect of variables such as drug treatment on brood size

To determine whether a treatment, such as exposure to CPT, IR etc. or the generation of the P0 hermaphrodite (e.g. brood size of F1 vs F10), had a significant effect on brood size, Two-way ANOVA with replication was performed, with post hoc contrasts. Two-way ANOVA not only assesses the main effect of each independent variable (e.g. genotype vs treatment/generation) but also if there is any interaction between them. The results of the statistical analysis (and n-values for each experiment) can be found in section II of the Appendix.

One-way ANOVA was performed using the quantification data (see section 2.3.8) to determine whether there was a significant difference in auto

fluorescence between strains at a given age. Two-way ANOVA was used to test for interaction between genotype and age.

2.6.4 Spontaneous visible mutant frequency and the frequency of males

The percentage of visible mutants and males was calculated by dividing the brood size (of an individual hermaphrodite of a given genotype) by the number of visible mutants or males in that brood, and then multiplying by 100. The percentage was then averaged for each genotype and one-way ANOVA was performed as described previously.

2.6.5 Determining statistical differences in germline defects

To determine whether there was a statistically significant difference in the frequency of germline defects (see results chapters for the types of defects analysed), one-way ANOVA was performed. Either the percentage of germlines showing a particular defect, or the average number of defective mitotic cells/meiotic oocytes per germline was analysed. The results of the statistical analysis (and n-values for each experiment) can be found in section III of the Appendix.

2.6.6 Statistical analysis of the level of apoptosis

The number of apoptotic corpses, labelled either by TUNEL or the presence of CED-1::GFP, was counted either for the half of the germline closest to the eye piece (of the microscope being used) or the entire germline. The method used is specified for each experimental data set. Statistical analysis of the level of apoptosis, measured either by TUNEL or the presence of CED-1::GFP labelled

corpses, was performed in exactly the same way as that in section 2.6.2 (one-way ANOVA) and 2.6.3 (two-way ANOVA). The results of the statistical analysis (and n-values for each experiment) can be found in section III of the Appendix.

Statistical analysis of thrashing at 20°C and 25°C was performed in the same way as that outlined in section 2.6.2, using the number of thrashes rather than the number of progeny. Two-way ANOVA with post hoc contrasts was subsequently performed to determine whether temperature significantly affected the average thrash rate of worms.

2.6.7 Statistical analysis of DAF-16::GFP localisation

DAF-16::GFP nuclear localisation at 20°C and 25°C was determined by counting the number of GFP-positive nuclei per worm, calculating and average and performing one-way ANOVA. Two-way ANOVA was used to test whether there was a statistically significant difference between DAF-16::GFP nuclear localisation at 20°C vs 25°C. The same method was performed for worms that were heat shocked, but instead of simply counting GFP-positive nuclei in the entire worm, counts were divided between the head region (anterior) of the worm and the posterior half of the worm.

Chapter 3 – A *C. elegans* model of Werner syndrome

3.1 Introduction

3.1.1 Werner syndrome

Segmental progeroid or 'accelerated ageing' syndromes such as Werner syndrome (WS) can be used to study the complex process of normal human ageing (Kipling & Faragher, 1997). An advantage of using WS to elucidate potential mechanisms of ageing is that it results from mutation of a single gene, WRN (Yu et al, 1996).This could imply that WRN is a major regulator of healthspan and longevity. Alternatively, WRN could just be required for normal healthspan. Either way, the relative importance of the helicase and the exonuclease activities of WRN to ageing is still unclear, despite extensive studies (Cox & Faragher, 2007; Crabbe et al, 2004; Dhillon et al, 2007; Kamath-Loeb et al, 2004; Kashino et al, 2005; Machwe et al, 2007; Rodriguez-Lopez et al, 2002; Rodriguez-Lopez et al, 2007; Sidorova et al, 2008). Dissection of the relative contributions of the helicase and exonuclease domains to genome stability and ageing is thus critical for a proper molecular understanding of the biology of WS, and in the search for drugs to treat age-related diseases.

As discussed in chapter 1 (section 1.6.3), current models of WS are limited. In order to establish a wholly novel model system to study WRN orthologues, I used the nematode worm, *C. elegans*, which provides a robust and well-characterised model system for studying lifespan and age-related morbidities

(Kenyon, 2010b; McElwee et al, 2004; Partridge, 2010). Like other invertebrates, the WRN helicase and exonuclease activities are predicted to be encoded by two separate genes (*wrn-1* and *mut-7*, respectively (Ketting et al, 1999; Lee et al, 2004); see also Figure 3.1 and 3.2), thus allowing analysis of mutation or partial knock down of each of these activities individually or in combination – something not achievable in human or mouse studies.

It is tempting to suggest that *wrn-1* and *mut-7* together reconstitute the same functional protein complex as human WRN. There is already precedent for this - yeast-two hybrid assays in *Arabidopsis thaliana* detected an interaction between a WRN exonuclease homologue, AtWRNexo (WEX) (Hartung et al, 2000) and one of seven RecQ helicases, AtRecQI2, suggesting that complementation of WRN activities *in trans* is possible (Plchova et al, 2003). Encouragingly, WEX is also related to *C. elegans mut-7* (Plchova et al, 2003), lending further support to the suggestion that *mut-7* encodes the worm orthologue of the exonuclease domain of hWRN.

Although *C. elegans* could prove to be a useful model of WS, there are several drawbacks. For instance, worms lack MDM2 (the major negative regulator of p53) and p19/Arf (the negative regulator of MDM2) homologues, although other DNA damage response pathways are still preserved (such as the ATM/ATR pathway). Furthermore, both apoptosis and senescence are postulated to play key roles in mammalian ageing and both result from p53 activation (see the review by Serrano, 2014), but it remains to be seen what role (if any) apoptosis and senescence have in worm ageing, since apoptosis in adult worms is restricted to the germline, and adult somatic cells are quiescent, differentiated cells, which (up until recently) are believed to be unable to become senescent.

3.1.2 *mut-7*

Studies of *C. elegans mut-7* have primarily focused on roles in transposon silencing and RNA interference (Ketting et al, 1999; Sijen & Plasterk, 2003; Tabara et al, 1999; Tops et al, 2005). MUT-7, which is located in protein complexes both in the nucleus and the cytoplasm (Tops et al, 2005), was first identified in a screen for mutants in which the transposon Tc1, normally silenced in the germline, was active (Collins et al, 1987; Ketting et al, 1999). As well as the Tc1 transposon, many other transposons of unrelated sequence were also found to be active in *mut-7* mutants, resulting in a mutator phenotype (Ketting et al, 1999). Several strains containing *mut-7* mutations were also found to be resistant to RNAi, suggesting that MUT-7 is required for RISC-mediated RNA degradation, further supported by the finding that MUT-7 is complexed with RDE-2 in the cytoplasm (Tops et al, 2005), Furthermore, it is via this mechanism that MUT-7 is required for silencing transposons in the germline – guided by transposon-derived dsRNA, MUT-7 degrades transposon-derived message, which in turn prevents the production of transposase and transposition in the germline, thus maintaining genome stability (Ketting et al, 1999). In addition to transposon silencing and RNAi, *mut-7* is also required for co-suppression (Ketting & Plasterk, 2000), which may be mediated (at least in part) by the same molecular machinery as RNAi and transposon silencing. The post-transcriptional gene silencing role of MUT-7 is also conserved in *Arabidopsis*, since WEX has also been shown to be required for these processes (Glazov et al, 2003). While I am predominantly interested in investigating potential ageing effects of MUT-7 as a putative WRNexo homologue, these important roles of MUT-7 in RNAi and transposon silencing

(Rizzon et al, 2003; Tops et al, 2005) must be always borne in mind when assessing phenotypes consequent on *mut-7* mutation. Furthermore, the hypermutator phenotype of *mut-7* mutants can result in unexpected secondary mutations that impact adversely on worm fitness and longevity – for instance *bus* mutants are generated at high frequency in a *mut-7* background (Gravato-Nobre et al, 2005).

3.1.3 *wrn-1*

The *C. elegans wrn-1* locus encodes the worm orthologue of human WRN helicase ((Lee et al, 2004), see also Fig 3.1). Purified recombinant WRN-1 protein expressed from *C. elegans wrn-1* cDNA (Hyun et al, 2008a) was confirmed to have 3'→ 5' helicase activity *in vitro* with substrate specificity similar to that of hWRN helicase, suggesting that WRN-1 may, like hWRN, function in aspects of DNA metabolism including replication, recombination and repair (reviewed in (Cox & Faragher, 2007)). Further in support of this suggestion, the helicase activity of WRN-1 has been shown to be stimulated by RPA-1 (Hyun et al, 2008a; Hyun et al, 2012). One potentially interesting difference is the reported ability of *C. elegans* WRN-1 to unwind long forked duplexes of 34-bp (Hyun et al, 2008a), for which hWRN helicase requires the concerted action of the WRN exonuclease domain (Opresko et al, 2001). The question as to whether the putative exonuclease MUT-7 acts co-ordinately with WRN-1 has yet to be addressed.

In worms, WRN-1 appears to be an important determinant of longevity, since normal N2 worms (i.e. wild type for *wrn-1*) have been shown to have a reduced lifespan and premature appearance of age-associated autofluorescence and

other aging phenotypes upon exposure to *wrn-1* RNAi (Lee et al, 2004). This has also been observed for a *wrn-1* mutant strain (Dallaire et al, 2012; Lee et al, 2010a), and the frequency of premature ageing phenotypes is increased when such strains are treated with ionizing radiation (IR) (Lee et al, 2004).

3.1.4 Aims of this chapter:

- To assess protein domain structure and sequence similarities between human *WRN* and potential *C. elegans* homologues.
- To assess lifespan in worms mutant for putative *C. elegans* WRN homologues.
- To investigate whether lifespan correlates with other biomarkers of ageing in worms mutant for *wrn-1* or *mut-7.*
- To generate and investigate ageing phenotypes in *wrn-1; mut-7* double mutants.
- To assess camptothecin sensitivity of worms mutant for *C. elegans* WRN homologues.

3.2 Results

3.2.1 Bioinformatics suggest that *C. elegans* WRN-1 and MUT-7 are homologues of human WRN

In order to verify previous claims that *wrn-1* and *mut-7* represent the closest worm homologues of human WRN helicase and exonuclease domains respectively (Ketting et al, 1999; Lee et al, 2004), I conducted comparative analysis using BLAST-P with a query sequence of either the intact hWRN protein sequence or isolated functional domains (Table 3.1; domains are shown schematically in Figure 3.1).

Whilst homology is very high between hWRN and the whole of WRN-1 protein sequence (BLAST-P e = $1x10^{-124}$, Table 3.1), there is much lower homology between hWRN and MUT-7 (BLAST-P e = $3x10^{-8}$). This difference is partly due to the presence of not only the RecQ helicase domain, but also many additional domains in *wrn-1* which are also present in hWRN (Table 3.1 and Figure 3.1). By contrast, MUT-7 only contains the conserved DEDDy 3'-5' exonuclease domain found in RNase D, WRN, and similar proteins (Table 3.1). Consequently, when aligning only the exonuclease domain of hWRN to MUT-7, homology is higher (BLAST-P e = $9x10^{-9}$).

Although MUT-7 is the highest hit obtained from a BLAST-P search against human WRN, a putative protein product of an adjacent locus, *ZK1098.3*, also shares some homology with human WRN (BLAST-P e = $5x10^{-8}$ for full length hWRN, e= $2x10^{-9}$ within the exonuclease domain, Table 3.1), although at a lower homology than MUT-7, (as indicated by the hatched yellow box in Fig 3.1). Provocatively, this putative protein shares extensive homology with MUT-7

(BLAST-P e=1x10-148), suggesting that ZK1098.3 may have arisen via a gene duplication event. Aligning ZK1098.3 protein (Uniprot accession number P34603) to MUT-7 and the exonuclease domain of human WRN (residues 78-300) shows conservation of key aspartates and a glutamate that are critical in human WRN for co-ordination of magnesium necessary for in-line attack of the phosphodiester bond during DNA cleavage, while the tyrosine is thought to mediate interaction with DNA bases (Perry et al, 2006). Hence the presence of all the key residues of the DEDDy 3'-5' exonuclease in both MUT-7 and ZK1098.3 suggests that either or both proteins could be functional exonucleases (Figure 3.2). Since it is therefore plausible that either mut-7 or ZK1098.3 might encode a functional homologue of the exonuclease domain of hWRN, I initially included both genes in my studies of WRN-dependent ageing in worms.

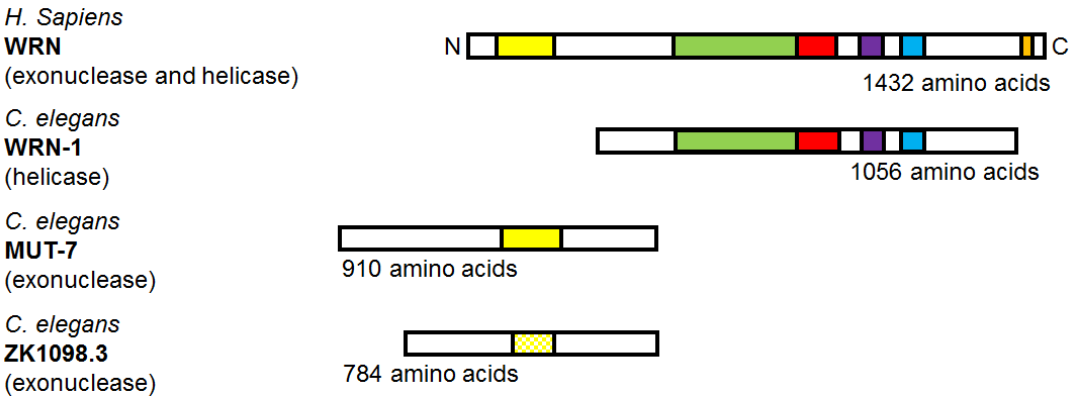

Figure 3.1: Schematic representation of hWRN and putative homologues in *C. elegans* (not to scale). Key domains are shown: DEDDy 3'-5' exonuclease (yellow); RecQ helicase (green); RQC (red); NTS (purple); HRDC (blue), and NLS (orange).

a) Conserved domains	b) Residues in hWRN	c) e value when BLAST-P against WRN-1	d) e value when BLAST-P against MUT-7	e) e value when BLAST-P against ZK1098.3
Entire WRN	1- 1432	$1x10^{-124}$	$3x10^{-8}$	$5x10^{-8}$
DEDDy exonuclease	38 - 236	no match	$9x10^{-9}$	$2x10^{-9}$
RecQ	538 - 1010	$1x10^{-108}$	no match	no match
DEDXc, DEAD-like helicase superfamily	565 - 705	$3x10^{-34}$	no match	no match
HELICc	759 - 867	$8x10^{-40}$	no match	no match
RQC	958 - 1015	$8x10^{-13}$	no match	no match
NTS	949 - 1092	$3x10^{-12}$	Two matches; 0.43 and 1	no match
HRDC	1156 - 1229	$3x10^{-7}$	Two matches	no match
HTH_40	1257 - 1352	no match	Three matches; 0.07, 2.8 and 4.3	no match
NLS	1370 - 1375	no match	no match	no match
NLS	1403 - 1404	no match	no match	no match

Table 3.1: **Homology between human WRN and potential homologues in *C. elegans*.** BLAST-P searches were performed using as query the listed hWRN residues (column b) which correspond to specific domains found in hWRN (column a), against *C. elegans* WRN-1 (column c), MUT-7 (column d) or ZK1098.3 (column e); expect-values (e-values) from BLAST-P searches are shown where matches were found. Sequence alignments can be found in the Appendix.

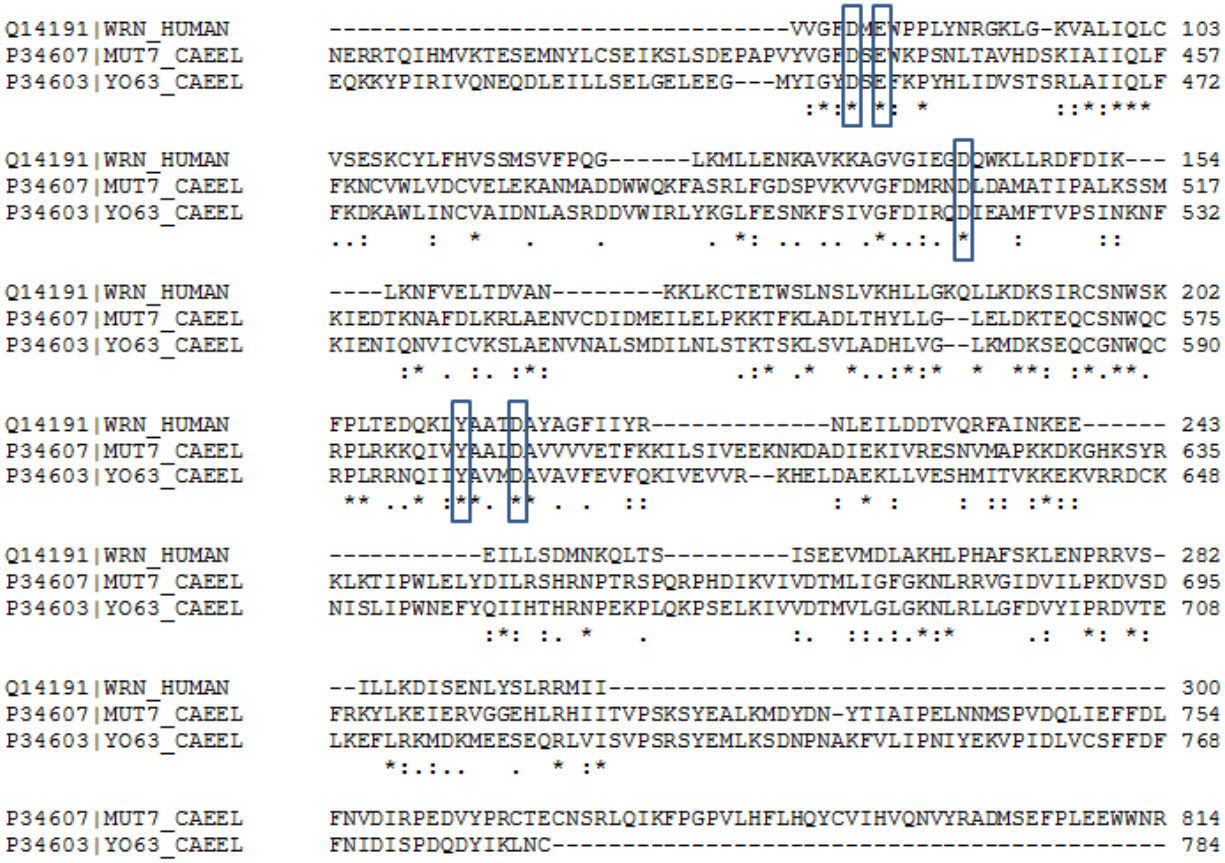

Figure 3.2: Alignment between human WRN exonuclease domain (residues 78-300), MUT-7 and ZK1098.3 (putative protein product of ZK1098.3). Blue boxes indicate key catalytic residues of DEDDy 3'→5' exonucleases. CLUSTAL-W was used to generate the alignment using FASTA protein sequences with Uniprot accession numbers Q14191 (human WRN), P34607 (*C. elegans* MUT-7) and P34603 (*C. elegans* ZK1098.3).

3.2.2 Worm strains bearing mutations in WRN homologues

In order to assess whether the putative WRN homologues had any impact on worm lifespan or other markers of ageing, it was necessary to obtain genetically pure stains and to monitor such strains regularly to ensure that the causative mutation was still present. Two homozygous deletion mutant strains were obtained for *wrn-1*: *gk99* carries a 196-bp deletion in *wrn-1*, while strain *tm764* has a 456-bp deletion in the *wrn-1* gene (see Figure 3.3A). The deletion in *wrn-1(gk99)* mutants removes the ATG start codon, causes a frame shift and is reported to be a null (Lee et al, 2010a). It is this strain that has been reported to show premature ageing phenotypes on mutation (Dallaire et al, 2012; Lee et al, 2010a). By contrast, *wrn-1(tm764)* mutants have a deletion from the fifth exon into the following intron (Figure 3.3A), which removes the RecQ helicase motif and is likely to abolish the helicase activity of WRN-1 without necessarily eliminating all of the protein. Consistent with the idea that this allele is not null, a protein can be detected in *wrn-1(tm764)* animals by immunofluorescence with an antibody raised against an N-terminal peptide of WRN-1 (Lee et al, 2010a); although the precise identify of this protein product is uncertain, it is possibly a truncated form of WRN-1. A third *wrn-1* allele, *gk116*, contains a deletion of 513 bp removing the 5' coding region of *wrn-1*, as well as part of the 3'UTR of an upstream gene, *tag-184*. This gene is the upstream gene of the operon *CEOP2250*, which also contains *wrn-1*, and thus phenotypes arising from this mutation could be also be attributed to *tag-184* as well as *wrn-1*. Furthermore, there is also a lesion in the *dpy-10* gene in *wrn-1(gk116)*. Since the *wrn-*

1(gk116) strain is genetically complex and furthermore homozygous-inviable, it was unsuitable for use in the studies conducted in this thesis.

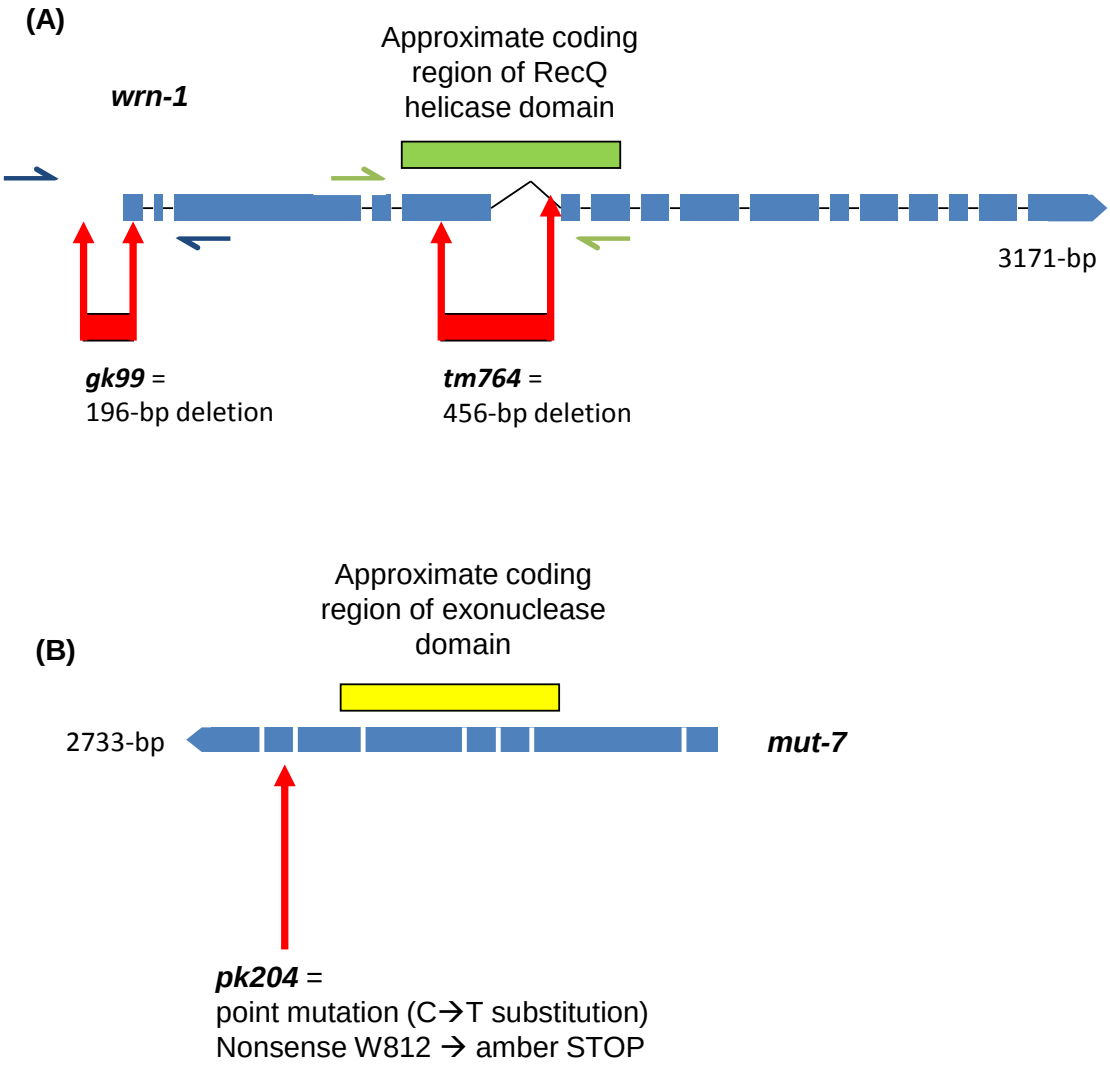

Figure 3.3: Schematic representation of the *wrn-1* and *mut-7* alleles used in this study. (A) The coding region of *wrn-1* (blue bars = exons) with relative positions of the *gk99* deletion (196 bp, left hand red bar) and the *tm764* deletion (456 bp right hand red bar). Also shown is the approximate coding region of the helicase domain (green bar) and the relative positions of the genotyping primers for *wrn-1(gk99)* and *wrn-1(tm764)* (blue and green arrows, respectively). (B) The coding region of *mut-7* (blue bars = exons). Note that *mut-7* is in the opposite orientation to *wrn-1.* The relative position of the *pk204* point mutation is indicated by the red arrow. Also shown is the approximate coding region of the exonuclease domain (yellow bar).

For the study of *mut-7,* the homozygous point mutant, *mut-7(pk204),* was used (Figure 3.3B). This is a nonsense mutation, in which a cytosine is replaced by a thymine, which results in the deletion of 98 amino acids from the C terminus of MUT-7 by introducing an amber stop codon. Given that the phenotypes of *mut-7(pk204)* are as severe as those of homozygous deletion strain *mut-7(pk720)* (in which *mut-7* and *ZK1098.4* (*GCN3* homologue) are completely deleted) it is likely that *mut-7(pk204)* is a null allele (Ketting et al, 1999).

Analysis of the second potential WRN exonuclease-like gene, *ZK1098.32,* utilised the allele *tm2546.* This is a complex mutation, consisting of a 369-bp deletion and a 14-bp insertion covering exons 3 and 4 out of the total 6 exons. This mutation results in a frame shift and is likely to be null. Worms homozygous for this allele are viable (www.wormbase.org).

In order to ensure that all strains carried the appropriate mutation, and to verify that they bred true, I developed several genotyping strategies to distinguish wild type (WT) from mutant alleles, since none of the alleles was associated with overt visible phenotypes. These strategies and their validation are described in Chapter 2 (Materials and Methods) section 2.3.11.

Prior to phenotypic analysis, all strains were out-crossed at least 4 times (and verified using the genotyping PCRs described in section 2.3.11 and in figure 2.2) and had been grown as homozygous mutants for several generations (unless otherwise stated) at 20°C.

3.2.3 Homozygous *wrn-1* or *mut-7* mutants have a reduced lifespan relative to N2

In order to determine whether mutation of either *wrn-1* or *mut-7* impacts on lifespan, I conducted lifespan assays by picking individual worms to agar plates with OP50 bacteria (as a food source) and transferring every two days until after the egg laying period. End of life was scored as lack of movement on physical stimulation with a platinum wire (repeated 3 times).

Homozygous mutation of either *wrn-1* helicase or *mut-7* presumptive WRN exonuclease significantly reduced both the maximum life span and the median (50%) survival of adult worms grown compared to N2 (Fig 3.4B), as indicated by a shift to the left of the lifespan curves of the mutants relative to that of N2 (Figure 3.4A). This was true for both *wrn-1(gk99),* as previously reported (Lee et al, 2010a) and also for *wrn-1(tm764)* (compare blue and green survival curves, Figure 3.4A). However, the life span curve of homozygous *ZK1098.3(tm2546)* mutants (putative WRN-2 i.e. second exonuclease with homology to WRN exonuclease) was indistinguishable from that of N2 worms (Figure 3.4A and B). Therefore, loss of function of either *wrn-1* or *mut-7* decreases lifespan under these conditions (at 20^{o}C); by contrast, mutation of *ZK1098.3* has no significant effect. Consequently, *mut-7* is a stronger candidate for the WRN exonuclease homologue that *ZK1098.3*. These data also suggest that loss of the RecQ helicase domain (*wrn-1(tm764)*) reduces lifespan in *C. elegans* as much as total absence of the WRN-1 protein (*wrn-1(gk99)*), implying that the region of WRN deleted in *wrn-1(tm764)* mutants is necessary for longevity. This may suggest that wrn-1 helicase activity *per se* is a determinant

of lifespan, or that the deleted region may provide a platform for recruitment of other functional proteins (see also Chapter 5).

A

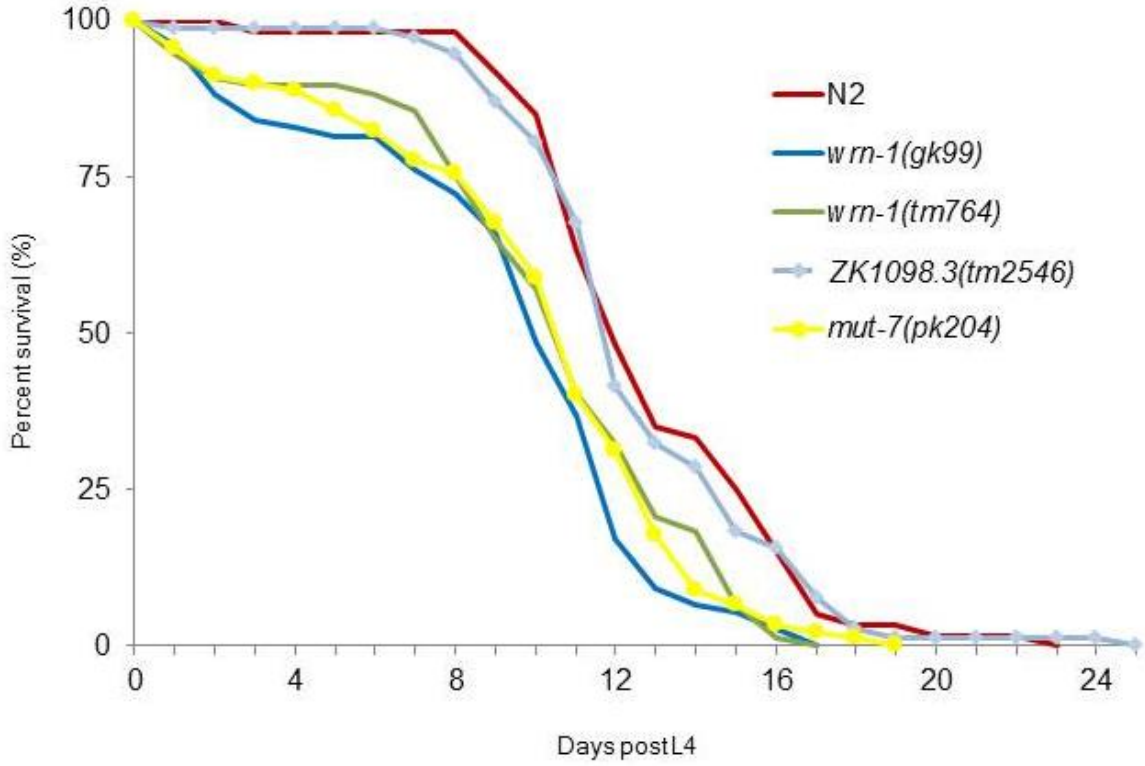

B

Strain	Maximum life span	Day at <50%	*n*
N2	23	12	60
wrn-1(gk99)	17	10	76
wrn-1(tm764)	17	11	77
ZK1098.3(tm2546)	25	12	77
mut-7(pk204)	19	11	90

Figure 3.4: Lifespan is decreased in *wrn-1* and *mut-7* mutants. Adult lifespan (post-L4) at 20°C, of *C. elegans* homozygous for mutations in *wrn-1, mut-7* or *ZK1098.3* compared to N2. (A) Lifespan curves plotted as number of animals surviving against time post-L4 (n values for each genotype are given in part B) (B) Median (50%) and maximum lifespans derived from data shown in (A). Day 0 = time at which worms reached larval stage L4.

3.2.4 *wrn-1* and *mut-7* mutants show premature signs of ageing

Since worms with mutations in either *wrn-1* or *mut-7* show a reduced life span (Figure 3.4), it was important to establish whether this phenotype was a result of premature ageing, rather than a result of general poor health or loss of fitness. Ageing in worms is associated with an accumulation of gut autofluorescence, attributed to lipofuscin, and a decline in tissue integrity (Garigan et al, 2002; Hosokawa et al, 1994; Klass, 1977; Russell & Seppa, 1987) which is particularly noticeable in the head region and the gonad of the ageing worm (Garigan et al, 2002). If short-lived mutants are short-lived because ageing is accelerated, one would expect to see the appearance of biomarkers of ageing in mutant worms at an earlier chronological age compared to WT controls. Therefore, both lipofuscin accumulation and tissue deterioration were used to assess the rate of ageing of worms mutant for the putative WRN homologues.

As shown in Figure 3.5, WT N2 worms at 2 and 4 days post-L4 show no detectable autofluorescence, whereas autofluorescence is observed in the intestine of *wrn-1* and *mut-7* mutants as early as 2 and 4 days post-L4, and continues to increase in brightness up to day 10 of adulthood. Lipofuscin began to accumulate in WT N2 worms at around day 6 (data not shown) and can be clearly detected at 10 days post L4. Thus, lipofuscin accumulates in *wrn-1* and *mut-7* mutant worms at an early age when compared to N2, indicating that the reduced lifespan phenotype in *wrn-1* and/or *mut-7* homozygous mutant worms is likely to be due to premature ageing. This was also confirmed by analysing tissue degeneration, which followed the same pattern – mutants showed loss of

tissue integrity at earlier ages that their N2 counterparts (data not shown, though see Chapter 5 Figure 5.3 and 5.4).

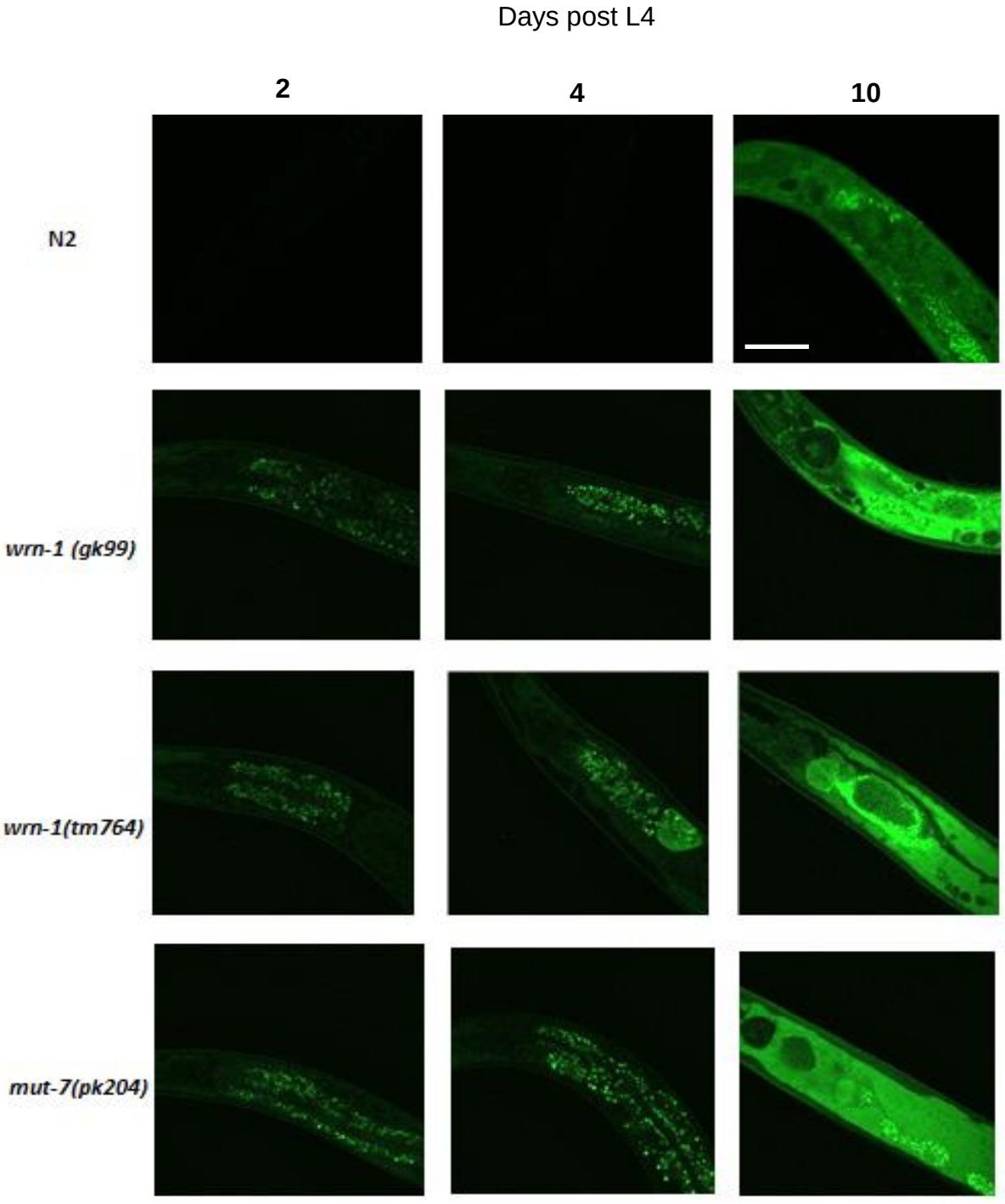

Figure 3.5: Lipofuscin accumulates prematurely in *wrn-1* and *mut-7* mutant worms. Representative confocal images of lipofuscin accumulation in ageing worms of various genotypes. N2 control worms and worms homozygous for either *wrn-1(gk99), wrn-1(tm764),* or *mut-7(pk204)* were imaged at 2, 4, and 10 days post L4 and assessed for the presence of autofluorescence,

representing lipofuscin. Note that black boxes are images of worms which had no detectable autofluorescence (N2 at day 2 and 4 post L4). Images were taken using a Leica TCS SP5 II confocal microscope under standardised scanning conditions. Excitation wavelength = 488 nm. The peak emission spectrum was set for FITC and centred around 520 nm. Scale bar = 100µm.

3.2.5 Can FUdR be used to reduce manual handling when analysing lifespan of *wrn-1* mutant worms?

When performing lifespan analysis, experimental animals must be transferred to fresh NGM plates every 24 to 48 hours during the first 4-6 days of the experiment in order to separate them from their progeny. Since this process is time consuming, the chemical FUdR has become widely used in *C. elegans* aging studies, in order to prevent hatching of progeny during lifespan experiments (Gandhi et al, 1980; Sutphin & Kaeberlein, 2009). At concentrations used for aging studies (50-100 µg/ml), FUdR has been reported not to alter the longevity of wild type N2 animals (Hosono et al, 1982). However, some genes influence longevity differently depending on whether FUdR is present or not (Aitlhadj & Sturzenbaum, 2010; Van Raamsdonk & Hekimi, 2011).

To assess whether the use of FUdR affected the longevity of *wrn-1(tm764)* mutant worms, lifespan was measured for *wrn-1(tm764)* homozygous mutant populations grown on OP50 either with or without FUdR. The lifespan of the worms maintained on FUdR was significantly longer than that of the worms maintained without FUdR (log rank test (OASIS) p=0.0003) (Figure 3.6).

Because of the strong association between longevity and maintenance of health through the lifecourse, I then tested whether *wrn-1(tm764)* mutant worms maintained on FUdR (which exhibited increased longevity) also had extended

healthspans (i.e. slower rate of biological ageing). To do this, pharyngeal pumping rate and lipofuscin accumulation were assessed. Comparison of *wrn-1(tm764)* mutant worms maintained on FUdR with WT worms also maintained on FUdR suggested that rate of biological ageing in the *wrn-1(tm764)* worms was approximately equal to, or slower than, that in WT worms (data not shown). Since both the lifespan and healthspan of *wrn-1(tm764)* worms were affected by the use FUdR, this compound was therefore not used in any subsequent experiments.

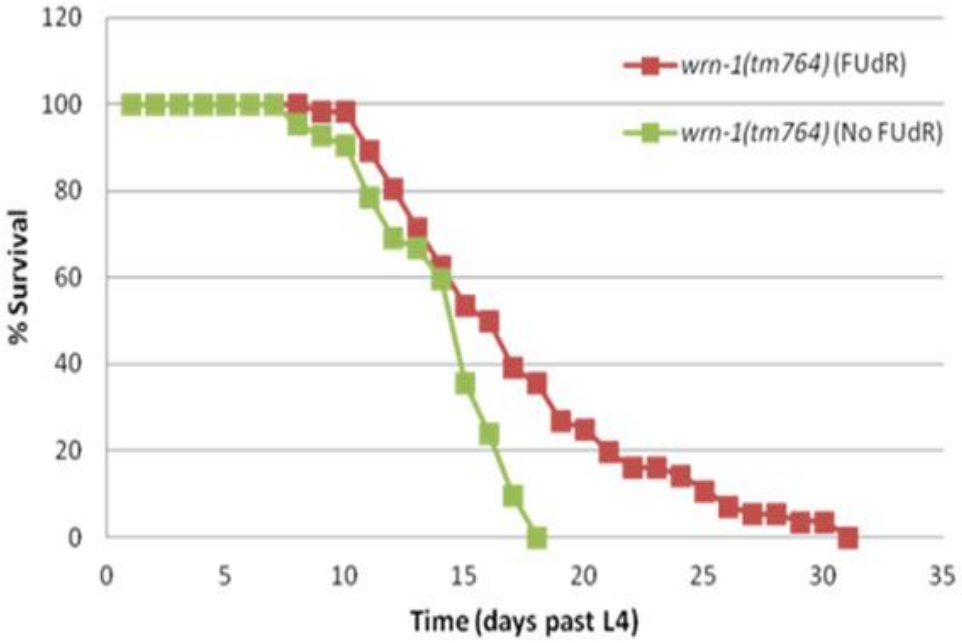

Strain	Maximum life span	Day at <50%	*n*
wrn-1(tm764) - no FUdR	18	14	42
wrn-1(tm764)- FUdR	31	15	56

Figure 3.6: The effect of FUdR on the lifespan of *wrn-1(tm764)* homozygotes at 20°C. This analysis was performed by H. Cantwell, an undergraduate student whom I was supervising. Both FUdR treated and untreated worms were picked every other day during the egg laying period to avoid potential differences in lifespan brought about by manual handling.

3.2.6 The reduced lifespan of *wrn-1(tm764)* homozygotes can be rescued by injection of a fosmid containing *wrn-1*

Although my data above suggest that premature ageing is associated with homozygous mutation of *wrn-1* and *mut-7* (Figures 3.4 and 3.5), the observed reduction in lifespan and premature appearance of autofluorescence could be attributed to a linked second site mutation (not easily removed by outcrossing) that may be present in the background of one or more of these strains. In order to test the hypothesis that a second site mutation, rather than mutation of *wrn-1 per se*, is responsible for the premature ageing observed in the *wrn-1(tm764)* strain, transgenic worms were generated in which the WT *wrn-1* gene was introduced into *wrn-1(tm764)* homozygotes. If mutation of *wrn-1* is the cause of the reduced lifespan, then the deficit should be rescued in the transgenic worms, and consequently the lifespan curve should be similar to that of WT controls. If a linked second site mutation is responsible, then the decreased lifespan phenotype of *the wrn-1(tm764)* strain will not be rescued (unless the linked mutation affects a gene also found on the fosmid).

Generation of transgenic worms by germline injection of fosmids has a relatively low success rate. To ensure selection of genuine transgenic animals, N2 and *wrn-1(tm764)* strains were crossed into the homozygous *unc-119(ed3)* background, which generated worms which were phenotypically uncoordinated. Rescue of the *unc-119* phenotype by injection of a WT *unc-119* transgene was used either solely (in *unc-119(ed3)* homozygotes and in *wrn-1(tm764);unc-119(ed3)* homozygotes to generate the appropriate control strains, AW869 and AW898, respectively) or in parallel with fosmid injection (into *wrn-1(tm764);unc-*

119(ed3) to generate the *wrn-1* rescue strain, AW931) to permit selection of transgenic worms on the basis of recovered motility. The presence of the fosmid was confirmed by PCR genotyping of *wrn-1*. Lifespan analysis at 20°C was then conducted by selecting L4 hermaphrodites (from strains AW898, AW931 and AW869) which did not display an uncoordinated phenotype. Though at least two lines were obtained for the controls and the rescued worms, only one line of each was assayed, since it is important to select lines which have a similar transmission rate. In the case of AW898, AW931, and AW869, the transmission rate was approximately 60-70%.

As demonstrated in Figure 3.7, the lifespan curve of strain AW898 (*wrn-1* mutant) is shifted to the left of the control strain, AW869. Inspection of the lifespan curve of AW898 shows that both the maximal lifespan, and the time at which fewer than 50% AW898 worms in the assay were still alive is significantly reduced (see Figure 3.7B), consistent with my earlier findings (eg Figures 3.4) that worms homozygous for *wrn-1(tm764)* are shorter lived than WT worms. However, the opposite is true for AW931. This strain represents worms homozygous for *wrn-1(tm764)* which had been co-injected with *unc-119*+ and a fosmid containing WT *wrn-1*. When the lifespan curve of AW931 is compared to that of the WT control, it is shifted to the right. Furthermore, both the maximum and median lifespans of AW931 worms were greater than those observed for the control strain, AW869 (Figure 3.7B). Therefore, *wrn-1(tm764)* homozygotes which have been co-injected with a fosmid containing WT *wrn-1* have a longer lifespan than *wrn-1(tm764)* homozygotes which have not been rescued for *wrn-1*. Significantly, the lifespan of the rescued worms was greater than that of the

control strain, suggesting that *wrn-1* overexpression may enhance longevity (see Discussion).

A

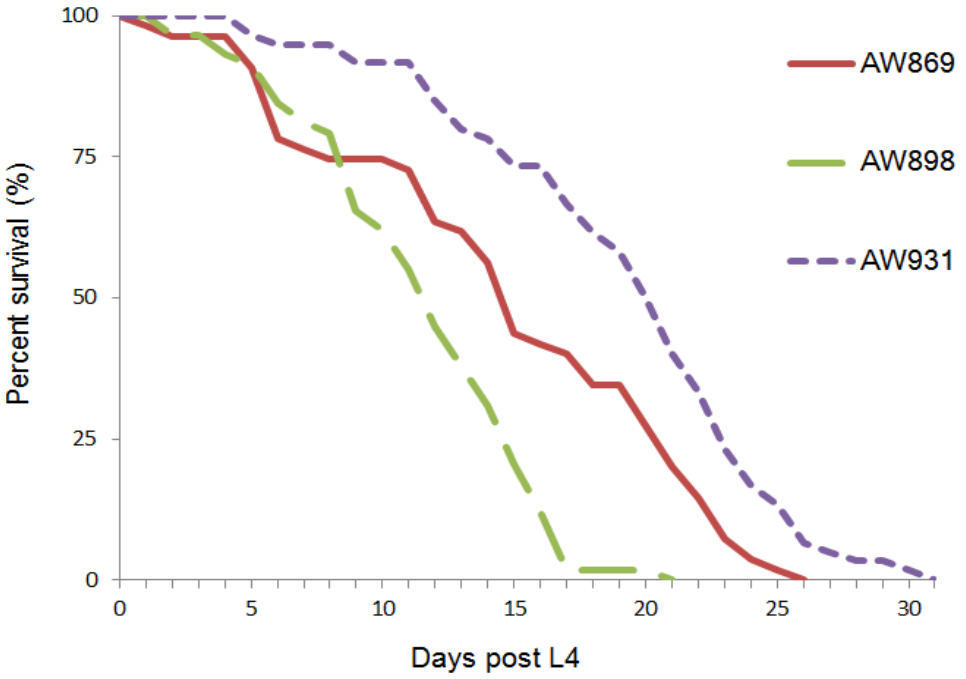

B

Strain name	Phenotype	Genotype	Maximum lifespan	50% survival	n
AW869	WT	*unc-119(ed3)IIIlouEx723[unc-119+]*	26	15	55
AW898	*wrn-1(tm764)* homozygote	*wrn-1(tm764)II;unc-119(ed3)IIIlouEx743[unc-119+]*	21	12	58
AW931	*wrn-1* rescue	*wrn-1(tm764)II;unc-119(ed3)IIIlouEx768[unc-119+ + fosmid]*	31	21	60

Figure 3.7: Multicopy *wrn-1* expression increases longevity. Adult lifespan of transgenic worms at 20°C. Lifespan survival curves: AW869 (red) represents the WT control strain, AW898 (green) represents the *wrn-1(tm764)* homozygous strain, and AW931 (purple) is essentially identical to AW898, but was co-injected with fosmid which carries a WT copy of *wrn-1*. Since transmission of the *unc-119* injection marker was not 100%, only non-uncoordinated L4 worms were used in the lifespan assay. Day 0 = day at which worms were L4. (B) Table summarising the maximal lifespan and 50% survival of each strain.

3.2.7 *wrn-1(tm764)* and *mut-7(pk204),* but not *wrn-1(gk99),* cause a reduction in brood size relative to N2

During general strain maintenance, it became apparent that *mut-7(pk204)* worms and *wrn-1(tm764)* worms had a noticeably lower brood size compared with N2 or the *wrn-1(gk99)* strain, previously characterised (Lee et al, 2004). When this observation was quantified by a standard brood size assay, the brood size of *mut-7(pk204)* was confirmed to be significantly lower ($p<0.01$) than that of N2 (Figure 3.8). In addition, *wrn-1(tm764)* worms also displayed a significantly reduced brood size relative to N2 ($p<0.01$ and $p=0.8$, respectively). However, the number of viable offspring of *wrn-1(gk99)* homozygotes was indistinguishable from N2. This is the first phenotypic difference to be reported between the two *wrn-1* alleles.

3.2.8 Germline apoptosis is increased in *wrn-1(tm764)* and *mut-7(pk204)* homozygotes, but not in *wrn-1(gk99)* homozygotes

To investigate possible causes of decreased brood size, a microscopic analysis of the gonad was conducted. In particular, I wished to establish whether an increase in germline apoptosis might contribute towards the decrease in brood size. Terminal deoxynucleotidyl transferase dUTP nick end labelling (TUNEL) was used to detect DNA fragmentation (a marker of apoptosis) in gonads isolated from worms of various genotypes. In this assay, terminal deoxynucleotidyl transferase catalyses the addition of FITC-labelled dUTP to DNA ends, such as those formed on DNA fragmentation during apoptosis.

When samples are visualised using a fluorescence microscope, cells undergoing apoptosis will be labelled green.

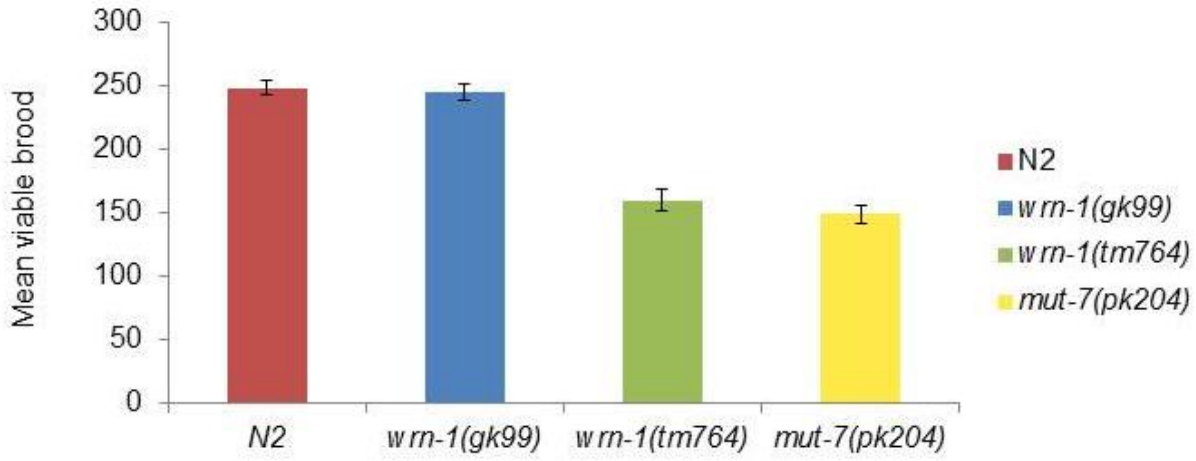

Figure 3.8: Brood size analysis in *wrn-1* and *mut-7* mutants. Average number of viable progeny of N2 (red), and worms homozygous for *wrn-1(gk99)* (blue), *wrn-1(tm764)* (green) and *mut-7(pk204)* (yellow), all maintained at 20°C. The number of viable progeny (i.e. larvae) was counted for at least 10 individual hermaphrodites for each of the four strains. The mean viable brood size for each strain was calculated and is shown ± SEM. There was no significant difference in average brood size of N2 and *wrn-1(gk99)* worms (*p=0.80*), or between *wrn-1(tm764)* and *mut-7(pk204)* mutants (*p=0.14*). However, there was a significant difference in average brood size between N2 and *wrn-1(tm764)* worms, and between N2 and *mut-7(pk204)* animals (*p<0.01*). Significance was calculated using the student t test (2 tailed).

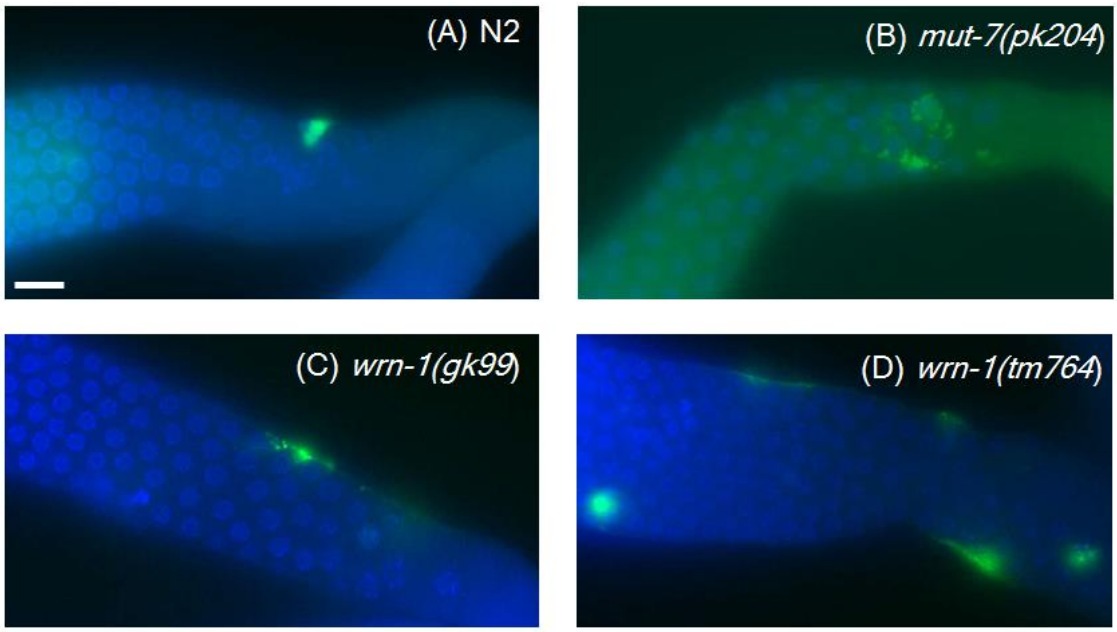

Figure 3.9: Increased germline apoptosis in *wrn-1* and *mut-7* single mutants. Representative images of germline apoptosis in dissected hermaphrodite gonads. Gonads were dissected from N2 (A*), mut-7(pk204)* (B), *wrn-1(gk99)* (C), and *wrn-1(tm764)* (D) homozygotes. TUNEL staining (green) was used to identify apoptotic nuclei. DNA was stained with DAPI (blue). Scale bar = 10µm.

As shown in Figure 3.9, low level TUNEL staining (i.e. on average, one or two green nuclei per gonad arm, as seen in panel A) was detected in dissected N2 hermaphrodite gonads, indicating a low level of apoptosis in the loop region of the gonad arm in N2 worms, which is expected under normal growth conditions. This low level of apoptosis is likely to be physiological germ cell apoptosis, which occurs in the absence of any known stress (Gumienny et al, 1999; Lettre & Hengartner, 2006). Dissected gonads from hermaphrodites homozygous for either *wrn-1(tm764)* or *mut-7(pk204)* showed more TUNEL-positive nuclei than N2 worms (Figure 3.9, panels B and D, respectively), whilst the number of TUNEL positive nuclei detected in gonads dissected form *wrn-1(gk99)* homozygotes was similar to that observed in N2 gonads (Figure 3.9, panel C). Therefore, *wrn-1(gk99)* homozygotes display normal levels of apoptosis. When comparing the extent of apoptosis (Figure 3.9) with brood size (Figure 3.8), an inverse correlation can be detected, suggesting that the lower brood size of *wrn-1(tm764)* and *mut-7(pk204)* worms may result from apoptotic loss of meiotic nuclei in the gonad prior to formation of functional oocytes. It is of note that *wrn-1(gk99)* and *wrn-1(tm764)* show such marked differences in brood size and levels of apoptosis. Potential causes of apoptosis (e.g. physiological versus DNA-damage induced) are discussed in more detail in Chapter 4.

3.2.9 Differential sensitivity of mutant worms to camptothecin

A hallmark feature of WS patient-derived cells is their hypersensitivity to specific DNA damaging agents. In particular, human WS fibroblasts (Bird et al, 2013) and lymphoblastoid cells (Poot et al, 1999) are hypersensitive to

camptothecin (CPT), a topoisomerase I inhibitor. CPT prevents DNA religation following the formation of a DNA nick by topoisomerase I. This in itself causes DNA damage (single strand breaks), though the toxicity of CPT is considered to be the result of a replication fork colliding with the cleavage complex (CPT-DNA-Topo I), thus converting the single stranded nick to a double-strand break during S-phase of the cell cycle (Squires et al, 1991).

In order to assess the sensitivity of worms to camptothecin, I measured the brood size of animals treated with this genotoxic agent and compared that to the brood size of untreated worms. When N2 and *wrn-1(gk99)* worms were treated with 0.15 mM CPT, the average brood size of these strains dropped approximately 31% and 23% respectively (Figure 3.10), indicative of a normal response to significant DNA damage in the gonad. While CPT significantly reduced brood size in both these strains ($p<0.01$ for treated compared with untreated), there was no significant effect of the *gk99* allele compared with WT on either the normal brood size or its response to CPT ($p=0.28$). Remarkably, CPT treatment had no further effect on the already low brood size of *wrn-1(tm764) worms* ($p=0.71$); the brood size of untreated *wrn-1(tm764)* worms was very similar to that post-treatment of N2 and *wrn-1(gk99)* (Figure 3.10). This may indicate that *wrn-1(tm764)* worms already experience high intrinsic levels of DNA damage that are not further exacerbated by CPT. In contrast, *mut-7(pk204)* worms appear hypersensitive to CPT treatment, with a drop in average brood size of 59% ($p<0.01$). This is consistent with the hypersensitivity of *Drosophila WRNexo* mutants to CPT (Saunders et al, 2008).

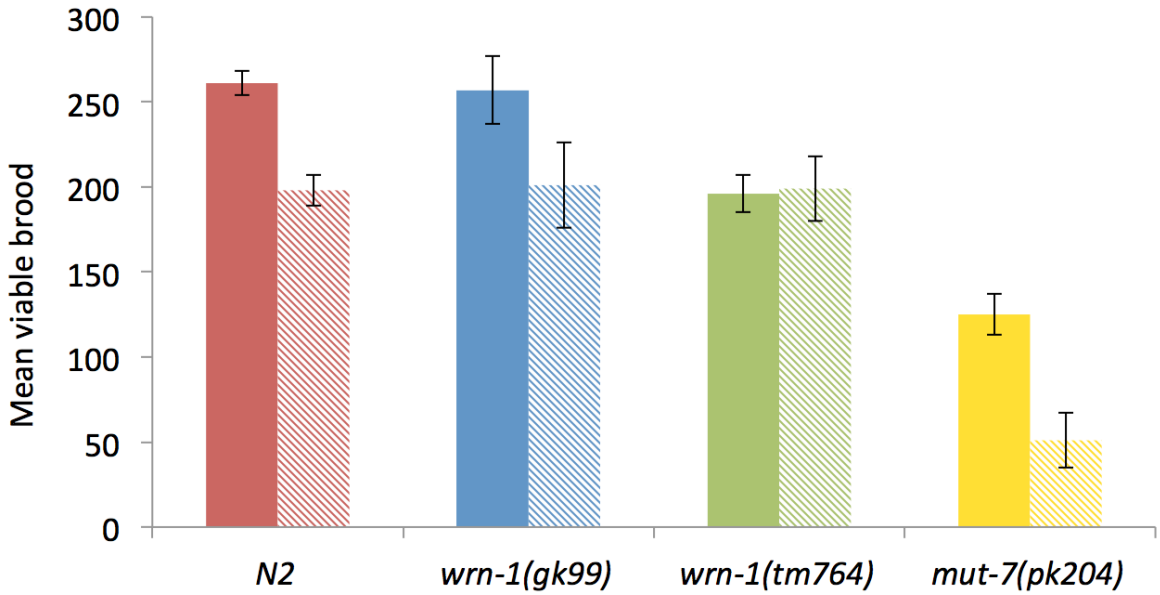

Figure 3.10: CPT sensitivity of *wrn-1* and *mut-7* homozygotes and N2 control worms. Average brood size of hermaphrodite worms maintained at 20°C was used as a read-out of CPT sensitivity. The number of viable progeny of N2 (red), *wrn-1(gk99)* (blue), *wrn-1(tm764)* (green), and *mut-7(pk204)* (yellow) was counted for hermaphrodites which had been incubated with 0.15mM CPT (dashed bars) or DMSO control (solid bars) for two hours at the L4 stage. The number of viable progeny was counted for 20 worms per strain per condition; mean brood sizes per worm are shown ± SEM.

3.2.10 Analysis of *wrn-1;mut-7* double mutants

Having established that *wrn-1* and *mut-7* single mutants have phenotypes reminiscent of WRN mutations in other systems, double mutants consisting of *mut-7(pk204)* in combination with either *wrn-1(gk99)* or *wrn-1(tm764)* were generated to more closely recapitulate human WS by loss of both WRN helicase and putative exonuclease activities. Since I had already shown that mutation of either *wrn-1* or *mut-7* was detrimental to *C. elegans* lifespan (Figure 3.4), double mutants were predicted to be even less viable, possibly even difficult to generate. By contrast however, double mutants were generated surprisingly easily. I originally came to select double homozygous animals from *wrn-1/wrn-1;unc-32 dpy-18/mut-7* animals (see section 2.3.4 and figure 2.1) having neglected the crosses over a holiday period. I expected not to be able to easily recover double homozygous mutants. However, these were markedly over-represented in the population, suggesting some possible selective advantage in being homozygous for both mutations. This is an anecdotal observation, however, and was not robustly quantified. PCR genotyping was performed to verify that these fitter strains did indeed carry mutant alleles for both *wrn-1* and *mut*-7. My next experiments revolved around phenotypic analysis of these double mutants.

3.2.11 Lifespan analysis of *wrn-1;mut-7* double mutants

In order to ascertain the effect of double mutation of both *wrn-1* and *mut-7* on lifespan at 20°C, *wrn-1;mut-7* homozygous mutant hermaphrodites were assayed each day post L4 for survival. Figure 3.11 shows the survival curve for *wrn-1(gk99);mut-7(pk204)* and *wrn-1(tm764);mut-7(pk204)* double mutant strains (dark blue and dark green lines, respectively), compared with *wrn-1* and *mut-7* single mutants, and N2 control worms. As shown in Figure 3.11, the maximal life span of the double *wrn-1;mut-7* mutants was reduced compared to N2, as indicated by a shift to the left of the survival curves relative to that of N2. However, the 50% survival was intermediate between that of the single mutants and N2 worms.

3.2.12 Brood size analysis for *wrn-1;mut-7* double mutants

Since double *wrn-1;mut-7* mutants show enhanced lifespan compared with the single mutants (Figure 3.11 above), it was important to assess whether this was also reflected in other readouts of fitness. I therefore measured brood size of the double mutants (Figure 3.12). Both double mutants (dark blue and dark green bars) showed a similar reduction in brood size to each other, though the brood size was significantly higher than for the *mut-7(pk204)* single mutants ($p<0.01$). Interestingly, mutation of *mut-7* in a *wrn-1(gk99)* background was significantly detrimental to brood size compared with *wrn-1(gk99)* single mutants ($p<0.01$), but conversely, beneficial when compared with *mut-7(pk204)* alone. The average brood size of *wrn-1(gk99);mut-7(pk204)* and *wrn-*

1(tm764);mut-7(pk204) was not significantly different from that of *wrn-1(tm764)* single mutants (*p = 0.69* and *0.13*, respectively).

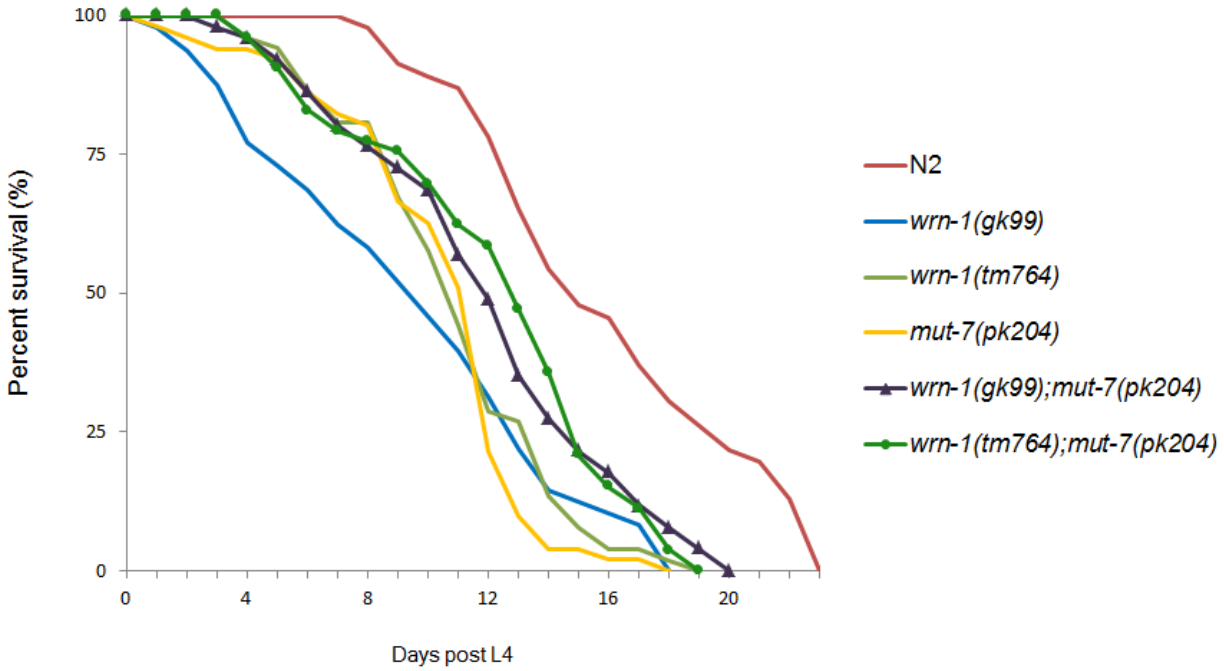

Strain	Maximum life span	Day at <50% survival	*n*
N2	24	16	54
wrn-1(gk99)	19	11	48
wrn-1(tm764)	20	12	52
mut-7(pk204)	19	12	55
wrn-1(gk99);mut-7(pk204)	21	13	51
wrn-1(tm764);mut-1(pk204)	20	14	53

Figure 3.11: Adult lifespan of homozygous single and double *wrn-1* and *mut-7* mutants, and of N2 control worms, at 20°C. (A) Lifespan curves, plotted as % of animals alive at each day post-L4. Red = N2 (WT control). Light blue = *wrn-1(gk99)*. Light green = *wrn-1(tm764).* Yellow e = *mut-7(pk204).* Dark blue = *wrn-1(gk99);mut-7(pk204).* Dark green = *wrn-1(tm764);mut-7(pk204).* Day 0 = the day at which worms were L4. (B) Median (50% survival) and maximal lifespans and n values for strains shown in (A).

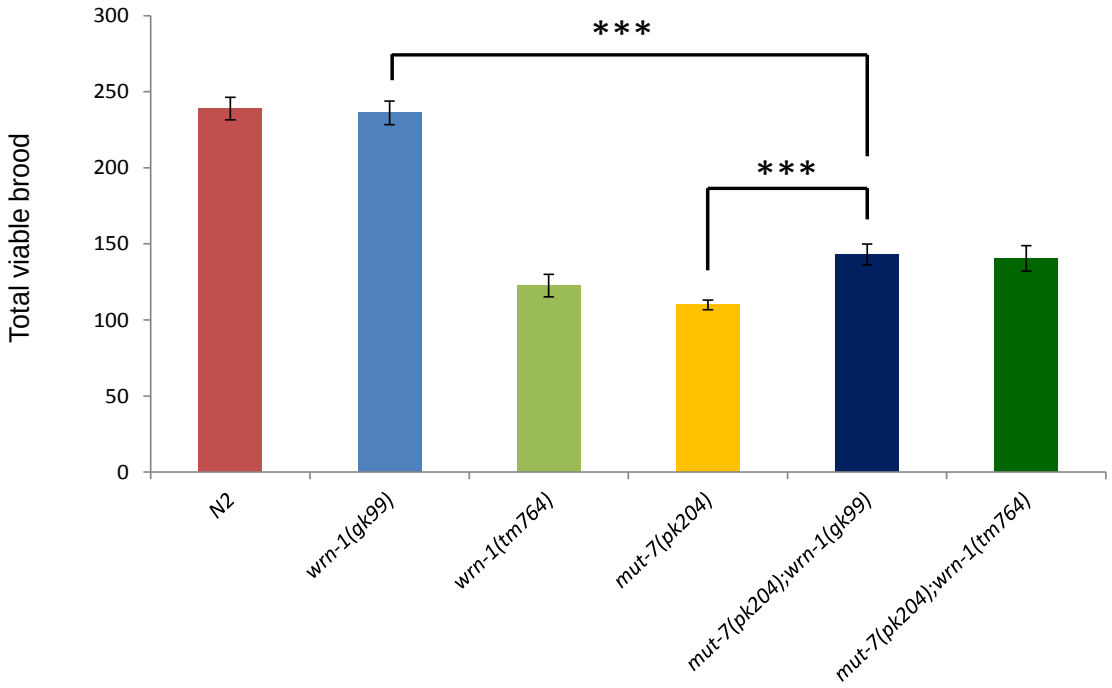

Figure 3.12: Decreased brood size in *wrn-1;mut-7* double mutants. The number of viable progeny (i.e. larvae) was counted for at least 10 individual hermaphrodites of each strain and averaged to give the mean brood size. Mean brood size ± SEM is shown for N2 (red), *wrn-1(gk99)* (blue), *wrn-1(tm764)* (green), *mut-7(pk204)* (yellow), *wrn-1(gk99);mut-7(pk204)* (dark blue) and *wrn-1(tm764);mut-7(pk204)* (dark green). Significance was calculated using student t test (2 tailed) where *** represents p<0.01.

3.2.13 Both *wrn-1(gk99);mut-7(pk204)* and *wrn-1(tm764);mut-7(pk204)* double mutants display elevated germline apoptosis

Although the brood size of *wrn-1:mut-7* double mutants was higher than that of *mut-7(pk204)* or *wrn-1(tm764)* single mutants, brood size was still lower than N2 (Figure 3.12). As I had previously found that decreased brood size in the *wrn-1(tm764)* and *mut-7(pk204)* single mutants correlated with increased germ line apoptosis (Figures 3.8 and 3.9), it was therefore important to test whether the slight decrease in brood size of the *wrn-1;mut-7* double mutants was a result of excessive germline apoptosis. Once again, the TUNEL method was employed. As illustrated in Figure 3.13, both *wrn-1(gk99);mut-7(pk204)* and *wrn-1(tm764);mut-7(pk204)* double mutants displayed an increased number of TUNEL-labelled (green) nuclei in gonads dissected from hermaphrodites (panels C and D, respectively), compared to the number seen in N2 worms (panel A). Therefore, *wrn-1;mut-7* double homozygous mutants have elevated levels of germline apoptosis in comparison to N2 worms, as assayed by TUNEL.

Apoptosis can also be identified by the appearance of ‘button’ like nuclei which appear to stick out from the plane of view under Nomarski optics. In Figure 3.13, one of these ‘button’ nuclei can be seen in the N2 gonad (arrow, panel A’), whilst many more are observed in *wrn-1(gk99);mut-7(pk204)* worms (arrows, panel C’). The same was also true for *wrn-1(tm764);mut-7(pk204)* worms (data not shown). Therefore, the apparently wild type level of apoptosis seen in *wrn-1(gk99)* worms (panel C, Figure 3.9) is increased by the presence

of *mut-7(pk204),* in the *wrn-1(gk99);mut-7(pk204)* double mutant (panel C and C', Figure 3.13).

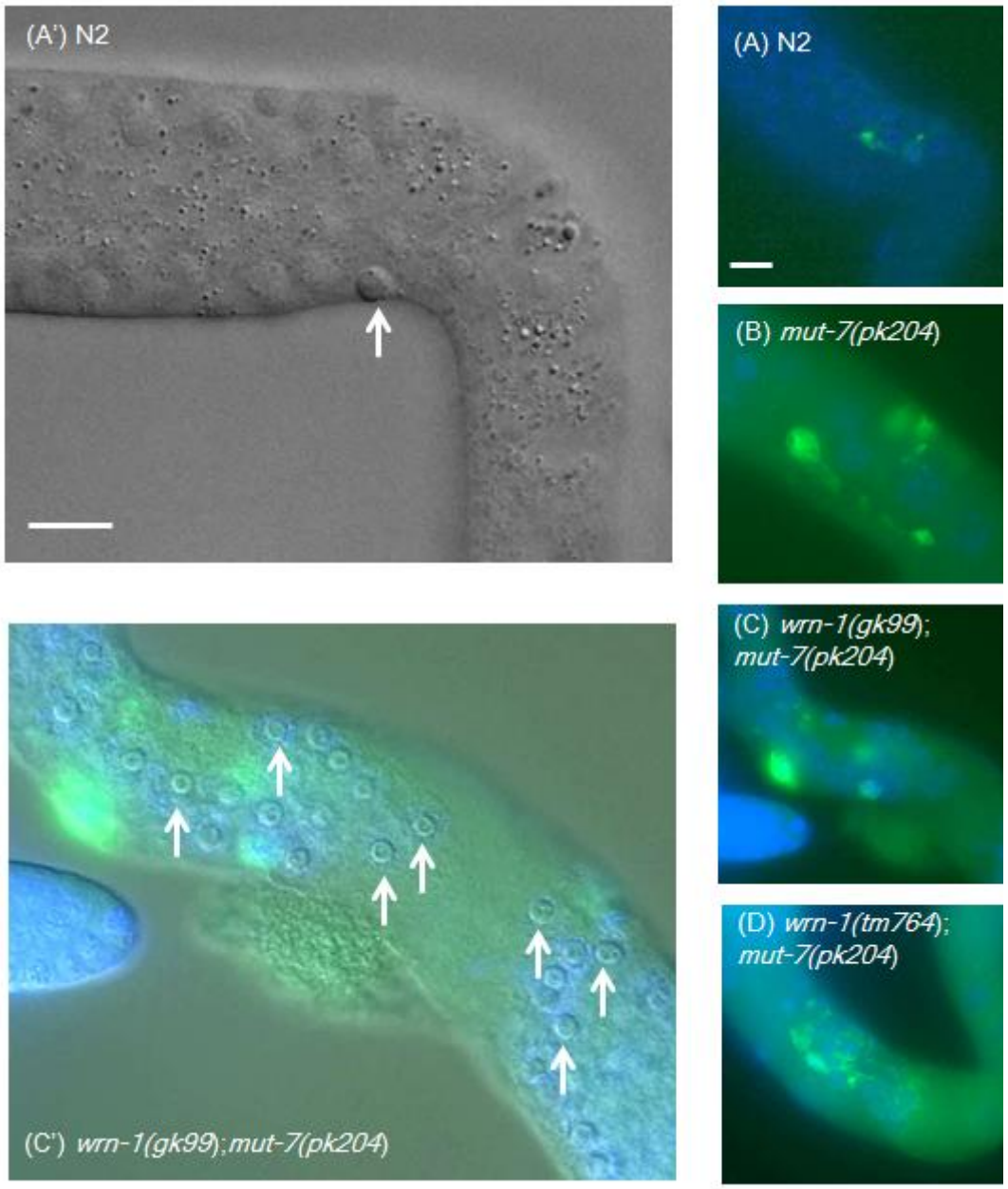

Figure 3.13: Germline apoptosis in *wrn-1;mut-7* double mutants. Representative Nomarski and fluorescence microscopy images of germline apoptosis in dissected hermaphrodite gonads. Gonads were dissected from N2 (A and A'*),* or worms homozygous for the following mutations*: mut-7(pk204)* (B), *wrn-1(gk99);mut7(pk204)* (C and C'); *wrn-1(tm764);mut-7(pk204)* (D). TUNEL staining (green) was used to identify apoptotic nuclei and DNA was counterstained with DAPI (blue). (For images of single mutants *wrn-1(tm764)* and *wrn-1(gk99)*, see Figure 3.9). Arrow heads indicate 'button nuclei', which, in addition to the appearance of TUNEL stain, also mark cell death and can be used as an alternative or additional measure of germline apoptosis. Note that in

panel C', for simplicity only a subset of 'button nuclei' are highlighted with arrows. Scale bar = 10µm.

3.2.14 *wrn-1;mut-7* double mutants are insensitive to CPT treatment

Since all three single mutants showed differing sensitivities to CPT treatment when brood size was assayed (Figure 3.8 above), it was necessary to ask what the sensitivity of the *wrn-1;mut-7* double mutants would be. Therefore, the CPT sensitivity of the double mutants was assayed at the same time as the single mutants and N2 control worms. Again, the total number of viable progeny with and without CPT treatment was used as a measure of CPT sensitivity.

Analysis of the sensitivity of the *wrn-1;mut-7* double mutants to CPT revealed a somewhat unexpected result (Figure 3.14). Though *mut-7(pk204)* confers hypersensitivity to the topoisomerase I inhibitor CPT when in an otherwise WT background (yellow bars, Figure 3.14), sensitivity is lost and no decrease in brood size is observed when it is combined with either of the *wrn-1* alleles (dark blue bars - *wrn-1(gk99);mut-7(pk204) p=0.74*, and dark green bars – *wrn-1(tm764);mut-7(pk204) p=0.90*). This may not seem so surprising in the case of *wrn-1(tm764);mut-7(pk204),* given that *wrn-1(tm764)* on its own is insensitive to the treatment (light green bars, Figure 3.14), but neither *wrn-1(gk99)* or *mut-7(pk204)* single mutants show insensitivity. This suggests that *wrn-1(tm764)* individually, or the combined loss of both WRN homologues confers the insensitivity.

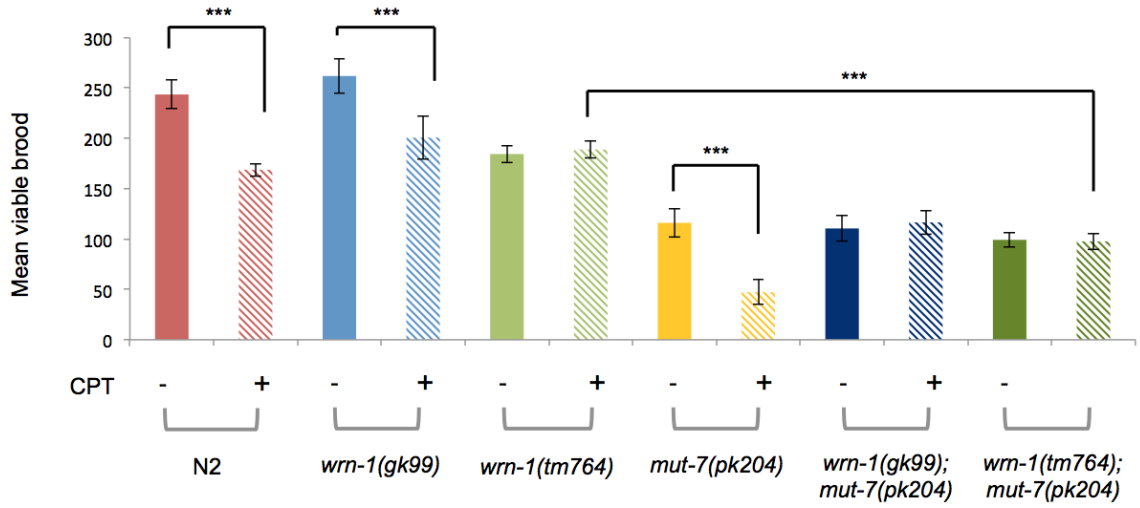

Figure 3.14: CPT sensitivity of *wrn-1* and *mut-7* single and double homozygotes. Average brood size of hermaphrodite worms maintained at 20°C was used as a read-out of CPT sensitivity. The number of viable progeny of N2 (red bars), *wrn-1(gk99)* (blue bars), *wrn-1(tm764)* (green bars), *mut-7(pk204)* (yellow), *wrn-1(gk99);mut-7(pk204)* (dark blue bars) and *wrn-1(tm764);mut-7(pk204)* (dark green bars) was counted for hermaphrodites which had been incubated with 0.15mM CPT (dashed bars) or DMSO vehicle control (solid bars) for two hours at the L4 stage. The number of viable progeny was counted for 20 worms per strain per condition; mean brood sizes are shown ± SEM.

3.3 Discussion

C. elegans provides an excellent model for the study of ageing. Besides the short life span, quick reproductive cycle, ease of genetics and isogenic nature of this nematode, the greatest asset of the model for studying WS is the fact that the genome of *C. elegans* encodes putative orthologues of both the hWRN helicase and exonuclease activities. Furthermore, since they are encoded by separate genes, (helicase by *wrn-1* and exonuclease by either *mut-7* or possibly *ZK1098.3*), this permits the evaluation of loss of either one of these genes, or both in combination – something which many existing WS models lack.

3.3.1 *wrn-1* and *mut-7* are both required for normal lifespan regulation

Comparative bioinformatics confirms previous reports that *wrn-1* and *mut-7* are hWRN homologues (Ketting et al, 1999; Lee et al, 2004), and this is bolstered by phenotypic evidence presented here, notably the premature ageing phenotypes and reduced lifespan of the mutants. The *wrn-1* single mutants, *wrn-1(gk99)* and *wrn-1(tm764)* represent an allelic series which can be used to dissect the contributions made by the RecQ helicase activity and by other domains present in WRN-1. This further confirms that *C. elegans* can be used as a good model of WS and that conclusions drawn from experiments in this system should be relevant to human WS and normal ageing alike.

Furthermore, being able to study the single mutants and the double mutants separately has revealed previously unappreciated differences between the exonuclease and helicase components. While mutation of either *wrn-1* or *mut-7* reduces lifespan, simultaneous mutation of these genes appears to be less detrimental – the lifespan of *wrn-1;mut-7* double mutants is intermediate between that of WT (N2) and either single mutant. At first this may seem counterintuitive – one might expect the combination of two mutations, which individually decrease median lifespan, to show an even more severe reduction of median lifespan. However, the apparent improvement could be reconciled if the effects of the loss of *wrn-1* and/or *mut-7* are considered. Since we expect *wrn-1* and *mut-7* to act in the same pathway (since hWRN exonuclease and helicase activities display coordinated activity (Opresko et al, 2001), loss of one of these components could result in a partially functioning pathway. Perhaps this partially functioning pathway causes the worm problems simply by running at low capacity or efficiency, by generating a substrate or complex that is in some way toxic to the cell, or by perturbing homeostasis, thus resulting in a decrease in median life span. However, if both components are lost (as in the case of *wrn-1;mut-7* double mutants), then the dysfunctional pathway becomes completely non-functional. Complete loss of a biologically important pathway would be expected to have some negative impact to the worm (in this case, a decrease in median life span) but perhaps not such a negative impact as partial loss, since a parallel redundant pathway could take over (for instance, one involving one of the other three RecQ homologues). Moreover, loss of an entire pathway may not result in as toxic lesions as those generated by a dysfunctional pathway. There is precedence for this. For example, loss of

53PB1 rescues BRCA1 deficiency in mouse embryonic stem cells, even though both mutations are deleterious by themselves (Bouwman et al, 2010), and chemical inhibition of NAT10 can correct defects associated with mutation of *LMNA* in cells derived from Hutchinson-Gilford progeria patients (Larrieu et al, 2014).

The less severe phenotype of the *wrn-1;mut-7* double mutant worms makes sense of the striking observation that the double mutants were surprisingly easy to recover from overgrown crosses. This, like the lifespan data implies that the double mutants are more viable than *wrn-1* or *mut-7* single mutants.

3.3.2 *wrn-1* appears to be a bona fide anti-gerontogene

Interestingly, transgenic expression of *wrn-1* by injection of a fosmid containing WT *wrn-1* was not only able to rescue the reduced lifespan of *wrn-1(tm764)* homozygotes, but actually increased the lifespan (both the maximum and the median lifespan) of these worms, beyond that of WT controls (Figure 3.7). Since transgenic worms produced by microinjection usually carry large extrachromosomal arrays that contain many copies of the injected DNA, and the lines used had a transmission rate of approximately 60-70%, *wrn-1* may be over-expressed in the rescued strain and this might account for the increased lifespan. If this is true, then the level of *wrn-1* expression appears to be important for longevity and would suggest that *wrn-1* is a true anti-gerontogene, not only limiting lifespan when it is mutated, but increasing it when it is over-expressed. It remains to be verified whether *wrn-1* is indeed over-expressed in these worms. Intriguingly, if *wrn-1* over-expression is the cause of the observed

longevity, then WT *wrn-1* expression in the germline is unlikely to be required, since repetitive arrays are strongly silenced in germ line nuclei (Kelly et al, 1997). It is important to note that these experiments were performed with a fosmid. The reason for this was the complex genomic structure of *wrn-1,* which is part of an operon (*CEOP2250*). This makes it very difficult to predict the important regulatory regions required for stable gene expression. Therefore, at this stage I cannot exclude the possibility that some other gene function on the fosmid contributes to the longevity phenotype.

3.3.3 Exogenous DNA damage sensitivity in double versus single mutants

While mutation of WRN exonuclease has been shown to result in hypersensitivity to the topoisomerase I inhibitor camptothecin (CPT) in flies (Saunders et al, 2008), it was unknown what the effect of mutating WRN helicase would be. In this *C.elegans* model of WS, mutation of *mut-7*, like that of DmWRNexo, also results in hypersensitivity to CPT. However, helicase *wrn-1(tm764)* mutants display insensitivity to CPT, which is also true of *wrn-1;mut-7* double mutants (Figure 3.14). This finding reinforces the hypothesis concerning partial biochemical pathways impacting on lifespan but provides more direct biochemical clues suggesting that the WRN helicase may unwind CPT-collapsed forks back, allowing exonuclease cleavage and resection. Without exonuclease activity, the resected fork may be toxic, while without the helicase activity an alternative pathway of homologous recombination or translesion synthesis may avoid toxicity.

3.3.4 Is the reduced brood size of *wrn-1* and *mut-7* single and double mutants indicative of endogenous DNA damage?

Even in the absence of exogenous DNA damage, *wrn-1(tm764)* and *mut-7(pk204)* mutants display a reduced brood size. There can be a number of reasons for a reduced brood size. Given that hWRN is known to be required to maintain genome stability, it is possible that in *wrn-1(tm764)* and *mut-7(pk204)* worms there is pronounced genomic instability caused by the mutation of these WRN homologues. Indeed, transposition has been reported in *mut-7(pk204)* strains, which leads to genomic instability in these worms (Ketting et al, 1999). Elevated germline apoptosis, as I found in *wrn-1(tm764)* and *mut-7(pk204)* mutants (Figure 3.9 and 3.13), would be an expected response to genomic instability, and this is further investigated in Chapter 4.

Genomic instability would be highly detrimental to the germline if left unchecked, and various mechanisms are in place to ensure fidelity is maintained. For instance, DNA damage signalling can lead to the induction of cell cycle arrest whilst damage is repaired, or in more severe cases it can induce apoptosis (Gartner et al, 2000). Both of these mechanisms would ensure that genomic errors are not passed on to the next generation. Genomic stability in *wrn-1* and *mut-7* mutants is investigated in Chapter 4.

Though both *wrn-1(gk99)* and *wrn-1(tm764)* display a reduced lifespan and premature ageing, they differ in brood size, the level of germline apoptosis, and sensitivity to CPT. The phenotypic differences observed for the two *wrn-1* alleles can help to tease apart the functional importance/requirements of the

RecQ helicase activity and other domains of WRN-1 in various aspects of ageing and DNA metabolism. These allelic differences are explored further in subsequent chapters.

3.3.5 Lifespan effects of *wrn-1* mutation appear to be highly context dependent

The lifespan of *wrn-1(tm764)* homozygotes is greatly extended upon treatment with FUdR, and this correlates with improvements in other readouts of ageing. The effect of FUdR on the lifespan of *wrn-1(tm764)* could prove to be informative in terms of ascertaining the function of *wrn-1* in lifespan regulation, since the effect of FUdR on lifespan probably defines another ageing pathway which should be analysed. In fact, several other studies have confirmed that at certain concentrations, FUdR can have an effect on lifespan. For instance, the lifespan of mutant *tub-1* (Aitlhadj & Sturzenbaum, 2010) and *gas-1* (Van Raamsdonk & Hekimi, 2011) worms is significantly increased in the presence of FUdR. Therefore it is likely that FUdR can alter different lifespan-determining signalling pathways, and current research has begun to shed light onto the mechanism behind the lifespan extending effects of FUdR (Angeli et al, 2013; Feldman et al, 2014). It is intriguing that the lifespan curves of *wrn-1(tm764)* mutant grown in the presence and absence of FUdR appear very similar for the decline in survival of the first ~50% of the populations examined, but diverge after this (see Figure 3.6). The difference if the shape of these survival curves may point towards a mechanism which influences ageing. For instance, it seems plausible that FUdR may act on one or several pathway(s) or processes which have little impact on young adults but become important to worms in late

life. Very recently, it has been demonstrated that FUdR converges on alternative regulatory signals that modulate *C. elegans* proteostasis capacity – in the presence of FUdR, effective induction of heat shock response is maintained during adulthood, and protein folding capacity is also improved (Feldman et al, 2014). Another study by Lithgow et al (Angeli et al, 2013) revealed that FUdR not only improves homeostasis but also stress resistance and healthspan in WT worms, and these effects are independent of DAF-16, DAF-12, and HSF-1 pathways, but dependent on FEM-3, implying that inhibition of oocyte production can improve protein homeostasis in *C. elegans.* In light of these recent studies, the late-life benefit of FUdR to the longevity of *wrn-1(tm764)* mutants may be attributed to improved protein homeostasis, which further implies that protein homeostasis is compromised in these mutants under standard conditions, and this becomes particularly detrimental in later-life.

Not only did the FUdR result dictate how future lifespan experiments were to be performed, it also demonstrated that the lifespan of *wrn-1(tm764)* worms could be drastically altered by a single intervention. This, combined with the small, but significant increase in the median lifespan of *wrn-1(tm764);mut-7(pk204)* double mutants relative to *wrn-1(tm764)* single mutants suggests that the outcome of *wrn-1* mutation on ageing may be context dependent. This avenue will be explored in later chapters.

Chapter 4 - The impact of *wrn-1*, *mut-7*, and *cep-1* mutation on genomic stability.

4.1 Introduction

4.1.1. Genome instability in Werner syndrome

Human WRN protein is intimately involved in all aspects of DNA metabolism, including replication, recombination, repair, telomere maintenance and transcription. Cell culture studies have suggested that loss of WRN results in problems with non-homologous end-joining (Oshima et al, 2002), base excision repair (Harrigan et al, 2006), errors in homologous recombination (Saintigny et al, 2002), and problems with maintaining processive replication fork progression (Rodriguez-Lopez et al, 2002). This has been reinforced by *in vitro* studies with purified WRN, showing helicase and exonuclease activity on DNA structures implicated in various aspects of DNA transactions (Table 4.1). On the basis of these *in vitro* and cell-based studies, different roles have been ascribed to the helicase and exonuclease activities of WRN, for example requiring that the helicase unwinds duplex DNA past a lesion to allow exonuclease cleavage (eg at a replication fork) (Rodriguez-Lopez et al, 2002; Rodriguez-Lopez et al, 2007; Sidorova, 2008; Sidorova et al, 2013; Sidorova et al, 2008), or branch migration via helicase activity in Holliday junction resolution through non-recombinational pathways (Saintigny et al, 2002). It is likely that both helicase and exonuclease act in concert (though possibly sequentially) in mammalian cells (Opresko et al, 2001; Opresko et al, 2004).

WRN helicase substrates	WRN exonuclease substrates
3'-recessed duplex	3'-recessed duplex
Bubble duplex	Bubble duplex
D-loop duplex	D-loop duplex
Duplex with a 5'-flap	
Forked duplex	
G-quadruplex	
Holliday junction	Holliday junction
Partial duplex	
Triplex	
NOT blunt duplex	
NOT 5'-recessed duplex	
	Looped duplex
	Nicked loop duplex

Table 4.1: WRN *in vitro* substrates. WRN helicase and exonuclease have been shown *in vitro* to possess substrate specificity towards DNA structures listed above.

Given the pleotropic nature of WRN and the critical processes in which it acts, it is not surprising that loss of function of the protein, as in progeroid human Werner syndrome, results in marked genome instability, characterised in patient cells as high levels of chromosomal translation and extensive deletions, leading to a high incidence of cancer in WS patients (Goto et al, 1996). Indeed, WRN

has been classified as a gatekeeper tumour suppressor (Chu & Hickson, 2009; Hickson, 2003; Kinzler & Vogelstein, 1997), presumably acting either to prevent the formation of deleterious DNA structures that predispose to instability or to remove them once formed. In this chapter, I sought to examine whether WRN-1 and/or MUT-7 regulate genome stability, and if so, to start to probe possible mechanisms by which they may act.

4.1.2 *wrn-1* and DNA damage

While there is little published literature on the role of C. elegans wrn-1 in genome stability, one report suggests that it is involved in instigating a mitotic checkpoint in response to replication stress (e.g. hydroxyurea treatment), and that it also functions in the DNA damage response (DRR) in a signalling pathway involving ATL-1 (ATR homologue) in the intra-S phase checkpoint, and upstream of ATM-1 and RPA-1 in response to IR-induced DNA damage (Lee et al, 2010a). This report conflicts to some extent with what is known for human WRN (e.g. WRN is thought to act downstream of ATM/R signalling), though it has been reported to complex with the proteins in a ‘ménage a trois’ with MRN (Cheng et al, 2004; Pichierri et al, 2012) and is implicated not only in dealing with problems during DNA replication ((Rodriguez-Lopez et al, 2002; Sidorova et al, 2008) but also in checkpoint response. It is therefore important to reassess the importance of WRN-1 in genome stability in the worm, especially as I have developed a model which allows me to study the impact of loss of function of either the helicase (WRN-1) or the nuclease (MUT-7) or both together (see chapter 3).

4.1.3 Biology of the *C. elegans* germline

Since the somatic tissue of an adult worm is post-mitotic, DNA damage checkpoints function specifically in the germline. It is imperative that genome integrity is maintained in the germline, since this is the immortal cell lineage which is passed on from one generation to the next. Thus, defects in DNA repair, apoptosis, cell cycle arrest and other DNA damage checkpoint signalling pathways will result in germline aberrations, which are likely to have detectable phenotypic effects (Craig et al, 2012; Gartner et al, 2004; Sakashita et al, 2010).

The reproductive system of *C. elegans* is made up of three major components: the egg-laying apparatus, the somatic gonad, and the germline (figure 4.1, and see www.wormatlas.org). Together, the somatic gonad and the germline form two symmetrical U-shaped tubes or arms. These share the egg laying apparatus. *C. elegans* hermaphrodites produce both oocytes and sperm. Though sperm are only produced during larval stage L4, oocytes are produced throughout the adult life of the worm, and gamete precursors are organised both spatially and temporally along the gonad arm. This distal-proximal polarity begins with a population of mitotic stem cells at the distal tip ((a) in Figure 4.1), which migrate proximally along the gonad arm, progressing through successive stages of meiotic prophase I until they arrest at diakinesis ((e) in Figure 4.1). This is the point at which gametogenesis occurs, and individual oocytes can be seen past the loop region, in the proximal end of the gonad arm. Germ cells in the distal region have incomplete borders and are syncytial, sharing the central canal (rachis), but cellularisation is complete at gametogenesis.

Germline nuclei can be visualised directly by staining fixed dissected gonads with 4',6-diamidino-2-phenylindole (DAPI), as demonstrated in Figure 4.1. Mitotic nuclei are of similar size and appearance to each other, with relatively diffuse chromatin and slightly brighter DAPI staining at the periphery (panel a). The zone of mitosis extends for typically 20 cells, and at any one time, about 1-2 nuclei in this zone appear as mitotic (M)-bodied which are easily distinguished from other mitotic nuclei by their highly condensed chromatin. As these mitotic cells progress proximally along the gonad arm, they move away from the influence of the distal tip cell (DTC, marked by * in figure 4.1), which blocks entry into meiosis via expression of LAG-2. Once beyond DTC signalling, the mitotic nuclei then transition into the early phases of meiosis I. Nuclei in the transition zone can also be distinguished from mitotic nuclei using DAPI, as they show crescent-shaped staining of condensed DNA (panel b). As nuclei progress more proximally, they grow in size and show a characteristic 'bowl of spaghetti' staining pattern, indicative of homologous chromosomes undergoing synapsis during the pachytene stage (panel c). At the loop region (indicated by the blue curve in figure 4.1), a subset of pachytene nuclei undergo apoptosis, while survivors progress into diplotene stage of meiosis (d) and line up in the proximal arm of the gonad. Here the nuclei advance into diakinesis and at this stage six pairs of highly condensed meiotic chromosomes can be seen (panel e). Oocytes remain arrested until maturation occurs; they can then be fertilised as they are pulled into the spermatheca and complete meiosis. Eggshell secretion commences and the embryo then passes to the uterus where it can be released via the vulva.

Thus, the spatial organisation of the worm germline and its experimental accessibility (e.g. to allow DNA staining), permits examination not only of various stages of mitosis and meiosis, but also of chromosomal complement and integrity - under normal conditions in WT and mutant worms, and after genotoxic insult (Craig et al, 2012; Gartner et al, 2004; Sakashita et al, 2010).

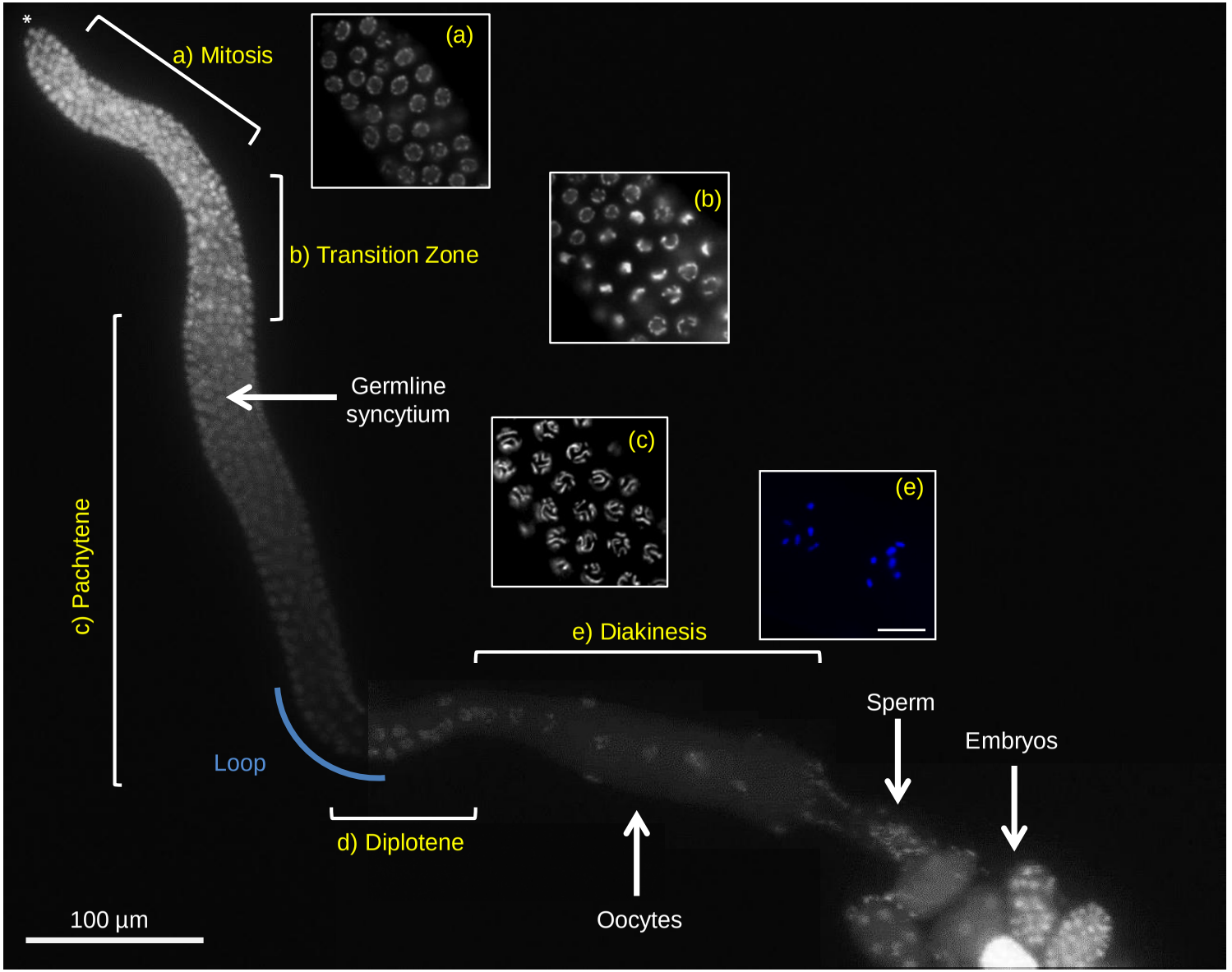
*
a) Mitosis
(a)
b) Transition Zone
(b)
Germline
syncytium
(c)
(e)
c) Pachytene
e) Diakinesis
Sperm
Embryos
Loop
d) Diplotene
100 µm
Oocytes

Figure 4.1: Organisation of the adult *C. elegans* hermaphrodite germline, as revealed by DAPI staining. Germline nuclei are arranged in a well-defined temporal/spatial gradient in the germline syncytium. Changes in organisation and appearance of DAPI-stained chromosomes allow for identification of these stages. At the distal tip of the gonad arm, nuclei undergo mitotic proliferation (a). As nuclei leave the influence of the distal tip cell (indicated by *), they enter meiosis in the transition zone region (b). Nuclei in the transition zone correspond to the leptotene and zygotene stages of meiosis, where homologous chromosomes begin to pair. Here they also acquire polarised organisation within the nuclei, creating a crescent-like appearance of DAPI signal (b – see close-up panel). Nuclei then progress into pachytene (c), where chromosomes re-disperse throughout the nuclei and homologues become fully paired and aligned (synapsis). This gives the characteristic 'bowl of spaghetti' appearance to the DAPI signal (see panel c). Apoptosis of pachytene nuclei occurs in the loop region (blue), and surviving nuclei progress to diplotene (d) and then into diakinesis, during which time the nuclear volume increases, oocytes become cellularised, and chromosomes condense. At diakinesis (e), six pairs of homologous chromosomes (six bivalents) attached to each other by chiasmata, can be clearly distinguished by the appearance of 6 well-spaced DAPI bodies.

4.1.4 Aims of the chapter

In this chapter, I set out to investigate whether:

- mutation of *wrn-1* and *mut-7,* alone or in combination, affects genome stability
- genome instability results in excess apoptosis in *wrn-1* and *mut-7* mutants
- the *C. elegans p53* homologue (*cep-1*) is required for DNA-damage dependent apoptosis in *wrn-1* and *mut-7* mutants
- the response to various DNA damaging agents supports the suggested role for WRN-1 in damage signaling checkpoints

4.2 Results

4.2.1 Homozygous *mut-7* and *wrn-1* mutants display hallmarks of a mutator phenotype

Morphologically, homozygous *wrn-1* and *mut-7* single and double mutant animals appear superficially WT. However, initial analysis of *wrn-1(tm764)* and *mut-7(pk204)* single and double mutants revealed low brood sizes (chapter 3). Furthermore, *mut-7(pk204)* mutant strains displayed an elevated occurrence of male worms (data not shown), consistent with the previously reported high incidence of males (Him) phenotype for this strain (Grabowski et al, 2005). An increase in the occurrence of males was also apparent in *wrn-1* mutant strains, but to a lesser degree than in *mut-7(pk204)* single mutant and *wrn-1(tm764);mut-7(pk204)* double mutant strains (data not shown).

In addition to the observed Him-phenotype, when maintaining *wrn-1* and *mut-7* mutant strains, the appearance of phenotypically identifiable animals (i.e. not phenotypically WT) was also seen, including dumpy, uncoordinated, long, and small worms (data not shown). In *C. elegans*, the Him phenotype and the occurrence of heritable phenotypic variants are both indicators of germline instability, and are characteristic of mutator strains.

Although anecdotal, this suggests that genomic instability may be one of the consequences of *wrn-1* and/or *mut-7* mutations, and therefore in depth analysis of genome instability was undertaken.

4.2.2 Analysis of the germlines of *wrn-1* and *mut-7* mutants reveals mitotic defects

Genome instability in the germline of *C. elegans* can be visualised directly by staining fixed dissected gonads with DAPI. As shown in figure 4.2, the mitotic nuclei of N2 worms are of uniform size and shape, and are evenly spaced. However, various mitotic defects are observed in the germlines of *wrn-1* and *mut-7* single and double homozygous mutants (figure 4.2). For both alleles of *wrn-1*, abnormalities included anaphase bridges (b, figure 4.2), an increase in the number of M-bodies in the mitotic region (b and c, figure 4.2), and large gaps between the mitotic nuclei (c, figure 4.2) Enlarged mitotic nuclei, indicative of (at least partial) cell cycle arrest, were also observed, though at a low penetrance (data not shown).

Mitotic abnormalities were also identified in the germlines dissected from *mut-7(pk204)* homozygotes (d, figure 4.2). The most prominent phenotype was the presence of enlarged mitotic nuclei (see arrow heads, panel d, figure 4.2). Enlarged nuclei were, on the whole, larger than the observed enlarged nuclei in *wrn-1* single mutants and more numerous. Similarly, *wrn-1;mut-7* double mutants also show increased numbers of enlarged mitotic nuclei (e and f). Since enlarged mitotic nuclei indicate implementation of cell cycle arrest, this suggests that *mut-7(pk204)* mutants exhibit persistent DNA damage or stress, which in turn activates a check point response.

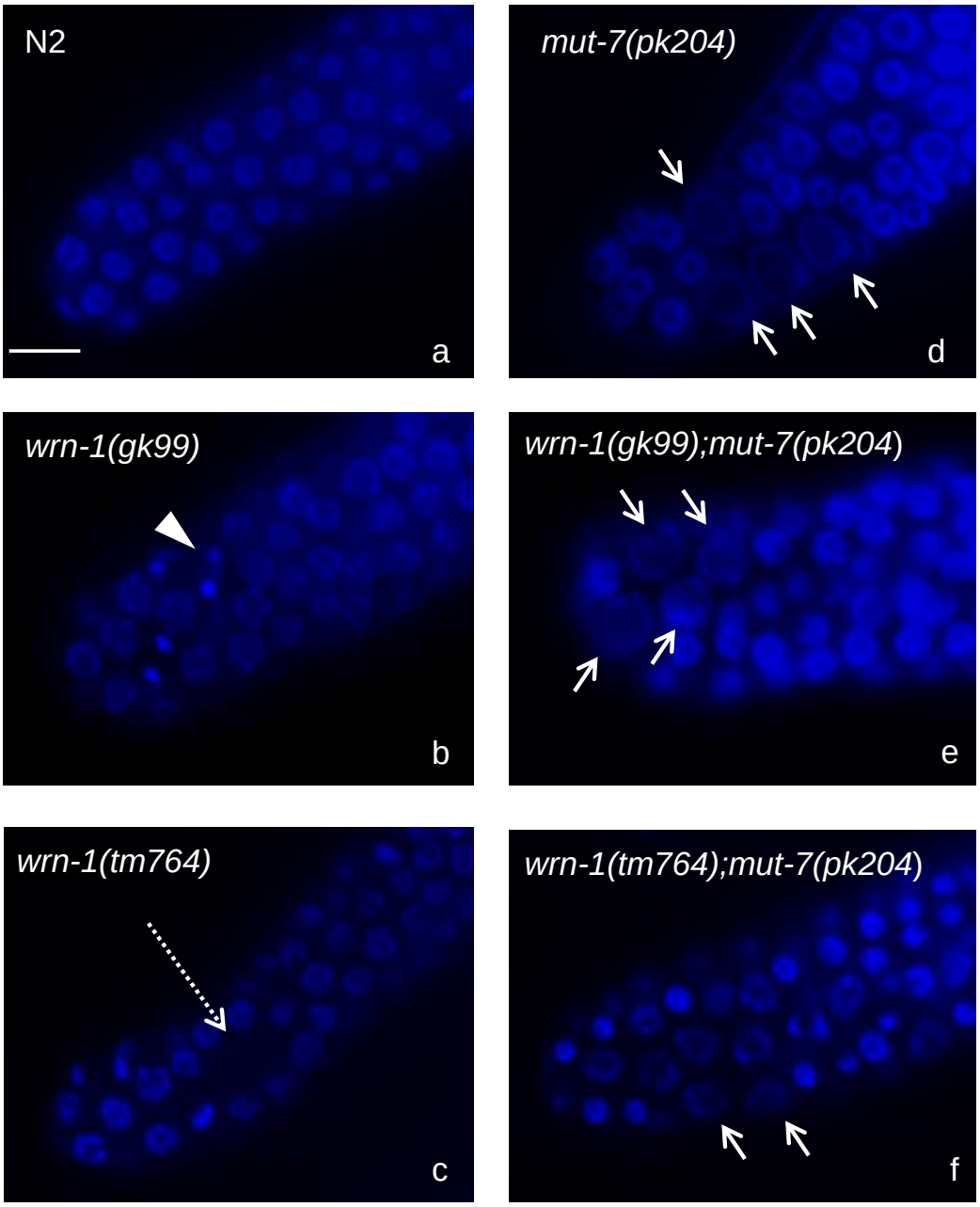

Figure 4.2: Germline defects in *wrn-1* and *mut-7* mutants. Representative images of DAPI-stained (blue) mitotic germline nuclei from dissected gonads. Germlines were dissected from: N2 (a); *wrn-1(gk99)* (b);*wrn-1(tm764)* (c); *mut-7(pk0204)* (d); *wrn-1(gk99)* ;*mut-7(pk0204)* (e); and *wrn-1(tm764)* ;*mut-7(pk0204)* (f) adult (2 days post L4) hermaphrodites. Mitotic nuclei in the germlines of N2 (control) worms are evenly spaced and similarly sized, and up to one mitotic figure can be seen at any one time (in panel a, no mitotic bodies can be seen). Arrow head (b) indicates an anaphase bridge; dashed arrow (c) indicates a large gap in between the mitotic nuclei; and arrows (d, e and f) indicate enlarged mitotic nuclei (indicative of activation of the mitotic checkpoint response. Scale bar = 10 um.

4.2.3 Meiotic defects are evident in the germlines of *wrn-1* and *mut-7* mutants

To further assess genome instability, dissected gonads were also analysed for meiotic defects – specifically, defects which give rise to observable chromosomal defects (such as fragmentation), and abnormal complements of chromosomes. In WT worms (N2, panel a, figure 4.3, and panels a and b, figure 4.4), oocytes that have arrested at diakinesis show six DAPI spots, corresponding to the six bivalent chromosomes (5 autosomes and 1 X). These DAPI spots appear relatively similar in size and are generally evenly spaced. However, in some *wrn-1* oocytes, this is not the case. Clumping of DAPI bodies is common (*wrn-1(tm764),* panel b, figure 4.3), and in such cases it is hard to confirm how many DAPI spots there are. In some oocytes, only five (and in some instances, fewer) DAPI spots can be visualised (*wrn-1(gk99)*, panel c, figure 4.3), which correlates with the increased occurrence of males in *wrn-1* strains, causes by non-disjunction. The frequency of all defects, both mitotic and meiotic, was found to increase at higher temperatures i.e. when strains were maintained at 25 ºC rather than 20ºC, suggesting that temperature stress may synergise. This temperature effect has been previously reported for *mut-7(pk204)* worms (Ketting et al, 1999).

Similarly, abnormal DAPI staining is observed in the oocytes of *mut-7(pk204)* single mutants (panel d, figure 4.3, and panels c – f, figure 4.4), and in *wrn-1(gk99);mut-7(pk204)* and *wrn-1(tm764);mut-7(pk204)* double mutants (panels e and f, respectively, figure 4.3, and panels g and h, and I and j, respectively, figure 4.4). Closer inspection of DAPI-stained oocytes from these strains (figure 4.4), revealed a variety of chromosomal defects. Abnormal complements of

chromosomes can often be seen – for instance, in the *mut-7(pk204)*-derived oocyte in panel c (figure 4.4), only five DAPI spots were identified. Again, occurrence of oocytes with five rather than six bivalent chromosomes reflects the Him phenotype documented for this strain (Ketting et al, 1999). Univalency was also noted (panel I, figure 4.4, indicated by the arrow), although the occurrence of univalency was less frequent than the appearance of abnormal numbers of bivalents. Chromosome fragmentation was commonly identified (panel d, figure 4.4). A particularly striking feature of *mut-7(pk204)* single and double mutants was the appearance of elongated chromosomes (e, f, and j, figure 4.4), reminiscent of those reported to be telomere-telomere fusion chromosomes in germline mortal strains (Ahmed & Hodgkin, 2000). Similarly to *wrn-1* mutants, chromosome clumping was also detected in *mut-7(pk204)* single and double mutant strains (g, figure 4.4).

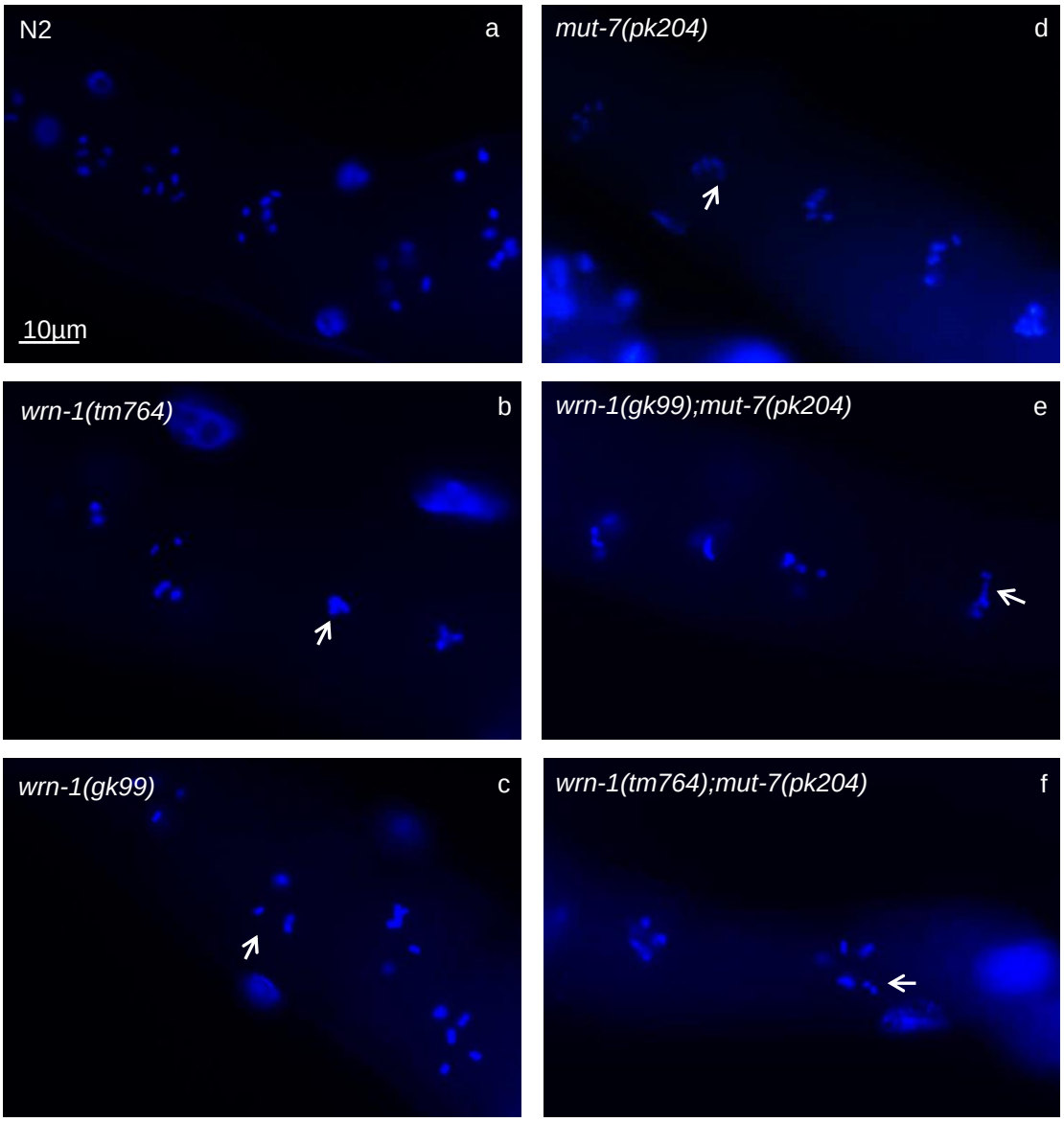

Figure 4.3: Meiotic defects in *wrn-1* and *mut-7* mutants. Representative images of multiple DAPI-stained meiotic germline nuclei (specifically, oocytes) in intact gonad arms. Germlines were dissected from: N2 (a); *wrn-1(gk99)* (b) ;*wrn-1(tm764)* (c); *mut-7(pk0204)* (d); *wrn-1(gk99)* ;*mut-7(pk0204)* (e); and *wrn-1(tm764)* ;*mut-7(pk0204)* (f) adult (2 days post L4) hermaphrodites. Photos were chosen based on the chance occurrence of all DAPI-bodies being in the same plane of view, for as many oocytes in one germline as possible. This permits counting of chromosomes. In the oocytes of N2 (control) worms, 6, well-spaced, similarly sized DAPI bodies can be identified in most of the oocytes of a given germline (a). Some DAPI bodies are missed due to being hidden from view by another DAPI body in the plane directly above it. This issue can be addressed by using 3D-imaging available via confocal microscopy, in conjunction with PI staining (see figure 4.5). Arrows highlighting examples of: chromosomes clumping (b); fewer than six DAPI bodies (c and d); chromosome fusions (e); and possible univalency (f). Scale bar = 10 um.

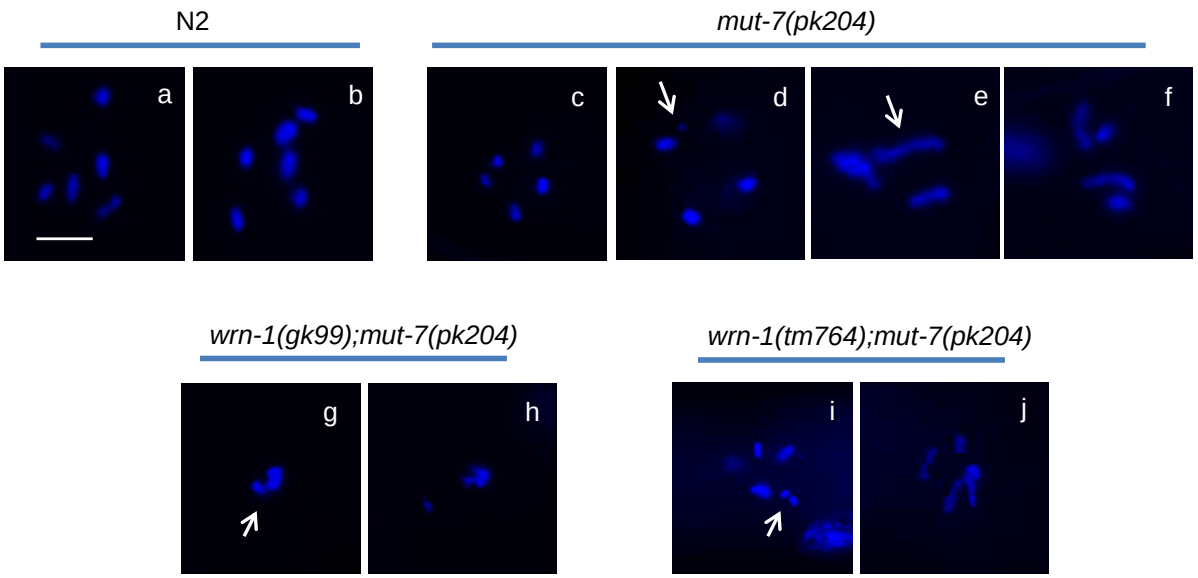

Figure 4.4: Representative images of DAPI-stained meiotic germline nuclei (specifically, oocytes) from dissected gonads. Oocytes dissected from: N2 (a and b); *mut-7(pk0204)* (c - f); *wrn-1(gk99)* ;*mut-7(pk0204)* (g and h); and *wrn-1(tm764)* ;*mut-7(pk0204)* (i and j) adult (2 days post L4) hermaphrodites. In the oocytes of N2 (control) worms, 6, well-spaced, similarly sized DAPI bodies can be identified. Arrows highlighting examples of: chromosome fragments (d); chromosome fusions (e); and possible univalent chromosomes (i). Scale bar = 10 um.

Next, I used confocal microscopy to confirm these chromosome defects. This allowed 180^0 images to be obtained in a Z-stack, thus enabling the accurate counting of chromosomes in oocytes (figure 4.5) and the removal of possible artefacts due to chromosome superimposition (these would be difficult to distinguish with conventional fluorescence microscopy). The confocal microscope available did not possess a UV laser – therefore, propidium iodide (PI) staining was used in place of DAPI. Abnormal numbers of chromosomes (b,c and d, figure 4.5), along with chromosome fragments (arrow, panel d, figure 4.5), and chromosome clumping (b, c and d, figure 4.5) were confirmed (note, only PI staining of N2, and *wrn-1(gk99);mut-7(pk204)* homozygotes is shown in figure 4.5, but single *wrn-1* and *mut-7* mutants showed similar results (data not shown).

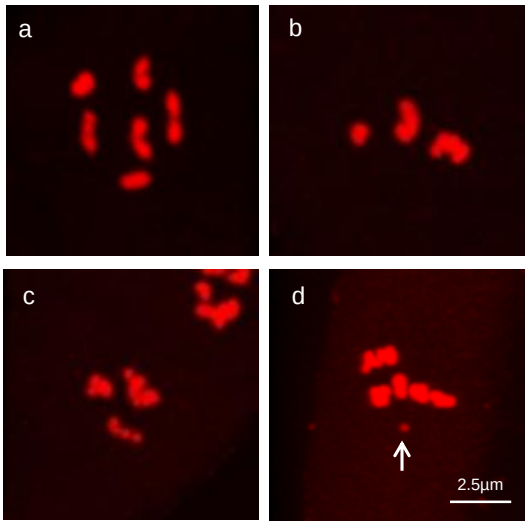

Figure 4.5: Confocal imaging of oocyte defects. Propidium iodide (PI) staining of meiotic chromosomes from N2 (a) and *wrn-1(tm764); mut-7(pk204)* double mutant worms (b-d). In N2, meiotic chromosomes progress from diplotene to diakinesis, becoming highly condensed. In each arrested oocyte, six discrete bivalents can be seen by staining with PI (panel a). In *wrn-1(tm764); mut-7(pk204)* homozygotes, fewer than or greater than six PI-stained bodies are frequently observed, as well as chromosome clumping (b), fusions (c) and fragmentation (arrow, d). Chromosome clumping makes counting the number of PI-stained bodies difficult, but can be circumvented to some extent by using 3D-imaging software. The presented images are stills from 3D-reconstructions. Scale bar = 2.5µm.

4.2.4 Genomic instability makes these strains problematic to maintain as homozygotes

Given the apparent genomic instability evident in *wrn-1* and *mut-7* mutants, I was concerned about the consequences of keeping homozygous mutant strains growing for many generations as phenotypes could be secondary consequences of genomic instability. For this reason, early on in my thesis work, I sought ways to balance my stocks. Fresh strains were obtained from the CGC, extensively outcrossed, and then balanced by crossing with an appropriate balancer. In the case of *wrn-1, mIn1(II)* was used, and for *mut-7, hT2(I;III)* was used. This allowed both strains to be maintained as balanced heterozygotes, with the added convenience that both balancers are marked with a pharyngeal GFP.

When required, worms were simply homozygosed by picking non-GFP progeny. For some experiments, it was important to distinguish F1 homozygous progeny from those of later generations. Thus the impact of the loss of WRN homologues over successive generations could also be evaluated.

Problems quickly became apparent in the case of balanced *mut-7* stocks. It became increasingly difficult to genotype them by using two different PCR-based strategies. My eventual conclusion was that the *hT2* balancer somehow broke down when kept in *trans* to *mut-7*, allowing WT worms to be produced. Heterozygous *mut-7* phenotypes have previously been reported (Ketting et al, 1999), so perhaps some kind of genomic instability leading to balancer rearrangement can occur in *mut-7* heterozygotes. This became so problematic that I terminated experiments with *mut-7* at this point.

4.2.5 Similar germline defects are observed in homozygous *wrn-1* mutants that have been maintained as balanced heterozygotes

I was very worried that the genome instability phenotypes previously observed may have a secondary consequence of the mutator phenotype. I checked this by repeating the analysis of *wrn-1* homozygotes with worms derived from balanced stocks. In both *wrn-1(gk99)* and *wrn-1(tm764),* homozygous mutants derived from balanced heterozygotes, the same range of meiotic and mitotic phenotypes were observed (figure 4.6). Thus, the germline defects observed are not a secondary consequence of genomic instability, but are directly attributable to *wrn-1* mutation.

Although heterozygous phenotypes have been reported for *mut-7(pk204)* (Ketting, 1999), none have been reported for *wrn-1* mutants. Since I did not test for heterozygous phenotypes, this is a caveat of using the ‘balanced’ strains.

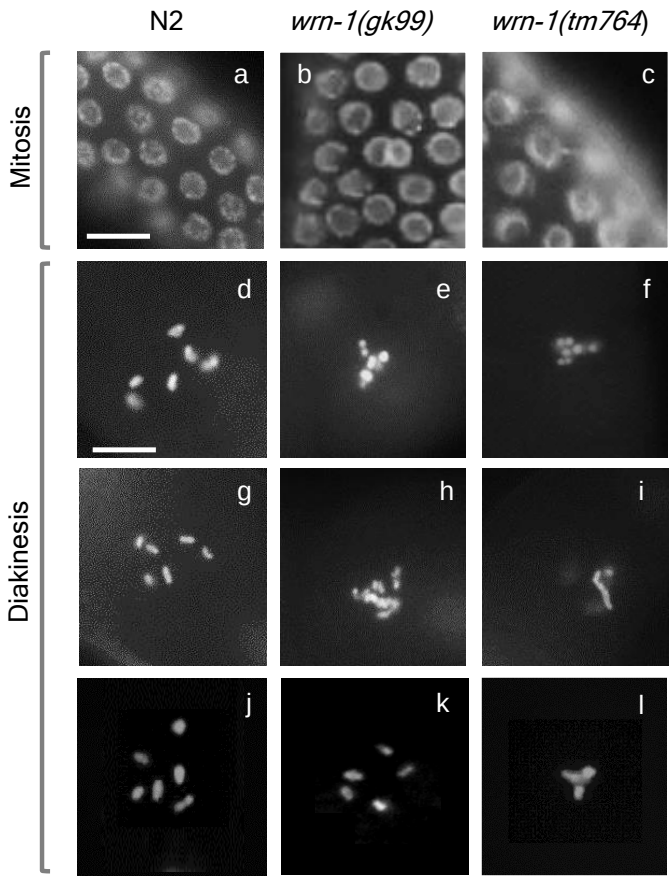

Figure 4. 6: Germline defects in *wrn-1* mutants. Representative images of DAPI-stained mitotic and meiotic germline nuclei. Gonads were dissected from N2 (a, d, g, and j), *wrn-1(gk99)* (b, e, h and k), and *wrn-1(tm764)* (c, f, I, and l) adult (2 days post L4) hermaphrodites. Scale bars = 10µm.

4.2.6 Is germline apoptosis in *wrn-1(tm764)* worms dependent on *cep-1*?

As seen in chapter 3, *wrn-1(tm764)* mutants (and *mut-7(pk204)* mutants) display elevated levels of germline apoptosis, presumed to be the result of increased genomic instability. Intriguingly, *wrn-1(gk99)* worms showed approximately WT levels of apoptosis in the germline, yet genomic instability was also evident in this strain. In order to determine whether the observed increase in apoptosis in *wrn-1(tm764)* germlines was DNA damage-dependent, *wrn-1* mutants (F1 progeny of balanced heterozygotes) were crossed into a *cep-1* null background.

cep-1;wrn-1 double mutants were assayed for germline cell death using the TUNEL method as discussed in Chapter 3. In addition to TUNEL, a second, complimentary method for detecting apoptosis was used in the case of *wrn-1* mutants, since there was initial uncertainty about the level of apoptosis observed via TUNEL. This method employs CED-1::GFP (expressed by engulfing cells) which specifically labels cell corpses that are in the process of being engulfed. In N2 worms, only a small portion of cell corpses will be surrounded by CED-1::GFP at any given moment in time (corresponding to low levels of physiological germline apoptosis). Crossing *wrn-1(gk99)* and *wrn-1(tm764)* into the CED-1::GFP reporter strain confirmed previous data obtained by the TUNEL method – high levels of CED-1::GFP-surrounded corpses could be seen in *wrn-1(tm764)* worms but not *wrn-1(gk99)* worms (figure 4.7).

TUNEL staining performed on *cep-1(gk138)* germlines indicated a low level of apoptosis under both normal conditions (figure 4.7) and after genetic insult (section 4.2.10). Thus, *cep-1* is required for DNA-damage induced apoptosis, in agreement with previous reports (Derry et al, 2001; Gartner et al, 2000; Greiss et al, 2008; Schumacher et al, 2001). When *cep-1(gk138);wrn-1(gk99)* and *cep-1(gk138);wrn-1(tm764)* germlines were stained with TUNEL (figure 4.7), a low level of apoptosis was observed under all conditions tested. Therefore, the elevated level of apoptosis seen in *wrn-1(tm764)* mutants was abrogated in *cep-1(gk138)* double mutants, indicating that apoptosis induced by DNA damage in these mutants requires functional *cep-1*.

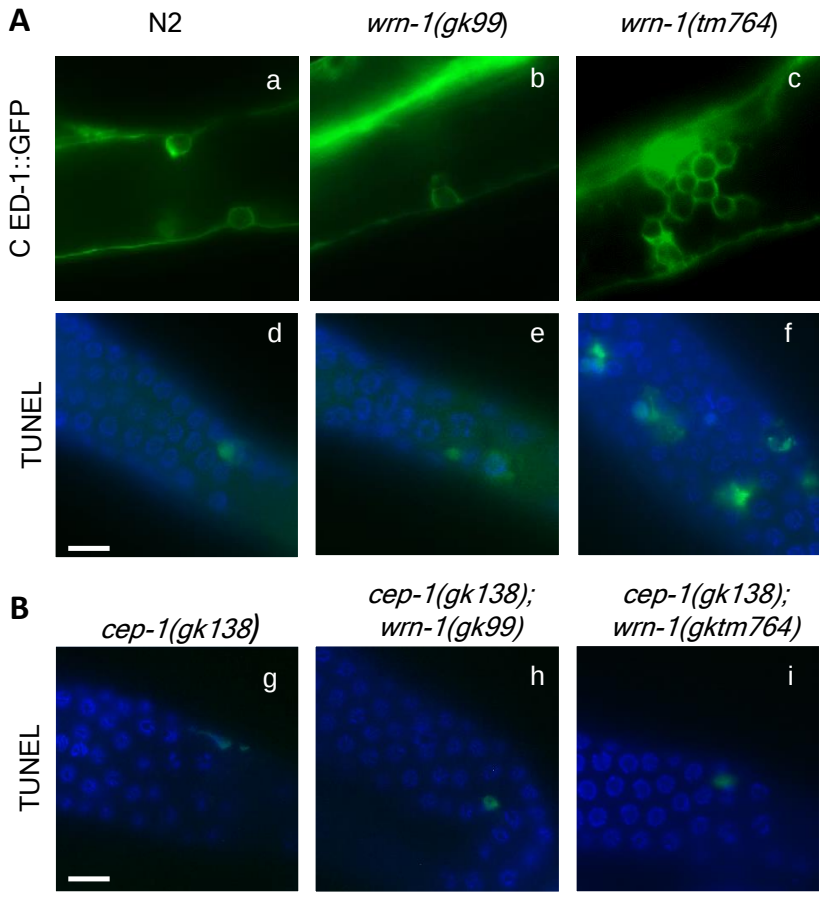

Figure 4.7: Elevated germline apoptosis in *wrn-1(tm764)* homozygotes is *cep-1*-dependent. (A) Germline apoptosis was assessed in N2, *wrn-1(gk99),* and *wrn-1(tm764)* homozygotes using either CED-1::GFP (a-b, respectively) or TUNEL staining (d-f, respectively) as markers of apoptotic corpses (both, green). (B) To ascertain whether increased germline apoptosis was *cep-1*-dependent, *wrn-1(gk99)* and *wrn-1(tm764)* homozygotes were crossed into the *cep-1(gk138)* mutant background, and apoptosis was visualised by TUNEL staining (green). Homozygous *cep-1(gk138)* (g), *cep-1(gk138);wrn-1(gk99)* (h), and *cep-1(gk138);wrn-1(tm764)* (i) gonads were dissected and used in this analysis. DNA was stained with DAPI. Scale bar = 10µm.

4.2.7 Mild genomic instability in *cep-1* single mutants

Consistent with published data, occasionally, germlines from *cep-1* single mutants displayed one or two oocytes which contained only 5 DAPI bodies (figure 4.8), which is likely to reflect the Him phenotype documented for this

strain (Derry et al, 2001). *cep-1* single mutants also displayed elevated levels of M-bodies in the mitotic region, but no other overt phenotypes were detected.

4.2.8 Germline defects are also observed in *cep-1;wrn-1* worms

Although the abrogation of elevated apoptosis in *wrn-1(tm764)* by the presence of *cep-1(gk138)* would suggest that the observed cell death is DNA-damage- and *cep-1* -dependent, another possibility is that the *cep-1;wrn-1* double mutants no longer display genome instability, and hence no apoptosis would be required or elicited regardless of the cells ability (or inability) to do so. In light of this possibility, the germlines of *cep-1(gk138);wrn-1(gk99)* and *cep-1(gk138);wrn-1(tm764)* worms were examined for evidence of genomic instability.

Like the *wrn-1* single mutants, both double mutants displayed defects in nuclei found in both the mitotic and meiotic regions (figure 4.9). In the mitotic region (A, figure 4.9), there was evidence of anaphase bridges, chromosome fragmentation and a greater than normal number of M-bodies (indicative of either an anaphase-to-metaphase transition defect, or possibly over proliferation). In the arrested oocytes (B (j), figure 4.9), chromosome fragmentation could be seen, as well as abnormal numbers of bivalents (fewer and greater than the WT six).

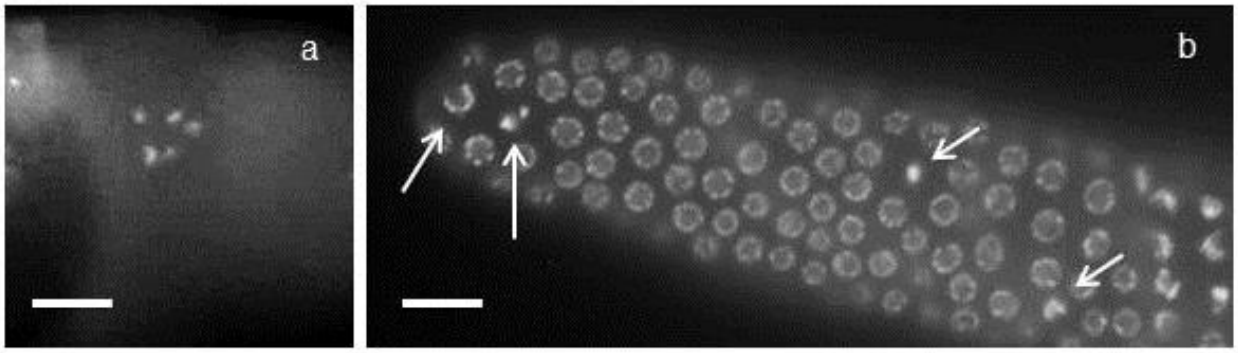

Figure 4. 8: Limited genomic instability in germlines from *cep-1(gk138)* worms. Representative images of DAPI-stained mitotic (b) and meiotic (a) nuclei from the dissected gonads of *cep-1(gk138) animals.* Oocytes were occasionally observed to show only 5 DAPI bodies (a), which reflects the Him phenotype documented for this strain. Increased numbers of mitotic bodies (arrows, b) are observed in the mitotic region of the germline. No other overt phenotypes were observed.

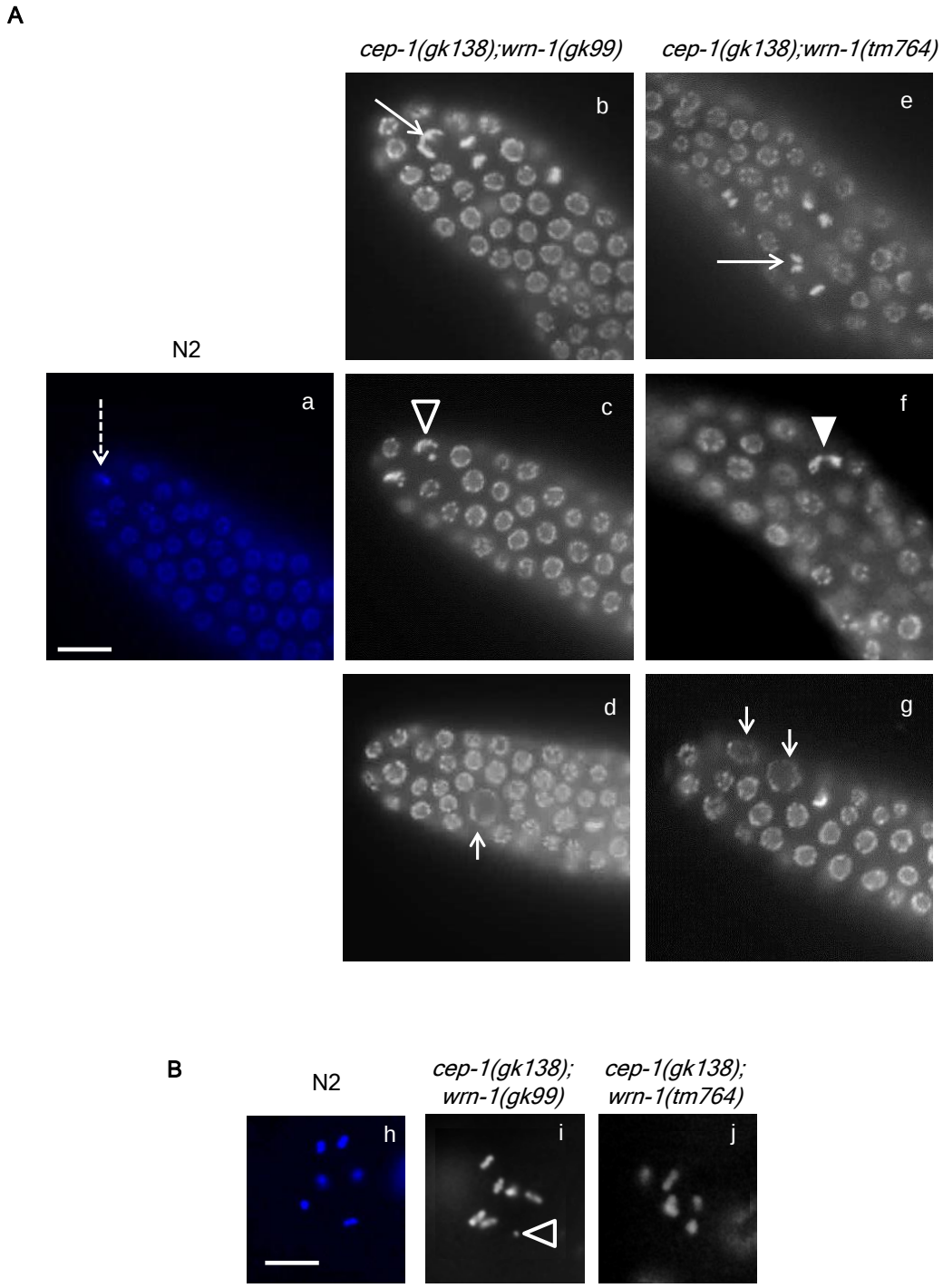

Figure 4.9: Genomic instability in the germlines of *cep-1;wrn-1* double mutants. Representative images of DAPI-stained mitotic and meiotic germline nuclei from the dissected gonads of: N2 (a (mitotic) and h (meiotic)); *cep-1(gk138);wrn-1(gk99)* (b, c, and d (mitotic) and I (meiotic); and *cep-1(gk138);wrn-1(tm764)* (e, f, and g (mitotic), and j (meiotic)) adult (2 days post L4) hermaphrodites. Dashed arrow indicating: a normal mitotic figure (a); long arrows indicating abnormal mitotic figures (b and e); empty arrow head indicating mitotic (c) and meiotic (i) fragmentation; filled arrow head indicating an anaphase bridge (f); arrows indicating enlarged nuclei (d and g); and chromosome fragments (i). Scale bars = 10µm.

4.2.9 Germline mortality is evident in *cep-1(gk138);wrn-1(gk99)* and *wrn-1(gk99)* mutant strains

The germline is an immortal lineage which is normally passed through generations indefinitely, but there are a group of *C. elegans* mutants, termed Mrt mutants (mortal germline) in which the fecundity of mutant strains decreases over successive generations until they reach sterility (Ahmed & Hodgkin, 2000).The Mrt phenotype can result from several different kinds of germline defects, including genomic instability. I next tested whether the Mrt phenotype was observed in *cep-1* and *wrn-1* single and double mutants. In order to do this, I counted the brood size of different strains every few generations up to generation F76, with strains maintained at two different temperatures, 20°C degrees and 25°C.

The data in figure 4.10 shows brood sizes from mutant strains maintained at 20°C up to F32. Brood sizes fluctuated somewhat unpredictably making it difficult to draw clear conclusions. However, it seems that *cep-1(gk138)* mutants displayed progressive loss of fertility between generation F1 and F32. The same could be said for *wrn-1(gk99), wrn-1(tm764)* and *cep-1(gk138);wrn-1(gk99)* mutants, although there were exceptions to the general trend. For example, the F32 generation of both *wrn-1(gk99)* and *wrn-1(tm764)* showed an unexpected rise in fecundity. What is clear, however, is that *cep-1(gk138);wrn-1(tm764)* double mutants had an unexpectedly large brood size at all generations assayed, relative to N2.

Next, I performed the assay at 25°C for many more generations, in an attempt to uncover more subtle Mrt phenotypes. Given the labour intensity of counting whole brood sizes for each of the strains involved, I utilised a scoring scheme

as outlined in figure 4.11. This method has been previously reported to act as a reliable read out of germline mortality (Ahmed & Hodgkin, 2000).

The data is shown in table 4.2. Strikingly, *cep-1(gk138)* mutants displayed improved fertility outcomes at 25°C compared with 20°C, maintaining a normal or relatively normal brood size after even 76 generations. *wrn-1(gk99)* mutants, on the other hand, had a much more severe mortal germline phenotype, being sterile or almost sterile in the later generations assayed in this study.*wrn-1(tm764)* mutants had a much less severe phenotype, displaying only medium reductions in brood size at the end of the study. *cep-1(gk138);wrn-1(gk99)* double mutants displayed the more severe phenotype reminiscent of *wrn-1(gk99)* single mutants, although these double mutants appeared better off than *wrn-1(gk99)* single mutants. Similar to what was observed at 20°C, *cep-1(gk138);wrn-1(tm764)* double mutants exhibited a normal or higher than normal brood size throughout the experiment.

A

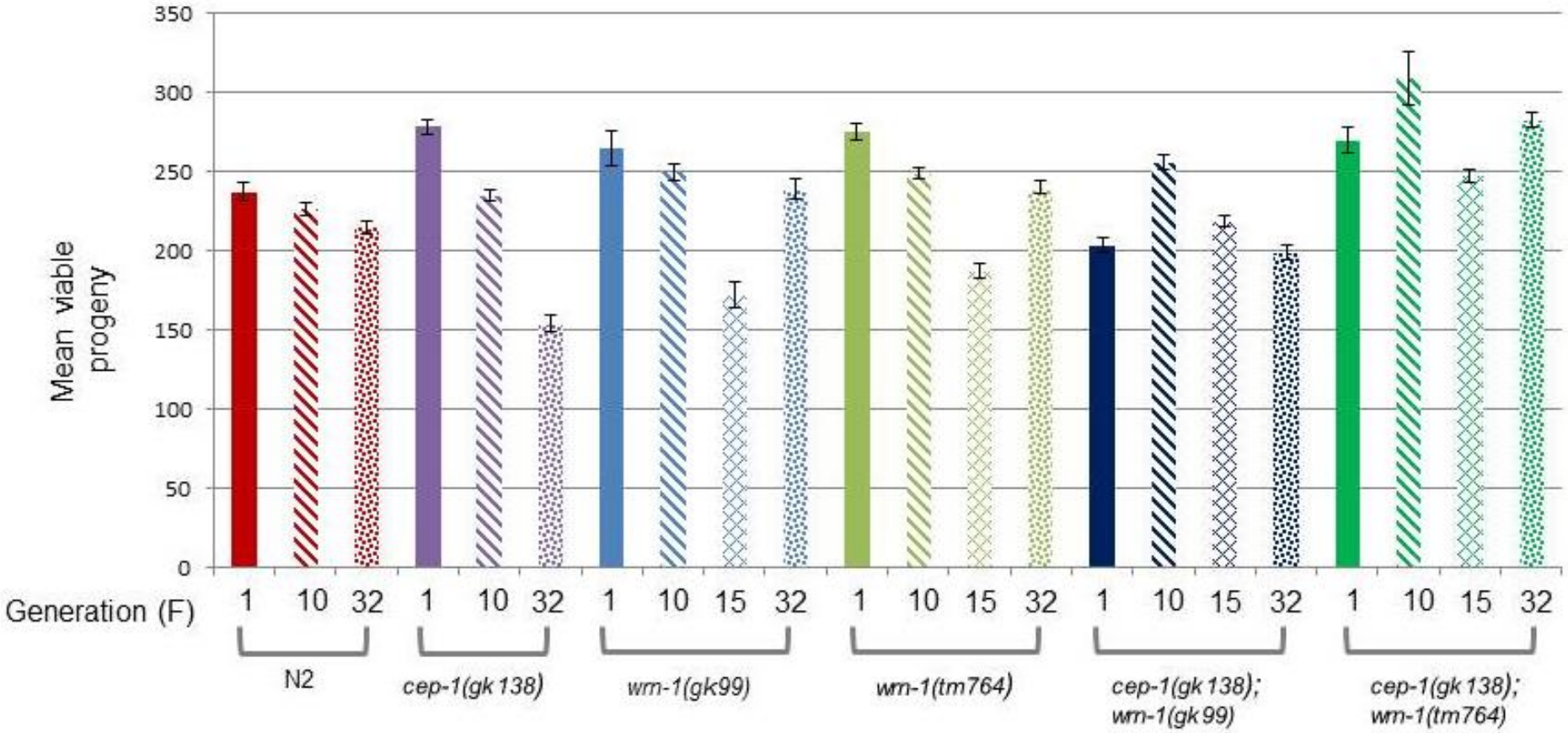
Mean viable progeny
350
300
250
200
150
100
50
0
Generation (F)
1 10 32 1 10 32 1 10 15 32 1 10 15 32 1 10 15 32 1 10 15 32
N2
cep-1(gk138)
wm-1(gk99)
wm-1(tm764)
cep-1(gk138); wm-1(gk99)
cep-1(gk138); wm-1(tm764)

Figure 4.10 (previous page): Germline mortality in *wrn-1* and *cep-1* mutants. Mean number of viable progeny at different generations for *wrn-1* and *cep-1* single and double homozygous mutants, and N2 control worms at 20°C. N2 (red bars), *cep-1(gk138)* (purple bars);*wrn-1(gk99)* (light blue bars), *wrn-1(tm764)* (light green bars), *cep-1(gk138);wrn-1(gk99)* (dark blue bars) and *cep-1(gk138);wrn-1(tm764)* (dark green bars). The number of viable progeny (i.e. larvae) was counted for at least 50 individual hermaphrodites and averaged to give the mean viable brood size for each of the six strains. The number of progeny was counted for hermaphrodites at different generations (F1, F10, F15 (but not for N2 and *cep-1(gk138)* and F32) after being homozygozed (since worm stocks were maintained as balanced heterozygotes). Error bars ± SEM.

A

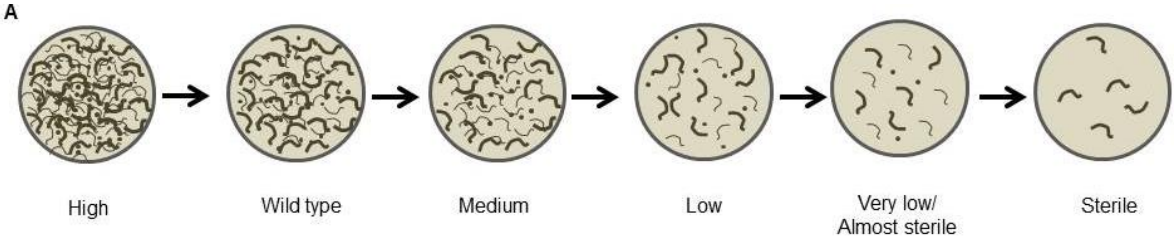

B

Symbol	Meaning in terms of relative progeny number
H	High (compared to WT)
WT	Wild type levels
M	Medium brood
L	Low brood
VF	Very low brood (≤50)
A	Almost sterile (≤15)
X	Sterile

Figure 4.11: Mortal germline mutants eventually become sterile. A – schematic representation of the progressive decline in brood size with subsequent generations, until the strain eventually becomes sterile. B – a key indicating the definition of each symbol used to indicate relative brood size in the germline mortality assay (table 4.2).

Strain	Plates	F1	F10	F32	F40	F46	F48	F49	F52	F54	F55	F56	F58	F64	F67	F71	F76
N2	A	WT	WT	WT	WT	WT	WT	WT	WT	WT	WT	WT	WT	WT	WT	WT	WT
	B	WT	WT	WT	WT	WT	WT	WT	WT	WT	WT	WT	WT	WT	WT	WT	WT
	C	WT	WT	WT	WT	WT	WT	WT	WT	WT	WT	WT	WT	WT	WT	WT	WT
	D	WT	WT	WT	WT	WT	WT	WT	WT	WT	WT	WT	WT	WT	WT	WT	WT
	E	WT	WT	WT	WT	WT	WT	WT	WT	WT	WT	WT	WT	WT	WT	WT	WT
cep-1(gk138)	A	WT	WT	M	M	WT	WT	WT	M	WT	WT	WT	M	WT	WT	WT	WT
	B	M	WT	M	L	M	M	M	WT	WT	WT	WT	WT	WT	M	M	M
	C	WT	WT	M	M	WT	WT	WT	M	WT	M	M	WT	WT	WT	WT	WT
	D	WT	M	M	M	M	L	M	WT	WT	WT	WT	WT	M	M	L	M
	E	WT	WT	M	WT	M	M	M	M	M	M	WT	M	WT	WT	WT	WT
wrn-1(gk99)	A	WT	WT	M	M	L	M	M	VF	L	L	M	A	L	L	A	X
	B	WT	WT	WT	M	M	M	L	VF	VF	VF	L	M	L	M	A	A
	C	WT	WT	WT	WT	M	M	M	M	M	M	VF	VF	VF	X	X	X
	D	WT	WT	M	M	VF	VF	VF	VF	A	A	X	X	X	X	X	X
	E	WT	M	M	M	VF	VF	VF	L	L	L	L	VF	M	A	X	X
wrn-1(tm764)	A	WT	WT	M	WT	L	WT	WT	M	WT	WT	H	WT	WT	WT	M	M
	B	WT	M	WT	M	M	M	M	M	WT	WT	WT	WT	M	WT	M	M
	C	M	M	WT	WT	WT	M	M	L	M	M	M	M	M	M	WT	M
	D	WT	M	M	M	M	M	M	L	M	M	M	L	M	L	M	M
	E	WT	M	M	M	WT	M	M	M	WT	M	VF	L	WT	WT	WT	M
cep-1(gk138); wrn-1(gk99)	A	WT	WT	M	L	M	L	L	M	L	VF	VF	L	L	M	L	VF
	B	WT	WT	WT	M	M	L	L	M	M	WT	M	M	M	M	L	M
	C	M	M	L	M	VF	A	A	X	X	X	X	X	X	X	X	X
	D	M	WT	M	M	WT	A	VF	VF	AS	X	X	X	X	X	X	X
	E	M	WT	WT	M	L	L	M	L	VF	VF	VF	A	VF	L	L	VF
cep-1(gk138); wrn-1(tm764)	A	WT	H	WT	WT	H	WT	M	WT	M	L	VF	M	M	WT	WT	WT
	B	H	H	H	WT	H	WT	H	H	H	WT	WT	H	WT	H	H	H
	C	H	H	H	H	WT	H	WT	H	H	WT	H	H	WT	H	H	H
	D	H	H	WT	WT	H	H	WT	H	H	WT	WT	H	WT	WT	H	WT
	E	H	H	H	H	H	H	H	WT	H	H	H	WT	WT	WT	WT	H

Table 4.2 (previous page): Brood size drops progressively in *wrn-1/cep-1* mutants. Five L4 hermaphrodites were picked onto petri dishes seeded with

OP50 and allowed to lay for 3 days (at 25°C, 4 days if 20°C). After 3 days, five L4 worms from the next generation (i.e. the offspring of the worms which had initially been picked to the plate) were picked onto fresh OP50 plates, and the cycle started again. Each time that L4s were picked, the generation (e.g. F32) and approximate brood size (see figure 4.11) was recorded until the strain became sterile (in which case only the five, infertile hermaphrodites would be left on a plate). Five plates (A-E) were set up for each strain at each temperature (20°C and 25°C).

4.2.10 DNA damage response in *wrn-1* and *cep-1* mutants

Genomic instability could be caused by failure to arrest the cell cycle in response to damage, failure to undergo apoptosis, or failure to repair such damage, or a mixture of all three. In order to try to distinguish between these possibilities, I used exogenous DNA damage in assays of cell cycle arrest and subsequent responses.

4.2.10.1 *wrn-1* and *cep-1* are not required for cell cycle arrest in response to HU exposure

Hydroxyurea (HU) is an indirect inhibitor of DNA synthesis, and chronic exposure of *C. elegans* hermaphrodites to HU initiates a checkpoint which monitors S-phase progression. In WT worms (figure 4.12 A) HU causes a block in the proliferation of mitotic germ cells which results in a characteristic DAPI stain – the number of mitotic nuclei is reduced and these are enlarged and have diffuse DAPI staining. Furthermore, condensed M-bodies are absent after HU treatment. When these same nuclei are viewed by Nomarski microscopy (DIC), the change in size and number can also be seen. Intriguingly, there is no

explanation in the literature why nuclear size increases when cell cycle progression is inhibited.

When germlines from *wrn-1(gk99)*, *wrn-1(tm764)* or *cep-1(gk138)* HU treated worms were stained with DAPI, they showed the same phenotype as N2 worms (figure 4.12 A and B). Similarly, when *cep-1;wrn-1* double mutants were analysed, they too displayed the characteristic checkpoint response of cell cycle arrest (figure 4.12 B). Therefore, neither *wrn-1* nor *cep-1* are required for cell cycle arrest in response to replication blockage induced by HU. This conflicts with data reported by *Lee et al*, in which *wrn-1* was claimed to be required for cell cycle arrest in response to HU (Lee et al, 2010a; Lee et al, 2004). However, analysis of the DAPI staining reported in their paper would suggest that there is indeed cell cycle arrest, in line with what was observed in my studies.

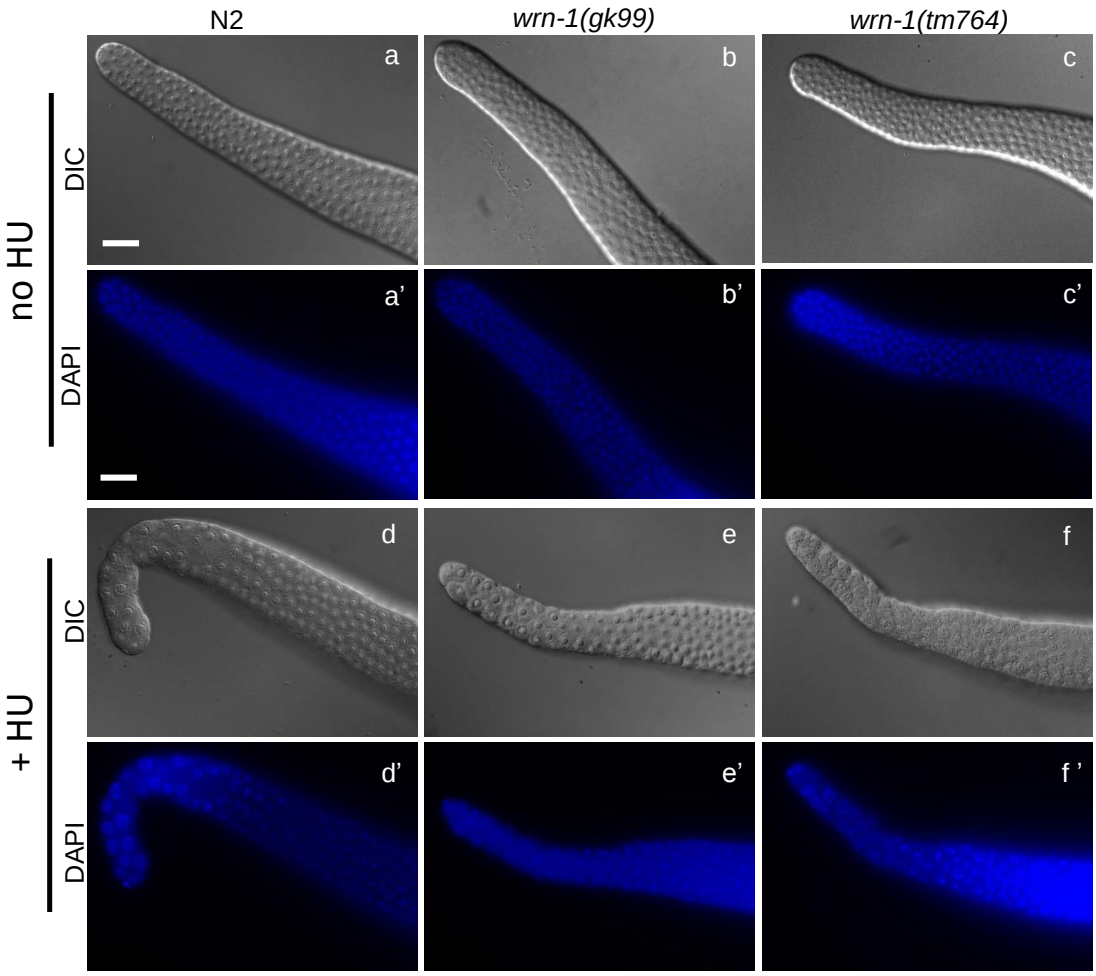

Figure 4.12: Assessment of HU-induced germ cell proliferation arrest. Morphological changes in mitotic germline nuclei after 12 hours of HU exposure were assessed by DAPI staining and Nomarski microscopy in the dissected gonads from N2 (a, a', d, and d'), *wrn-1(gk99)* (b, b', e, and e'), and *wrn-1(tm764)* (c, c', f, and f'). Scale bar = 20µm. Mitotic nuclei were reduced in number and increased in nuclear volume in all strains after HU exposure, compared to untreated controls, indicating that the mitotic S-phase checkpoint is intact

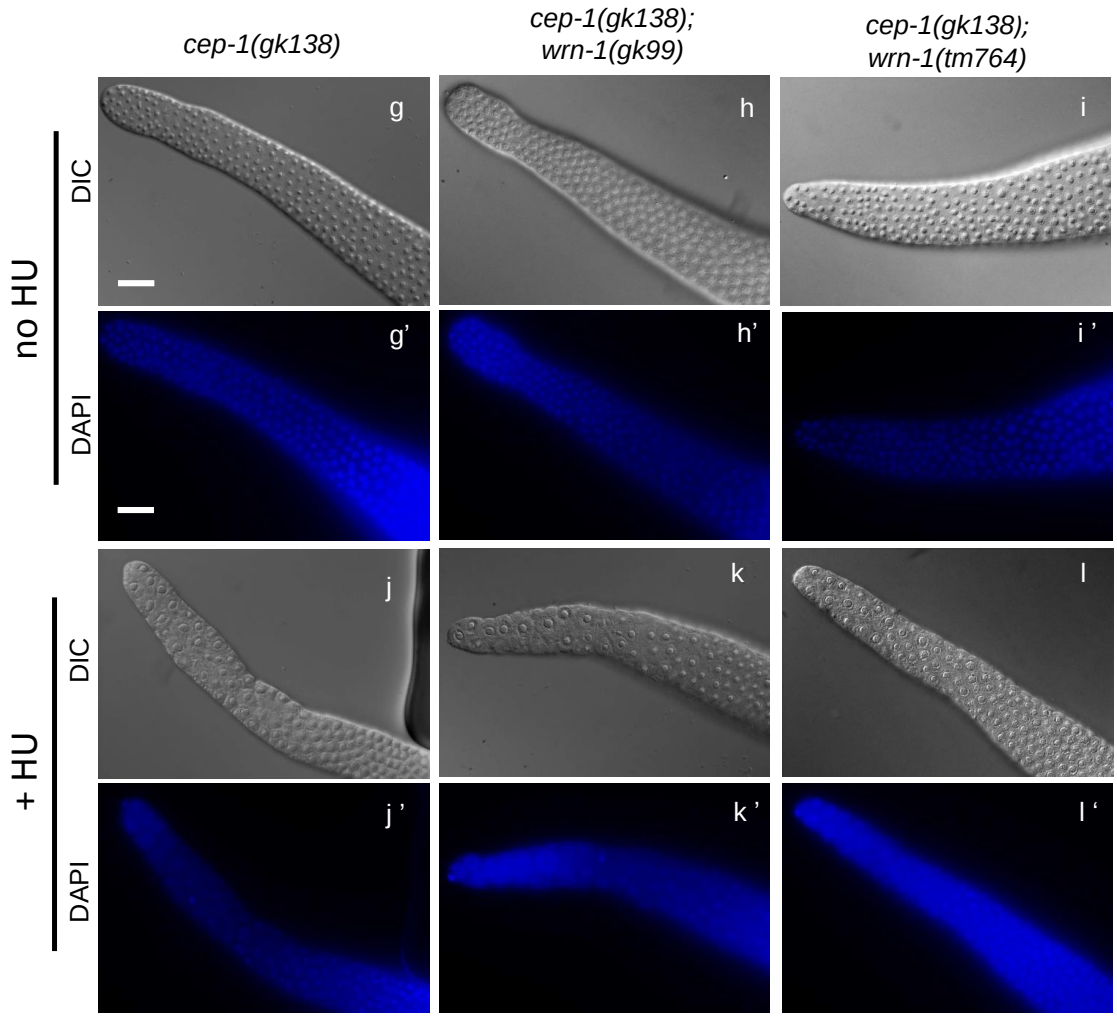

Figure 4.12 continued: Morphological changes in mitotic germline nuclei after 12 hours of HU exposure were assessed by DAPI staining and Nomarski microscopy in the dissected gonads from *cep-1(gk138)* (g, g', j, and j'), *cep-1(gk138);wrn-1(gk99)* (h, h', k, and k'), and *wrn-1(tm764);cep-1(gk138)* (i, i', l, and l'). Scale bar = 20µm. Mitotic nuclei were reduced in number and increased in nuclear volume in all strains after HU exposure, compared to untreated controls, indicating that the mitotic S-phase checkpoint is intact

4.2.10.2 *Wrn-1* and *cep-1* are not required for cell cycle arrest in response to IR

Ionizing radiation (IR) is another genotoxic stress which can induce cell cycle arrest of mitotic germ cells (Craig et al, 2012; Gartner et al, 2004; Gartner et al, 2000; Sakashita et al, 2010). IR causes the same morphological changes in germline nuclei as HU – fewer and enlarged nuclei with a diffuse pattern of DAPI stain. Lee et al have reported that *wrn-1* is required for cell cycle arrest in response to IR (Lee et al, 2010a). However, my data shows that all five strains appear to display the same response to IR as WT (figure 4.15, 4.16), when germlines are analysed 12 hours post irradiation (60 Gy).

4.2.10.3 *wrn-1* mutants display a huge increase in apoptosis after IR treatment

Whereas mitotic germ cells can arrest cell cycle progression in response to IR, germ cells in the late pachytene region have been shown to undergo apoptosis (Craig et al, 2012; Gartner et al, 2008; Gartner et al, 2004; Gartner et al, 2000; Sakashita et al, 2010). Although the mitotic arrest checkpoint can be seen after 12 hours post treatment with IR, at 48 hours nuclei in the pachytene region of meiosis undergo apoptosis. Given the time it takes for nuclei to proceed from mitosis to meiosis in the germline, the presumption is that those nuclei that have arrested the cell cycle in mitosis in response to the IR insult are not all able to repair the damage and thus some of them undergo apoptosis when they proceed to the pachytene region. Thus, when TUNEL staining is performed on gonads that have been dissected from worms which had been exposed to IR 48

hours previously, differences in the apoptotic checkpoint response may be seen.

The data shown in figure 4.17 demonstrated that IR caused an increase in apoptosis in the germlines of N2 worms, as expected. *cep-1(gk138)* single mutants did not show a significant elevation in apoptosis, consistent with previous reports (Derry et al, 2001; Schumacher et al, 2001). Similarly, both *cep-1;wrn-1* double mutants showed low levels of apoptosis, consistent with the requirement for *cep-1* in DNA damage-induced apoptosis. Both *wrn-1(gk99)* and *wrn-1(tm764)* single mutants displayed a massive increase in apoptosis, way beyond that observed under untreated conditions.

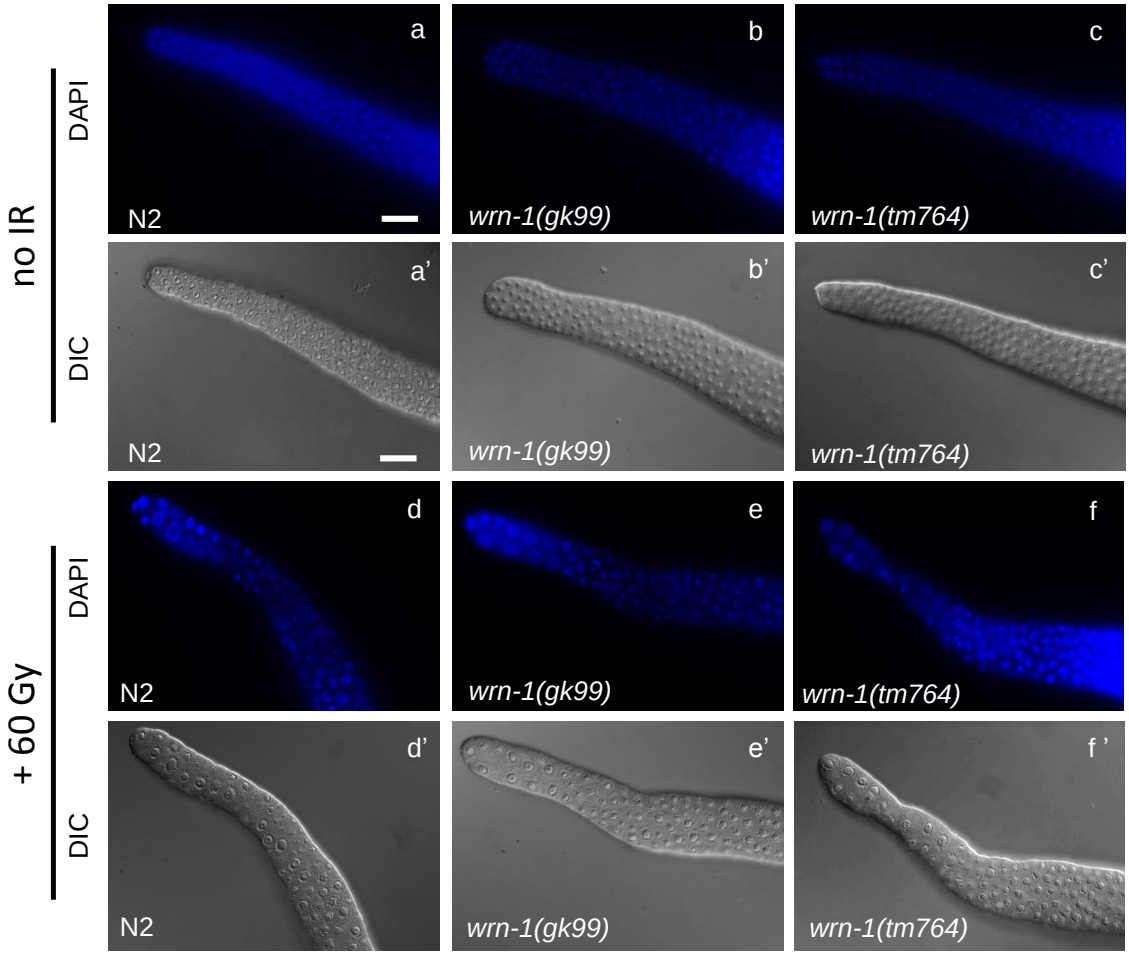

Figure 4.15: (See next page).

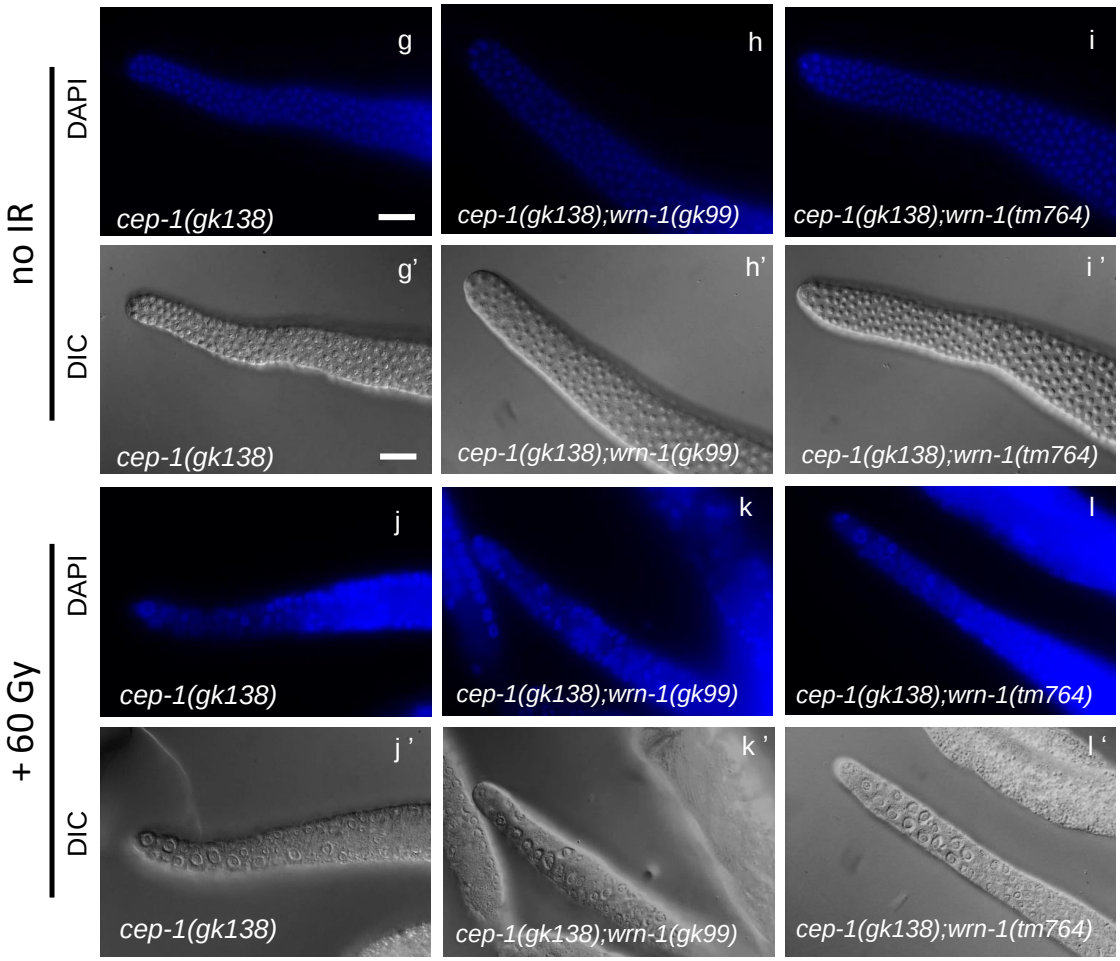

Figure 4.16 (continued): Assessment of IR-induced germ cell proliferation arrest. Figure shows morphological changes in mitotic germline nuclei, 12 hours post IR (60 Gy), were assessed by DAPI staining and Nomarski in the dissected gonads from N2 (a, a', d, and d'), *wrn-1(gk99)* (b, b', e, and e'), and *wrn-1(tm764)* (c, c', f, and f') (figure A), and from *cep-1(gk138)* (g, g', j, and j'), *cep-1(gk138);wrn-1(gk99)* (h, h', k, and k'), and *wrn-1(tm764);cep-1(gk138)* (i, i', l, and l') (figure B). Scale bar = 20µm. Mitotic nuclei were reduced in number and increased in nuclear volume in all strains after 60 Gy IR compared to non-irradiated controls, indicating that the mitotic checkpoint response to IR is intact in these worms.

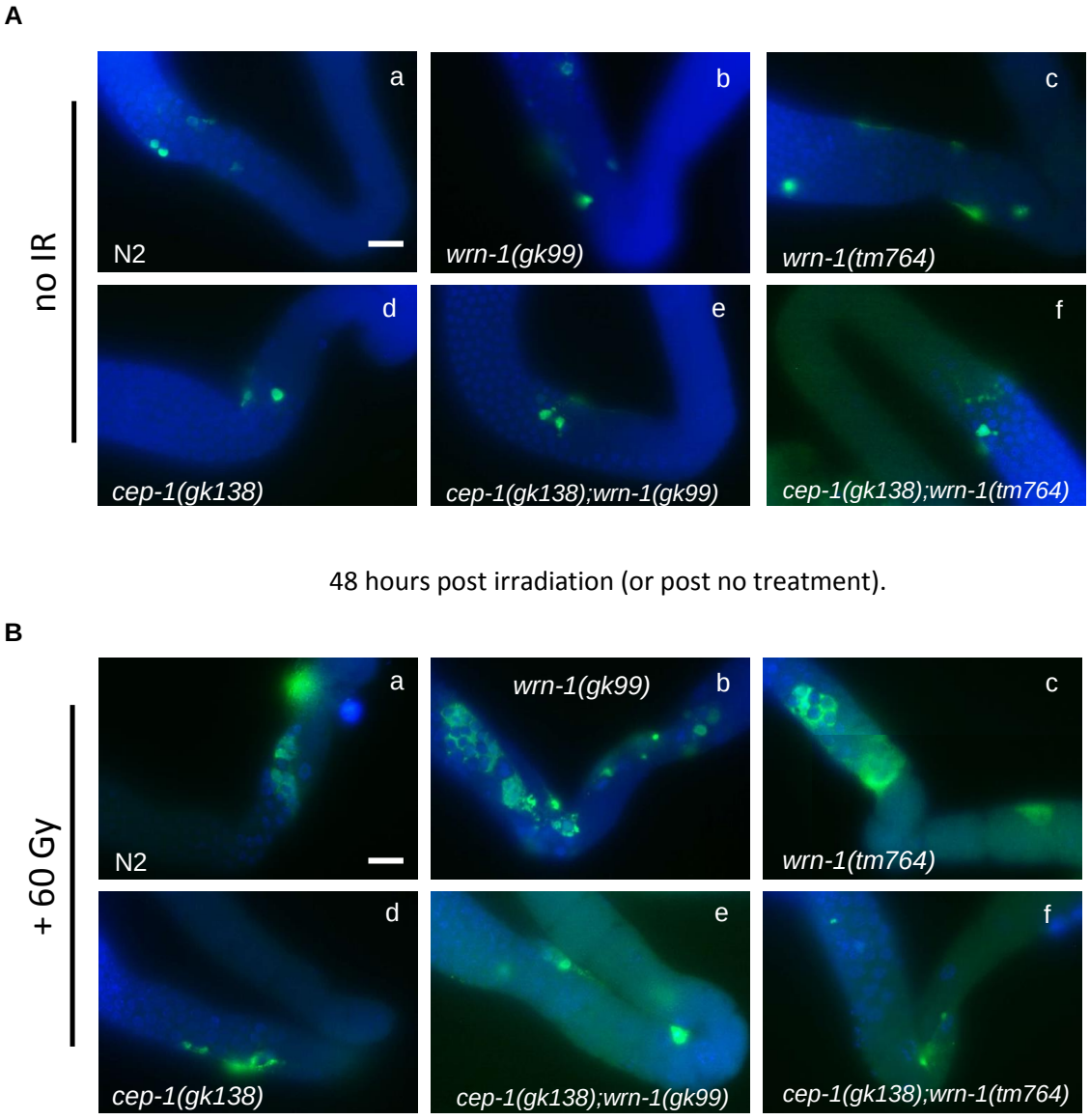

Figure 4.17: Germline apoptosis 48 hours post irradiation (60 Gy).TUNEL staining was performed on the dissected gonads of worms which had been irradiated 48 hours prior to analysis (B) or left untreated (A). The level of apoptosis was observed in the germlines of N2 (a); *wrn-1(gk99)* (b); *wrn-1(tm764)* (c); *cep-1(gk138)* (d); *cep-1(gk138);wrn-1(gk99)* (e), and *wrn-1(tm764);cep-1(gk138)* (f). Scale bar = 20µm.

4.2.10.4 *wrn-1* and *cep-1* single and double mutants display profound genomic instability in response to IR irradiation

Cytological examination 48 hours after irradiation revealed profound defects in oocyte chromosomes from germlines of *wrn-1* and *cep-1* single and double mutants, suggesting massive genomic instability (figure 4.18). As expected, oocytes from N2 germlines appeared WT, showing 6 well-spaced bivalents, of approximately equal size, shape and compactness/density. Oocytes from both *wrn-1* alleles showed a multitude of chromosome abnormalities, including changes in chromosome number and what appeared to be elongated chromosomes, possibly corresponding to end-on-end chromosome fusions (arrow heads, figure 4.18). In addition, chromosome fragmentation is prevalent.

Unlike *wrn-1* mutants, irradiation of *cep-1(gk138)* did not result in the appearance of elongated chromosomes, but unusual chromosome morphology was observed, with chromosomes (possibly bivalents) showing clumpy appearance. Again, abnormal numbers of DAPI spots were observed, and some oocytes appeared to show complete univalency of chromosomes, whilst others showed more extensive chromosome fragmentation.

Both *cep-1;wrn-1* double mutant phenotypes were more severe than any of the single mutants, with oocytes displaying extensive chromosome fragmentation, where the entire genome appeared to be completely shattered.

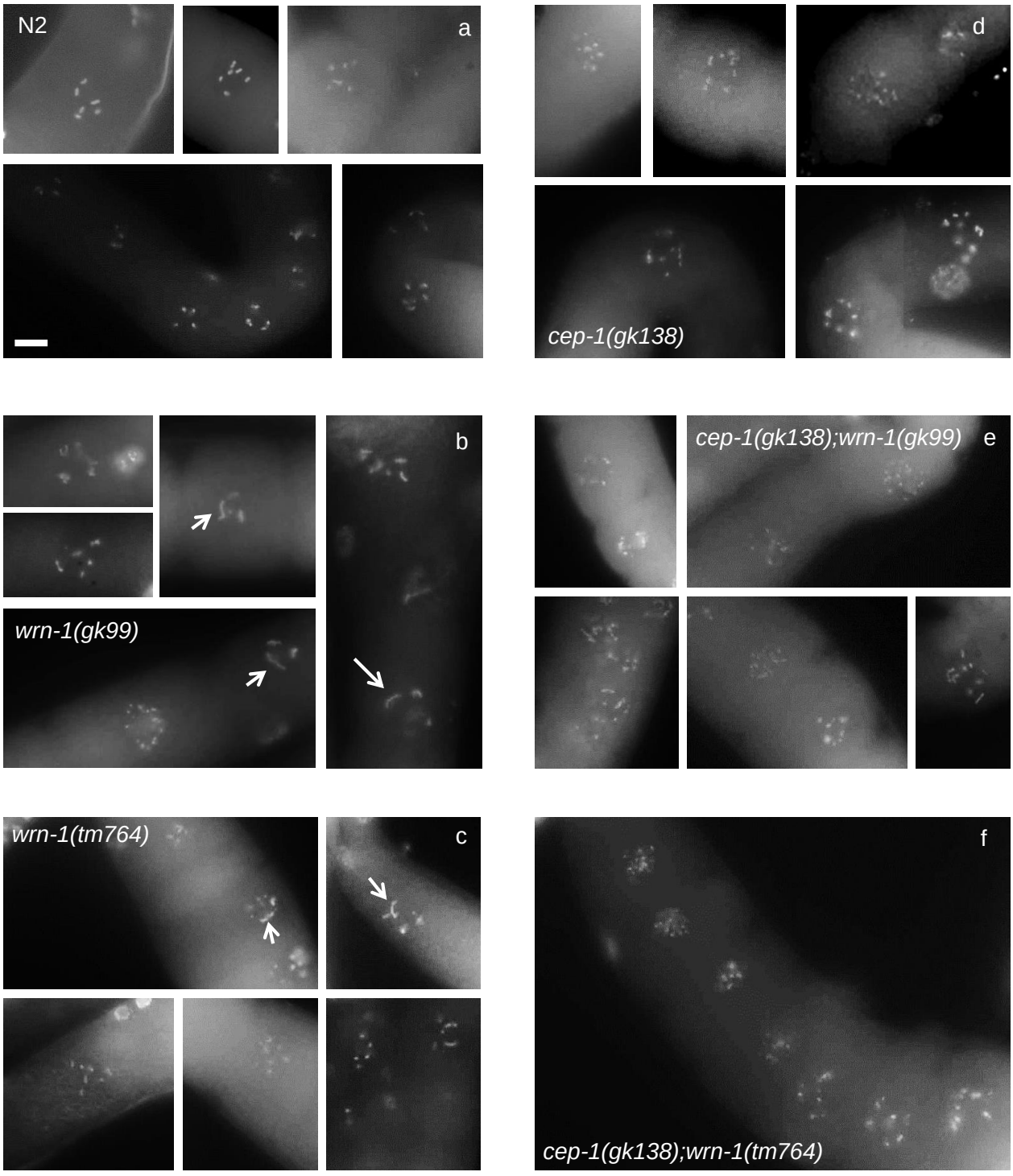

Figure 4.18 : Chromosome defects in the germlines of worms 48 hours post IR treatment. Shown are representative images of: N2 control (a); *wrn-1(gk99)* (b); *wrn-1(tm764)* (c); *cep-1(gk138)* (d); *cep-1(gk138); wrn-1(gk99)* (d); and *cep-1(gk138); wrn-1(tm764)* (e). Arrows indicate what appear to be elongated chromosomes, possibly end-on-end chromosome fusions.

4.2.10.5 Progeny viability after IR irradiation of *wrn-1* and *cep-1* single and double mutants

Since mutation of either *wrn-1* or *cep-1* results in severe chromosomal defects when worms are irradiated, one might suspect that offspring production and survival would be severely affected. Therefore, embryonic and larval survival was assayed for each strain, after IR treatment and under normal growth conditions.

Irradiation of N2 hermaphrodites causes the total brood (taken to be the total number of eggs laid, whether viable or not) to drop by 32% (figure 4.19 and table 4.3), with an overall percentage reduction of viable brood of around 57%. Surprisingly, the total brood of *cep-1(gk138)* worms only drops by 10%, with an overall decrease of viable progeny after treatment of around 42%. Thus, *cep-1(gk138)* mutants appear to perform better than WT following IR treatment.

In contrast, both alleles of *wrn-1* were significantly worse off following IR treatment, with a decrease in viable brood of 69% and 66% for *wrn-1(gk99)* and *wrn-1(tm764),* respectively (table 4.3 and figure 4.19). Mutation of *cep-1* in *wrn-1* mutants appeared to offer some protection following IR treatment, with percentage decrease in viable broods of 56% and 52% for *cep-1(gk138);wrn-1(gk99)* and *cep-1(gk138);wrn-1(tm764)* respectively, similar to WT levels.

It is intriguing that although all five mutant strains show severe DNA damage after IR, they are still able to produce a reasonable number of viable progeny. In the case of the *cep-1* bearing strains, this is even more intriguing since these strains are unable to undergo DNA damage-induced apoptosis. This suggests that *cep-1* normally functions to eliminate any potentially damaged nuclei,

possibly by sensing or signalling the presence of damage. *wrn-1* mutants show the biggest reduction in progeny viability, which could suggest that *wrn-1* normally acts in a repair pathway, limiting the amount of damage after irradiation.

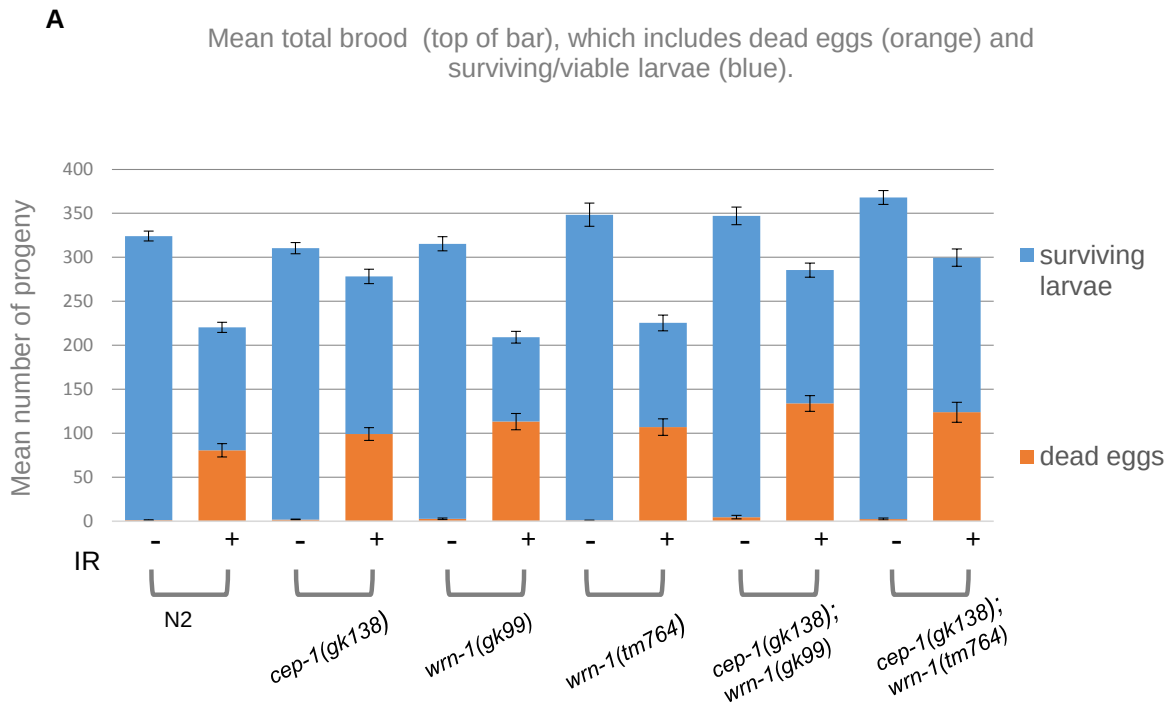

Figure 4.19: Sensitivity of WT, and *cep-1* and *wrn-1* single and double mutant L4 stage worms to IR (60 Gy). (A) The mean number of viable larvae (blue) and the mean number of dead eggs (orange) produced over a 12 hour period per five worms is shown for worms treated with 60 Gy IR (+) and those which remained untreated (-). The mean total number of progeny (the sum of viable larvae + dead eggs) is determined by the top of each blue bar. The number of dead eggs and viable larvae were counted for N2, *cep-1(gk138), wrn-1(gk99), wrn-1(tm764), cep-1(gk138);wrn-1(gk99),* and *cep-1(k138);wrn-1(tm764)*, with (+) and without (-) IR exposure at the L4 stage.

	Untreated (no IR)			+ IR (60 Gy)							
Strain	**Mean total brood No IR (chart A)**	**Mean number of dead eggs No IR (chart A)**	**% viability No IR**	**Mean total brood +IR (chart A)**	**Mean number of dead eggs +IR (chart A)**	**Mean % viability +IR (chart B)**	**Mean % embryonic lethality +IR (chart C)**	**IR-induced % decrease in total brood relative to untreated worms**	**% total brood after IR relative to total brood when no IR (chart D)**	**% viable brood after IR (relative viable brood of non IR treated worms, chart E)**	**% decrease in viable brood after IR (relative to viable brood of non IR treated worms)**
N2	324	1	100	220	81	63	37	32	68	43	57
cep-1(gk138)	310	2	99	278	99	64	36	10	90	58	42
wrn-1(gk99)	315	3	99	209	113	46	54	34	66	31	69
wrn-1(tm764)	348	1	100	226	107	52	48	35	65	34	66
cep-1(gk138); wrn-1(gk99)	347	5	99	286	134	53	47	18	82	44	56
cep-1(gk138); wrn-1(tm764)	368	3	99	300	124	59	41	19	81	48	52

Table 4.3: Sensitivity of WT, and *cep-1* and *wrn-1* single and double mutant L4 stage worms to IR (60 Gy). A summary of the data obtained from assaying brood size with and without IR (figure 4.19).

4.2.10.6 Both *wrn-1* and *cep-1* are required for the response to CPT, but not cell cycle arrest

Exposing worms to the topoisomerase I inhibitor, camptothecin (CPT) results in single stranded DNA lesions which affect replication fork progression and must be repaired in order to prevent the generation of double strand breaks (Squires et al, 1991). In the germline, mitotic cells can initiate cell cycle arrest as part of the S-phase check point in response to replication stress, thus allowing time for repair. If cells fail to repair such breaks then apoptosis must be executed in order to remove the genetically damaged cell from the germline nuclei population.

When N2 worms are exposed to CPT, enlarged mitotic nuclei are observed, indicative of a functional check point response (figure 4.20). Likewise, all *wrn-1* and *cep-1* single and double mutants show enlarged mitotic nuclei after CPT treatment, suggesting that the S phase checkpoint is intact in *wrn-1* and *cep-1* mutants.

Despite the S phase check point remaining intact in these mutants, DNA damage is evident in all mutant strains after CPT exposure. While WT oocytes display the expected number of DAPI spots corresponding to six chromosome bivalents, the number and morphology of DAPI spots in the oocytes of *wrn-1* or *cep-1* mutants varies.

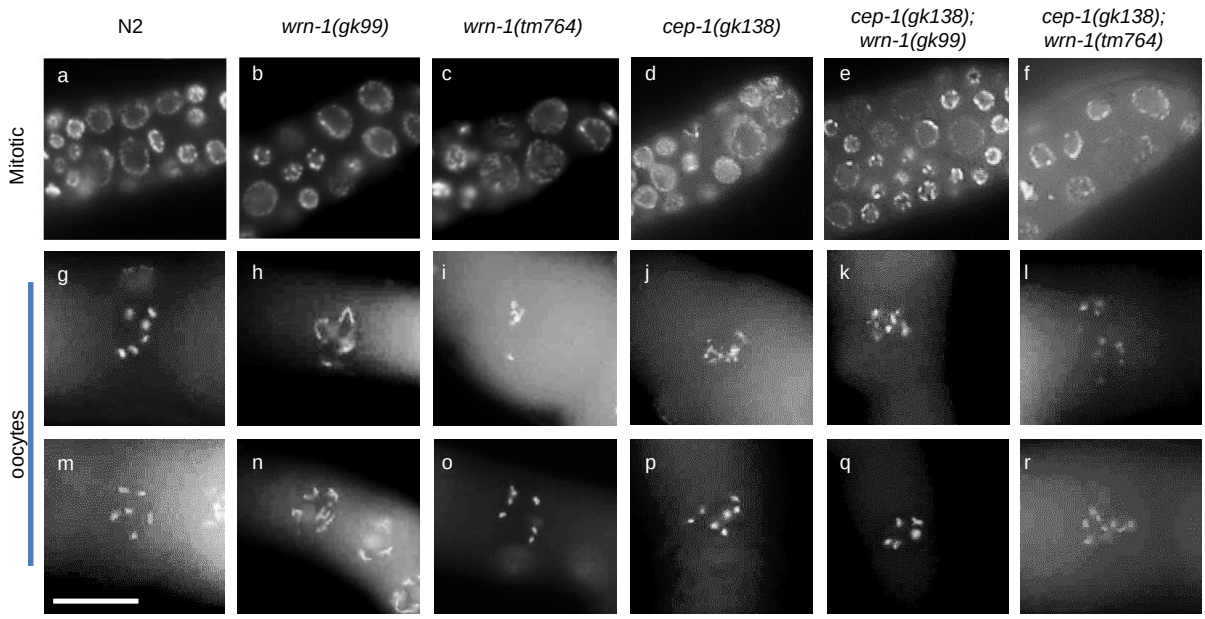

Figure 4.20: Assessment of CPT-induced germ cell proliferation arrest and DNA damage in *wrn-1* and *cep-1* mutants. Morphological changes in mitotic germline nuclei 12 hours (a-f) and 48 hours (g-r) post CPT treatment were assessed by DAPI staining of dissected gonads from: N2 (a); *wrn-1(gk99)* (b); *wrn-1(tm764)* (c); *cep-1(gk138)* (d); *cep-1(gk138);wrn-1(gk99)* (e), and *wrn-1(tm764);cep-1(gk138)* (f). Mitotic nuclei were reduced in number and increased in nuclear volume in all strains after CPT exposure, compared to untreated controls (not shown), indicating that the mitotic checkpoint is intact in these strains. The appearance of DAPI bodies in the oocytes of CPT-treated worms of the following genotypes was also assessed: N2 (g and m); *wrn-1(gk99)* (h and n); *wrn-1(tm764)* (I and o); *cep-1(gk138)* (j and p); *cep-1(gk138);wrn-1(gk99)* (k and q), and *wrn-1(tm764);cep-1(gk138)* (l and r). Six DAPI stained bodies could be identified in the oocytes of N2 worms post CPT treatment. Scale bar = 20µm.

As discussed previously, any cells in which DNA damage persists must be eliminated via programmed cell death. Consequently, N2 worms treated with CPT show elevated TUNEL stain 48 hours after treatment (figure 4.21). Similarly, the level of apoptosis is also increased in both *wrn-1* mutants, However, *cep-1* bearing strains all fail to show an increase in CPT-induced apoptosis, indicating that *cep-1* is required for DNA damage dependent apoptosis in response to CPT treatment, as would be expected.

Since the cell cycle arrest check point appears intact in *wrn-1* and *cep-1* mutants, but DNA damage is evident in both single and double mutants, this implies a DNA repair defect as opposed to a check point defect.

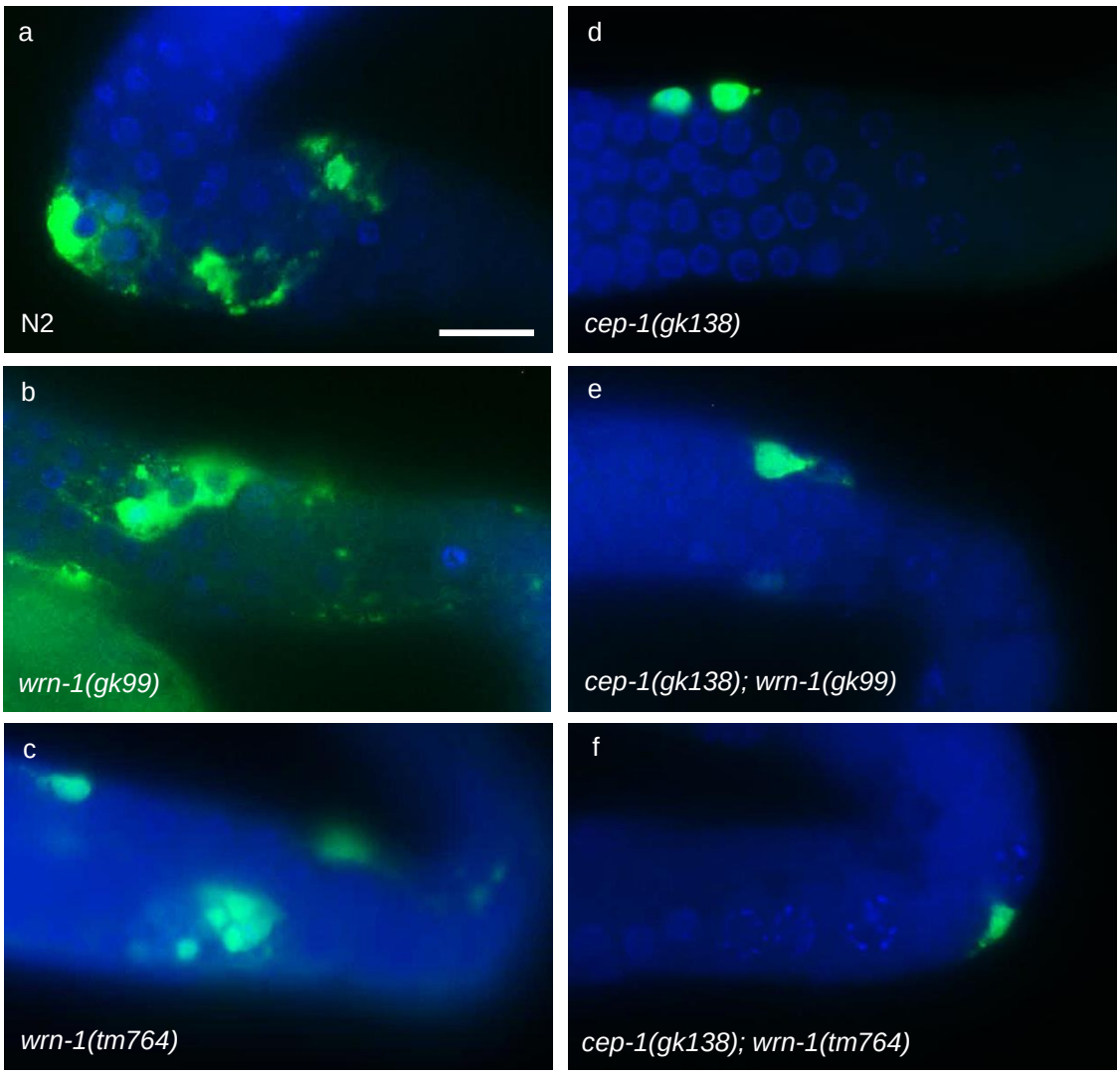

Figure 4.21: Germline apoptosis 48 hours post CPT treatment. TUNEL staining (green) was performed on the dissected gonads of worms which had been treated with CPT for 2 hours, 48 hours prior to analysis (the same analysis was performed on untreated worms (not shown). The level of apoptosis was observed in the germlines of N2 (a); *wrn-1(gk99)* (b); *wrn-1(tm764)* (c); *cep-1(gk138)* (d); *cep-1(gk138);wrn-1(gk99)* (e), and *wrn-1(tm764);cep-1(gk138)* (f). DNA was stained with DAPI (blue). Scale bar = 20µm.

4.3 Discussion

Genotoxic stress constantly challenges the replication of genetic information and its maintenance. Since the germ line of *C. elegans* (and that of all metazoa) comprises cells which are both immortal and pluripotent, it is critical that genotoxic stress and damage arising from it is both sensed and repaired or the cell removed entirely in order to maintain genome integrity of the organism and that of its future offspring.

My data suggests that neither *wrn-1* nor *cep-1* are required for cell cycle arrest in response to any of the genotoxic stressors examined in this chapter. However, both are required to maintain genome instability, not only after exogenous insults, but also under normal growth conditions, since germline defects are present (though at a relatively low frequency) even when worms are not treated with any DNA damaging agent.

From these data, I propose that *wrn-1* is required for the repair of DNA damage, whilst *cep-1* is required for the elimination of cells in which damage is irreparable, via the induction of apoptosis.

4.3.1 The response of *cep-1* to DNA damage must be carefully balanced

I and others have demonstrated that *cep-1* is required for apoptosis in response to DNA damage. Eliminating damaged cells is important in order to ensure that the genetic information carried in the germline is transmitted from one generation to the next, faithfully. If it is not, then the survival of the species is

threatened. However, if too many cells are eliminated, then the propagation of the species also suffers, since progeny production will be limited. The data presented in this chapter would suggest that as well as removing damaged cells, *cep-1* also induces apoptosis in cells which could go on to produce viable gametes. Therefore, the response of *cep-1* is one of over-reaction – a belt and braces, if you like – where the induction of a *cep-1* response causes, rather than solves problems (though, it does solve the problem of irreparable damage). The response of *cep-1* to stress requires a balancing act between beneficial outcomes such as removal of critically damaged cells, and the detrimental side effects of *cep-1* activity, such as removal of viable gametes. This mirrors the scenario observed for p53 and apoptosis in mammalian tissue . Though removal of damaged cells by apoptosis is a potent tumour suppressor mechanism, it can also deplete renewable tissues of proliferation-competent progenitor or stem cells. In turn, this depletion can compromise the structure and function of tissues – a hallmark of ageing. In light of this, the next chapter explores the role of *cep-1* and *wrn-1* in normal and premature ageing.

4.3.2 Why is germline apoptosis elevated in untreated *wrn-1(tm764)* worms but not *wrn-1(gk99)*?

Since *cep-1* is the *C. elegans* homologue of the human tumour suppressor protein, p53 (Derry et al, 2001; Greiss et al, 2008; Schumacher et al, 2001), it is possible that *wrn-1* is required for DNA-damage dependent apoptosis in the germline, since hWRN physically interacts with p53 and has been shown to be required for p53-dependent apoptosis (Spillare et al, 1999), and therefore it is possible that *wrn-1* is required for *cep-1* dependent apoptosis in the germline of

C. elegans. The *wrn-1(gk99)* is allele is reported to be a null (Lee et al, 2010a), and therefore if *wrn-1* is required for *cep-1*-induced apoptosis, then this would explain the low levels of apoptosis in this strain under normal conditions. In comparison, an antibody raised against an N-terminal peptide of WRN-1 was able to detect WRN-1 protein in the *wrn-1(tm764)* bearing strain, suggesting that a mutant form of WRN-1 is produced in these worms. The deletion in this strain removes the RecQ helicase domain of *wrn-1*, so whatever the actual identity of this mutant WRN-1 protein is, we can at least infer that it is lacking this enzyme activity. Since *wrn-1(tm764)* but not *wrn-1(g99)* displays an increase in *cep-1* dependent apoptosis under normal growth conditions, but both strains display genome instability in their germlines, it is tempting to speculate that the RecQ helicase domain of *wrn-1* (and by extrapolation, perhaps that of hWRN) is dispensable for *cep-1*/p53-dependent apoptosis, but other parts of WRN-1 are required for CEP-1-induced apoptosis. For instance, hWRN is known to interact with a wide variety of proteins (figure 4.1), and maintaining these protein-protein interactions may be critical for the induction of apoptosis.

Somewhat unexpectedly, however, *wrn-1(gk99)* as well as *wrn-1(tm764)* shows an increase in *cep-1*-dependent apoptosis in response to IR and CPT, suggesting that *wrn-1* might be required for *cep-1* dependent apoptosis only in response to specific types of DNA damage, or that apoptosis in response to severe DNA damage does not require *wrn-1*. Alternatively, it could be that *wrn-1* is required for DNA damage apoptosis in response to persistent rather than transient damage.

4.3.3 Unexpected fecundity of *cep-1* mutants

When the brood size of *wrn-1* and *cep-1* single and double mutants was assayed, *cep-1(gk138);wrn-1(tm764)* worms were found to have a brood size which was not only higher than that of either single mutant, but also that of WT, implying that when brood size is used as a read-out of success, *cep-1(gk138);wrn-1(tm764)* worms perform better than WT. Given my observation that *cep-1(gk138)* single mutants irradiated with IR show the smallest decrease in viable progeny production relative to untreated worms, this suggests that WT *cep-1* acts to limit progeny production in the face of DNA damage – whether that be endogenous (i.e. that caused by mutation of *wrn-1*) or exogenous (i.e. that caused by IR) damage. Does *cep-1* function to limit other aspects of physiology? The data presented in chapter 5 would suggest so.

Strikingly, the brood size of *cep-1(gk138)* single mutants was improved when this strain was maintained at 25°C rather than 20°C, whereas the brood size of WT worms decreases with increased temperature (Byerly et al, 1976). Is the improvement of fecundity of *cep-1(gk138)* worms at the higher temperature reflective of a more general improvement to other stresses, or is this case specific? Given that *cep-1(gk138)* worms showed greater viability of progeny after IR, relative to WT, I speculate that *cep-1* mutants may perform better in the context of other types of stress. This is explored in chapter 6.

Chapter 5 – Genetic interaction of *wrn-1* and *cep-1* reveal an unexpected lifespan extension phenotype

5.1 Introduction

5.1.1 The *C. elegans* p53 homologue, *cep-1*

Unlike higher organisms which have three p53 family members (p53, p63 and p73 (Augustin et al, 1998; Jost et al, 1997; Kaghad et al, 1997; Osada et al, 1998; Schmale & Bamberger, 1997; Senoo et al, 1998; Trink et al, 1998; Yang et al, 1998)and reviewed in (Dotsch et al, 2010; Yang et al, 2002; Yang & McKeon, 2000)), worms possess only one p53 gene (*cep-1*) (Derry et al, 2001; Jolliffe & Derry, 2013), which has a role in stress-induced apoptosis in the germline of these animals (Derry et al, 2007; Derry et al, 2001; Greiss et al, 2008; Schumacher et al, 2001; Schumacher et al, 2005). On a structural basis, the p53 family members p63 and p73, which are known to be important to normal development, have been suggested to be evolutionarily more ancient than p53 (Chi et al, 1999; Dotsch et al, 2010; Jolliffe & Derry, 2013; Lu & Abrams, 2006). Ultimately, all three proteins are thought to have arisen from a common ancestor that may be related to CEP-1 (Huyen et al, 2004).

It has been argued that CEP-1 might be more accurately described as p63 or p73. This is supported by the fact that CEP-1 contains a carboxy-terminal SAM domain, which is present in p63 and p73, but not p53 (Dotsch et al, 2010; Ou et al, 2007). Furthermore, p63 and p73 are known to affect DNA damage-induced

germ cell apoptosis (Flores et al, 2002; Levine et al, 2011; Suh et al, 2006). However, *cep-1* is considered to be more related to p53, since its principal function is to protect the germline from the effects of genotoxic damage (via the induction of apoptosis), and *cep-1* mutants do not show any overt developmental phenotypes (Derry et al, 2001). Despite a low degree of sequence homology of the DNA binding domain of CEP-1 and p53, they exhibit very similar DNA binding specificity (Dotsch et al, 2010; Huyen et al, 2004). Furthermore, both *C. elegans* BH3 domain-only proteins needed for efficient DNA damage-induced apoptosis, EGL-1 and CED-13, are transcriptionally induced by *cep-1* upon IR and UV irradiation (Schumacher et al, 2001; Schumacher et al, 2005; Stergiou et al, 2007).This response appears to be functionally equivalent to the p53-dependent transcriptional induction of mammalian BH3 domain-only proteins like PUMA and NOXA (Oda et al, 2000; Yu et al, 2001). Another possibility is that CEP-1 action represents a composite p53/p63 role. This has been suggested in light of experiments in which the CEP-1 transcriptional network was compared with the transcriptional targets of the human p53 family (Derry et al, 2007). This revealed considerable overlap between CEP-1-regulated genes and homologues regulated by human p63 and p53. Overall, however, CEP-1 is considered to be a p53 homologue, and is proving to be instrumental in elucidating the more recently discovered functions of p53 (see chapter 1).

As discussed in chapter 1, p53 is a sequence-specific DNA binding transcription factor that induces cell cycle arrest or apoptosis in response to DNA damage, and in doing so acts as a potent tumour suppressor (Lane & Levine, 2010; Levine, 1997; Vogelstein et al, 2000). The critical role played by

p53 in cancer is evident from the fact that in more than half of all human tumours, p53 function is inactivated (for instance, by missense mutations that target its sequence-specific DNA binding domain) (Hollstein et al, 1999). Whether *cep-1* acts as a tumour suppressor equivalent to p53 is moot, given the lack of somatic tumours in worms. However, germ line 'tumours' have been reported, including those arising from endoreduplication of mitotic cells in the gonad (McGee et al, 2012), and a role for *cep-1* in limiting these types of 'tumours' has been demonstrated (McGee et al, 2012). Worms mutant for *glp-1* or *gld-1* develop a different kind of germline tumour – these grow more rapidly and consist of intact germline nuclei, while the age-related endreduplication tumours grow more slowly and contain regions that are both cellularized and acellular (Francis et al, 1995a; Francis et al, 1995b; Pinkston et al, 2006). A study showed that *cep-1* does not affect the number of mitotic cells in germline tumour mutants or the shortened lifespan of these mutants (Pinkston et al, 2006). Therefore, it is likely that *cep-1* has a different mechanistic function in *C. elegans* tumours from *gld-1* and *glp-1* mutants compared to mammals (Levine, 1997). Recently, however, a role for CEP-1in limiting tumour size in *glp-1* mutants after UVC treatment was demonstrated (Hoffman et al, 2014). In addition to the role of CEP-1 in DNA damage-dependent apoptosis, CEP-1 has also been demonstrated to be required for DNA repair (Hoffman et al, 2014). Therefore, it is possible that worm p53 may act as guardian of the germline much like mammalian p53.

C. elegans mutant for *cep-1* have been reported to have a shortened lifespan at 25°C (Arum and Johnson, 2007), and either an increased or decreased lifespan depending on the level of mitochondrial stress (Baruah et al, 2014; Ventura et

al, 2009).*cep-1* mutants also display defects in germline apoptosis in response to DNA damage though not in response to physiological cues (Derry et al, 2007; Derry et al, 2001; Schumacher et al, 2001) . While it is still contested whether *cep-1* serves a p53-like tumour suppressor role in worms, I propose that its activities extend beyond regulation of germline apoptosis to regulation of worm longevity, particularly in response to genotoxic or other stresses. Moreover, I argue that *cep-1* interacts genetically with *wrn-1* and that this interaction is important in modulating lifespan.

5.2 Results

5.2.1 The combination of *wrn-1(tm764)* and *cep-1(gk138)* significantly and unexpectedly increases the lifespan of *C. elegans* at 20°C

In order to determine whether the mutation of *cep-1* would affect the lifespan of worms carrying a mutation in *wrn-1,* the survival of worms harbouring mutations in either or both of these genes was measured at 20°C, and the lifespan of N2 worms was used as a control. As revealed in chapter 3, mutation of *wrn-1* reduces the lifespan of *C. elegans* relative to N2 worms. Similarly, the lifespan of *cep-1(gk138)* single mutants was also reduced in comparison to N2 worms (see figure 5.1), suggesting that *cep-1* is required to maintain normal lifespan at this temperature.

Strikingly, *cep-1(gk138)*;*wrn-1(tm764)* double mutants had a significantly increased lifespan, far beyond that of N2 controls (figure 5.1). This result was somewhat unexpected at first sight and was made even more intriguing by the fact that *cep-1(gk138);wrn-1(gk99)* worms did not display this lifespan extension (figure 5.1). As it would happen, this allelic difference would prove highly informative for the mechanistic understanding of how the combinatorial loss of p53 and *wrn-1* activity could lead to such a large lifespan extension and is discussed in chapter 6.

What is really striking about the lifespan extension observed for *cep-1(gk138);wrn-1(tm764)*, is the delay in the onset of mortality, as indicated by the extended plateau part of the lifespan curve (figure 5.1) for this strain. For instance, at the time point at which 50% survival is reached for the single

mutants *cep-1* and *wrn-1* (around 17 days post L4), approximately 90% of the *cep-1(gk138);wrn-1(tm764)* animals are still alive. These double mutants reach 50% survival at roughly 27 days post L4.

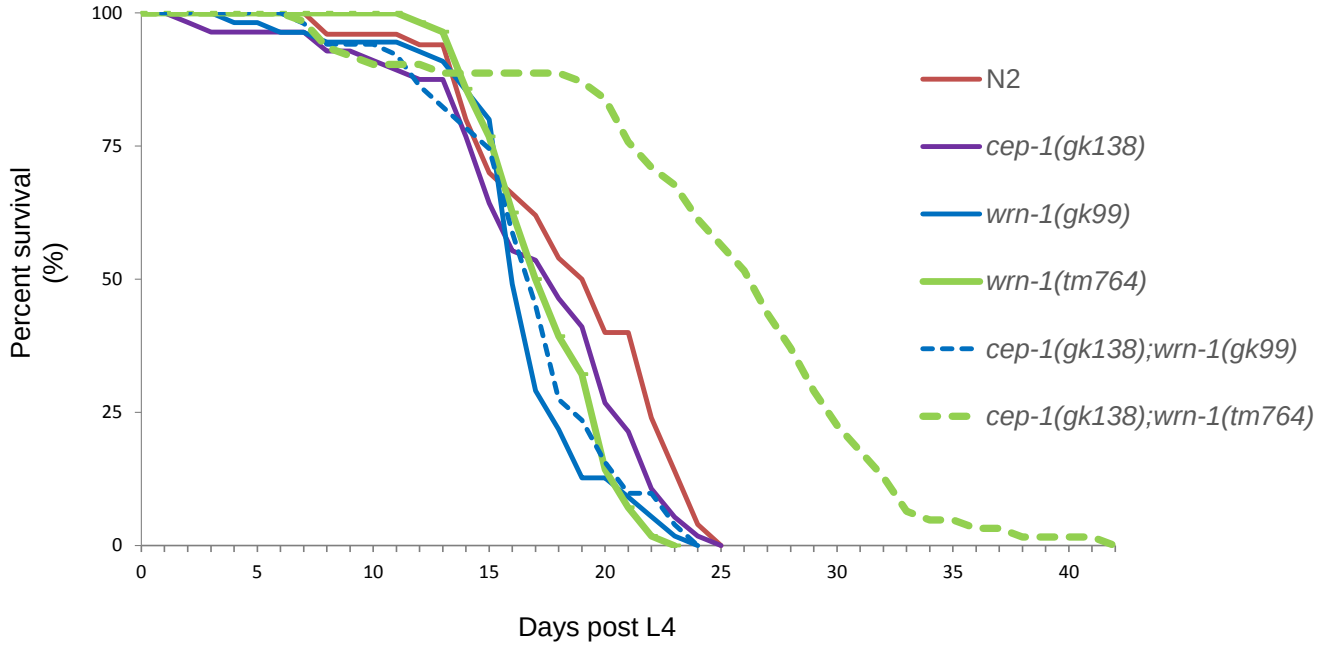

Figure 5. 1: Unexpected synthetic superviability of *cep-1;wrn-1* double mutants. Lifespan of *wrn-1* and *cep-1* single and double mutant worms relative to N2 worms, at 20°C. *n* values for the experiment shown: N2 = 50; *cep-1(gk138)* = 56; *wrn-1(gk99)* = 55; *wrn-1(tm764) = 56; cep-1(gk138);wrn-1(gk99)* = 51; and *cep-1(gk138);wrn-1(tm764)= 62.*

5.2.2 *cep-1(gk138);wrn-1(tm764)* double mutants are not only longer lived but also have an extended healthspan.

Ageing well is arguably more important than *living longer*, therefore I sought to confirm whether these long lived mutants also had an increased healthspan. The shape of the survival curve alone hinted that this was the case and phenotypic analysis confirmed this.

From the photographs in figures 5.2 and 5.3, it is clear that worms mutant for either *wrn-1* or *cep-1* look phenotypically 'older' and 'sicker' in appearance. The same is true for *cep-1(gk138);wrn-1(gk99)* worms, whilst *cep-1(gk138);wrn-1(tm764)* hermaphrodites on the other hand look much more youthful in comparison. Even at this relatively low magnification, tissue deterioration is visible in the single mutants and *cep-1(gk138);wrn-1(gk99)* doubles, and even in N2 worms, though to a somewhat lesser degree, at 7 days post L4. With increasing age, the length of a worm decreases due to shrinkage (of the cuticle), and consequently N2, *wrn-1* and *cep-1* single mutants and *cep-1(gk138);wrn-1(gk99)* worms all appear shorter in length compared to *cep-1(gk138);wrn-1(tm764)*. At day 14 (figure 5.3), *cep-1(gk138);wrn-1(tm764)* mutants retain a youthful appearance, whilst all of the other strains assessed look even more aged and show even greater tissue deterioration. This prolonged youthful appearance of *cep-1(gk138);wrn-1(tm764)* worms mirrors the lifespan curve see in figure 5.1.

Further support for the extended healthspan of *cep-1(gk138);wrn-1(tm764)* was obtained from high magnification images of worms at various ages. As figure 5.4 shows, looking at images taken of worms 10 days post L4 for example, tissue deterioration is already obvious in both the head region (particularly the pharynx, panel A figure 5.4) and in the mid-body of the worm (panel B, figure 5.4), where the intestine and the gonad are hard to identify. In the case of *cep-1(gk138);wrn-1(tm764)* worms, tissue deterioration is less evident and organs can still easily be identified, again indicating that these worms are healthier for a longer of period of time compared to N2 worms and the single mutants (and the *cep-1(gk138);wrn-1(gk99)* double mutant).

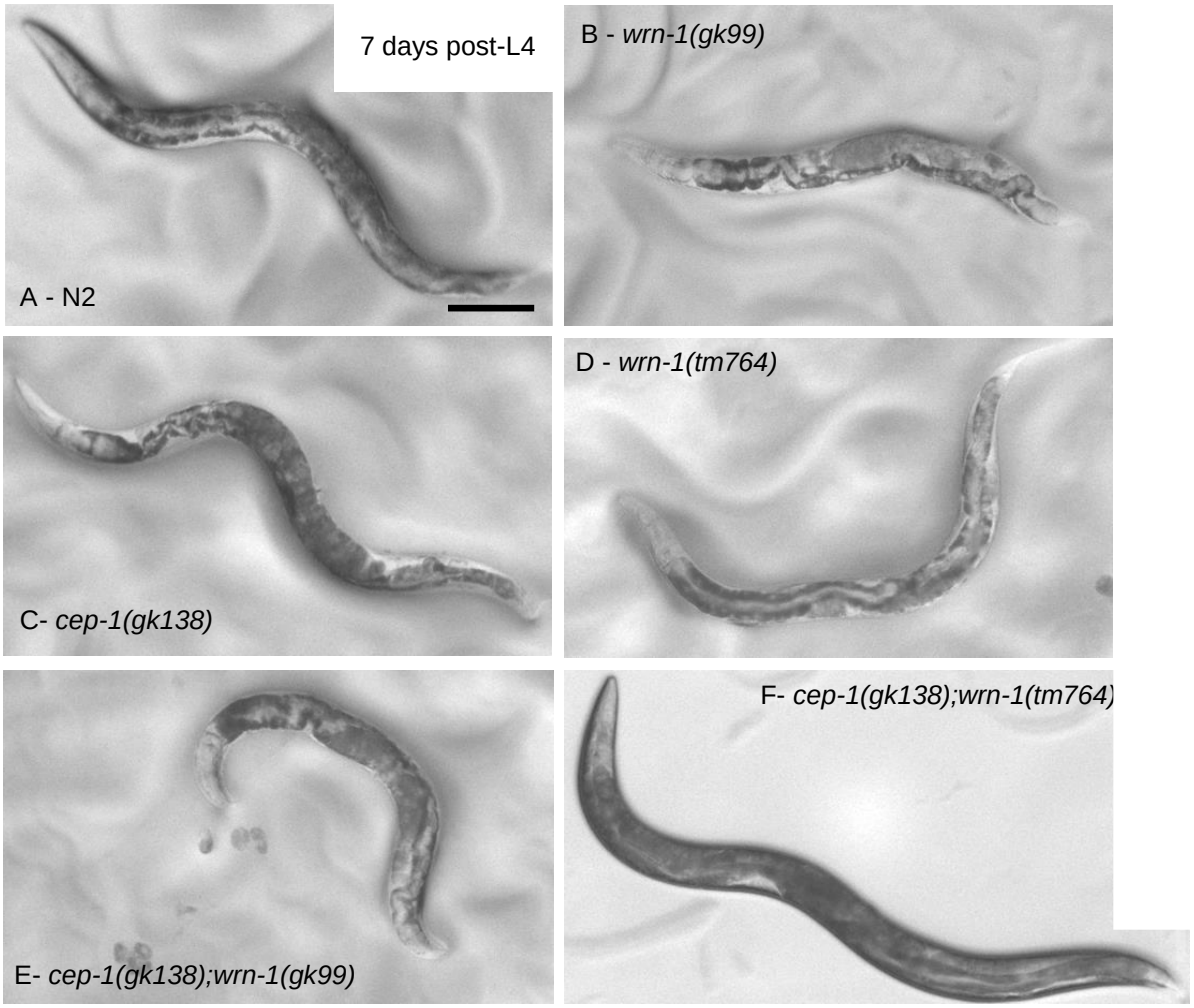

Figure 5.2: Delayed ageing of *cep-1;wrn-1* double mutants 7 days post-L4. The appearance of worms 7 days post-L4 at 20°C. Representative photographs of hermaphrodites 7 days post L4 at 20°C. (A) N2, (B) *wrn-1(gk99)*, (C) *cep-1(gk138)*, (D) *wrn-1(tm764)*, (E) *cep-1(gk138);wrn-1(gk99)* ,and (F) *cep-1(gk138);wrn-1(tm764).* Scale bar = 100µm.

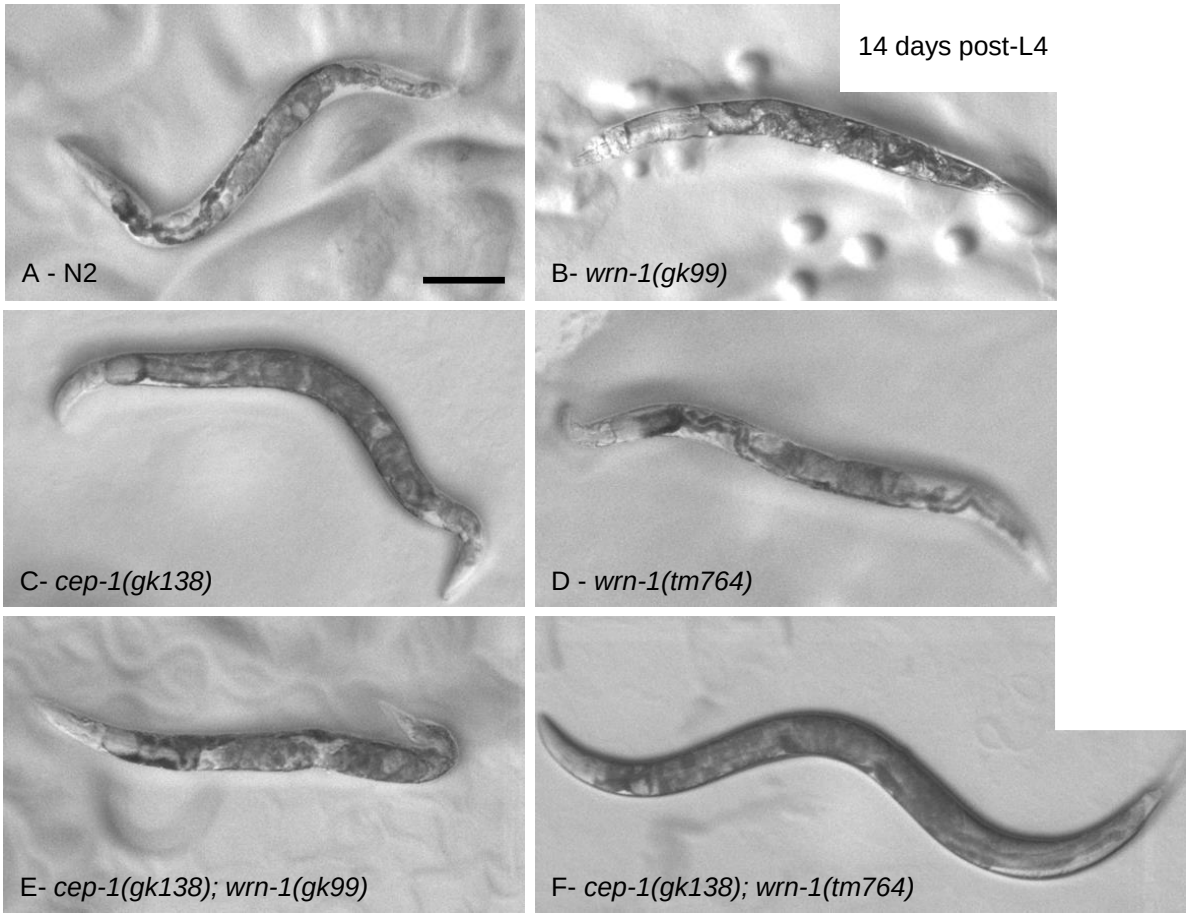

Figure 5.3: Delayed ageing of *cep-1;wrn-1* double mutants 14 days post-L4. The appearance of worms 14 days post-L4 at 20°C. Representative photographs of hermaphrodites 14 days post L4 at 20°C. (A) N2, (B) *wrn-1(gk99)*, (C) *cep-1(gk138)*, (D) *wrn-1(tm764)*, (E) *cep-1(gk138);wrn-1(gk99)* ,and (F) *cep-1(gk138);wrn-1(tm764).* Scale bar = 100µm. Note the extensive tissue deterioration and lack of sigmoidal body shape in all strains apart from *cep-1(gk138);wrn-1(tm764).*

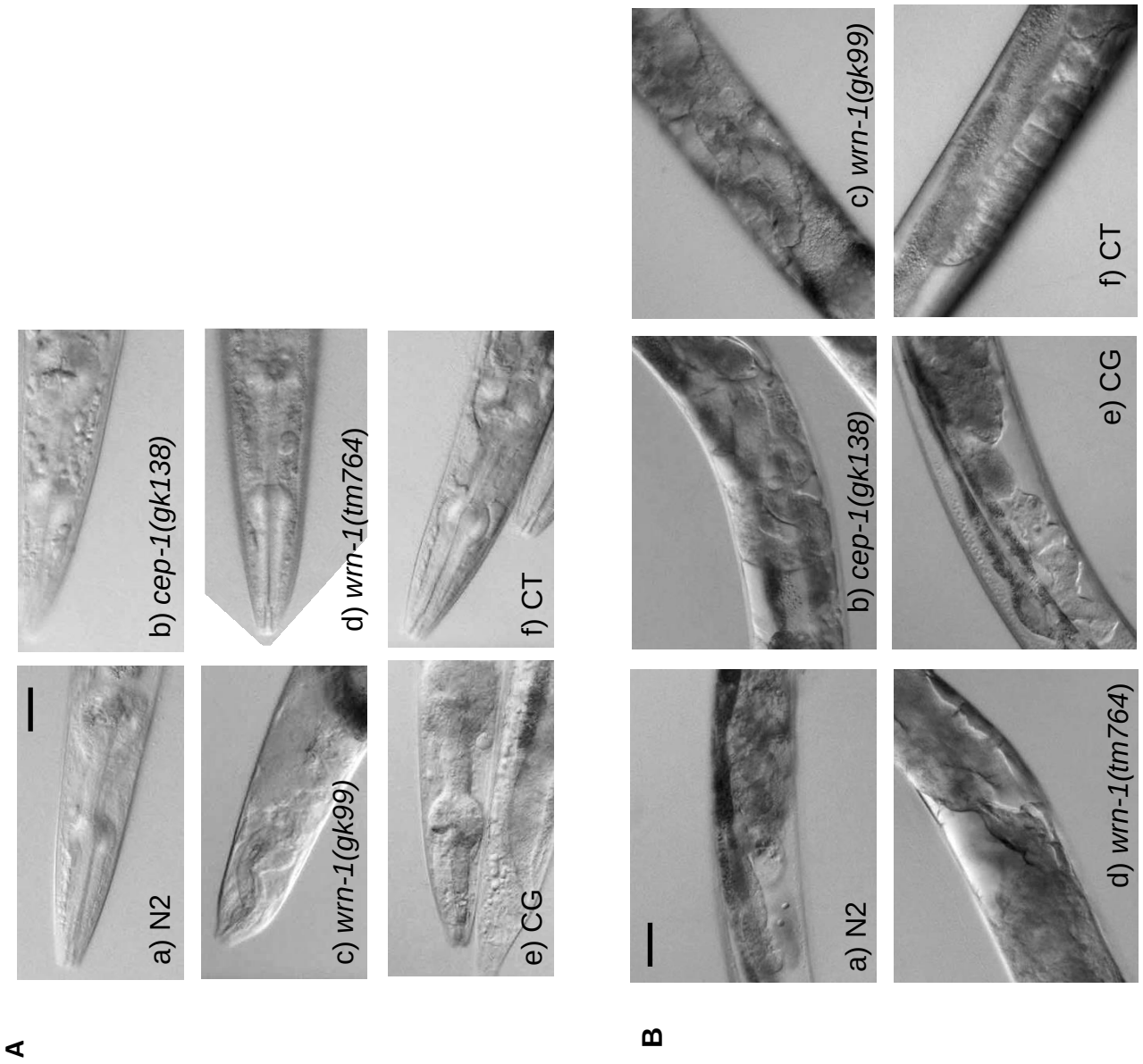

Figure 5.4: High magnification images of A) the head region, and B) the mid-body of worms 10 days post L4. Shown are representative images of: (a) N2; (b) *cep-1(gk138)*; (c) *wrn-1(gk99);* (d) *wrn-1(tm764);* (e) CG = *cep-1(gk138);wrn-1(gk99);* and (f) CT = *cep-1(gk138);wrn-1(tm764).*A) The morphology of the pharynx becomes less distinct with age, due to tissue deterioration and appearance of lipid droplets, however, tissue integrity appears to be maintained in *cep-1(gk138);wrn-1(tm764)* (panel A, f) worms of the same chronological age. B) tissue deterioration of the gonad and the intestine is also evident in worms 10 days post L4, however the gonad and intestine can still be distinguished in *cep-1(gk138);wrn-1(tm764)* worms (image B, f). Scale bar = 100µm.

Furthermore, the lack of the characteristic ‘sigmoidal’ body shape of all worms except the long –lived double mutant also suggests that locomotion has severely declined in these worms, and measurement of the thrashing rate for worms in liquid media confirms this (figure 5.5). In all strains but *cep-1(gk138);wrn-1(tm764)*, the thrash rate declined with age (i.e. it declines between graphs A, B, C and D. However, the thrash rate for *cep-1(gk138);wrn-1(tm764)* remains high, and at all ages examined the spread of the average number of thrashes between individual worms is much less than that seen for all the other strains. Therefore, analysis of thrashing rates demonstrates that *cep-1(gk138);wrn-1(tm764)* worms have a prolonged healthspan as well as lifespan, since locomotive capabilities are maintained even in later life.

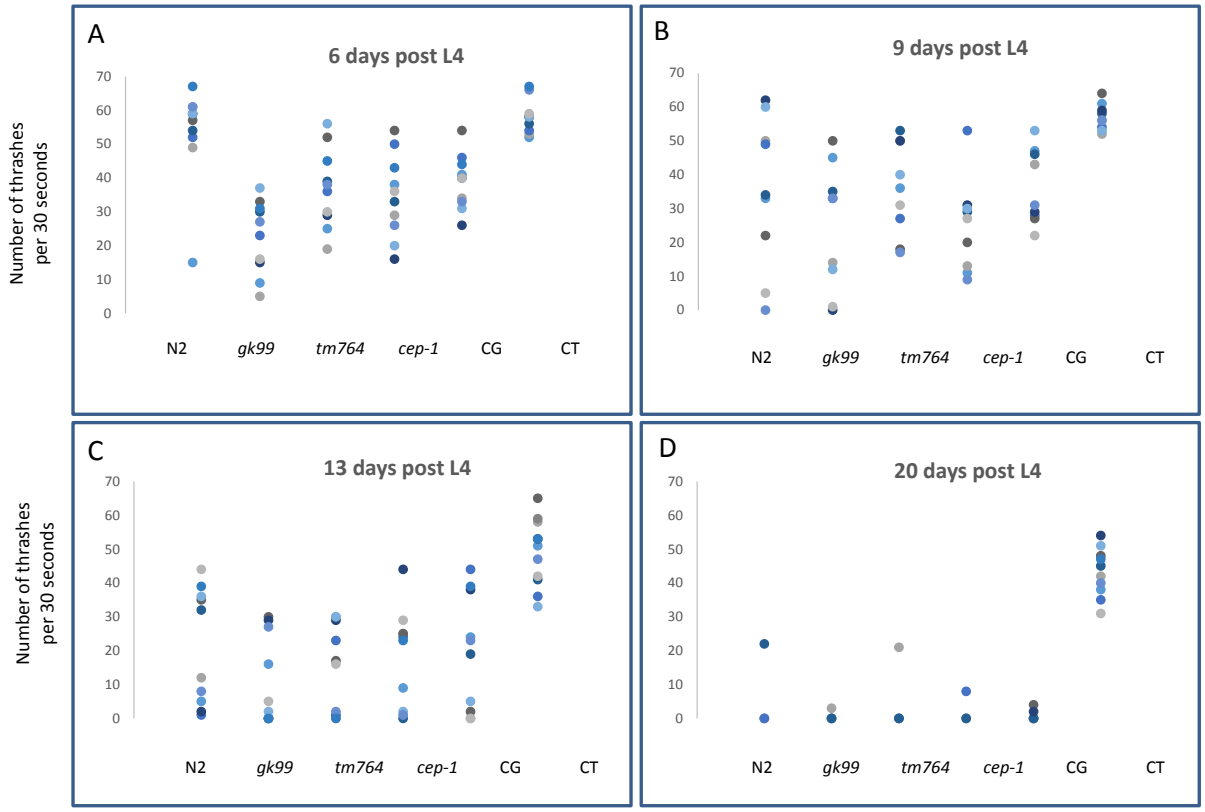

Figure 5.5: Healthspan assessment in *wrn-1/cep-1* mutants. Graphical representation of the number of thrashes performed in a 30 second period for individual worms of a given genotype. Each point corresponds to a different worm, all of which had been maintained at 20 degrees . Each graph corresponds to worms at a different number of days post L4. As worms age, the thrash rate declines. However, the thrash rate of *cep-1(gk138);wrn-1(tm764)* worms remains high, even when assessed at 20 days post L4 (graph D). *Gk99 = wrn-1(gk99)*, *tm764 = wrn-1(tm764*), *cep-1 = cep-1(gk138)*, CG = *cep-1(gk138);wrn-1(gk99),* CT = *cep-1(gk138);wrn-1(tm764).*(D) at this time point (20 days post L4) few worms remained alive for all the strains except for *cep-1(gk138);wrn-1(tm764)*, so consequently there are fewer data points.

Another feature of ageing worms is the appearance and growth of so-called 'germline tumours'. These are not tumours in the traditional sense – instead they arise from endoreduplcation of unfertilised oocytes, resulting in large chromatin masses which initially build up in the uterus and spread into the rest of the gonad and eventually fill up the entire diameter of the worm. Since these germline masses are associated with ageing in the worm and are also detrimental, I sought to determine whether appearance of this age-associated phenotype was also delayed in *cep-1(gk138);wrn-1(tm764)* worms. As figure 5.6 shows, this is indeed the case. These worms on average show fewer chromatin masses compared to age –matched worms of all other genotypes examined, including N2.

Figure 5. 6 (see next page): Germline tumours in aged *wrn-1/cep-1* mutants. Representative images of age-related endoreduplication in worms 8 days post L4**.** Photographs of whole worms stained with DAPI were used to qualitatively assess the appearance of chromatin masses. Scale bar = 200 µm. Compared to worms of the same age but of different genotypes, *cep-1(gk138);wrn-1(tm764)* worms on average show fewer chromatin masses.

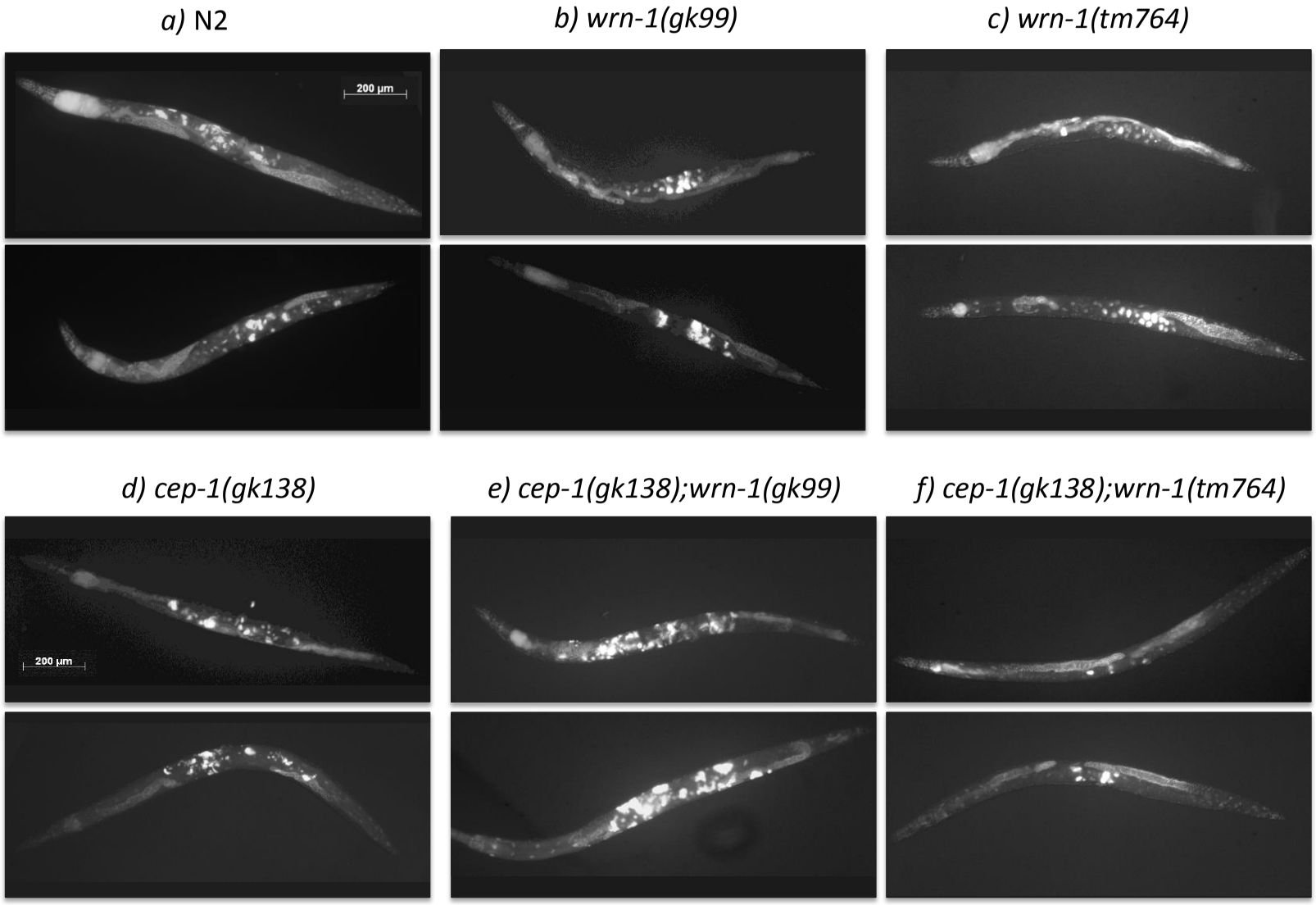
a) N2
b) wrn-1(gk99)
c) wrn-1(tm764)
200 µm
d) cep-1(gk138)
e) cep-1(gk138);wrn-1(gk99)
f) cep-1(gk138);wrn-1(tm764)
200 µm

5.2.3 The extreme longevity of *cep-1(gk138);wrn-1(tm764)* worms is completely dependent on *daf-16*

Epistasis with *daf-16* (mutation of which shortens lifespan (Kenyon et al, 1993; Lin et al, 1997; Ogg et al, 1997)) is a commonly used experimental tool to begin to investigate the molecular basis of lifespan extension phenotypes in *C. elegans*. In order to determine whether the longevity of *cep-1(gk138);wrn-1(tm764)* mutants is *daf-16* dependent, RNAi of *daf-16* was performed on this strain and on N2 as a control (figure 5.7.A). As expected, the lifespan of N2 worms in which *daf-16* is knocked down is reduced compared to the lifespan of N2 worms treated with bacteria carrying the empty vector control (maximum lifespan = 18 and 24 days, respectively), indicating that the RNAi was working in this experiment. The same RNAi performed on *cep-1(gk138);wrn-1(tm764)* completely abrogated the lifespan increase observed in these mutants on the empty vector control (maximum lifespan = 41 and 22 days, respectively), demonstrating the complete dependency of this lifespan extension phenotype on *daf-16*. This point is further emphasised when looking at the time point where less than 5% of *cep-1(gk138);wrn-1(tm764)* worms treated with *daf-16* RNAi are alive – here, over 95% of this strain grown on the empty vector-expressing control bacteria survive. RNAi of *daf-16* also reduced the healthspan of both N2 and *cep-1(gk138);wrn-1(tm764)* worms (figure 5.7.B), resulting in the lack of youthful appearance by 13 days post L4, compared to empty vector controls.

Intriguingly, these data also suggested that the bacterial strain used in this experiment, HT115, further improves the healthspan of *cep-1(gk138);wrn-1(tm764)* worms in the case where empty vector is used, since the plateau

region of the curve is both extended and is at a higher survival percentage compared to that seen when the worms are grown on OP50 (around 95-97% survival compared to a plateau at around 90% when the double mutant is grown on OP50, figure 5.1). For worms grown on HT115, the time point (in days) at which 50% of the *cep-1(gk138);wrn-1(tm764)* worms remain viable is doubled compared with controls (figure 5.7), whereas for worms grown on OP50, the effect, whilst highly significant, is slightly less extreme (figure 5.1).

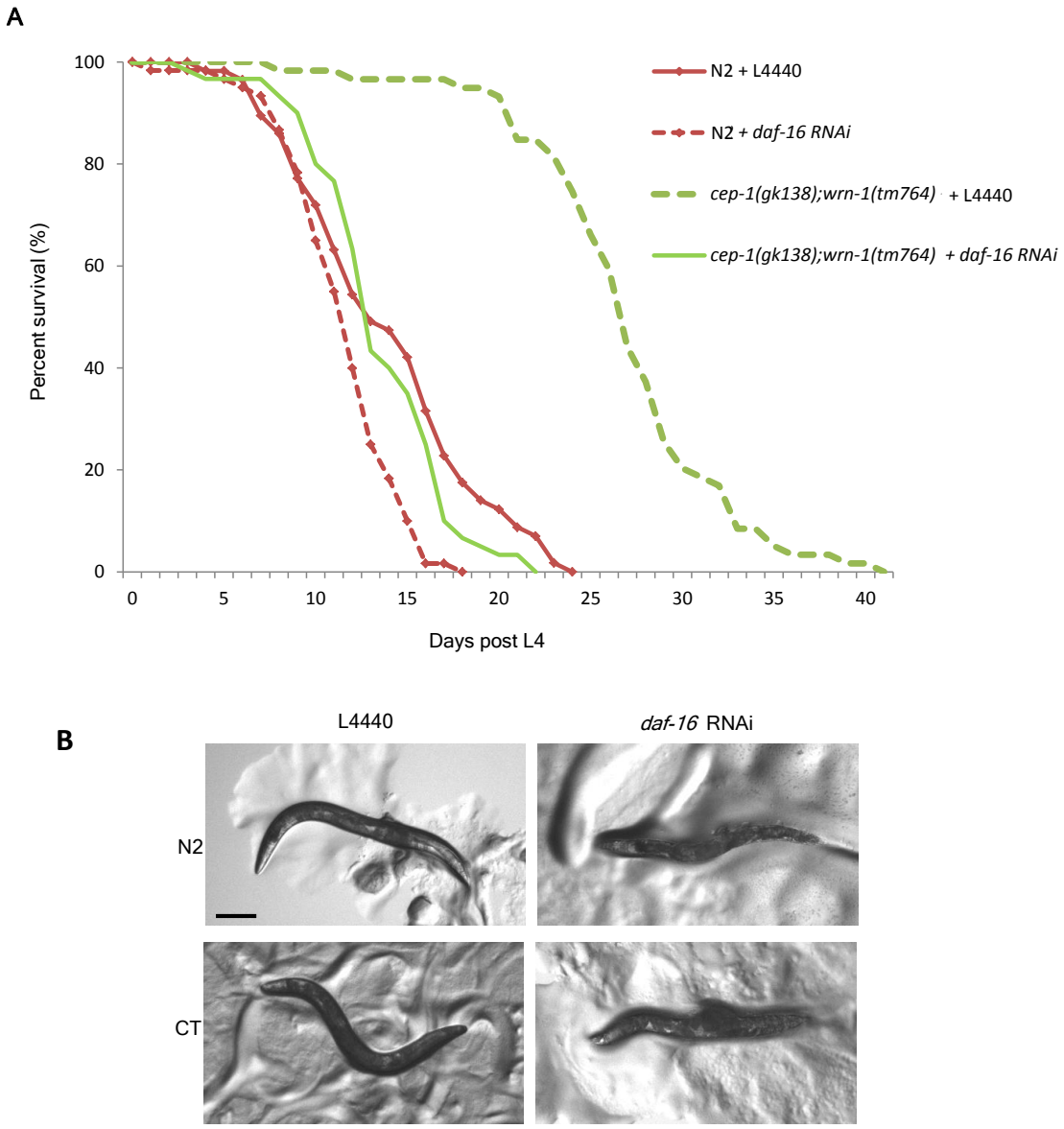

Figure 5.7: The longevity of *cep-1(gk138);wrn-1(tm764)* is completely dependent on *daf-16*. A) The effect of *daf-16* RNAi on the lifespan of the long-lived *cep-1(gk138);wrn-1(tm764)* double mutant, at 20°C. Knock-down of *daf-16* in N2 worms shortens the lifespan of these worms. When *daf-16* is knocked-down in *cep-1(gk138);wrn-1(tm764),* the increased lifespan of this strain is completely abolished. Therefore, the longevity of these worms is completely dependent on *daf-16.* L4440 was used as the empty vector control. B) Representative photographs of whole worms at 13 days post L4. Knockdown of *daf-16* by RNAi also ameliorates the healthspan of *cep-1(gk138);wrn-1(tm764).* Double mutants fed on empty vector appear youthful in comparison to those treated with *daf-16* RNAi. CT = *cep-1(gk138);wrn-1(tm764).* Scale bar = 200µm.

5.2.4 The longevity of *cep-1(gk138);wrn-1(tm764)* double mutants correlates with increased DAF-16::GFP nuclear localisation

In many but not all long-lived mutants which show *daf-16*-dependent longevity, DAF-16 is nuclear. Since the genetic combination of *wrn-1(tm764)* and *cep-1(gk138)* extends the lifespan of *C. elegans* in a *daf-16*-dependent manner, I asked whether this double mutant causes DAF-16 nuclear accumulation. All strains were crossed into a DAF-16::GFP (TJ356) background and the subcellular localisation of this reporter was compared between strains, and at different ages.

As expected, DAF-16::GFP was found to be expressed in most cell types and was predominantly cytoplasmic in WT worms maintained at 20 degrees (figure 5.8, panel a). Furthermore, the subcellular localisation of DAF-16::GFP did not change with age in these worms. Overall, the same was true for *wrn-1* and *cep-1* single mutants, and for *cep-1(gk138);wrn-1(gk99)* double mutant (figure 5.8, panels b-e), although there was variability in the subcellular localisation between worms of a given strain – some worms did show nuclear DAF-16::GFP, though the majority did not. This variation could be caused by differing population densities between plates, since overcrowding has been shown to cause translocation of DAF-16 to the nucleus (Henderson & Johnson, 2001) and this was found to be true in the case of these strains (data not shown). However, DAF-16::GFP is more prominently nuclear localised in *cep-1(gk138);wrn-1(tm764)* than in WT, and this becomes more evident with age (for instance by 7 days post L4, figure 5.8, panel f) and with increased temperature (see next chapter). In summary, although there is a greater

tendency for the long lived *cep-1(gk138);wrn-1(tm764)* to show nuclear DAF-16::GFP, this is by no means complete in terms of the number of nuclei or the number of worms it is seen in. Thus, complete nuclear localisation of DAF-16 is not required for the longevity of this strain.

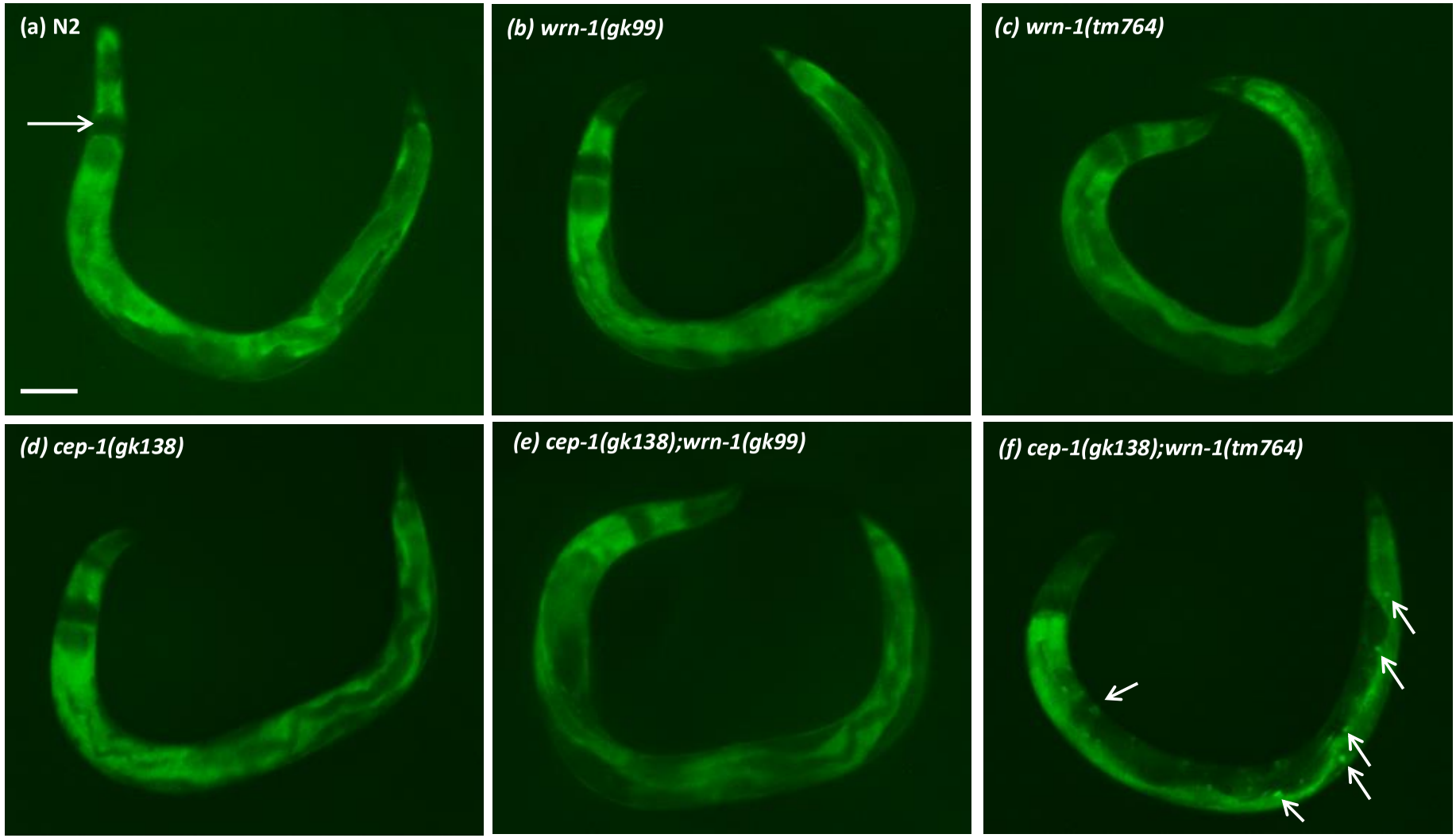
(a) N2
(b) wrn-1(gk99)
(c) wrn-1(tm764)
(d) cep-1(gk138)
(e) cep-1(gk138);wrn-1(gk99)
(f) cep-1(gk138);wrn-1(tm764)

Figure 5. 8: Localisation of DAF-16::GFP in *cep-1/wrn-1* mutants.
Representative images of DAF-16::GFP localisation in worms maintained at 20°C. Images were taken at 7 days post L4. DAF-16::GFP is predominantly cytoplasmic and widely expressed (except in the pharynx (arrow, panel a) and germline) in all strains (a-e), but a higher proportion of worms and cells show nuclear DAF-16::GFP (arrows) in *cep-1(gk138);wrn-1(tnm764)* double mutants (f). Scale bar = 100µm.

5.2.5 The neomorphic lifespan extension phenotype seen in *cep-1(gk138);wrn-1(tm764)* may not be specific to just *wrn-1*, but other RecQ helicases

The unexpected finding that *wrn-1(tm764)* and *cep-1(gk138)* alleles, when mutated individually have reduced life span, whereas double mutants display extreme longevity, begged the question whether this was a gene-specific phenomenon, or whether it could be recapitulated by other mutant combinations. When *cep-1(gk138)* was crossed into another RecQ helicase mutant, *him-6(ok412)* (Bloom syndrome homologue (Grabowski et al, 2005)), the lifespan of these double mutants also appeared to be greater than that of either single mutant, though the effect was much less pronounced. 60% of *cep-1(gk138);him-6(ok412)* double mutants were viable at time points when *cep-1* or him-6 single mutants displayed ≤20% viability (see figure 5.9). Although this is only a modest increase in lifespan, it is important to note that *him-6(ok412)* is phenotypically a lot sicker than *wrn-1(tm764)* worms, having a greatly reduced brood size and high incidence of males, as well as a mortal germline phenotype (Grabowski et al, 2005). Since the loss of *cep-1* in a *wrn-1(tm764)* background does not ameliorate the genomic instability seen in these worms (figure 4.8), it is unlikely that the genomic instability phenotypes of *him-6(ok412)* single mutants is abrogated in a *cep-1(gk138)* background either. Perhaps the more severe genomic instability in *him-6(ok412)* somewhat masks the longevity produced by the presence of *cep-1(gk138),* and hence the lifespan extension seen in the double mutants is not as great as that observed for *cep-1(gk138);wrn-1(tm764).*

It is intriguing to recall at this point that we have already encountered the phenomenon of *wrn-1* mutation leading to a lifespan extension in the context of FUdR treatment (figure 3.6).

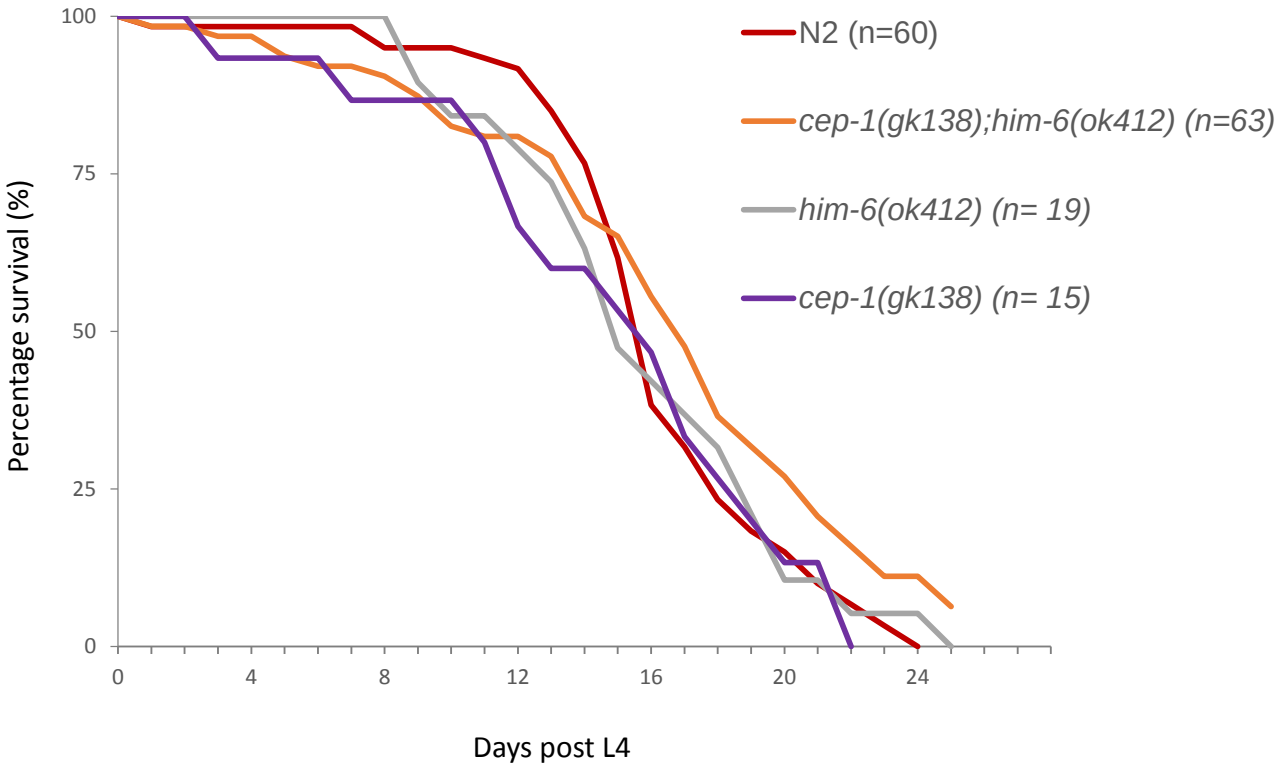

Figure 5.9: Preliminary lifespan analysis of *cep-1(gk138)* and *him-6(ok412)* single and double mutants. The lifespan of N2 control worms and *cep-1(gk138);him-6(ok412)* double and single mutants was assayed at 20°C. The lifespan of *him-6(ok412)* was found to be similar to that published (Grabowski et al, 2005), and was not significantly different from that of *cep-1(gk138)*. *cep-1(gk138);him-6(ok412)* double mutants show an increased lifespan relative to N2 worms, suggesting that the lifespan of the double mutant is improved relative to either single mutant. Given the low *n* numbers for this experiment, these results are preliminary.

5.3 Discussion

Mutation of *wrn-1* is detrimental at the cellular level (see chapter 4 – mutation of *wrn-1* causes genomic instability) and also at the organismal level, since *wrn-1* mutants have a shortened lifespan. Mutation of *cep-1* also reduces the lifespan of *C. elegans*. However, the combination of mutations in both of these genes surprisingly results in strikingly improved organismal lifespan under the conditions outlined in this chapter. Furthermore, not only is the lifespan of *cep-1(gk138);wrn-1(tm764)* increased, but the healthspan of these worms is also enhanced. The long life and extended healthspan of these worms is completely dependent on *daf-16*, a master regulator of ageing.

This synthetic interaction is striking for several reasons. To my knowledge, there are no other examples in the literature of two mutations, which individually are detrimental to lifespan but in combination are not only beneficial but rescue the lifespan deficit of the single mutants *beyond* that of WT. Other recent reports have focused on identifying genetic or chemical factors which individually produce an unfavourable phenotype but together rescue this phenotype to WT or nearly-WT levels. For example, I discussed an example of this in chapter 3, relating to mutation of BRCA1 and 53BP1 (Bouwman et al, 2010), and NAT10 and LMNA (Larrieu et al, 2014). Synthetic viability would seem a suitable term to describe this phenomenon. However, the genetic interaction observed in the case of *cep-1(gk138);wrn-1(tm764)* is not simply one in which the WT phenotype (in this case, WT lifespan) is restored, but the phenotype is actually enhanced or improved far beyond that of WT. Since there is no precedence for a genetic phenomenon like this in the literature, deciding

on suitable terminology for this is difficult. However, '*synthetic super-viability*' probably best describes the phenotypic consequence of the combination of *wrn-1(tm764)* and *cep-1(gk138).*

Another intriguing point regarding this synthetic super-viability is that despite being long lived and 'healthier' for longer, these worms still display genomic instability and are highly sensitive to DNA damaging agents (see chapter 4). The genomic instability observed in *wrn-1* mutants and indeed in WS cells has been postulated to play a causal role in the premature ageing seen in *wrn-1* worms and WS patients. So why, then, do *cep-1(gk138);wrn-1(tm764)* worms not age prematurely, despite also showing genomic instability? The damage theory of ageing speculates that the accumulation of damage to DNA and to other macromolecules drives ageing (Kirkwood, 1998; Kirkwood, 2002; Kirkwood, 2005; Kirkwood & Kowald, 1997; Kowald & Kirkwood, 1996). If this were true, then *cep-1(gk138);wrn-1(tm764)* would not be long lived. This disagreement can be reconciled if, perhaps, it is not DNA damage (or other types of damage) *per se*, that causes ageing, but the sensing and/or response to that damage. DNA damage is a form of stress which activates (or is sensed and responded to by) p53. Since p53 is activated not only by DNA damage, I wanted to address the question whether the lack of sensing or response to other types of stress by p53/*cep-1* could have a similar lifespan extending effect in a *cep-1* mutant background. The data presented in chapter 6 begins to address this question.

5.3.1 Is extreme longevity specific to *cep-1(gk138);wrn-1(tm764)*?

Although *cep-1(gk138);wrn-1(tm764)* represents an interesting case of longevity in its own right, it is important to address whether the extended lifespan is specific to a) the particular alleles used, and b) the combination of *wrn-1* and *cep-1*. At first, it is a curious fact that *cep-1(gk138)* extends the lifespan of *wrn-1(tm764)* but not that of *wrn-1(gk99)*. A worrying possibility would be that an unknown background mutation in either of the *wrn-1* strains is responsible for the difference in longevity when *cep-1(gk138)* is present. As we will see in the next chapter, this is not the case. It also seems likely that synthetic super-viability is not restricted to just the combination of *wrn-1* and *cep-1*, since *cep-1(gk138);him-6(ok412)* also show a modest enhancement of lifespan despite the two single mutants being short lived (figure 5.9). Furthermore, as described in chapter 3, *wrn-1(gk99);mut-7(pk204)* and *wrn-1(tm764);mut-7(pk204)* showed synthetic viability (note, I have not referred to this as 'super' viability since the lifespan of the double mutants was not greater than that of WT), showing that both alleles of *wrn-1* can be combined with another lifespan reducing mutation to increase lifespan beyond that of the single mutants.

In chapter 3 (figure 3.6), the short lifespan of *wrn-1(tm764)* worms could also be modulated by FUdR – in this case, beyond the lifespan observed for WT controls. Does this represent another example of synthetic super viability? Strictly speaking, it does not, since FUdR treatment of WT worms does not causes a decrease in lifespan (Gandhi et al, 1980; Hosono et al, 1982; Mitchell et al, 1979; Sutphin & Kaeberlein, 2009). However, this is a further example

demonstrating that the lifespan of *wrn-1(tm764)* worms can be modulated, and the influence of *wrn-1(tm764)* on ageing appears to be highly context-dependent (in some instances it results in longevity, while in others it limits it). The very different lifespan trajectories of *wrn-1(tm764)* in a *cep-1(gk138)* background versus treatment with FUdR (i.e. the difference in the shape of the lifespan curves, despite both representing an increased lifespan –see figures 3.6 and 5.1) suggests that the mechanisms responsible for increased longevity in each instance may be different. The lifespan curve of *wrn-1(tm764)* worms grown in the presence of FUdR mirrors that of untreated *wrn-1(tm764)* worms up until 50% of the worms assayed had died (figure 3.6). After this point the lifespan curves diverge, with rapid mortality observed for untreated worms, and a slower rate of death for those treated with FUdR. This suggests that FUdR alters mid- to late-life ageing. In contrast, the lifespan curve of *cep-1(gk138);wrn-1(tm764)* double mutants (figure 5.1) suggests that ageing is improved from the beginning of adulthood (or possibly before), since the onset of mortality is significantly delayed relative to *wrn-1(tm764)* single mutants. Therefore, *cep-1(gk138);wrn-1(tm764)* worms have a slower rate of ageing and consequently remain healthy for longer. In conclusion, I suggest that the longevity mechanisms behind lifespan extension of *cep-1(gk138);wrn-1(tm764)* mutants differ (to at least some degree) from the mechanisms at play when FUdR is used. Further epistasis analysis should enable such mechanisms to be teased apart.

5.3.2 How does SSV work?

The longevity observed for *cep-1(gk138);wrn-1(tm764)* strains cannot be explained by the 'disposable soma' theory of ageing. The theory stipulates that organisms reproduce at the expense of long life (Kirkwood & Holliday, 1979), allocating resources to producing the production of offspring rather than maintenance of the soma, with the consequence that late-life fitness is neglected, resulting in early death. Although there are many reports of long lived *C. elegans* strains which produce fewer progeny than WT, for instance, those which have had their germlines ablated (Arantes-Oliveira et al, 2002; Hsin & Kenyon, 1999) , *cep-1(gk138);wrn-1(tm764)* on the other hand have a larger brood size than WT (figure 4.11), demonstrating that progeny production can be uncoupled from longevity. Perhaps this result can also be reconciled by the possibility that a sensing or response mechanism is disrupted by the loss of *cep-1*.

However, this brings us back to the question – why does the combination of *wrn-1(tm764)* and *cep-1(gk138)* improve lifespan *beyond* that of WT? Perhaps the combined mutation of both of these genes establishes a physiological state which favours long life. Broadly speaking, this might resemble hormesis – the induction of enhanced survival and robustness by exposure to transient, low level stress, which is protective against a future stress (Cypser & Johnson, 2002; Cypser et al, 2006; Johnson et al, 2000; Johnson et al, 2002). In addition to protection from future stress, the induction of hormesis can also induce protective mechanisms which not only combat potential stress, but concomitantly improve the day-to-day functioning of the organism, for instance, by the induction of heat shock proteins (Olsen et al, 2006). In order to

distinguish this phenomenon from hormesis in the broader sense (the dose-response relationships of treatments (e.g., chemical) that are beneficial at a low level but harmful at a higher level (Calabrese & Baldwin, 1999; Calabrese et al, 1999), it has been classified as stress-induced hormesis (Gems & Partridge, 2008). The 'stress' in this instance is the result of the mutation of *wrn-1*, and may or may not be a direct causes of the observed genome instability. It is possible that the stress experienced by *wrn-1(tm764)* single mutants has hormetic-like properties which are masked or suppressed by the presence of functional *cep-1*(because *cep-1* senses and responds to this stress). When *cep-1* is lost, as is the case in *cep-1(gk138);wrn-1(tm764),* then perhaps the hormetic capabilities of *wrn-1(tm764)* mutation are revealed and hence, lifespan and healthspan is increased beyond that of WT.

However, there is an important difference between how hormesis is more often understood, and what might be responsible for the longevity of *cep-1(gk138);wrn-1(tm764)*. For instance, increased longevity in *C. elegans* by exposure to high levels of oxygen has been attributed to hormesis. In this instance, hormesis was produced by *transient* stress, which is protective against a future stress (Cypser & Johnson, 2002). In contrast, the stress produced by *wrn-1(tm764)* mutation is present throughout the entire life of the worm. In other words, *wrn-1(tm764)* worms experience chronic stress rather than transient stress. However, the stress-induced hormesis hypothesis would suggest that even constant levels of stress (of the right kind) can induce a hormetic response. If stress-induced hormesis is the mechanism behind the *cep-1(gk138);wrn-1(tm764)* longevity phenotype, then searching for other synthetic superviability combinations in *cep-1* single mutants might be a fruitful

area of future investigation. This is discussed more fully in the final discussion (chapter 7).

Chapter 6 – investigating the physiological basis of synthetic super viability

6.1 Introduction

Having discovered the synthetic super viability (SSV) phenotype of *cep-1(gk138);wrn-1(tm764)* worms, I next wanted to investigate the physiological basis of SSV and also the proposed allele specificity with respect to *wrn-1*.

It has been reported that increased lifespan is associated with an increased stress resistance (see table 6.1 and references therein, and also (Johnson et al, 2000; Johnson et al, 2002; Lithgow, 2000; Lithgow & Walker, 2002)). Thus, the first logical step would be to test whether *cep-1(gk138);wrn-1(tm764)* animals also show increased stress resistance. This approach should give insight into likely pathways impacted by concomitant mutation of both *wrn-1* and *cep-1*.

With respect to the allele specificity, one possibility is that *wrn-1(tm764)* creates a particular type or level of stress, normally sensed and counteracted by the *cep-1* pathway, whereas *wrn-1(gk99)* does not. If such stress is not dealt with (via the action of *cep-1*), and is below the level at which it becomes overtly detrimental, then it could induce a hormetic-like response, the outcome of which is enhanced longevity. It could be that the chronic stress produced in *wrn-1(gk99)* animals is below the level that would trigger this hormetic-like response. To test this, I began to investigate whether changing the amount of stress in the *wrn-1(gk99)* background (and also in *wrn-1(tm764)*) could alter lifespan in a *cep-1* dependent manner.

Gene	Lifespan	Stress resistance
age-1	increased (a)	increased resistance to: oxidative stress (b), thermal (a), heavy-metal (c), and pathogenic stress (d)
akt-1 and akt-2	weakly increased (e) (f)	weakly increases resistance to oxidative and thermal stress (g)
clk-1	increased (h)	increased oxidative stress resistance in daf-2 mutant background (i)
daf-16	decreased (j)	decreased thermotolerance (k); no effect on resistance to UV, oxidative, or pathogenic stress (d) (l)
daf-18	decreased (m) (n)	decreased resistance to oxidative stress (o)
daf-2	increased (p)	increased resistance to thermal (a), oxidative (i), heavy-metal (c), and pathogenic stress (d)
eat-2	increased (q)	increased thermotolerance (q) (r)
glp-1	increased (s)	increased resistance to pathogenic stress (t)
hsf-1	decreased (j)	decreased resistance to thermal, oxidative, and pathogenic stress (ez).
isp-1	increased (x) (y)	increased resistance to oxidative stress (x) (y)
sgk-1	increased (g)	increased resistance to thermal and oxidative stress (g)
sir-2	decreased (z)	decreased resistance to thermal, oxidative, and UV stress (z)
skn-1	decreased (az)	decreased resistance to oxidative stress (az)
sod-1	weakly decreased (bz)	decreased resistance to oxidative stress (bz) (cz)
sod-2	slightly increased (dz)	decreased resistance to oxidative stress (bz) (dz)

Table 6. 1: Table summarising genes involved in regulating ageing, and the stress resistance phenotypes associated with mutation of that gene (see next page for references).

Note that this is a limited list of genes which have been demonstrated to contribute to the biology of ageing**.** References are as follows: (a) = (Babar et al, 1999), (b) = (Larsen, 1993), (c) = (Barsyte et al, 2001), (d) = (Garsin et al, 2003), (e) = (Zhang et al, 2008), (f) = (Hu et al, 2006), (g) = (Hertweck et al, 2004), (h) = (Lakowski & Hekimi, 1996), (i) = (Honda & Honda, 1999), (j) = (Hsu et al, 2003), (k) = (Yanase et al, 2002), (l) = (Hyun et al, 2008b), (m) = (Dorman et al, 1995), (n) = (Larsen et al, 1995), (o) = (Masse et al, 2008), (p) (Kenyon et al, 1993), (q) = (Houthoofd et al, 2002), (r) = (Hansen et al, 2007), (s) = (Arantes-Oliveira et al, 2002), (t) = (TeKippe & Aballay), (u) = (Walker et al, 2003), (v) = (Zhang et al, 2009), (w) = (Singh & Aballay, 2006), (x) = (Feng et al, 2001), (y) = (Sedensky & Morgan, 2006), (z) = (Wang & Tissenbaum, 2006), (az) = (An & Blackwell, 2003), (bz) = (Yang et al, 2007), (cz) = (Doonan et al, 2008), (dz) = (Van Raamsdonk & Hekimi, 2009). (ez) = (Singh, 2006)

6.2 Results

6.2.1 *cep-1* determines longevity in a temperature-dependent manner

The lifespan of *C. elegans* varies inversely with temperature (Hosono et al, 1982) and this is subject to active regulation (Lee & Kenyon, 2009). Consequently, mutation or alteration of pathways involved in this regulation can alter the relationship between temperature and lifespan. Furthermore, it is known that increasing temperature can, of itself, induce stress in worms, and this can trigger a hormetic response under certain conditions, thereby increasing stress tolerance as well as lifespan (Lithgow et al, 1995). Firstly, I asked whether increasing the temperature at which worms were maintained could alter the lifespan of *wrn-1* and *cep-1* single and double mutants.

The first thing to note from this experiment (figure 6.1) is that shifting WT worms from a constant temperature of 20°C to 25°C results in a decrease in lifespan, as expected, with 50% survival decreasing from around 18 days at 20°C to

around 10 days at 25°C. Similarly, the lifespan of both *wrn-1(gk99)* and *wrn-1(tm764)* maintained at 25°C also decreased relative to the observed lifespan of these mutants at 20°C. Thus, the lifespan of *wrn-1* mutants is inversely proportional to temperature, under the conditions tested.

Significantly, however, increasing the temperature to 25°C caused *cep-1(gk138)* mutants to live longer than N2 worms (figure 6.1, A), whereas *cep-1* lifespan is reduced relative to WT when grown at 20°C (figure 6.1, B). Hence, *cep-1(gk138)* mutant lifespan displays the opposite relationship to temperature compared with WT, suggesting that temperature stress on its own is sufficient to synergise with loss of *cep-1* to enhance lifespan.

In the case of the double mutants, both *cep-1(gk138);wrn-1(gk99)* and *cep-1(gk138);wrn-1(tm764)* display SSV at 25°C. Therefore, SSV is not specific to the *tm764* allele of *wrn-1* but is also observed in *gk99* mutants shifted to 25°C. Furthermore, the extent of SSV is even more marked in *cep-1(gk138);wrn-1(tm764)* double mutants at 25°C, where 50% survival is almost doubled relative to WT, compared with at 20°C, where there is more like a 50% increase. Taken together, these data suggest that temperature stress and stress associated with mutation of *wrn-1* are additive, being enough to trigger the SSV response in *wrn-1(gk99)* mutants at 25°C, as well as further enhancing the response of *wrn-1(tm764)* to loss of *cep-1*.

To summarise, this experiment suggests that a combination of either: temperature shift and loss of *cep-1; or wrn-1(tm764)* and loss of *cep-1; or wrn-1(gk99)* plus temperature shift and loss of *cep-1*; induce the physiological conditions in which SSV is observed, because *cep-1* acts as a

sensor/responder to stress induced by all of these conditions. Thus, the SSV is not allele specific to *wrn-1(tm764)*, but could be envisaged to be triggered by other types of stress.

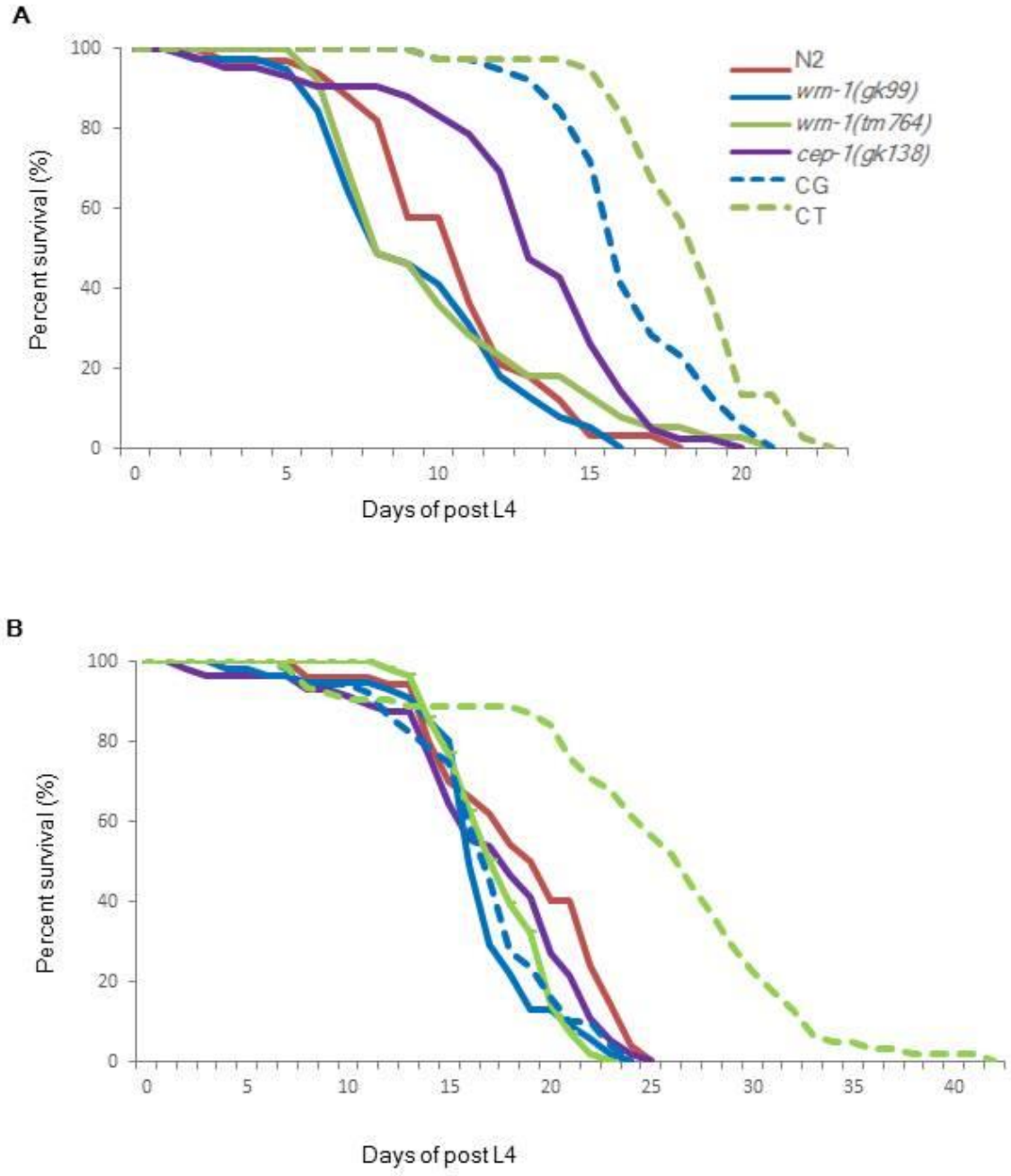

Figure 6.1: Effects of moderate temperature stress on SSV. Lifespan of worms maintained at 25°C. Increasing the temperature from 20°C ([B], as shown previously in chapter 5, figure 5.2, included here for ease of comparison) to 25°C [A], increases the lifespan of *cep-1(gk138)* bearing worms. CG = *cep-1(gk138);wrn-1(gk99),* CT = *cep-1(gk138);wrn-1(tm764).*Note that the x-axes in A and B are not to the same scale.

6.2.2 The longevity phenotype of *cep-1*-bearing strains is associated with an increased healthspan at this temperature

In order to establish whether the increase in lifespan of *cep-1*-bearing strains was accompanied by an increase in healthspan, motility and appearance were assayed (figure 6.2).

The average thrashing rate of each strain at 25°C (figure 2, part A and B) was proportional to the lifespan observed for that strain at this higher temperature (figure 6.1, A). Once again *cep-1(gk138);wrn-1(tm764)* showed the best motility, but this time *cep-1(gk138);wrn-1(gk99)* also displayed enhanced motility compared with WT, as does the *cep-1(gk138)* single mutant, although to a lesser extent. Conversely, both *wrn-1* single mutants performed poorly compared to WT controls. Thus, not only does *cep-1(gk138)* confer an increase in lifespan relative to N2 at 25°C to both alleles of *wrn-1*, as well as on its own,, but also an increase in motility, a marker of health span.

A

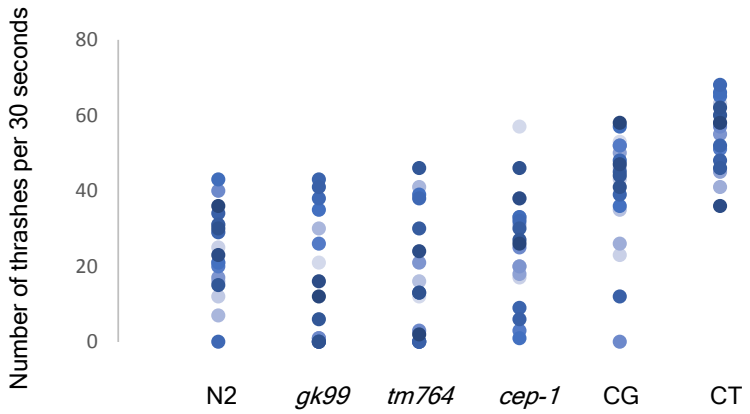

B

N2	*wrn-1(gk99)*	*wrn-1(tm764)*	*cep-1(gk138)*	*cep-1(gk138); wrn-1(gk99)*	*cep-1(gk138); wrn-1(tm764)*
24	13.55	14.9	25.5	40.35	55.65

C

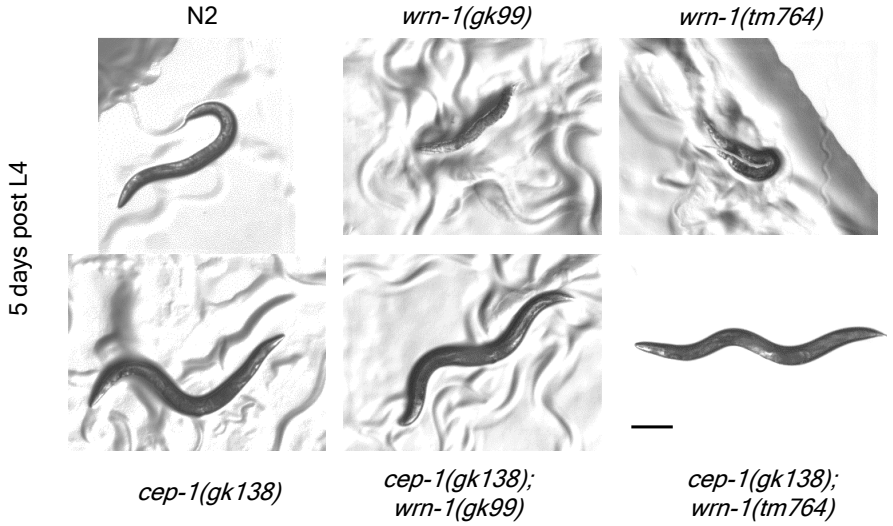

Figure 6. 2: Healthspan of *cep-1/wrn-1* mutant worms grown at 25°C. (A) Number of thrashes per 30 seconds in liquid culture as a measure of motility. All worms are 5 days post L4 when assessed. Once again *cep-1(gk138);wrn-1(tm764)* shows the best motility, though *cep-1(gk138)* and *cep-1(gk138);wrn-1(gk99)* have improved motility at 25°C compared to at 20°C. (B) Average number of thrashes for each strain at 25°C, 5 days post L4. (C) Representative photographs of worms 5 days post L4. *wrn-1(gk99)* and *wrn-1(tm764)* appear shorter than N2, with gross tissue deterioration evident, as well as lack of movement (as indicated by the lack of sigmoidal body shape). In contrast, *cep-1(gk138), cep-1(gk138);wrn-1(gk99)* and *cep-1(gk138);wrn-1(tm764)* all look healthier in appearance relative to N2. Their bodies have not shrank and tissue morphology does not show clear signs of deterioration. Therefore, these strains have an extended health span at 25°C. Scale bar = 200µm. CG = *cep-1(gk138);wrn-1(gk99)* , CT = *cep-1(gk138);wrn-1(tm764).*

6.2.3 Distribution of DAF-16::GFP in mutant strains at 25°C

Since the long lived *cep-1(gk138);wrn-1(tm764)* showed an increase in DAF-16::GFP nuclear localisation at 20°C, I next assessed DAF-16::GFP localisation in worms maintained at 25°C (figure 6.3). Given the correlation between DAF-16::GFP localisation and longevity at 20°C, strains which were long lived at the higher temperature might be expected to show an increase in the proportion of DAF-16::GFP positive nuclei.

Once again, DAF-16 was found to be expressed in most cell types and was predominantly cytoplasmic in WT worms maintained at 25°C (figure 6.3 (A), panel a). Overall, the same was true for *wrn-1* single mutants (figure 3 (A), panels c and d) although there was, as described in chapter 5, variability in the subcellular localisation between worms of a given strain – some worms did show nuclear DAF-16::GFP, though the majority did not. In fact, not only was an increase in nuclear DAF-16::GFP not observed in the majority of *wrn-1* mutants, but clear nuclear exclusion was evident (figure 6.4).

However, nuclear DAF-16::GFP expression was more prominent in *cep-1(gk138);wrn-1(tm764)* and also in *cep-1(gk138);wrn-1(gk99)* mutants (figure 6.3 A, panels e and f). In addition, *cep-1(gk138)* single mutants also appeared to have a higher proportion of nuclei showing nuclear DAF-16::GFP, at 25°C rather than 20°C (5.9), albeit less than in the double mutants. Thus, DAF-16::GFP is more likely to be nuclear in long lived worms. However, as was noted at 20°C, nuclear DAF-16::GFP localisation is by no means complete, thus the observed longevity is not dependent on complete nuclear localisation of DAF-16.

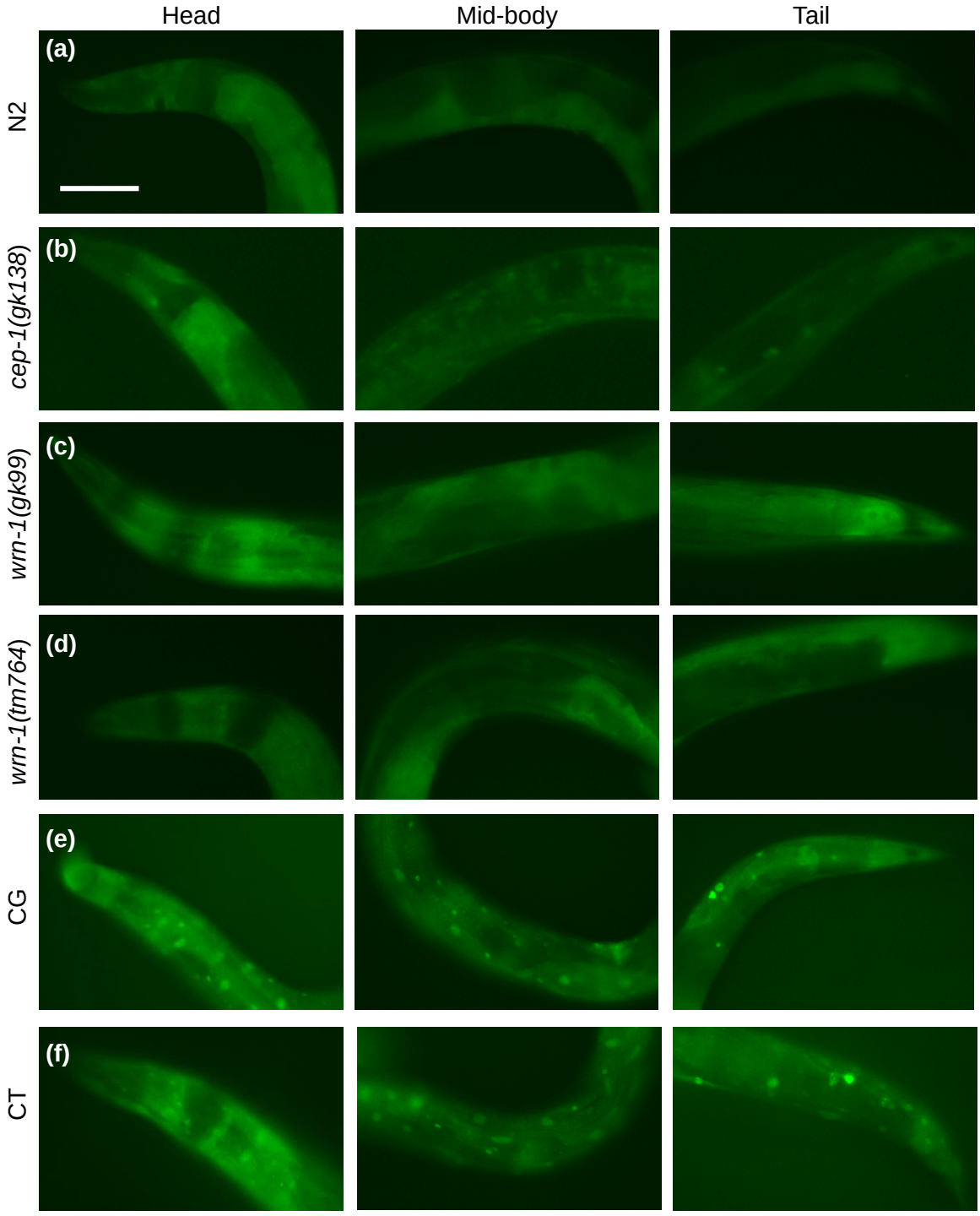

Figure 6. 3: DAF-16::GFP localisation in *cep-1/wrn-1* mutant worms maintained at 25°C. Images are representative and were taken at 6 days post L4. DAF-16::GFP is predominantly cytoplasmic in all strains, but a higher proportion of worms and cells show nuclear DAF-16::GFP in *cep-1;wrn-1* double mutants at 25°C (panels e and f). Increase in nuclear localisation of DAF-16::GFP is also observed in *cep-1(gk138)* (panel b) but to a lesser extent than *cep-1;wrn-1* doubles. Scale bar = 100µm. CG= *cep-1(gk138)wrn-1(gk99)*, CT= *cep-1(gk138)wrn-1(tm764).*

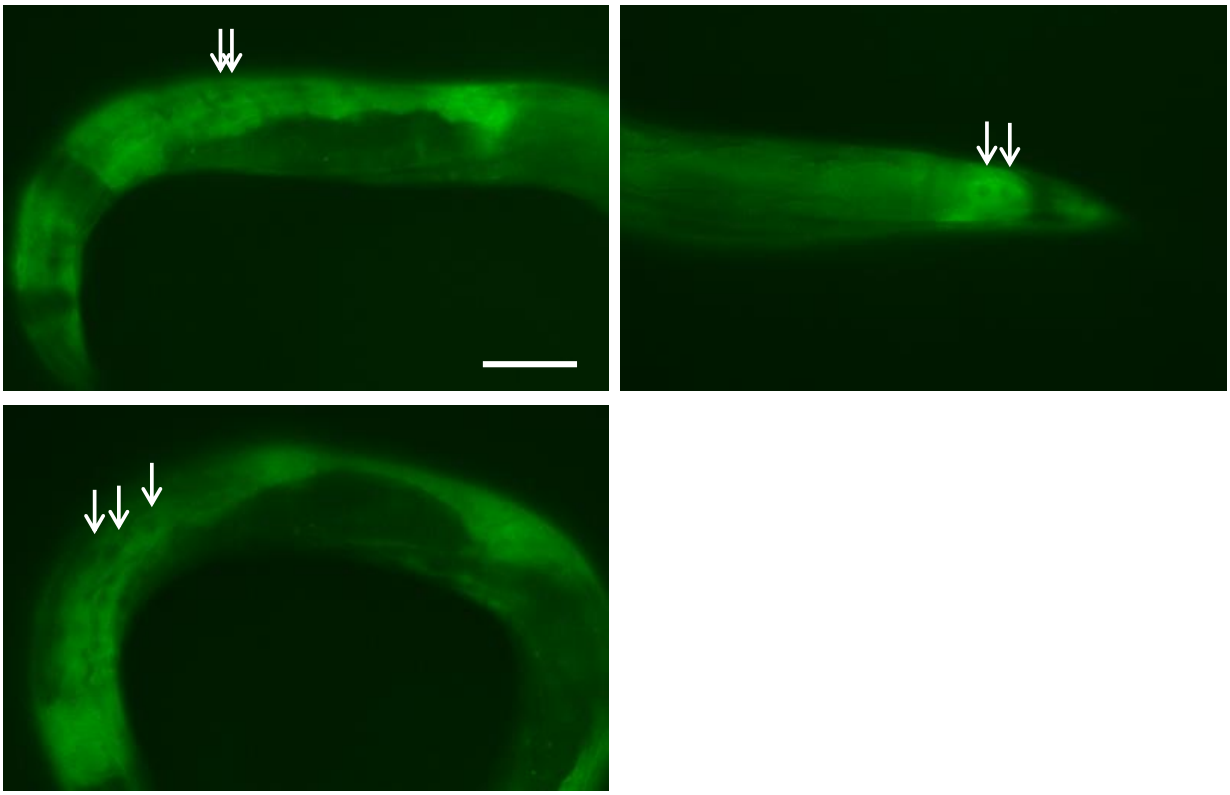

Figure 6. 4: DAF-16::GFP localisation in *wrn-1(gk99)* worms maintained at 25°C. Images are representative and were taken at 6 days post L4. DAF-16::GFP is predominantly cytoplasmic and in some instances, is clearly excluded from the nucleus (arrows). This was also observed in *wrn-1(tm764)* worms. Scale bar = 100µm.

6.2.4 *cep-1* mutants are resistant to ultraviolet irradiation, regardless of *wrn-1* mutation

Since *cep-1;wrn-1* are both long lived and resistant to thermal stress, I wanted to establish whether these mutants were also resistant to other types of stress. Therefore, strains were tested for resistance to UV light by assaying survival each day post irradiation. When 5-day post L4 hermaphrodites (i.e. adults post-egg laying) of the genotype *cep-1(gk138), cep-1(gk138);wrn-1(tm764)* or *cep-1(gk138);wrn-1(gk99)* were irradiated, they survived significantly longer than WT (figure 6.7), mirroring the effect of maintenance at 25°C (figure 6.1). Intriguingly, there is an allele-specific difference in the response of *wrn-1* single mutants to UV radiation, with *wrn-1(gk99)* showing enhanced sensitivity, whilst *wrn-1(tm764)* behaves like WT. This implies that UV sensitivity is not dependent on the RecQ helicase activity of *wrn-1.*

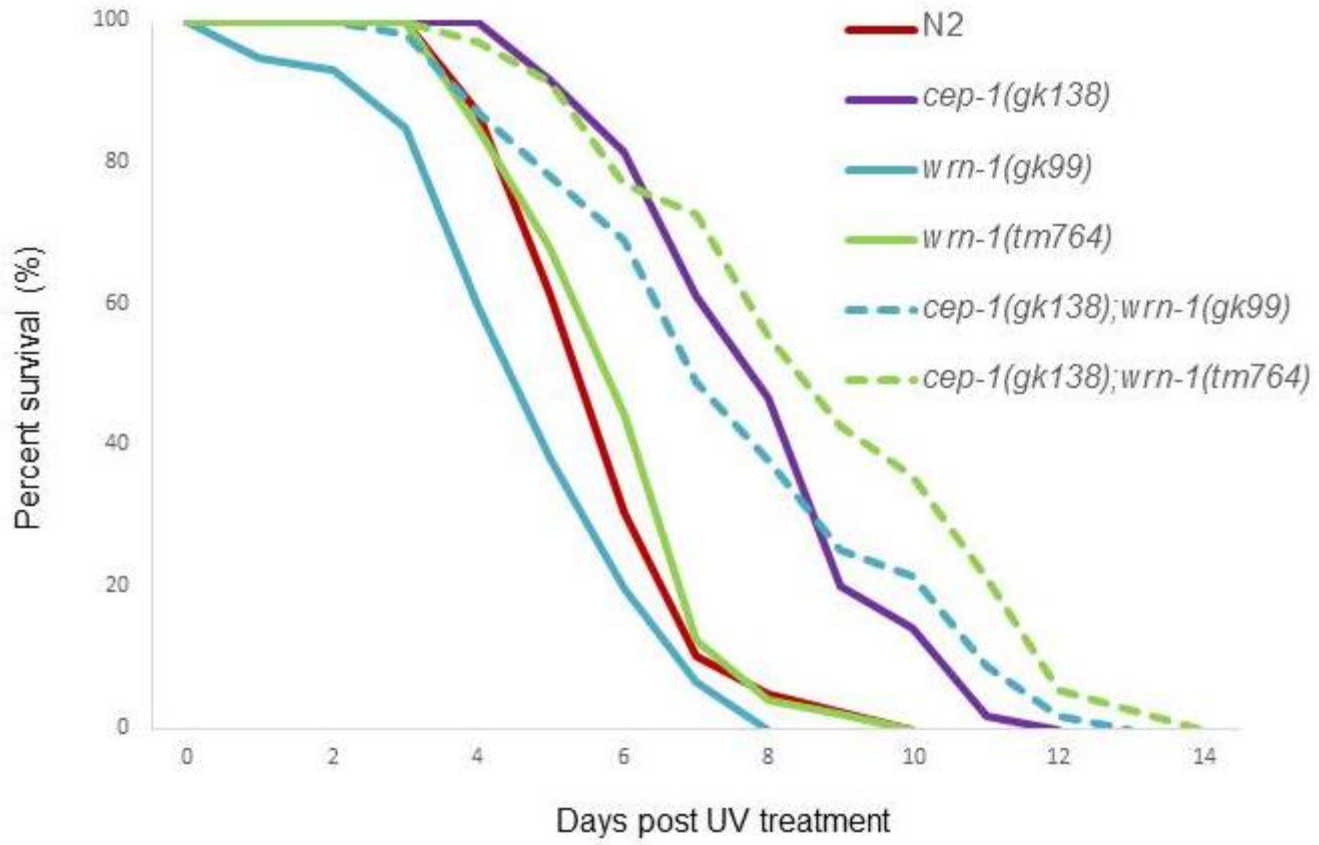

Figure 6. 5: Increased survival of *cep-1;wrn-1* double mutants following UV exposure. Survival at 20°C after UV irradiation of 5 day post L4 worms. Worms were irradiated with 1000 J/m2 and survival was scored every day. The survival of all strains except *wrn-1(m764)* was significantly different from that of N2. *wrn-1(gk99)* showed a reduced survival compared to WT, but a reduced survival relative to WT is also observed when not irradiated. Similarly, the lifespan of *cep-1(gk138);wrn-1(tm764)* is also long lived compared to N2, whether irradiated or not. However, *cep-1(gk138)* and *cep-1(gk138);wrn-1(gk99)* are short lived relative to WT at 20°C, but survive longer than WT when exposed to UV.

6.2.5 The long-lived *cep-1;wrn-1* double mutants display increased tolerance to chronic heat stress

Since many manipulations that increase longevity also increase resistance to a variety of stressors, I sought to confirm whether the long lived *cep-1;wrn-1* worms were also stress resistant. Conversely, would *wrn-1* and *cep-1* single mutants be more sensitive to stress than WT? Given that *cep-1* mutation can be both detrimental and beneficial to lifespan under different conditions, it is hard to predict from first principles whether *cep-1* worms would be inherently stress resistant.

Intrinsic thermal tolerance is assayed on worms not previously exposed to thermal stress, i.e. maintained at 20°C. Here, survival under lethal thermal stress (35°C) was measured as an indicator of stress tolerance (figure 6.6). When N2 worms 5 days post L4 are shifted up to this temperature, deaths start to occur at approximately 7 hours into treatment, and all worms are dead 12 hours after that (19 hours into treatment). As predicted given the longevity of c*ep-1;wrn-1* double mutants*,* these worms not only display a delayed onset of death, but the maximum survival under these conditions is increased. For example, ≥10% death occurs 11.5 hours after temperature shift for WT animals compared with 17 hours for c*ep-1(gk138);wrn-1(tm764)* double mutants, corresponding to a 48% increase in the time taken for 10% of the population to die. In terms of maximum survival under these conditions, the value is 24.5 hours for c*ep-1(gk138);wrn-1(tm764)* animals, versus 19 hours for N2. c*ep-1(gk138);wrn-1(gk99)* worms also display increased thermal tolerance, although the effects are more modest.

Conversely, both *wrn-1(gk99)* and *wrn-1(tm764)* single mutants are less thermotolerant than WT worms (figure 6.4), at least during the initial period of heat stress, although *wrn-1(gk99)* animals perform significantly worse in these conditions. Apart from the initial period of onset of death, *wrn-1(tm764)* worms appear to have a similar thermotolerance as WT worms, with respect to mean and maximal survival. On the other hand, *wrn-1(gk99)* animals show significantly reduced mean and maximal survival relative to N2 worms.

When *cep-1(gk138)* worms are shifted to 35°C at 5 days post L4, mean and maximal survival is increased relative to N2 worms, suggesting that *cep-1(gk138)* worms are intrinsically thermotolerant compared to WT, though not to the extent seen for *cep-1(gk138);wrn-1(tm764).*

A

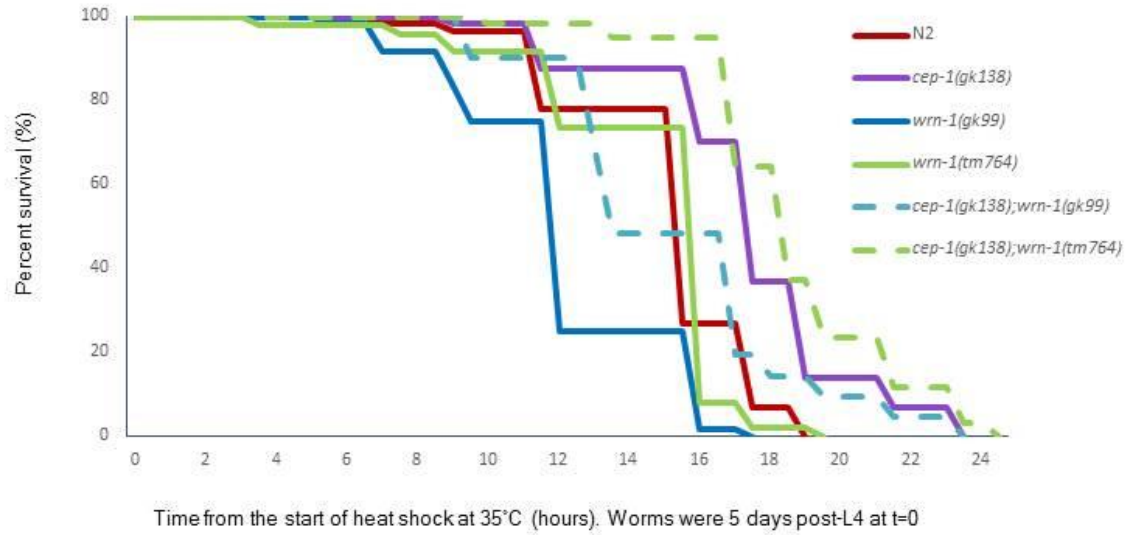

B

Strain	(a) Time at which worms start dying (hours)	(b) Time at which 90% or less are alive (hours)	(c) Time at which 50% or less are alive (hours)	(d) Time at which 0% alive (hours)	(e) % alive when 0% N2 are alive	(f) Time at which 10% are alive (hours)	(g) % alive when 10% N2 are alive	n value
N2	7	11.5	15.5	19	-	17.5	-	59
cep-1(gk138)	9	11.5	17.5	23.5	14%	21.5	39%	57
wrn-1(gk99)	5.5	9	12	17.5	0%	16	0%	60
wrn-1(tm764)	3.5	12	16*	19.5	2%	16	2%	49
cep-1(gk138);wrn-1(gk99)	9.5	13	13.5§	23.5	15%	19.5	19%	62
cep-1(gk138);wrn-1(tm764)	10	17	18.5	24.5	37%	23.5	64%	59

*73% at 16 hours but only 8% at 16.5 hours
§48% ar 13.5 hours, 19% at 17 hours

Figure 6. 6: Survival of *cep-1/wrn-1* mutants subjected to chronic heat stress. Intrinsic thermotolerance of worms 5 days post-L4. The percentage surviving was scored during a 35°C thermal stress assay. Note that due to the time take to assess each strain at each time point, not every time point was the same for each strain. (A) Survival curve for intrinsic thermotolerance at 35°C and (B) tabulated data from the survival assay. *cep-1(gk138);wrn-1(tm764)* displays the highest thermotolerance, showing the greatest delay in the onset of death compared to all other strains (B, column a), closely followed by *cep-1(gk138);wrn-1(gk99),* which itself was closely followed by *cep-1(gk138).* Both *wrn-1* mutants started to die prematurely relative to WT worms. The same pattern was observed for the maximum survival (B, column d) and the time at which 10% survival was reached (B, column f), though the maximum survival of *wrn-1(tm764)* was not significantly different from that of N2, and *cep-1(gk138)* was not significantly different from *cep-1(gk138);wrn-1(gk99)*. The same pattern was also observed when comparing the percentage alive at the point where 0% or 10% of N2 are alive (B, columns e and g, respectively), although at the point where 10% of N2 were alive, there were more *cep-1(gk138)* alive than *cep-1(gk138);wrn-1(gk99)* (39% and 19%, respectively),

and was echoed by the time at which 10% survival was reached (column f) and the time at which 50% or less were alive (B, column c). Broadly speaking, the survival of *wrn-1(tm764)* is not significantly different from that of N2, apart from the initial onset of death (B, column a). Furthermore, apart from the initial onset of death, *wrn-1(tm764)* performs better than *wrn-1(gk99)*. The allelic difference in thermotolerance for wrn-1 mutants might explain the difference seen between *cep-1(gk138)* and *cep-1(gk138);wrn-1(gk99)*, and also the latter with *cep-1(gk138);wrn-1(tm764).* Perhaps the (evidently) detrimental effect of *wrn-1(gk99)* is able to at least partially override the beneficial effects of *cep-1* in terms of thermotolerance when survival is measured.

6.2.6 Response of mutant strains to acute heat stress

In order to assess how well *wrn-1* and *cep-1* single and double mutant survive after transient heat shock, life span analysis was performed on worms which had been heat shocked for 2 hours at 33°C at L4, then returned to 20°C where they remained throughout the rest of the study (figure 6.7). Transient heat shock early in life markedly increased early life mortality for all strains, completely transforming the shape of the lifespan curves. Therefore, heat shock is detrimental to survival of young adults, regardless of genotype. Furthermore, all mutants showed higher death rates early on compared to N2, all reaching 50% survival before WT controls. However, the lifespan curves for both *cep-1(gk138);wrn-1(tm764)* and *cep-1(gk138);wrn-1(gk99)* double mutants crosses the WT curve shortly after this point. Thus, chronologically older *cep-1;wrn-1* double mutants showed better survival after heat shock than N2, with CT animals showing the longest maximum lifespan (32 days compared with 24 days for WT). Both *wrn-1* and *cep-1* single mutants performed poorly in this assay.

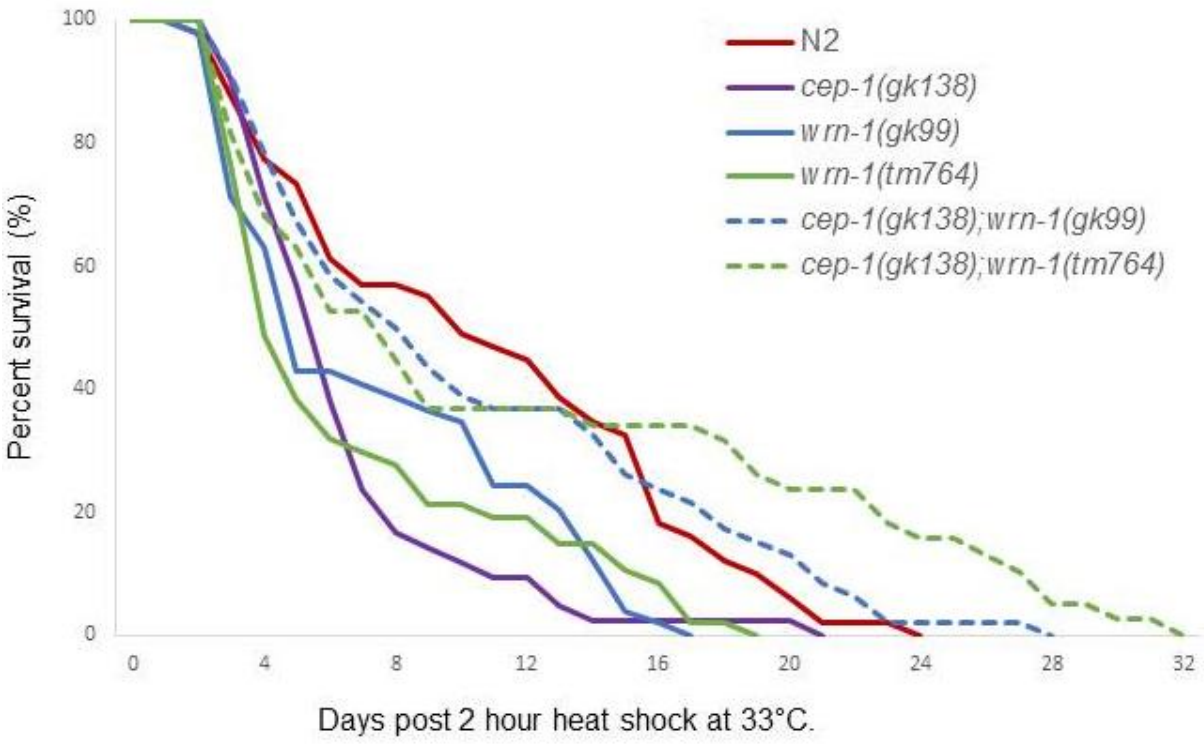

Figure 6. 7: Response of *cep-1/wrn-1* mutants to transient heat stress. Lifespan at 20°C after L4 worms were subjected to 2 hours of heat shock at 33°C. All strains including N2 show a sharp decrease in deaths in the first few days after heat shock. Initially, all strains respond poorly to transient heat shock compared to N2 worms, reaching 50% survival earlier than WT. *wrn-1* mutants show the most drastic decrease in survival, followed by *cep-1(gk138)*. Towards the latter part of the survival curve, *cep-1(gk138);wrn-1(tm764)* survival is improved and has a significantly greater maximum lifespan compared to N2 (32 days and 24 days, respectively. Therefore, *cep-1(gk138);wrn-1(tm764)* does has a better chance of survival after early life heat shock compared to WT worms, whereas *wrn-1* and *cep-1* single mutants are more sensitive to early life heat shock and die prematurely. Compared to survival at 20°C with no heat shock, *cep-1(gk138);wrn-1(gk99)* lives longer, and this longer life span is slightly greater than WT after heat shock, suggesting early life heat shock is beneficial to *cep-1(gk138);wrn-1(tm764)* in later (but not early) life. In the case of all strains, transient heat shock at L4 increases early life mortality.

6.2.7 DAF-16::GFP nuclear localisation after heat shock is limited by *cep-1*

Since DAF-16::GFP is known to relocate to the nucleus upon heat shock (Henderson & Johnson, 2001), and a difference in survival was observed for *wrn-1* and *cep-1* single and double mutants that had been subjected to various heat shock treatments compared to WT worms, the localisation of DAF-16::GFP after heat shock was examined in mutant strains. Given time constraints, I was only able to analyse DAF-16::GFP localisation in control versus *cep-1* single mutants. The results from this experiment are summarised in figure 6.8.

After 30 minutes of heat shock at 35°C, control worms begin to show some DAF-16::GFP nuclear localisation in cells at the anterior (the head, and the beginning of the intestine), though there is still a lot of cytoplasmic DAF-16::GFP. If control animals are left at 35°C for an entire hour, nuclear DAF-16::GFP is more frequently observed.

When the same manipulations are performed on *cep-1(gk138)* mutants, nuclear DAF-16::GFP expression is brighter after 30 minutes incubation at 35°C, and very bright after one hour, with these worms showing no visible cytoplasmic DAF-16::GFP at this time point. Therefore, loss of *cep-1* appears to promote DAF-16 nuclear localisation in response to heat shock.

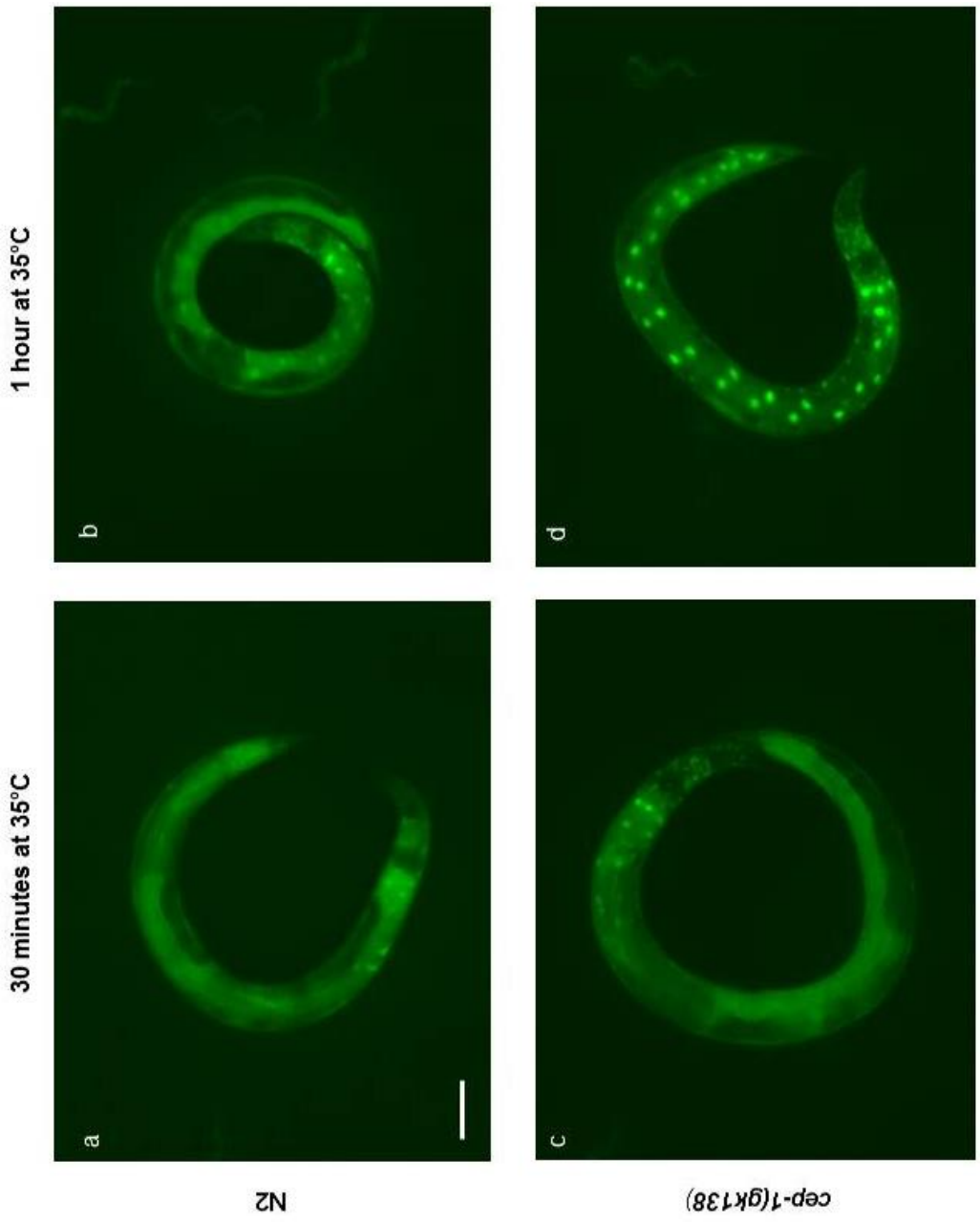

Figure 6. 8: Localisation of DAF-16::GFP in response to heat shock. DAF-16::GFP localisation was assayed in 1 day post L4 *cep-1(gk138)* single mutants and in the control strain (TJ356). Worms were shifted from 20°C to the heat shock temperature (35°C), and the localisation of DAF-16::GFP was visualised after 30 minutes or one hour of heat shock. After 30 minutes of heat shock, control strains (a) showed a low level of DAF-16::GFP expression in anterior nuclei. After one hour of heat shock, the level of expression and the number of DAF-16::GFP positive nuclei had increased (b). *cep-1(gk138)* mutants heat shocked for 30 minutes showed a greater number of DAF-16::GFP positive nuclei at this time point, compared to control worms, and the level of nuclear expression was brighter (c). After one hour of heat shock (d), the level of nuclear DAF-16::GFP expression and the number of DAF-16::GFP positive nuclei was not only higher than that observed after 30 minutes, but was also significantly higher than that seen in controls after one hour of heat shock.

6.3 Discussion

6.3.1 Allele specificity of SSV

The experiments presented in this chapter demonstrate that *cep-1(gk138);wrn-1(gk99)* as well as *cep-1(gk138);wrn-1(tm764)* display SSV. In the case of *cep-1(gk138);wrn-1(gk99),* SSV is observed in worms maintained at 25°C but not at 20°C, suggesting that additional insult in the form of mild heat stress is required to trigger SSV. These experiments are important for two reasons: firstly, they show that SSV is not specific to a single allele of *wrn-1*, a phenomenon which would be difficult to explain satisfactorily. Secondly, the data suggests that the physiological basis of SSV revolves around stress responses. The phenotypic differences between the two alleles are hypothesised to relate to the nature of the intrinsic stress generated in the two *wrn-1* mutants.

6.3.2 *cep-1* integrates environmental input to influence lifespan

It is very striking that *cep-1(gk138)* mutants have a reduced lifespan at 20°C but are longer lived at 25°C. My experiments help to clarify the confusion in the literature surrounding lifespan effects of *cep-1* mutation. For example, a previous report claims that *cep-1* mutants have extended lifespan (Arum & Johnson, 2007), but this experiment was performed at 25.5°C, and the results are not set in the context of the range of *cep-1*-associated lifespans that are observed under different temperature conditions. Similarly, recent work assessing the role of *cep-1* in determining life span of mitochondrial mutants

(Baruah et al, 2014; Ventura et al, 2009) also reported that *cep-1* mutants are long lived. This latter study claims that life span assays were performed at 20°C, but careful inspection of the supplementary materials and methods section show that not only was FUdR used (which can alter lifespan), but worms were maintained at 25°C for the first three days of adulthood in order to minimise potential vulval protrusions. These three days were included in the overall life span analysis.

Since my data shows that life span of *cep-1* mutants is longer at this temperature than at 20°C, this highlights not only the fact that life span of *cep-1* mutants is temperature dependent, but that care must be taken when selecting protocols for life span analysis. This is the first time a direct comparison of *cep-1* life span under different temperatures has been made.

Temperature is not the only factor which modulates *cep-1*-dependent longevity outcomes. For instance, mutation of *wrn-1* could compromise mitochondrial function, thus *cep-1* could be responding to altered ROS levels. This suggestion is supported by recent work that demonstrated that *cep-1* modulates longevity outcomes depending on the level of mitochondrial stress (Baruah et al, 2014; Ventura et al, 2009). The precise mechanism behind the likely hormesis in my SSV strains awaits investigation (see section 7.3).

Moreover, *cep-1* mutants appear to do well under conditions of UV stress and chronic heat stress, but not acute heat stress. Taken together, this data suggests that *cep-1*, or the *cep-1* pathway, acts as a central node for lifespan regulation, integrating multiple stress signals to dictate the appropriate response, which may have an influence on lifespan outcome. Under conditions

of stress, *cep-1* mounts a response, which may have a cost in terms of lifespan. Thus, *cep-1* single mutants display enhanced longevity under stressful conditions (and this includes *wrn-1* mutations). Under normal physiological conditions, *cep-1* presumably performs essential house-keeping tasks and thus *cep-1* mutants display reduced lifespan in the absence of stress.

6.3.3 DAF-16 localisation in response to heat stress

Longevity of *cep-1* and *cep-1;wrn-1* mutants at 25°C was correlated with higher levels of nuclear DAF-16::GFP, and the level appeared to be somewhat proportional to the extent of longevity.

Intriguingly, CEP-1 appears to have some role in the nuclear localisation of DAF-16 following heat stress, acting to limit DAF-16 nuclear localisation. Why would CEP-1do this? Perhaps this has to do with regulating the trade-off between stress response and longevity (presumably with the aim of reproducing). In the absence of *cep-1,* the stress goes unnoticed and DAF-16 is free to promote longevity by preferentially localising to the nucleus.

Of course, this would only apply when the stress is below some critical threshold above which it would be highly detrimental to the animal. *wrn-1* mutation seems to induce an optimal level of stress at which SSV can be observed in combination with *cep-1* mutation. In other situations where SSV is observed, for example in *him-6;cep-1* double mutants, the stress levels are such that the longevity benefit is more marginal.

Chapter 7 Final discussion

7.1 Summary of important conclusions

- *wrn-1* and *mut-7* mutant phenotypes recapitulate aspects of premature ageing, genomic instability, and sensitivity to DNA damaging agents. *wrn-1* overexpression appears to enhance longevity, suggesting that *wrn-1* acts as a bona-fide antigerontogene.
- Combination of *wrn-1* and *cep-1* mutations produces a novel and very striking enhanced lifespan and healthspan phenotype which I have termed synthetic super-viability (SSV). The SSV phenotype appears to be modulated by various environmental inputs such as temperature stress.
- Overall, therefore, my data suggest that *wrn-1* mutants have the latent potential to switch longevity outcomes, and that this switch is determined, at least in part, by *cep-1*.

7.2 The role of stress sensing in determining longevity outcomes

The really striking and unexpected result from this work is the synthetic super viability phenotype (SSV), which begs the immediate question - how does it work? As discussed in chapters 5 and 6, this is an entirely novel genetic phenomenon, with no obvious precedent in the literature. I previously mentioned Nietzsche's quote "that which does not kill us makes us stronger", as

being encapsulated biologically in the concept of hormesis (Gems & Partridge, 2008). Hormesis refers to the induction of enhanced survival and robustness by exposure to transient, low level stress (see chapter 5 discussion, and (Calabrese & Baldwin, 1999; Calabrese et al, 1999; Calabreseci, 1999; Cypser & Johnson, 2002; Cypser et al, 2006; Gems & Partridge, 2008; Olsen et al, 2006)). Mutation of *wrn-1* would certainly be expected to induce stress in the form of genome instability, and perhaps others (although this would be pervasive rather than transient). I hypothesise that SSV can be attributed to a hormetic-like response to *wrn-1* mutation, and that *cep-1* normally acts to limit this. In other words, it is not the stress *per se* that is life-limiting, it is the sensing and response to such stress that regulates longevity. p53 mutation can act to lengthen lifespan in the worm because these animals do not develop health consuming tumours. In other systems (e.g. mice), the physiological effects of mutating p53 in the context of increased cellular stress might be masked by the increased sensitivity to cancer in such models.

p53 is a famous tumour suppressor gene, although nowadays it is also thought of as a regulator of general cellular homeostasis, with roles in the DNA damage response, senescence, and metabolic regulation, to name but a few (Vousden & Lane, 2007). The level of p53 activity and the physiological context in which it is acting are critical in determining the response (see chapter 1, section 1.7). p53 activation must therefore be regarded as a compensatory response mounted in the face of cellular stress. This ought to be beneficial, but when damage is pervasive the capacity of tissues to regenerate can be attributed to excessive p53-dependent apoptosis and or/senescence of stem cell progenitors, for instance. Indeed, transient inhibition of p53 during radiotherapy

with pifithrin-α protects mice from excessive DNA damage-induced apoptosis (Strom et al, 2006) (Komarov et al, 1999), while a similar neuroprotective effect is observed in a mouse stroke model (Culmsee et al, 2001). When damage is pervasive, p53 response constitutes a problem and becomes deleterious accelerating ageing. For example, mutant mice that display premature ageing (due to persistent damage) show dramatic levels of senescence, apoptosis, and importantly, their progeroid phenotypes are suppressed by elimination of p53 (or indeed by elimination of p21 (Benson et al, 2009), or by elimination of senescent cells (Baker et al, 2011). An important distinction here, though, is that this does not produce a super viability phenotype – the intervention acts simply to suppress ageing phenotypes.

How does this idea apply to my worm model? Though *replicative* senescence is not a feature of worm ageing *per se*, since the adult soma is entirely post-mitotic, both somatic and germline cells could still exhibit senescence-like phenotypes, which, as in mammalian systems, could act to limit lifespan (Kuilman et al, 2010; Rodier & Campisi, 2011; Salminen et al, 2012). For instance, senescent cells display a 'senescence-associated secretory phenotype' (SASP), which contributes to the alteration in intercellular communication with age, known as 'inflammageing' (Kuilman et al, 2010; Rodier & Campisi, 2011; Salminen et al, 2012), and SASP is postulated to contribute to ageing. It is believed that the SASP creates a 'bystander' effect in which senescent cells can induce other cells to become senescent. This 'contagious ageing' can also be induced between neighbouring cells via gap-junction mediated cell-cell contacts and processes involving ROS (Nelson et al, 2012). Importantly, what this demonstrates is that while *C. elegans* may not

show a decline in replicative capacity as they age (since they are somatically post-mitotic throughout the entirety of adulthood), the senescence phenotype entails much more than just cell cycle arrest, and cells found in old worms may have other phenotypes reminiscent of senescent cells, and therefore could still promote ageing, by altering local tissue microenvironment or even the systemic milieu (Dimri et al, 1995; Linskens et al, 1995; Shelton et al, 1999).

Even if a senescence-like state cannot be acquired by the already non-dividing somatic cells of *C. elegans*, germline cells continue to proliferate and could, in theory, demonstrate cellular senescence. Furthermore, even if cellular senescence was not possible, these cells are, unlike adult somatic cells, able to undergo DNA-damage induced apoptosis – something which has also been demonstrated to cause ageing (Rodier et al, 2007; Shen & Tower, 2009).

How could germline genomic instability (or for that matter, germline ageing) influence somatic longevity? It has long been believed that organismal senescence – i.e. the lifespan of the individual organisms (or worm, in this case) – is dictated by the soma, and the germline was solely responsible for the inheritance of traits (to which the soma contributes nothing) (Kirkwood & Holliday, 1979). Therefore shifts in the physiology of the germline are inconsequential to the organismal longevity (but not, however, to germline senescence or mortality (Ahmed & Hodgkin, 2000)). Ermolaeva et al have recently provided evidence of a bidirectional cross-talk between the soma and germline, such that certain stresses (DNA damage, for instance) when applied to the germline, initiate protective stress signals that can protect the soma (Ermolaeva et al, 2013). This represents a systemic stress response to DNA damage that acts through an innate immune response pathway, and bolsters

protein homeostasis through the increased function of the ubiquitin/proteasome system. Therefore, the germline is a key tissue for sensing DNA damage (since DNA damage checkpoints function specifically in the germline (Gartner et al, 2000)), and subsequently communicating to somatic tissues under genotoxic stress.

Intriguingly, the somatic stress resistance is mediated by the ERK MAP kinase MPK-1 in germ cells, and triggers induction of putative secreted peptides associated with innate immunity (Ermolaeva et al, 2013). This bidirectional communication may explain the observed SSV in *cep-1;wrn-1* double mutants presented in this thesis. My hypothesis would be that *wrn-1* mutation leads to constitutive DNA damage/stress, which in turn causes persistent *cep-1*/p53 activation, and consequently, premature ageing. When *wrn-1* is mutated in the absence of *cep-1* (i.e. in a *cep-1* mutant background), the stress created by *wrn-1*-induced DNA damage can then be signalled to the soma (because no *cep-1* response is mounted in the germline), where protective responses are initiated, with the result that lifespan and healthspan are increased. It would be very interesting to see if blocking germline signalling suppresses SSV.

The response of *cep-1* to *wrn-1* mutation is somewhat analogous to autoimmunity, in which the immune system betrays its original function and aggravates, rather than alleviates problems (or put very simply, they both reflect processes which are initially positive but can consequently become bad when over activated). This is not unique to *cep-1*/p53, however, since many modulators of ageing can be viewed as being intended for the protection or maintenance of the organism (from the effects of nutrient deprivation, for instance), but when they are chronically activated they subvert their intended

purpose and generate further damage. For example, IIS down regulation reflects a defensive response, the aim of which is to minimise metabolism and growth in the face of damage (Garinis et al, 2008; Kenyon, 2010b; Schumacher et al, 2008a).This would also suggest that SSV is not unique to *cep-1;wrn-1*, and that other genetic combinations would also provoke SSV.

7.3 Important future work

Up until now, research has focused upon identifying additive or synergistic genetic interactions – where double mutants enhance the longevity associated with previously-identified single long-lived mutants, or suppressors of the shortened lifespan phenotype, in which WT longevity is restored. However, the novel type of genetic interaction represented by SSV suggests that screening for factors which individually shorten lifespan but together enhance it **beyond** WT lifespan offers an entirely new approach to the field of ageing and longevity research. The results presented in this thesis suggest that SSV is not limited to *cep-1;wrn-1* double mutants, therefore the obvious next step is to perform genetic screens for other SSV interactions.

RNAi based screens could identify more genes that create the same SSV interaction in a *wrn-1* or *cep-1* single mutant background. The molecular basis of SSV is very intriguing. One way to elucidate the molecular mechanism(s) behind SSV would be to screen for factors which, when silenced by RNAi (or using EMS mutagenesis), could suppress SSV in the *cep-1;wrn-1* background. For instance, RNAi knockdown of the *PTEN* homologue, *daf-18*, in the SSV strain would allow me to test the hypothesis that hormesis contributes to the extended longevity and healthspan of these worms (Cypser & Johnson, 2003)

(Cypser et al, 2006). Another possibility is that *cep-1* regulates *wrn-1* lifespan in response to oxidative stress. Lending support to this idea is the growing evidence that WRN depletion induces a metabolic shift that leads to oxidative stress and increased ROS (Kashino et al, 2003; Li et al, 2014; Massip et al, 2009; Pagano et al, 2005). This stress has been postulated to play an important role in the onset of phenotypes caused by the loss of WRN function, and is further supported by the fact that supplementing WRN mutant mice with Vitamin C restores healthy ageing (Kashino et al, 2003; Massip et al, 2009; Pagano et al, 2005). It is possible that mutation of *wrn-1* likewise causes oxidative stress, which could be the cause of the observed reduction in lifespan and increased stress sensitivity, which in turn require *cep-1*. This would be an interesting avenue to explore and one which could be tested via various approaches (testing the effect of paraquat (which causes the production of ROS) on lifespan, for example, or adding some anti-oxidant to the *cep-1;wrn-1* double mutant e.g. growing the worms on plates containing N-acetyl cysteine).

RNAi screens would be best performed in the first instance using a candidate gene approach, focusing on a set of approximately 500 genes from a group of likely candidate processes, such as innate immunity, chromatin regulation, stress and damage signalling, and hormesis. The set of candidates would be different for the suppressor screen compared with the screen for novel SSV mutant combinations.

Another possibility would be to perform RNA sequencing in *cep-1* and *wrn-1* single and double mutants to identify potentially informative changes in gene expression. It would also be very interesting to elucidate the tissue specificity of

SSV by performing tissue specific rescue experiments in *cep-1;wrn-1* double mutants.

This work should define the breadth of the SSV interaction and provide mechanistic insight. Ultimately, it is hoped that these studies will be translated into real life benefits for humans and healthy ageing.

Appendix

8 Statistical analysis of lifespan.

OASIS (Online Application for the Survival Analysis of Lifespan Assays Performed in Aging Research) is an online tool that helps conduct statistical tasks involved in analysing survival data. As well as performing appropriate statistical analyses, OASIS also allows the visualisation of survival data, by generating survival and log cumulative hazard plots. Consequently, statistical analysis of lifespan data generated during this thesis was performed using OASIS, specifically:

- Mean and median lifespan, including 95% confidence intervals and standard error.
- Log rank/Mantel-Cox test with Chi square, P-value, and Bonferroni P-value calculations. The Log rank test is a nonparametric test that is used for comparing two survival functions through overall lifespan data. Since OASIS generates all pair-wise comparison results, there may be an increase type I error. To adjust multiple testing, OASIS provides the corrected P-values with Bonferroni method, one of the most commonly used correction methods for multiple statistical comparisons.
- Fisher's Exact Test, to test different survival functions at specific time points instead of overall lifespan. The OASIS program can calculate the probability of observed data with Fisher's exact test at different time points. For the purpose of this thesis, P-values were calculated at 25%, 50%, 75% and 90%.
- Generating log cumulative hazard plots, because analysis of hazard function from lifespan data has gained popularity as the shape of the cumulative hazard plots has been proposed to reflect the rate of aging. Note that the plots cannot be labelled with italicised labels.
- Normalised Chow test, to verify the difference in the lifespan variations (using the log cumulative hazard plots). This particular statistical test examines whether the coefficients of two linear regressions on different normalized data sets are equal. Since researchers who perform survival analysis tend to be interested in examining the difference in slope rather than in determining the difference in y-intersect, before conducting the Chow test, OASIS normalises the log cumulative hazard data to have a mean of zero. Consequently, linear regression of each dataset has zero y-intersect. Thus, it is possible to examine the differences in the slopes of datasets.

8.1.1 I.I Statistical analysis for Figure 3.4 – Lifespan of *wrn-1, mut-7*, and *ZK1098.3* single mutants.

Name	No. of subjects	Restricted mean			Age in days at % mortality					
		Days	Std. error	95% C.I.	25%	50%	75%	90%	100%	95% Median C.I.
N2	60	13.05	0.42	12.23 ~ 13.87	11	12	15	17	24	12 ~ 12
wrn-1(gk99)	76	10.55	0.46	9.65 ~ 11.45	9	11	13	14	18	11 ~ 11
wrn-1(tm764)	78	10.37	0.45	9.49 ~ 11.25	8	11	13	15	17	10 ~ 11
mut-7(pk204)	90	11.24	0.43	10.41 ~ 12.08	10	12	14	15	20	11 ~ 12
ZK1098.3(tm2546)	77	13.74	0.38	13.00 ~ 14.48	12	13	16	18	26	13 ~ 13

Table App.1: Mean and median survival time for data presented in figure 3.4. C.I. indicates confidence interval.

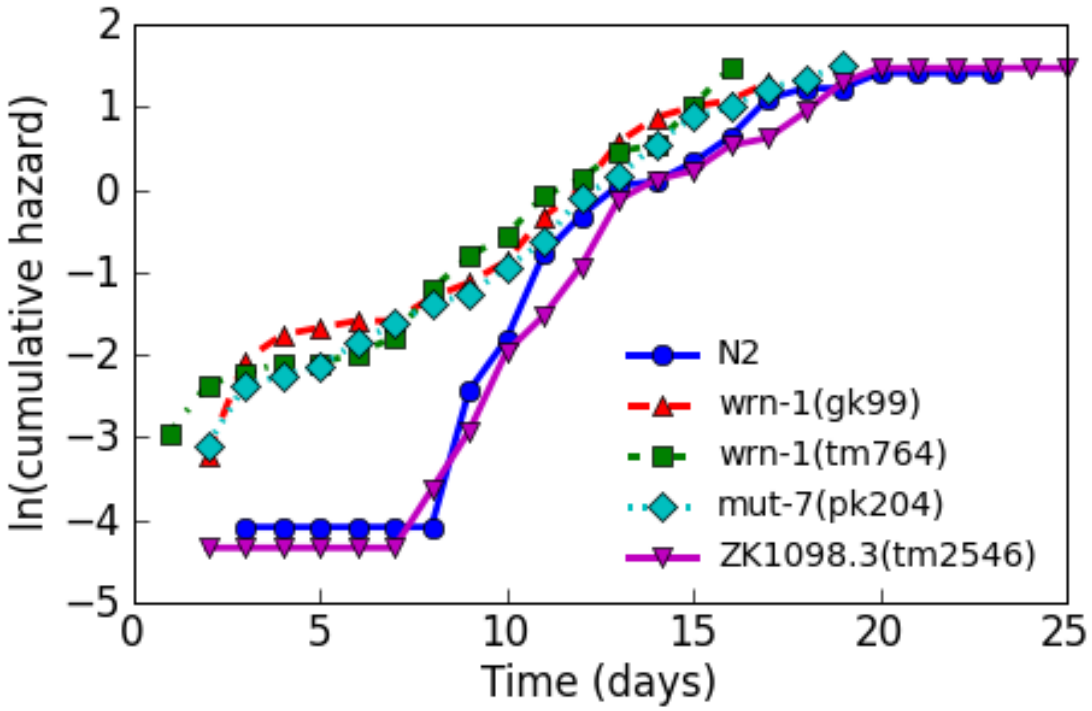

Figure App.1: Log Cumulative Hazard plot for Figure 3.4. The differences in slopes are analysed using a Normalised Chow Test (see Table App.2).

Condition	Log Rank Test			Fisher's Exact Test				Normalised Chow Test		
	Chi^2	**P-value**	**Bonferroni P-value**	**P-value at 25%**	**P-value at 50%**	**P-value at 75%**	**P-value at 90%**	**F-value**	**P-value**	**Bonferroni P-value**
N2 *v.s.* **wrn-1(gk99)**	9.03	0.0027	0.0106	0.017	0.221	0.0009	0.0775	1.83	0.1763	0.705
N2 *v.s.* **wrn-1(tm764)**	14.65	0.0001	0.0005	0.0004	0.0559	0.0468	0.0025	1.55	0.2266	0.9063
N2 *v.s.* **mut-7(pk204)**	4.51	0.0336	0.1346	0.0213	0.3195	0.0333	0.6837	2.83	0.0724	0.2895
N2 *v.s.* **ZK1098.3(tm2546)**	2.16	0.1414	0.5655	0.0327	0.4821	0.6531	0.4654	0.27	0.7672	1
wrn-1(gk99) *v.s.* **N2**	9.03	0.0027	0.0106	0.017	0.221	0.0009	0.0775	1.83	0.1763	0.705
wrn-1(gk99) *v.s.* **wrn-1(tm764)**	0.27	0.6004	1	0.3021	0.3303	0.6816	1	0.06	0.9413	1
wrn-1(gk99) *v.s.* **mut-7(pk204)**	2.01	0.1565	0.6261	0.7229	0.7496	0.0469	0.7734	0.02	0.9814	1
wrn-1(gk99) *v.s.* **ZK1098.3(tm2546)**	22.96	1.70E-06	6.60E-06	4.40E-05	0.0013	0.0006	0.0093	0.92	0.407	1
wrn-1(tm764) *v.s.* **N2**	14.65	0.0001	0.0005	0.0004	0.0559	0.0468	0.0025	1.55	0.2266	0.9063
wrn-1(tm764) *v.s.* **wrn-1(gk99)**	0.27	0.6004	1	0.3021	0.3303	0.6816	1	0.06	0.9413	1
wrn-1(tm764) *v.s.* **mut-7(pk204)**	2.78	0.0952	0.3808	0.1284	0.3354	1	0.5793	0.25	0.778	1
wrn-1(tm764) *v.s.* **ZK1098.3(tm2546)**	27.55	1.50E-07	6.10E-07	3.10E-05	1.30E-05	0.0003	0.0003	0.7	0.503	1
mut-7(pk204) *v.s.* **N2**	4.51	0.0336	0.1346	0.0213	0.3195	0.0333	0.6837	2.83	0.0724	0.2895
mut-7(pk204) *v.s.* **wrn-1(gk99)**	2.01	0.1565	0.6261	0.7229	0.7496	0.0469	0.7734	0.02	0.9814	1
mut-7(pk204) *v.s.* **wrn-1(tm764)**	2.78	0.0952	0.3808	0.1284	0.3354	1	0.5793	0.25	0.778	1
mut-7(pk204) *v.s.* **ZK1098.3(tm2546)**	12.59	0.0004	0.0015	0.0027	0.196	0.0316	0.0067	1.52	0.232	0.9281
ZK1098.3(tm2546) *v.s.* **N2**	2.16	0.1414	0.5655	0.0327	0.4821	0.6531	0.4654	0.27	0.7672	1
ZK1098.3(tm2546) *v.s.* **wrn-1(gk99)**	22.96	1.70E-06	6.60E-06	4.40E-05	0.0013	0.0006	0.0093	0.92	0.407	1
ZK1098.3(tm2546) *v.s.* **wrn-1(tm764)**	27.55	1.50E-07	6.10E-07	3.10E-05	1.30E-05	0.0003	0.0003	0.7	0.503	1
ZK1098.3(tm2546) *v.s.* **mut-7(pk204)**	12.59	0.0004	0.0015	0.0027	0.196	0.0316	0.0067	1.52	0.232	0.9281

Table App.2: Table showing the results of: Log Rank Tests (testing statistical significance over the entire lifespan); Fishers Exact Tests (statistical significance at specific time points); and Normalised Chow Tests (to test for variations in lifespans, specifically in relation to the slopes of the cumulative hazard plots) for the data presented in Figure 3.4.

8.1.2 I.II Statistical analysis for Figure 3.7 – Lifespan of *wrn-1* rescued worms.

Name	No. of subjects	Restricted mean			Age in days at % mortality					
		Days	Std. error	95% C.I.	25%	50%	75%	90%	100%	95% Median C.I.
AW869	55	14.80	0.90	13.03 ~ 16.57	8	15	21	23	26	13 ~ 17
AW898	58	11.59	0.56	10.49 ~ 12.68	9	12	15	17	21	10 ~ 13
AW931	60	19.30	0.76	17.81 ~ 20.79	15	21	23	26	31	18 ~ 21

Table App.3: Mean and median survival time for data presented in figure 3.7. C.I. indicates confidence interval.

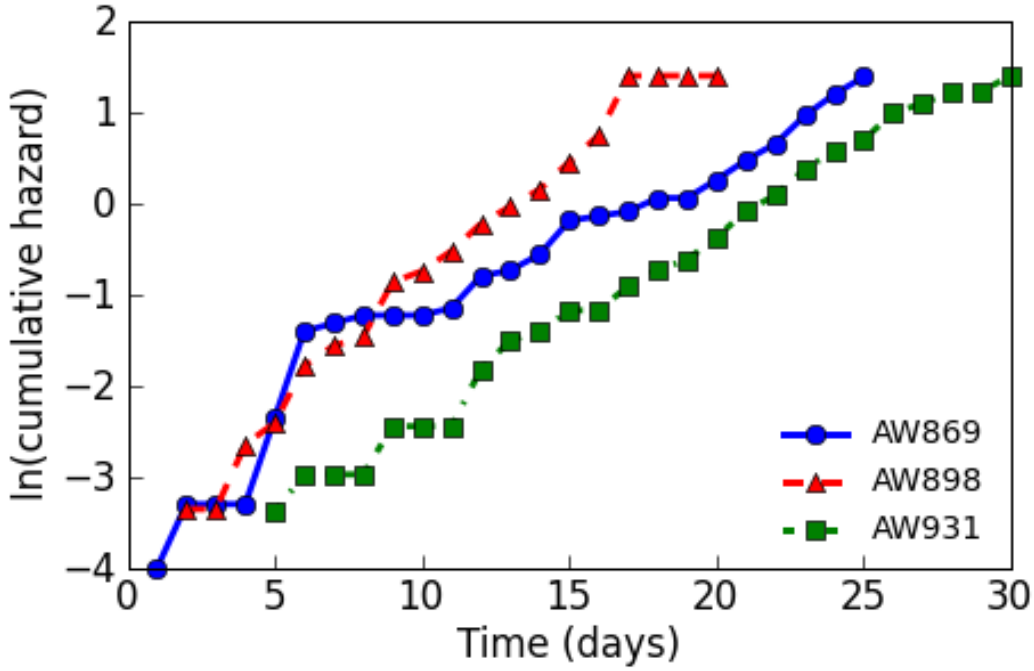

Figure App.2: Log Cumulative Hazard plot for Figure 3.7. The differences in slopes are analysed using a Normalised Chow Test (see Table App.4).

Condition	Log Rank Test			Fisher's Exact Test				Normalised Chow Test		
	Chi^2	**P-value**	**Bonferroni P-value**	**P-value at 25%**	**P-value at 50%**	**P-value at 75%**	**P-value at 90%**	**F-value**	**P-value**	**Bonferroni P-value**
AW869 *v.s.* **AW898**	17.02	3.70E-05	0.0001	0.3133	0.0145	1.50E-07	0.0002	12.9	4.80E-05	0.0001
AW869 *v.s.* **AW931**	12.1	0.0005	0.001	0.0102	0.005	0.0287	0.0334	0.1	0.9014	1
AW898 *v.s.* **AW869**	17.02	3.70E-05	0.0001	0.3133	0.0145	1.50E-07	0.0002	12.9	4.80E-05	0.0001
AW898 *v.s.* **AW931**	61.44	0.00E+00	0.00E+00	6.50E-06	7.70E-09	7.00E-09	0.0013	38.56	0.00E+00	0.00E+00
AW931 *v.s.* **AW869**	12.1	0.0005	0.001	0.0102	0.005	0.0287	0.0334	0.1	0.9014	1
AW931 *v.s.* **AW898**	61.44	0.00E+00	0.00E+00	6.50E-06	7.70E-09	7.00E-09	0.0013	38.56	0.00E+00	0.00E+00

Table App.4 (next page): Table showing the results of: Log Rank Tests (testing statistical significance over the entire lifespan); Fishers Exact Tests (statistical significance at specific time points); and Normalised Chow Tests (to test for variations in lifespans, specifically in relation to the slopes of the cumulative hazard plots) for the data presented in Figure 3.7.

8.1.3 I.III Statistical analysis for Figure 3.11 – Lifespan of *wrn-1* and *mut-7* single and double mutants.

Name	No. of subjects	Restricted mean			Age in days at % mortality					
		Days	Std. error	95% C.I.	25%	50%	75%	90%	100%	95% Median C.I.
N2	55	17.02	0.60	15.85 ~ 18.19	14	16	21	24	-	15 ~ 17
wrn-1(gk99)	48	10.56	0.70	9.19 ~ 11.94	6	11	14	18	19	8 ~ 12
wrn-1(tm64)	52	11.94	0.47	11.02 ~ 12.87	10	12	15	16	20	11 ~ 12
mut-7(pk204)	53	11.47	0.45	10.60 ~ 12.34	10	13	14	15	19	11 ~ 12
wrn-1(gk99);mut-7(pk204)	51	13.02	0.60	11.84 ~ 14.20	10	13	16	19	21	12 ~ 13
wrn-1(tm764);mut-7(pk204)	53	13.26	0.58	12.13 ~ 14.40	11	14	16	19	20	12 ~ 14

Table App.5: Mean and median survival time for data presented in figure 3.11. C.I. indicates confidence interval.

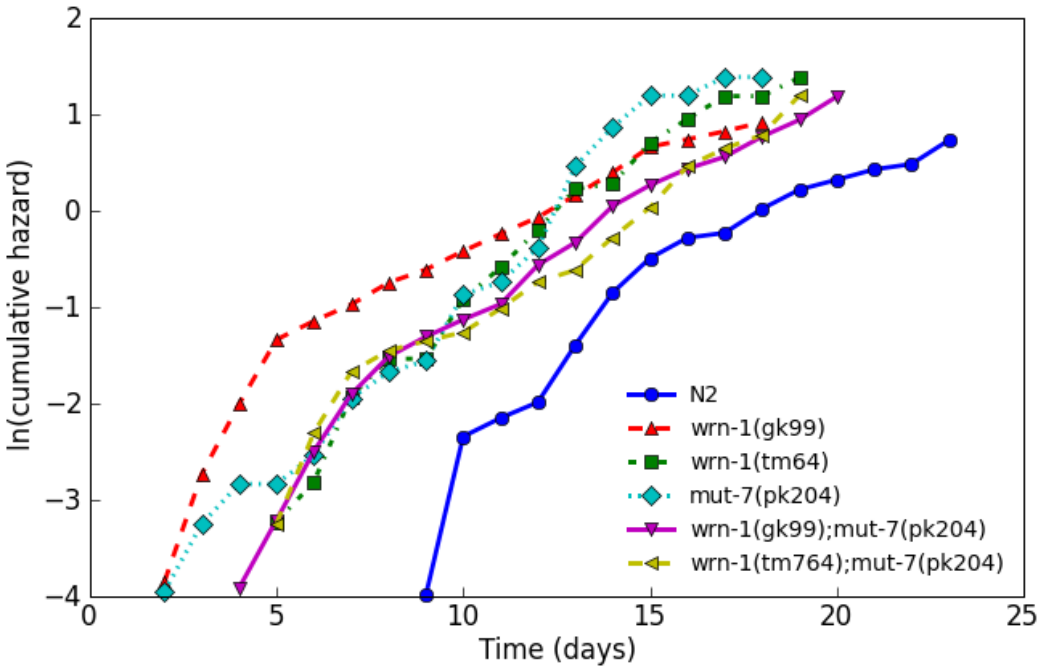

Figure App.3: Log Cumulative Hazard plot for Figure 3.11. The differences in slopes are analysed using a Normalised Chow Test (see Table App.6).

Condition	Log Rank Test			Fisher's Exact Test				Normalised Chow Test		
	Chi^2	P-value	Bonferroni P-value	P-value at 25%	P-value at 50%	P-value at 75%	P-value at 90%	F-value	P-value	Bonferroni P-value
N2 *v.s.* **wrn-1(gk99)**	34.5	4.30E-09	2.10E-08	1.40E-05	2.40E-05	0.0009	0.014	0.48	0.625	1
N2 *v.s.* **wrn-1(tm64)**	36.07	0.00E+00	0.00E+00	0.0003	0.0001	2.40E-05	0.0129	0.92	0.41	1
N2 *v.s.* **mut-7(pk204)**	48.87	0.00E+00	0.00E+00	0.0001	8.90E-10	3.20E-08	0.0128	2.88	0.0726	0.3629
N2 *v.s.* **wrn-1(gk99);mut-7(pk204)**	19.15	1.20E-05	0.0001	0.0005	0.0059	0.0036	0.0131	0.01	0.9859	1
N2 *v.s.* **wrn-1(tm764);mut-7(pk204)**	17.27	3.20E-05	0.0002	0.038	0.0564	0.0031	0.0128	0.08	0.9256	1
wrn-1(gk99) *v.s.* **N2**	34.5	4.30E-09	2.10E-08	1.40E-05	2.40E-05	0.0009	0.014	0.48	0.625	1
wrn-1(gk99) *v.s.* **wrn-1(tm64)**	0.38	0.5367	1	0.048	0.6882	1	0.2557	3.75	0.036	0.1799
wrn-1(gk99) *v.s.* **mut-7(pk204)**	0.08	0.7838	1	0.025	0.318	0.1	0.0815	8.71	0.001	0.0052
wrn-1(gk99) *v.s.* **wrn-1(gk99);mut-7(pk204)**	4.88	0.0272	0.136	0.0732	0.1085	0.1439	0.1181	1.07	0.3559	1
wrn-1(gk99) *v.s.* **wrn-1(tm764);mut-7(pk204)**	6.28	0.0122	0.0611	0.0795	0.0091	0.2993	0.7442	0.31	0.7366	1
wrn-1(tm64) *v.s.* **N2**	36.07	0.00E+00	0.00E+00	0.0003	0.0001	2.40E-05	0.0129	0.92	0.41	1
wrn-1(tm64) *v.s.* **wrn-1(gk99)**	0.38	0.5367	1	0.048	0.6882	1	0.2557	3.75	0.036	0.1799
wrn-1(tm64) *v.s.* **mut-7(pk204)**	0.95	0.3306	1	1	0.5596	0.3728	0.0927	0.68	0.5153	1
wrn-1(tm64) *v.s.* **wrn-1(gk99);mut-7(pk204)**	3.8	0.0512	0.2561	0.6685	0.0442	0.0914	0.1603	1.33	0.2796	1
wrn-1(tm64) *v.s.* **wrn-1(tm764);mut-7(pk204)**	5.47	0.0194	0.097	0.3933	0.0031	0.0121	0.0927	3.28	0.0535	0.2673
mut-7(pk204) *v.s.* **N2**	48.87	0.00E+00	0.00E+00	0.0001	8.90E-10	3.20E-08	0.0128	2.88	0.0726	0.3629
mut-7(pk204) *v.s.* **wrn-1(gk99)**	0.08	0.7838	1	0.025	0.318	0.1	0.0815	8.71	0.001	0.0052
mut-7(pk204) *v.s.* **wrn-1(tm64)**	0.95	0.3306	1	1	0.5596	0.3728	0.0927	0.68	0.5153	1
mut-7(pk204) *v.s.* **wrn-1(gk99);mut-7(pk204)**	8.11	0.0044	0.022	0.5278	0.0037	0.0019	0.0074	4.78	0.0157	0.0786
mut-7(pk204) *v.s.* **wrn-1(tm764);mut-7(pk204)**	13.15	0.0003	0.0014	0.3933	0.0001	4.40E-05	0.0313	9.14	0.0009	0.0044
wrn-1(gk99);mut-7(pk204) *v.s.* **N2**	19.15	1.20E-05	0.0001	0.0005	0.0059	0.0036	0.0131	0.01	0.9859	1
wrn-1(gk99);mut-7(pk204) *v.s.* **wrn-1(gk99)**	4.88	0.0272	0.136	0.0732	0.1085	0.1439	0.1181	1.07	0.3559	1
wrn-1(gk99);mut-7(pk204) *v.s.* **wrn-1(tm64)**	3.8	0.0512	0.2561	0.6685	0.0442	0.0914	0.1603	1.33	0.2796	1
wrn-1(gk99);mut-7(pk204) *v.s.* **mut-7(pk204)**	8.11	0.0044	0.022	0.5278	0.0037	0.0019	0.0074	4.78	0.0157	0.0786
wrn-1(gk99);mut-7(pk204) *v.s.* **wrn-1(tm764);mut-7(pk204)**	0	0.9727	1	0.8243	0.2383	1	0.4324	0.3	0.741	1
wrn-1(tm764);mut-7(pk204) *v.s.* **N2**	17.27	3.20E-05	0.0002	0.038	0.0564	0.0031	0.0128	0.08	0.9256	1
wrn-1(tm764);mut-7(pk204) *v.s.* **wrn-1(gk99)**	6.28	0.0122	0.0611	0.0795	0.0091	0.2993	0.7442	0.31	0.7366	1
wrn-1(tm764);mut-7(pk204) *v.s.* **wrn-1(tm64)**	5.47	0.0194	0.097	0.3933	0.0031	0.0121	0.0927	3.28	0.0535	0.2673
wrn-1(tm764);mut-7(pk204) *v.s.* **mut-7(pk204)**	13.15	0.0003	0.0014	0.3933	0.0001	4.40E-05	0.0313	9.14	0.0009	0.0044
wrn-1(tm764);mut-7(pk204) *v.s.* **wrn-1(gk99);mut-7(pk204)**	0	0.9727	1	0.8243	0.2383	1	0.4324	0.3	0.741	1

Table App.6: Table showing the results of: Log Rank Tests (testing statistical significance over the entire lifespan); Fishers Exact Tests (statistical significance at specific time points); and Normalised Chow Tests (to test for variations in lifespans, specifically in relation to the slopes of the cumulative hazard plots) for the data presented in Figure 3.11.

8.1.4 I.IV Statistical analysis for Figure 5.1 – Lifespan of *wrn-1* and *cep-1* single and double mutants at 20°C.

Name	No. of subjects	Restricted mean			Age in days at % mortality					
		Days	Std. error	95% C.I.	25%	50%	75%	90%	100%	95% Median C.I.
N2	50	17.76	0.61	16.57 ~ 18.95	14	18	21	23	24	16 ~ 20
cep-1(gk138)	56	16.25	0.65	14.97 ~ 17.53	14	17	20	22	24	15 ~ 18
wrn-1(gk99)	55	15.58	0.48	14.65 ~ 16.51	15	16	17	20	23	15 ~ 15
wrn-1(tm764)	56	16.64	0.35	15.95 ~ 17.33	15	16	19	20	22	15 ~ 17
cep-1(gk138);(wrn-1(gk99)	51	15.88	0.54	14.83 ~ 16.93	14	16	18	20	23	15 ~ 16
cep-1(gk138);wrn-1(tm764)	62	24.34	0.94	22.49 ~ 26.19	21	26	29	32	41	23 ~ 26

Table App.7: Mean and median survival time for data presented in figure 5.1. C.I. indicates confidence interval.

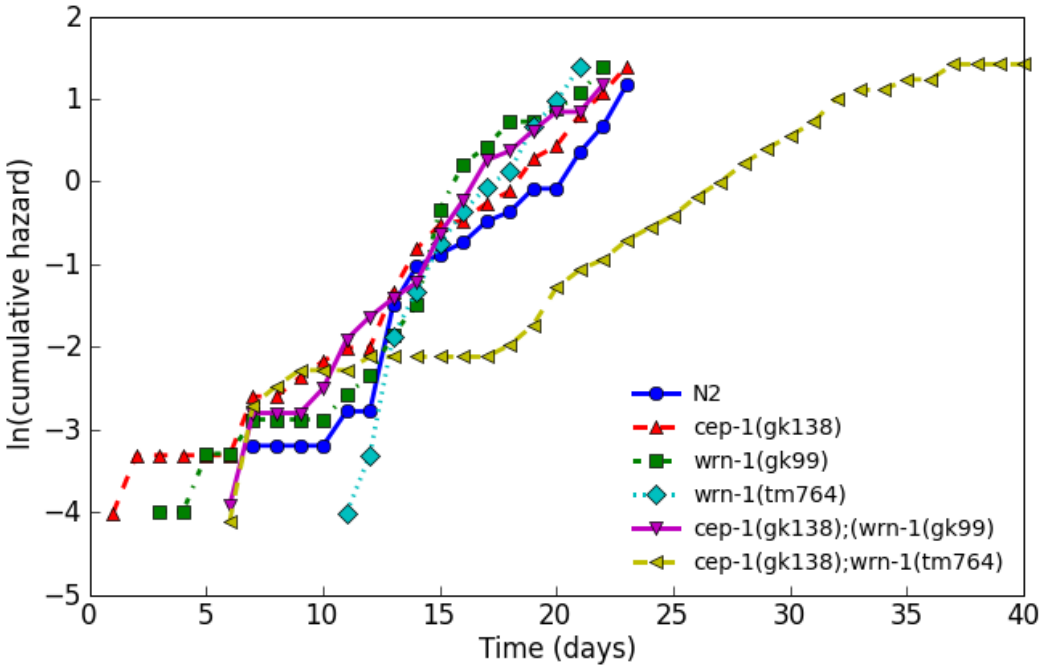

Figure App.4: Log Cumulative Hazard plot for Figure 5.1. The differences in slopes are analysed using a Normalised Chow Test (see Table App.8).

Condition	Log Rank Test			Fisher's Exact Test				Normalised Chow Test		
	Chi^2	P-value	Bonferroni P-value	P-value at 25%	P-value at 50%	P-value at 75%	P-value at 90%	F-value	P-value	Bonferroni P-value
N2 *v.s.* **cep-1(gk138)**	3.28	0.0699	0.3496	0.5438	0.4352	0.0769	0.1852	4.57	0.017	0.0852
N2 *v.s.* **wrn-1(gk99)**	11.4	0.0007	0.0037	0.1139	0.0009	0.0002	0.026	0.21	0.8094	1
N2 *v.s.* **wrn-1(tm764)**	10.21	0.0014	0.007	0.51	0.1721	0.0001	0.0041	12.91	0.0002	0.0008
N2 *v.s.* **cep-1(gk138);(wrn-1(gk99)**	7.4	0.0065	0.0327	0.6611	0.0085	0.0005	0.092	0.41	0.6666	1
N2 *v.s.* **cep-1(gk138);wrn-1(tm764)**	48.62	0.00E+00	0.00E+00	0.0001	1.10E-08	8.20E-09	0.001	35.58	0.00E+00	0.00E+00
cep-1(gk138) *v.s.* **N2**	3.28	0.0699	0.3496	0.5438	0.4352	0.0769	0.1852	4.57	0.017	0.0852
cep-1(gk138) *v.s.* **wrn-1(gk99)**	3.15	0.076	0.3799	0.0902	0.0121	0.0945	0.4893	7.4	0.0019	0.0094
cep-1(gk138) *v.s.* **wrn-1(tm764)**	1.89	0.1687	0.8434	0.2133	0.567	0.1596	0.1132	32.34	0.00E+00	0.00E+00
cep-1(gk138) *v.s.* **cep-1(gk138);(wrn-1(gk99)**	1.21	0.2714	1	0.298	0.4409	0.2386	1	11.92	0.0001	0.0005
cep-1(gk138) *v.s.* **cep-1(gk138);wrn-1(tm764)**	63.8	0.00E+00	0.00E+00	0.0001	1.30E-11	9.00E-10	0.0007	38.51	0.00E+00	0.00E+00
wrn-1(gk99) *v.s.* **N2**	11.4	0.0007	0.0037	0.1139	0.0009	0.0002	0.026	0.21	0.8094	1
wrn-1(gk99) *v.s.* **cep-1(gk138)**	3.15	0.076	0.3799	0.0902	0.0121	0.0945	0.4893	7.4	0.0019	0.0094
wrn-1(gk99) *v.s.* **wrn-1(tm764)**	0.98	0.323	1	0.1831	0.0328	0.0221	0.7422	8.91	0.0011	0.0054
wrn-1(gk99) *v.s.* **cep-1(gk138);(wrn-1(gk99)**	0.86	0.3545	1	0.3363	0.1083	0.6519	1	0	0.9956	1
wrn-1(gk99) *v.s.* **cep-1(gk138);wrn-1(tm764)**	75.49	0.00E+00	0.00E+00	4.80E-06	1.30E-13	2.10E-09	0.0007	52.74	0.00E+00	0.00E+00
wrn-1(tm764) *v.s.* **N2**	10.21	0.0014	0.007	0.51	0.1721	0.0001	0.0041	12.91	0.0002	0.0008
wrn-1(tm764) *v.s.* **cep-1(gk138)**	1.89	0.1687	0.8434	0.2133	0.567	0.1596	0.1132	32.34	0.00E+00	0.00E+00
wrn-1(tm764) *v.s.* **wrn-1(gk99)**	0.98	0.323	1	0.1831	0.0328	0.0221	0.7422	8.91	0.0011	0.0054
wrn-1(tm764) *v.s.* **cep-1(gk138);(wrn-1(gk99)**	0	0.9798	1	0.843	0.6994	1	0.7338	14.2	0.0001	0.0004
wrn-1(tm764) *v.s.* **cep-1(gk138);wrn-1(tm764)**	74.14	0.00E+00	0.00E+00	5.40E-06	9.40E-13	9.00E-10	0.0007	54.15	0.00E+00	0.00E+00
cep-1(gk138);(wrn-1(gk99) *v.s.* **N2**	7.4	0.0065	0.0327	0.6611	0.0085	0.0005	0.092	0.41	0.6666	1
cep-1(gk138);(wrn-1(gk99) *v.s.* **cep-1(gk138)**	1.21	0.2714	1	0.298	0.4409	0.2386	1	11.92	0.0001	0.0005
cep-1(gk138);(wrn-1(gk99) *v.s.* **wrn-1(gk99)**	0.86	0.3545	1	0.3363	0.1083	0.6519	1	0	0.9956	1
cep-1(gk138);(wrn-1(gk99) *v.s.* **wrn-1(tm764)**	0	0.9798	1	0.843	0.6994	1	0.7338	14.2	0.0001	0.0004
cep-1(gk138);(wrn-1(gk99) *v.s.* **cep-1(gk138);wrn-1(tm764)**	69.55	0.00E+00	0.00E+00	6.10E-07	1.00E-12	3.50E-09	0.001	54.99	0.00E+00	0.00E+00
cep-1(gk138);wrn-1(tm764) *v.s.* **N2**	48.62	0.00E+00	0.00E+00	0.0001	1.10E-08	8.20E-09	0.001	35.58	0.00E+00	0.00E+00
cep-1(gk138);wrn-1(tm764) *v.s.* **cep-1(gk138)**	63.8	0.00E+00	0.00E+00	0.0001	1.30E-11	9.00E-10	0.0007	38.51	0.00E+00	0.00E+00
cep-1(gk138);wrn-1(tm764) *v.s.* **wrn-1(gk99)**	75.49	0.00E+00	0.00E+00	4.80E-06	1.30E-13	2.10E-09	0.0007	52.74	0.00E+00	0.00E+00
cep-1(gk138);wrn-1(tm764) *v.s.* **wrn-1(tm764)**	74.14	0.00E+00	0.00E+00	5.40E-06	9.40E-13	9.00E-10	0.0007	54.15	0.00E+00	0.00E+00
cep-1(gk138);wrn-1(tm764) *v.s.* **cep-1(gk138);(wrn-1(gk99)**	69.55	0.00E+00	0.00E+00	6.10E-07	1.00E-12	3.50E-09	0.001	54.99	0.00E+00	0.00E+00

Table App.8: Table showing the results of: Log Rank Tests (testing statistical significance over the entire lifespan); Fishers Exact Tests (statistical significance at specific time points); and Normalised Chow Tests (to test for variations in lifespans, specifically in relation to the slopes of the cumulative hazard plots) for the data presented in Figure 5.1.

8.1.5 I.V Statistical analysis for Figure 5.7 – Lifespan of *cep-1;wrn-1* in the presence and absence of *daf-16* RNAi.

Name	No. of subjects	Restricted mean			Age in days at % mortality					
		Days	Std. error	95% C.I.	25%	50%	75%	90%	100%	95% Median C.I.
N2 L4440	57	12.89	0.65	11.62 ~ 14.17	9	12	16	20	23	11 ~ 14
N2 daf-16	59	10.78	0.36	10.08 ~ 11.48	9	11	13	15	17	10 ~ 11
CT L4440	59	26.05	0.72	24.63 ~ 27.47	23	26	29	32	40	25 ~ 26
CT daf-16	60	12.60	0.48	11.66 ~ 13.54	11	12	15	17	21	12 ~ 13

Table App.9: Mean and median survival time for data presented in figure 5.7. C.I. indicates confidence interval.

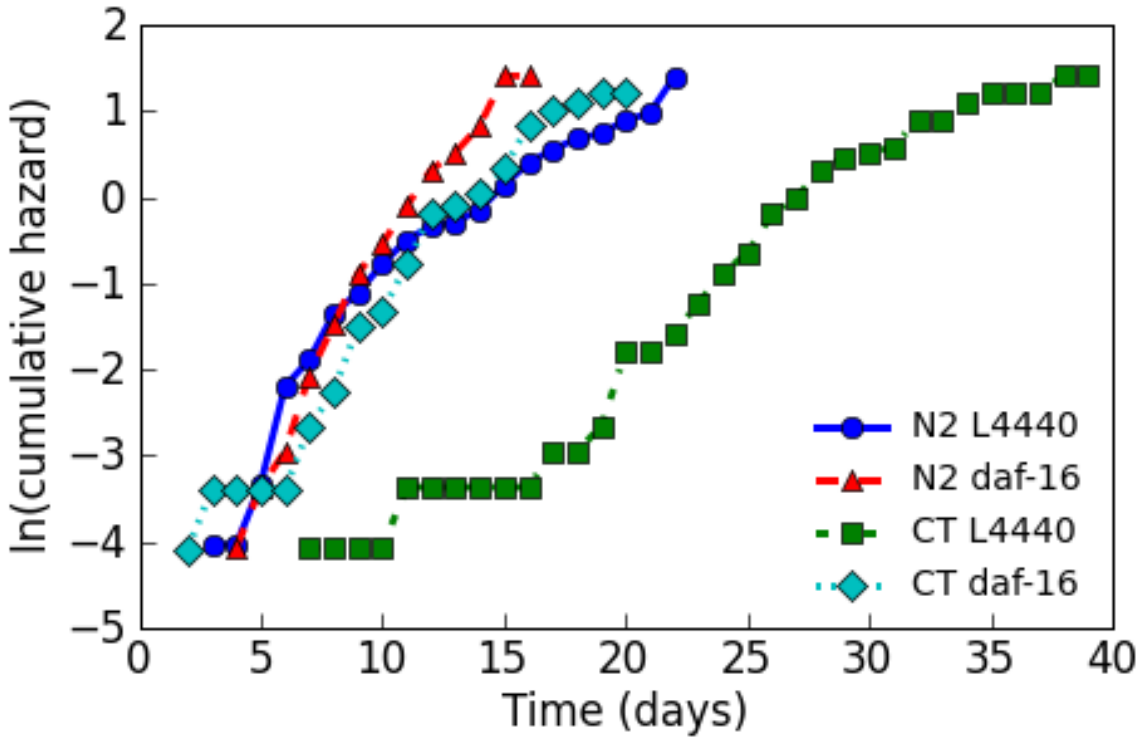

Figure App.5: Log Cumulative Hazard plot for Figure 5.7. The differences in slopes are analysed using a Normalised Chow Test (see Table App.10).

Condition	Log Rank Test			Fisher's Exact Test				Normalised Chow Test		
	Chi^2	**P-value**	**Bonferroni P-value**	**P-value at 25%**	**P-value at 50%**	**P-value at 75%**	**P-value at 90%**	**F-value**	**P-value**	**Bonferroni P-value**
N2 L4440 *v.s.* **N2 daf-16**	13.47	0.0002	0.0007	0.5505	0.1928	7.00E-06	0.0005	13.56	0.0001	0.0002
N2 L4440 *v.s.* **CT L4440**	109.4	0.00E+00	0.00E+00	2.00E-09	8.20E-13	9.20E-10	0.0006	5.28	0.0084	0.0252
N2 L4440 *v.s.* **CT daf-16**	1.21	0.2712	0.8136	0.157	0.5805	0.0798	0.1193	3.09	0.0583	0.175
N2 daf-16 *v.s.* **N2 L4440**	13.47	0.0002	0.0007	0.5505	0.1928	7.00E-06	0.0005	13.56	0.0001	0.0002
N2 daf-16 *v.s.* **CT L4440**	123.7	0.00E+00	0.00E+00	1.30E-11	1.50E-12	8.50E-10	0.0006	44.22	0.00E+00	0.00E+00
N2 daf-16 *v.s.* **CT daf-16**	13.92	0.0002	0.0006	0.1011	0.0536	0.0018	0.114	11.08	0.0003	0.0009
CT L4440 *v.s.* **N2 L4440**	109.4	0.00E+00	0.00E+00	2.00E-09	8.20E-13	9.20E-10	0.0006	5.28	0.0084	0.0252
CT L4440 *v.s.* **N2 daf-16**	123.7	0.00E+00	0.00E+00	1.30E-11	1.50E-12	8.50E-10	0.0006	44.22	0.00E+00	0.00E+00
CT L4440 *v.s.* **CT daf-16**	118.49	0.00E+00	0.00E+00	4.70E-11	5.70E-13	3.30E-10	0.0003	27.5	0.00E+00	0.00E+00
CT daf-16 *v.s.* **N2 L4440**	1.21	0.2712	0.8136	0.157	0.5805	0.0798	0.1193	3.09	0.0583	0.175
CT daf-16 *v.s.* **N2 daf-16**	13.92	0.0002	0.0006	0.1011	0.0536	0.0018	0.114	11.08	0.0003	0.0009
CT daf-16 *v.s.* **CT L4440**	118.49	0.00E+00	0.00E+00	4.70E-11	5.70E-13	3.30E-10	0.0003	27.5	0.00E+00	0.00E+00

Table App.10: Table showing the results of: Log Rank Tests (testing statistical significance over the entire lifespan); Fishers Exact Tests (statistical significance at specific time points); and Normalised Chow Tests (to test for variations in lifespans, specifically in relation to the slopes of the cumulative hazard plots) for the data presented in Figure 5.7.

8.1.6 I.VI Statistical analysis for Figure 5.9 – Lifespan of *cep-1* and *him-6* single and double mutants.

Name	No. of subjects	Restricted mean			Age in days at % mortality					
		Days	Std. error	95% C.I.	25%	50%	75%	90%	100%	95% Median C.I.
N2	59	15.54	0.44	14.68 ~ 16.40	14	15	17	21	23	15 ~ 15
cep-1(gk138);him-6(ok412)	62	15.90	0.70	14.52 ~ 17.28	13	16	20	24	-	15 ~ 16
him-6(ok412)	19	14.89	0.97	12.99 ~ 16.80	12	14	18	21	24	13 ~ 17
cep-1(gk138)	15	13.93	1.34	11.31 ~ 16.56	11	15	18	21	-	11 ~ 16

Table App.11: Mean and median survival time for data presented in figure 5.9. C.I. indicates confidence interval.

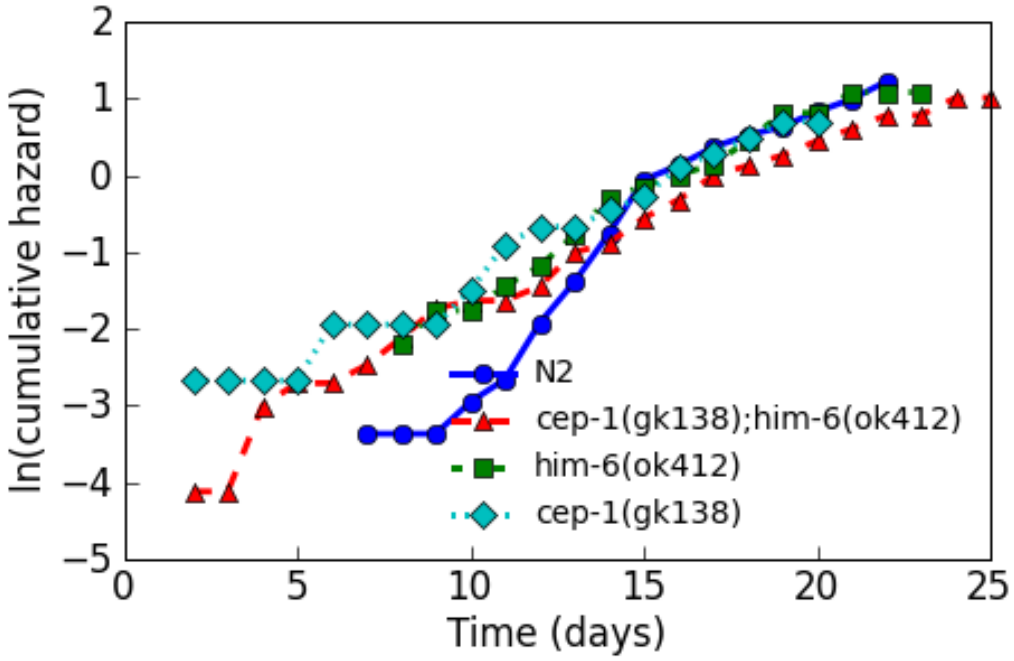

Figure App.6: Log Cumulative Hazard plot for Figure 5.9. The differences in slopes are analysed using a Normalised Chow Test (see Table App.12). Note that although statistical analysis suggests that there is no significant difference in lifespan between these strains (Table App.12), the y-intercept in the log cumulative hazard plot of *cep-1;him-6* double mutants was smaller than those of N2 and single mutants. Furthermore, these data are combined from two separate experiments, and the n values for the single mutants are much lower than those for N2 and the double mutants. Since, unlike all other lifespan experiments, this experiment was only performed once, this should be repeated at least twice more and statistical analysis performed again. This may reveal a statistical significance after all.

Condition	Log Rank Test			Fisher's Exact Test				Normalised Chow Test		
	Chi^2	**P-value**	**Bonferroni P-value**	**P-value at 25%**	**P-value at 50%**	**P-value at 75%**	**P-value at 90%**	**F-value**	**P-value**	**Bonferroni P-value**
N2 *v.s.* ***cep-1(gk138);him-6(ok412)***	3.81	0.0509	0.1528	0.3091	0.0692	0.099	0.1555	22.44	0.00E+00	1.00E-06
N2 *v.s.* ***him-6(ok412)***	0.01	0.9305	1	0.233	1	1	1	12.68	0.0001	0.0004
N2 *v.s.* ***cep-1(gk138)***	0.37	0.541	1	0.1902	0.7692	1	0.5762	23.12	1.00E-06	2.00E-06
cep-1(gk138);him-6(ok412) *v.s.* **N2**	3.81	0.0509	0.1528	0.3091	0.0692	0.099	0.1555	22.44	0.00E+00	1.00E-06
cep-1(gk138);him-6(ok412) *v.s.* ***him-6(ok412)***	1.83	0.1758	0.5273	0.7794	0.4376	0.2148	0.4436	0.37	0.6945	1
cep-1(gk138);him-6(ok412) *v.s.* ***cep-1(gk138)***	2.37	0.1239	0.3716	0.18	0.3899	0.3329	0.195	0.17	0.8481	1
him-6(ok412) *v.s.* **N2**	0.01	0.9305	1	0.233	1	1	1	12.68	0.0001	0.0004
him-6(ok412) *v.s.* ***cep-1(gk138);him-6(ok412)***	1.83	0.1758	0.5273	0.7794	0.4376	0.2148	0.4436	0.37	0.6945	1
him-6(ok412) *v.s.* ***cep-1(gk138)***	0.07	0.7879	1	0.462	1	1	1	1.09	0.3479	1
cep-1(gk138) *v.s.* **N2**	0.37	0.541	1	0.1902	0.7692	1	0.5762	23.12	1.00E-06	2.00E-06
cep-1(gk138) *v.s.* ***cep-1(gk138);him-6(ok412)***	2.37	0.1239	0.3716	0.18	0.3899	0.3329	0.195	0.17	0.8481	1
cep-1(gk138) *v.s.* ***him-6(ok412)***	0.07	0.7879	1	0.462	1	1	1	1.09	0.3479	1

Table App.12: Table showing the results of: Log Rank Tests (testing statistical significance over the entire lifespan); Fishers Exact Tests (statistical significance at specific time points); and Normalised Chow Tests (to test for variations in lifespans, specifically in relation to the slopes of the cumulative hazard plots) for the data presented in Figure 5.9.

8.1.7 I.VII Statistical analysis for Figure 6.1 – Lifespan of *wrn-1* and *cep-1* single and double mutants at 25°C.

Name	No. of subjects	Restricted mean			Age in days at % mortality					
		Days	Std. error	95% C.I.	25%	50%	75%	90%	100%	95% Median C.I.
N2	33	9.67	0.52	8.65 ~ 10.68	8	10	11	14	17	8 ~ 10
wrn-1(gk99)	39	8.46	0.52	7.44 ~ 9.48	6	7	11	13	15	6 ~ 9
wrn-1(tm764)	39	9.15	0.61	7.96 ~ 10.35	6	7	11	15	20	7 ~ 9
cep-1(gk138)	42	12.12	0.58	10.98 ~ 13.25	11	12	15	16	19	12 ~ 13
cep-1(gk138);wrn-1(gk99)	39	15.49	0.38	14.75 ~ 16.23	14	15	17	19	20	15 ~ 15
cep-1(gk138);wrn-1(tm764)	37	17.57	0.40	16.79 ~ 18.34	16	18	19	21	22	17 ~ 18

Table App.13: Mean and median survival time for data presented in figure 6.1. C.I. indicates confidence interval.

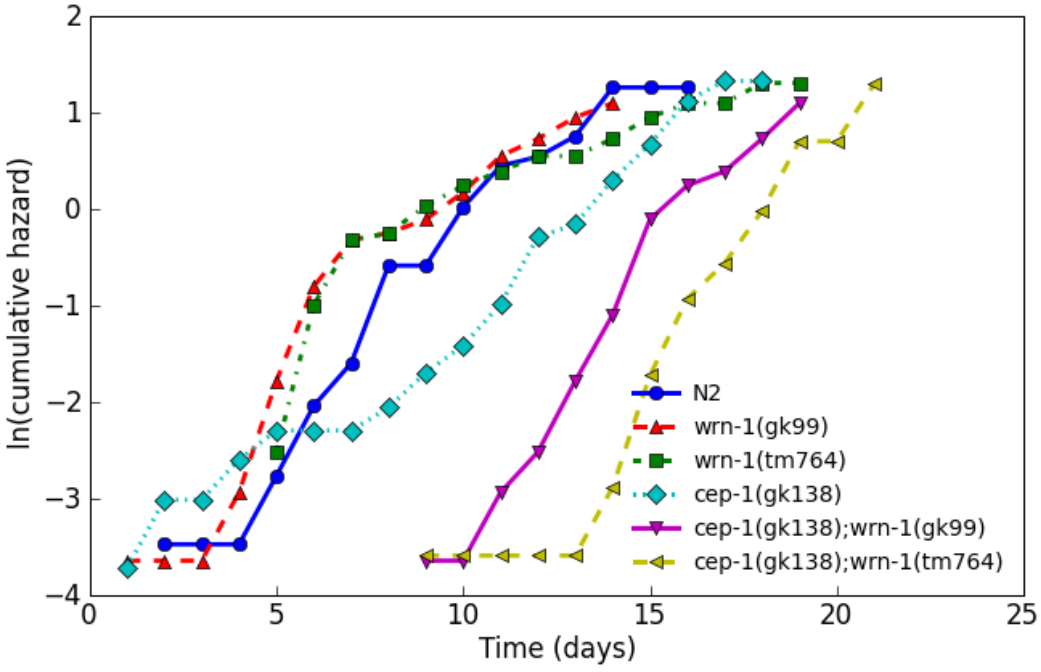

Figure App.7: Log Cumulative Hazard plot for Figure 6.1. The differences in slopes are analysed using a Normalised Chow Test (see Table App.14).

Condition	Log Rank Test			Fisher's Exact Test				Normalised Chow Test		
	Chi^2	P-value	Bonferroni P-value	P-value at 25%	P-value at 50%	P-value at 75%	P-value at 90%	F-value	P-value	Bonferroni P-value
N2 *v.s.* ***wrn-1(gk99)***	1.67	0.1965	0.9826	0.0062	0.2367	0.772	0.6954	0.05	0.9476	1
N2 *v.s.* ***wrn-1(tm764)***	0.11	0.7369	1	0.0062	0.0965	1	0.2088	14	0.0001	0.0004
N2 *v.s.* ***cep-1(gk138)***	13.22	0.0003	0.0014	0.0034	0.0001	0.0092	0.1264	7.19	0.0029	0.0145
N2 *v.s.* ***cep-1(gk138);wrn-1(gk99)***	51.56	0.00E+00	0.00E+00	7.80E-09	8.40E-10	0.0002	0.0581	4.97	0.0165	0.0827
N2 *v.s.* ***cep-1(gk138);wrn-1(tm764)***	68.22	0.00E+00	0.00E+00	2.60E-08	9.30E-13	3.60E-05	0.0556	1.47	0.2491	1
wrn-1(gk99) *v.s.* **N2**	1.67	0.1965	0.9826	0.0062	0.2367	0.772	0.6954	0.05	0.9476	1
wrn-1(gk99) *v.s.* ***wrn-1(tm764)***	0.96	0.328	1	0.8105	1	0.7799	0.4309	11.11	0.0004	0.0018
wrn-1(gk99) *v.s.* ***cep-1(gk138)***	22.52	2.10E-06	1.00E-05	0.0001	5.00E-06	0.014	0.0262	5.81	0.0077	0.0387
wrn-1(gk99) *v.s.* ***cep-1(gk138);wrn-1(gk99)***	62.61	0.00E+00	0.00E+00	7.00E-08	2.80E-12	4.40E-06	0.0545	2.55	0.1022	0.5108
wrn-1(gk99) *v.s.* ***cep-1(gk138);wrn-1(tm764)***	78.02	0.00E+00	0.00E+00	7.80E-08	1.50E-12	8.90E-06	0.0236	0.71	0.5017	1
wrn-1(tm764) *v.s.* **N2**	0.11	0.7369	1	0.0062	0.0965	1	0.2088	14	0.0001	0.0004
wrn-1(tm764) *v.s.* ***wrn-1(gk99)***	0.96	0.328	1	0.8105	1	0.7799	0.4309	11.11	0.0004	0.0018
wrn-1(tm764) *v.s.* ***cep-1(gk138)***	7.19	0.0073	0.0366	0.0001	4.90E-05	0.1673	1	6.14	0.006	0.0299
wrn-1(tm764) *v.s.* ***cep-1(gk138);wrn-1(gk99)***	30.82	2.80E-08	1.40E-07	7.00E-08	1.90E-07	0.0011	0.2002	25.14	2.00E-06	1.00E-05
wrn-1(tm764) *v.s.* ***cep-1(gk138);wrn-1(tm764)***	52.98	0.00E+00	0.00E+00	7.80E-08	7.00E-12	0.0001	0.1033	16.39	3.20E-05	0.0002
cep-1(gk138) *v.s.* **N2**	13.22	0.0003	0.0014	0.0034	0.0001	0.0092	0.1264	7.19	0.0029	0.0145
cep-1(gk138) *v.s.* ***wrn-1(gk99)***	22.52	2.10E-06	1.00E-05	0.0001	5.00E-06	0.014	0.0262	5.81	0.0077	0.0387
cep-1(gk138) *v.s.* ***wrn-1(tm764)***	7.19	0.0073	0.0366	0.0001	4.90E-05	0.1673	1	6.14	0.006	0.0299
cep-1(gk138) *v.s.* ***cep-1(gk138);wrn-1(gk99)***	18.77	1.50E-05	0.0001	1.10E-05	0.0001	0.0055	0.1007	27.88	0.00E+00	2.00E-06
cep-1(gk138) *v.s.* ***cep-1(gk138);wrn-1(tm764)***	48.32	0.00E+00	0.00E+00	6.40E-07	2.90E-10	0.0001	0.0193	12.31	0.0002	0.0008
cep-1(gk138);wrn-1(gk99) *v.s.* **N2**	51.56	0.00E+00	0.00E+00	7.80E-09	8.40E-10	0.0002	0.0581	4.97	0.0165	0.0827
cep-1(gk138);wrn-1(gk99) *v.s.* ***wrn-1(gk99)***	62.61	0.00E+00	0.00E+00	7.00E-08	2.80E-12	4.40E-06	0.0545	2.55	0.1022	0.5108
cep-1(gk138);wrn-1(gk99) *v.s.* ***wrn-1(tm764)***	30.82	2.80E-08	1.40E-07	7.00E-08	1.90E-07	0.0011	0.2002	25.14	2.00E-06	1.00E-05
cep-1(gk138);wrn-1(gk99) *v.s.* ***cep-1(gk138)***	18.77	1.50E-05	0.0001	1.10E-05	0.0001	0.0055	0.1007	27.88	0.00E+00	2.00E-06
cep-1(gk138);wrn-1(gk99) *v.s.* ***cep-1(gk138);wrn-1(tm764)***	13.93	0.0002	0.001	0.0001	0.0011	0.2562	0.2562	0.5	0.6119	1
cep-1(gk138);wrn-1(tm764) *v.s.* **N2**	68.22	0.00E+00	0.00E+00	2.60E-08	9.30E-13	3.60E-05	0.0556	1.47	0.2491	1
cep-1(gk138);wrn-1(tm764) *v.s.* ***wrn-1(gk99)***	78.02	0.00E+00	0.00E+00	7.80E-08	1.50E-12	8.90E-06	0.0236	0.71	0.5017	1
cep-1(gk138);wrn-1(tm764) *v.s.* ***wrn-1(tm764)***	52.98	0.00E+00	0.00E+00	7.80E-08	7.00E-12	0.0001	0.1033	16.39	3.20E-05	0.0002
cep-1(gk138);wrn-1(tm764) *v.s.* ***cep-1(gk138)***	48.32	0.00E+00	0.00E+00	6.40E-07	2.90E-10	0.0001	0.0193	12.31	0.0002	0.0008
cep-1(gk138);wrn-1(tm764) *v.s.* ***cep-1(gk138);wrn-1(gk99)***	13.93	0.0002	0.001	0.0001	0.0011	0.2562	0.2562	0.5	0.6119	1

Table App.14: Table showing the results of: Log Rank Tests (testing statistical significance over the entire lifespan); Fishers Exact Tests (statistical significance at specific time points); and Normalised Chow Tests (to test for variations in lifespans, specifically in relation to the slopes of the cumulative hazard plots) for the data presented in Figure 6.1.

8.1.8 I.VIII Statistical analysis for Figure 6.5 - Survival of *wrn-1* and *cep-1* single and double mutants after UV irradiation.

Name	No. of subjects	Restricted mean			Age in days at % mortality					
		Days	Std. error	95% C.I.	25%	50%	75%	90%	100%	95% Median C.I.
N2	39	4.97	0.22	4.55 ~ 5.40	4	5	6	7	9	4 ~ 4
cep-1(gk138)	49	7.18	0.26	6.68 ~ 7.69	6	7	8	10	11	6 ~ 7
wrn-1(gk99)	57	4.19	0.19	3.81 ~ 4.57	3	4	5	6	7	4 ~ 4
wrn-1(tm764)	47	5.17	0.20	4.77 ~ 5.57	4	5	6	7	9	5 ~ 5
cep-1(gk138);wrn-1(gk99)	55	6.78	0.35	6.10 ~ 7.46	5	6	9	10	12	6 ~ 7
cep-1(gk138);wrn-1(tm764)	70	8.03	0.30	7.43 ~ 8.63	6	8	10	11	13	7 ~ 8

Table App.15: Mean and median survival time for data presented in figure 6.5. C.I. indicates confidence interval.

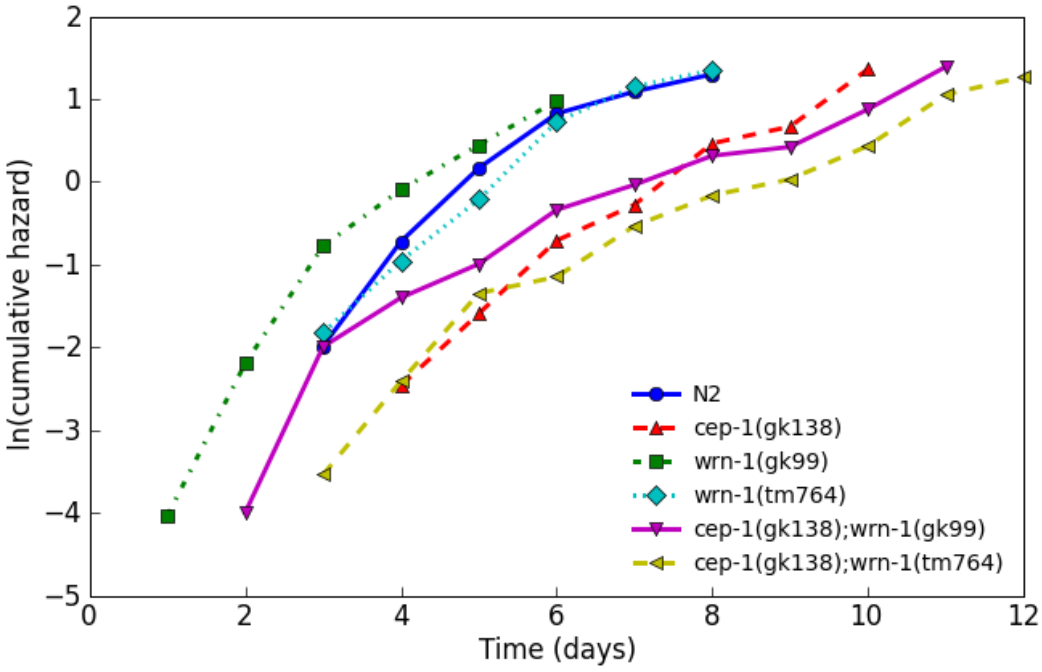

Figure App.8: Log Cumulative Hazard plot for Figure 6.5. The differences in slopes are analysed using a Normalised Chow Test (see Table App.16).

Condition	Log Rank Test			Fisher's Exact Test				Normalised Chow Test		
	Chi^2	P-value	Bonferroni P-value	P-value at 25%	P-value at 50%	P-value at 75%	P-value at 90%	F-value	P-value	Bonferroni P-value
N2 *v.s.* **cep-1(gk138)**	32.33	1.30E-08	6.50E-08	2.60E-06	7.40E-07	0.0197	0.016	0.05	0.9552	1
N2 *v.s.* **wrn-1(gk99)**	4.62	0.0316	0.1579	0.0105	0.061	0.7114	0.7114	1.75	0.2337	1
N2 *v.s.* **wrn-1(tm764)**	0.59	0.442	1	0.6502	0.2655	1	1	0.01	0.99	1
N2 *v.s.* **cep-1(gk138);wrn-1(gk99)**	19.07	1.30E-05	0.0001	0.1058	0.0001	0.0002	0.0739	0.61	0.5599	1
N2 *v.s.* **cep-1(gk138);wrn-1(tm764)**	48.21	0.00E+00	0.00E+00	4.00E-06	3.60E-08	2.60E-06	0.2946	1.16	0.3453	1
cep-1(gk138) *v.s.* **N2**	32.33	1.30E-08	6.50E-08	2.60E-06	7.40E-07	0.0197	0.016	0.05	0.9552	1
cep-1(gk138) *v.s.* **wrn-1(gk99)**	57.46	0.00E+00	0.00E+00	1.60E-08	4.40E-10	5.20E-10	0.0003	3.83	0.0627	0.3135
cep-1(gk138) *v.s.* **wrn-1(tm764)**	30.66	3.10E-08	1.50E-07	0.0003	8.20E-07	0.0078	0.0125	0.2	0.8225	1
cep-1(gk138) *v.s.* **cep-1(gk138);wrn-1(gk99)**	0	0.9536	1	0.2409	0.4285	0.6432	0.2098	0.71	0.5081	1
cep-1(gk138) *v.s.* **cep-1(gk138);wrn-1(tm764)**	7.6	0.0058	0.0292	0.2311	0.0114	0.002	0.1421	1.61	0.2365	1
wrn-1(gk99) *v.s.* **N2**	4.62	0.0316	0.1579	0.0105	0.061	0.7114	0.7114	1.75	0.2337	1
wrn-1(gk99) *v.s.* **cep-1(gk138)**	57.46	0.00E+00	0.00E+00	1.60E-08	4.40E-10	5.20E-10	0.0003	3.83	0.0627	0.3135
wrn-1(gk99) *v.s.* **wrn-1(tm764)**	8.96	0.0028	0.0138	0.0147	0.0119	0.3417	0.3417	1.98	0.2003	1
wrn-1(gk99) *v.s.* **cep-1(gk138);wrn-1(gk99)**	38.29	0.00E+00	0.00E+00	0.0001	4.70E-07	2.90E-08	0.0259	5.15	0.0243	0.1216
wrn-1(gk99) *v.s.* **cep-1(gk138);wrn-1(tm764)**	78.07	0.00E+00	0.00E+00	5.00E-10	2.60E-13	7.90E-10	0.1269	8.17	0.0058	0.0289
wrn-1(tm764) *v.s.* **N2**	0.59	0.442	1	0.6502	0.2655	1	1	0.01	0.99	1
wrn-1(tm764) *v.s.* **cep-1(gk138)**	30.66	3.10E-08	1.50E-07	0.0003	8.20E-07	0.0078	0.0125	0.2	0.8225	1
wrn-1(tm764) *v.s.* **wrn-1(gk99)**	8.96	0.0028	0.0138	0.0147	0.0119	0.3417	0.3417	1.98	0.2003	1
wrn-1(tm764) *v.s.* **cep-1(gk138);wrn-1(gk99)**	17.74	2.50E-05	0.0001	0.269	0.0001	3.00E-05	0.0602	0.88	0.4398	1
wrn-1(tm764) *v.s.* **cep-1(gk138);wrn-1(tm764)**	47.69	0.00E+00	0.00E+00	0.0004	1.10E-10	3.60E-07	0.1477	1.86	0.1972	0.9862
cep-1(gk138);wrn-1(gk99) *v.s.* **N2**	19.07	1.30E-05	0.0001	0.1058	0.0001	0.0002	0.0739	0.61	0.5599	1
cep-1(gk138);wrn-1(gk99) *v.s.* **cep-1(gk138)**	0	0.9536	1	0.2409	0.4285	0.6432	0.2098	0.71	0.5081	1
cep-1(gk138);wrn-1(gk99) *v.s.* **wrn-1(gk99)**	38.29	0.00E+00	0.00E+00	0.0001	4.70E-07	2.90E-08	0.0259	5.15	0.0243	0.1216
cep-1(gk138);wrn-1(gk99) *v.s.* **wrn-1(tm764)**	17.74	2.50E-05	0.0001	0.269	0.0001	3.00E-05	0.0602	0.88	0.4398	1
cep-1(gk138);wrn-1(gk99) *v.s.* **cep-1(gk138);wrn-1(tm764)**	6.61	0.0101	0.0506	0.4139	0.0711	0.0851	0.3833	0.01	0.9915	1
cep-1(gk138);wrn-1(tm764) *v.s.* **N2**	48.21	0.00E+00	0.00E+00	4.00E-06	3.60E-08	2.60E-06	0.2946	1.16	0.3453	1
cep-1(gk138);wrn-1(tm764) *v.s.* **cep-1(gk138)**	7.6	0.0058	0.0292	0.2311	0.0114	0.002	0.1421	1.61	0.2365	1
cep-1(gk138);wrn-1(tm764) *v.s.* **wrn-1(gk99)**	78.07	0.00E+00	0.00E+00	5.00E-10	2.60E-13	7.90E-10	0.1269	8.17	0.0058	0.0289
cep-1(gk138);wrn-1(tm764) *v.s.* **wrn-1(tm764)**	47.69	0.00E+00	0.00E+00	0.0004	1.10E-10	3.60E-07	0.1477	1.86	0.1972	0.9862
cep-1(gk138);wrn-1(tm764) *v.s.* **cep-1(gk138);wrn-1(gk99)**	6.61	0.0101	0.0506	0.4139	0.0711	0.0851	0.3833	0.01	0.9915	1

Table App.16: Table showing the results of: Log Rank Tests (testing statistical significance over the entire lifespan); Fishers Exact Tests (statistical significance at specific time points); and Normalised Chow Tests (to test for variations in lifespans, specifically in relation to the slopes of the cumulative hazard plots) for the data presented in Figure 6.5.

8.1.9 V.IX Statistical analysis for Figure 6.6 – Survival of *wrn-1* and *cep-1* single and double mutants under chronic heat stress (35°C).

Name	No. of subjects	Restricted mean			Age in days at % mortality					
		Days	Std. error	95% C.I.	25%	50%	75%	90%	100%	95% Median C.I.
N2	59	878.64	19.82	839.79 ~ 917.50	900	930	1020	1050	1110	- ~ -
cep-1(gk138)	57	1020.00	24.64	971.70 ~ 1068.30	930	1020	1110	1260	1380	- ~ -
wrn-1(gk99)	60	697.50	21.72	654.93 ~ 740.07	540	690	720	930	1020	- ~ -
wrn-1(tm764)	49	877.96	25.30	828.37 ~ 927.55	720	960	990	1020	1140	- ~ -
cep-1(gk138);wrn-1(gk99)	62	894.19	26.61	842.04 ~ 946.34	750	780	990	1140	1380	780 ~ 960
cep-1(gk138);wrn-1(tm764)	59	1100.85	20.93	1059.82 ~ 1141.87	990	1080	1140	1380	1440	- ~ -

Table App.17: Mean and median survival time for data presented in figure 6.6. C.I. indicates confidence interval.

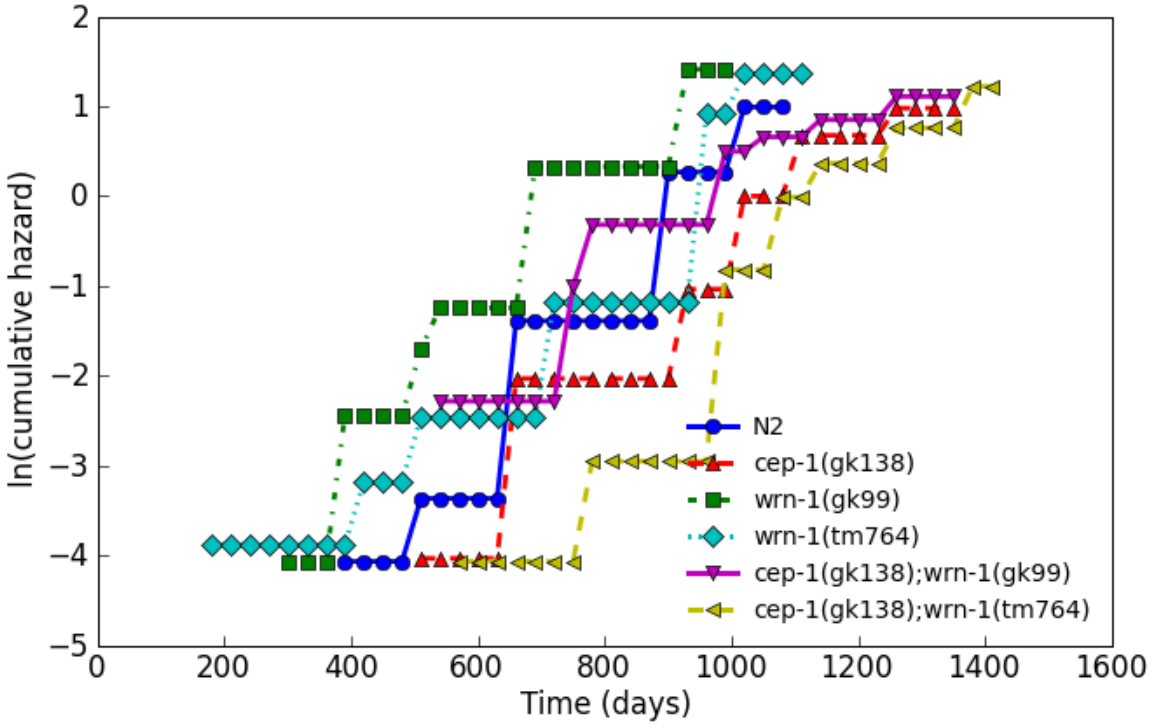

Figure App.9: Log Cumulative Hazard plot for Figure 6.6. The differences in slopes are analysed using a Normalised Chow Test (see Table App.18).

Condition	Log Rank Test			Fishers Exact Test				Normalised Chow Test		
	Chi^2	P-value	Bonferroni P-value	P-value at 25%	P-value at 50%	P-value at 75%	P-value at 90%	F-value	P-value	Bonferroni P-value
N2 *v.s.* ***cep-1(gk138)***	28.46	9.50E-08	4.80E-07	1.60E-11	6.00E-06	0.0001	0.0026	3.53	0.0369	0.1845
N2 *v.s.* ***wrn-1(gk99)***	17.64	2.70E-05	0.0001	6.70E-09	0.8367	4.40E-05	0.0573	0.13	0.8817	1
N2 *v.s.* ***wrn-1(tm764)***	0.69	0.4063	1	2.40E-06	2.40E-06	0.0132	0.3742	5.88	0.005	0.0249
N2 *v.s.* ***cep-1(gk138);wrn-1(gk99)***	0.71	0.3981	1	0.3091	0.0241	0.3896	0.0029	16.58	3.00E-06	1.70E-05
N2 *v.s.* ***cep-1(gk138);wrn-1(tm764)***	53.07	0.00E+00	0.00E+00	1.90E-13	0.0001	0.0001	0.0129	0.34	0.7104	1
cep-1(gk138) *v.s.* **N2**	28.46	9.50E-08	4.80E-07	1.60E-11	6.00E-06	0.0001	0.0026	3.53	0.0369	0.1845
cep-1(gk138) *v.s.* ***wrn-1(gk99)***	63.73	0.00E+00	0.00E+00	3.60E-12	5.60E-13	2.70E-08	0.0024	2.11	0.1319	0.6593
cep-1(gk138) *v.s.* ***wrn-1(tm764)***	24.57	7.20E-07	3.60E-06	0.8294	4.10E-11	5.00E-06	0.0358	0.6	0.5498	1
cep-1(gk138) *v.s.* ***cep-1(gk138);wrn-1(gk99)***	9.73	0.0018	0.0091	4.80E-06	2.00E-08	1	0.7086	6.15	0.004	0.0198
cep-1(gk138) *v.s.* ***cep-1(gk138);wrn-1(tm764)***	3.83	0.0502	0.251	0.5565	1	0.2378	0.5289	1.78	0.1788	0.8941
wrn-1(gk99) *v.s.* **N2**	17.64	2.70E-05	0.0001	6.70E-09	0.8367	4.40E-05	0.0573	0.13	0.8817	1
wrn-1(gk99) *v.s.* ***cep-1(gk138)***	63.73	0.00E+00	0.00E+00	3.60E-12	5.60E-13	2.70E-08	0.0024	2.11	0.1319	0.6593
wrn-1(gk99) *v.s.* ***wrn-1(tm764)***	52.96	0.00E+00	0.00E+00	1.50E-12	4.50E-07	0.1719	0.1719	4.08	0.0226	0.1131
wrn-1(gk99) *v.s.* ***cep-1(gk138);wrn-1(gk99)***	39.57	0.00E+00	0.00E+00	1.50E-12	9.20E-07	0.0021	0.0003	12.95	3.20E-05	0.0002
wrn-1(gk99) *v.s.* ***cep-1(gk138);wrn-1(tm764)***	108.75	0.00E+00	0.00E+00	2.50E-13	5.20E-13	1.70E-08	0.0061	0.05	0.9551	1
wrn-1(tm764) *v.s.* **N2**	0.69	0.4063	1	2.40E-06	2.40E-06	0.0132	0.3742	5.88	0.005	0.0249
wrn-1(tm764) *v.s.* ***cep-1(gk138)***	24.57	7.20E-07	3.60E-06	0.8294	4.10E-11	5.00E-06	0.0358	0.6	0.5498	1
wrn-1(tm764) *v.s.* ***wrn-1(gk99)***	52.96	0.00E+00	0.00E+00	1.50E-12	4.50E-07	0.1719	0.1719	4.08	0.0226	0.1131
wrn-1(tm764) *v.s.* ***cep-1(gk138);wrn-1(gk99)***	4.86	0.0275	0.1373	0.6777	3.20E-06	0.1105	0.0405	2.6	0.083	0.4148
wrn-1(tm764) *v.s.* ***cep-1(gk138);wrn-1(tm764)***	72.3	0.00E+00	0.00E+00	1.00E-12	8.10E-10	2.90E-06	0.0153	4.21	0.0198	0.0989
cep-1(gk138);wrn-1(gk99) *v.s.* **N2**	0.71	0.3981	1	0.3091	0.0241	0.3896	0.0029	16.58	3.00E-06	1.70E-05
cep-1(gk138);wrn-1(gk99) *v.s.* ***cep-1(gk138)***	9.73	0.0018	0.0091	4.80E-06	2.00E-08	1	0.7086	6.15	0.004	0.0198
cep-1(gk138);wrn-1(gk99) *v.s.* ***wrn-1(gk99)***	39.57	0.00E+00	0.00E+00	1.50E-12	9.20E-07	0.0021	0.0003	12.95	3.20E-05	0.0002
cep-1(gk138);wrn-1(gk99) *v.s.* ***wrn-1(tm764)***	4.86	0.0275	0.1373	0.6777	3.20E-06	0.1105	0.0405	2.6	0.083	0.4148
cep-1(gk138);wrn-1(gk99) *v.s.* ***cep-1(gk138);wrn-1(tm764)***	24.23	8.60E-07	4.30E-06	5.30E-09	4.90E-07	0.05	0.1978	13.04	2.50E-05	0.0001
cep-1(gk138);wrn-1(tm764) *v.s.* **N2**	53.07	0.00E+00	0.00E+00	1.90E-13	0.0001	0.0001	0.0129	0.34	0.7104	1
cep-1(gk138);wrn-1(tm764) *v.s.* ***cep-1(gk138)***	3.83	0.0502	0.251	0.5565	1	0.2378	0.5289	1.78	0.1788	0.8941
cep-1(gk138);wrn-1(tm764) *v.s.* ***wrn-1(gk99)***	108.75	0.00E+00	0.00E+00	2.50E-13	5.20E-13	1.70E-08	0.0061	0.05	0.9551	1
cep-1(gk138);wrn-1(tm764) *v.s.* ***wrn-1(tm764)***	72.3	0.00E+00	0.00E+00	1.00E-12	8.10E-10	2.90E-06	0.0153	4.21	0.0198	0.0989
cep-1(gk138);wrn-1(tm764) *v.s.* ***cep-1(gk138);wrn-1(gk99)***	24.23	8.60E-07	4.30E-06	5.30E-09	4.90E-07	0.05	0.1978	13.04	2.50E-05	0.0001

Table App.18: Table showing the results of: Log Rank Tests (testing statistical significance over the entire lifespan); Fishers Exact Tests (statistical significance at specific time points); and Normalised Chow Tests (to test for variations in lifespans, specifically in relation to the slopes of the cumulative hazard plots) for the data presented in Figure 6.6.

8.1.10 I.X Statistical analysis for Figure 6.7 – Survival of wrn-1 and cep-1 single and double mutants after transient heat stress (33°C for two hours).

Name	No. of subjects	Restricted mean			Age in days at % mortality					
		Days	Std. error	95% C.I.	25%	50%	75%	90%	100%	95% Median C.I.
N2	49	9.84	0.88	8.11 ~ 11.56	4	9	15	19	23	5 ~ 12
cep-1(gk138)	42	5.64	0.54	4.59 ~ 6.70	3	5	6	10	20	4 ~ 5
wrn-1(gk99)	49	6.57	0.67	5.25 ~ 7.89	2	4	10	14	16	3 ~ 8
wrn-1(tm764)	47	5.87	0.70	4.51 ~ 7.24	3	4	8	15	18	3 ~ 4
cep-1(gk138);wrn-1(gk99)	46	9.70	1.01	7.72 ~ 11.67	4	8	15	20	27	5 ~ 12
cep-1(gk138);wrn-1(tm764)	38	11.03	1.55	8.00 ~ 14.06	3	7	19	27	31	4 ~ 12

Table App.19: Mean and median survival time for data presented in figure 6.7. C.I. indicates confidence interval.

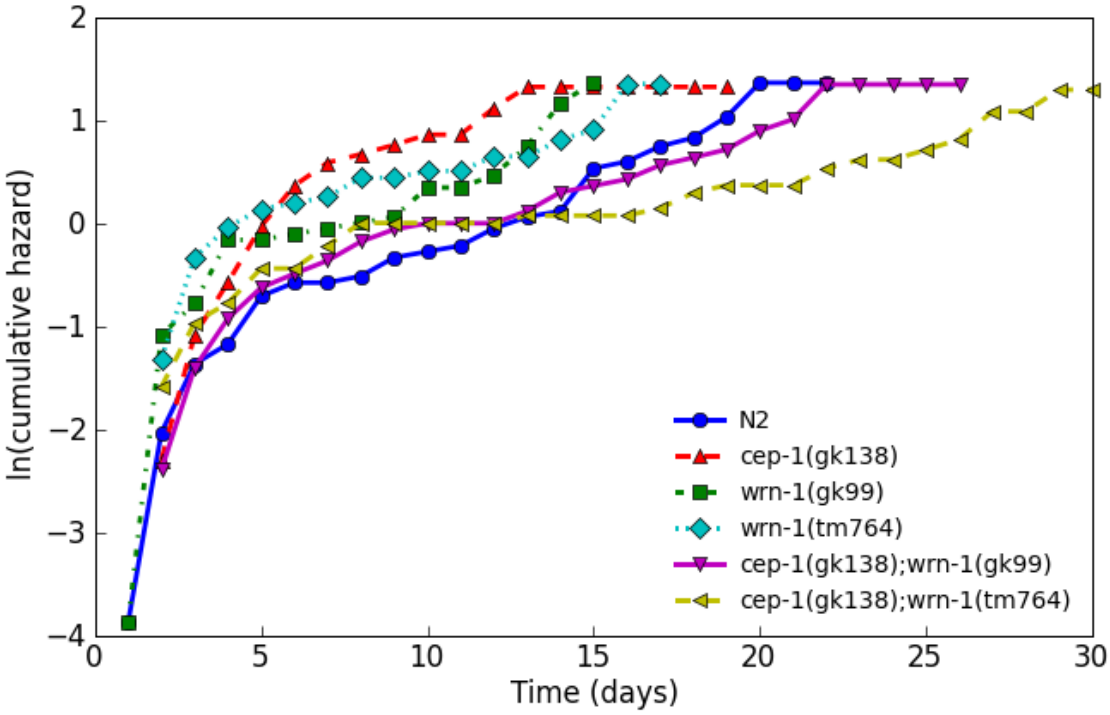

Figure App.10: Log Cumulative Hazard plot for Figure 6.7. The differences in slopes are analysed using a Normalised Chow Test (see Table App.20).

Condition	Log Rank Test			Fisher's Exact Test				Normalised Chow Test		
	Chi^2	P-value	Bonferroni P-value	P-value at 25%	P-value at 50%	P-value at 75%	P-value at 90%	F-value	P-value	Bonferroni P-value
N2 *v.s.* ***cep-1(gk138)***	13.11	0.0003	0.0015	0.6295	0.0015	0.0001	0.0347	0.13	0.882	1
N2 *v.s.* ***wrn-1(gk99)***	11.74	0.0006	0.0031	0.1838	0.1569	0.016	0.0057	0.74	0.4861	1
N2 *v.s.* ***wrn-1(tm764)***	11.54	0.0007	0.0034	0.0055	0.0046	0.0128	0.0309	1.89	0.1667	0.8335
N2 *v.s.* ***cep-1(gk138);wrn-1(gk99)***	0.13	0.7235	1	0.653	0.307	0.6167	0.3073	4.93	0.0118	0.0592
N2 *v.s.* ***cep-1(gk138);wrn-1(tm764)***	2.44	0.1182	0.5912	0.4627	0.1294	0.0767	0.0191	24.72	0.00E+00	0.00E+00
cep-1(gk138) *v.s.* **N2**	13.11	0.0003	0.0015	0.6295	0.0015	0.0001	0.0347	0.13	0.882	1
cep-1(gk138) *v.s.* ***wrn-1(gk99)***	1.08	0.2979	1	0.5038	0.2097	0.0142	0.1183	0.92	0.4095	1
cep-1(gk138) *v.s.* ***wrn-1(tm764)***	0	0.9871	1	0.0509	0.0913	0.3093	0.0615	0.72	0.4954	1
cep-1(gk138) *v.s.* ***cep-1(gk138);wrn-1(gk99)***	11.33	0.0008	0.0038	0.3809	0.0592	0.0028	0.0602	1.66	0.203	1
cep-1(gk138) *v.s.* ***cep-1(gk138);wrn-1(tm764)***	9.43	0.0021	0.0107	0.8107	0.2609	0.0165	0.004	10.86	0.0002	0.0008
wrn-1(gk99) *v.s.* **N2**	11.74	0.0006	0.0031	0.1838	0.1569	0.016	0.0057	0.74	0.4861	1
wrn-1(gk99) *v.s.* ***cep-1(gk138)***	1.08	0.2979	1	0.5038	0.2097	0.0142	0.1183	0.92	0.4095	1
wrn-1(gk99) *v.s.* ***wrn-1(tm764)***	0	0.9693	1	0.6448	0.6822	0.6242	0.2631	2.71	0.0845	0.4224
wrn-1(gk99) *v.s.* ***cep-1(gk138);wrn-1(gk99)***	9.02	0.0027	0.0134	0.1215	0.2205	0.0251	0.0021	5.09	0.0113	0.0564
wrn-1(gk99) *v.s.* ***cep-1(gk138);wrn-1(tm764)***	9.05	0.0026	0.0132	0.6554	0.3939	0.0188	0.0022	14.07	2.40E-05	0.0001
wrn-1(tm764) *v.s.* **N2**	11.54	0.0007	0.0034	0.0055	0.0046	0.0128	0.0309	1.89	0.1667	0.8335
wrn-1(tm764) *v.s.* ***cep-1(gk138)***	0	0.9871	1	0.0509	0.0913	0.3093	0.0615	0.72	0.4954	1
wrn-1(tm764) *v.s.* ***wrn-1(gk99)***	0	0.9693	1	0.6448	0.6822	0.6242	0.2631	2.71	0.0845	0.4224
wrn-1(tm764) *v.s.* ***cep-1(gk138);wrn-1(gk99)***	11.05	0.0009	0.0044	0.0049	0.0126	0.0535	0.0153	0.02	0.9804	1
wrn-1(tm764) *v.s.* ***cep-1(gk138);wrn-1(tm764)***	11.49	0.0007	0.0035	0.0815	0.0297	0.0244	0.0026	6.65	0.0032	0.0158
cep-1(gk138);wrn-1(gk99) *v.s.* **N2**	0.13	0.7235	1	0.653	0.307	0.6167	0.3073	4.93	0.0118	0.0592
cep-1(gk138);wrn-1(gk99) *v.s.* ***cep-1(gk138)***	11.33	0.0008	0.0038	0.3809	0.0592	0.0028	0.0602	1.66	0.203	1
cep-1(gk138);wrn-1(gk99) *v.s.* ***wrn-1(gk99)***	9.02	0.0027	0.0134	0.1215	0.2205	0.0251	0.0021	5.09	0.0113	0.0564
cep-1(gk138);wrn-1(gk99) *v.s.* ***wrn-1(tm764)***	11.05	0.0009	0.0044	0.0049	0.0126	0.0535	0.0153	0.02	0.9804	1
cep-1(gk138);wrn-1(gk99) *v.s.* ***cep-1(gk138);wrn-1(tm764)***	1.65	0.1991	0.9957	0.3301	0.666	0.1976	0.0204	12.93	3.00E-05	0.0001
cep-1(gk138);wrn-1(tm764) *v.s.* **N2**	2.44	0.1182	0.5912	0.4627	0.1294	0.0767	0.0191	24.72	0.00E+00	0.00E+00
cep-1(gk138);wrn-1(tm764) *v.s.* ***cep-1(gk138)***	9.43	0.0021	0.0107	0.8107	0.2609	0.0165	0.004	10.86	0.0002	0.0008
cep-1(gk138);wrn-1(tm764) *v.s.* ***wrn-1(gk99)***	9.05	0.0026	0.0132	0.6554	0.3939	0.0188	0.0022	14.07	2.40E-05	0.0001
cep-1(gk138);wrn-1(tm764) *v.s.* ***wrn-1(tm764)***	11.49	0.0007	0.0035	0.0815	0.0297	0.0244	0.0026	6.65	0.0032	0.0158
cep-1(gk138);wrn-1(tm764) *v.s.* ***cep-1(gk138);wrn-1(gk99)***	1.65	0.1991	0.9957	0.3301	0.666	0.1976	0.0204	12.93	3.00E-05	0.0001

Table App.20: Table showing the results of: Log Rank Tests (testing statistical significance over the entire lifespan); Fishers Exact Tests (statistical significance at specific time points); and Normalised Chow Tests (to test for variations in lifespans, specifically in relation to the slopes of the cumulative hazard plots) for the data presented in Figure 6.7.

9 Statistical analysis of brood size

10 Statistical analysis for Figure 3.8 – brood size of *wrn-1* and *mut-7* single mutants.

Single Factor/One-way ANOVA

Summary:

Groups	*Count*	*Sum*	*Average*	*Variance*
N2	10	2389	239	556
wrn-1(gk99)	9	2125	236	538
wrn-1(tm764)	10	1226	123	540
mut-7(pk204)	9	989	110	88

ANOVA:

Source of Variation	*SS*	*df*	*MS*	*F*	*P-value*	*F crit*
Between Groups	139892	3	46631	106.5406	2.32E-17	2.882604
Within Groups	14881	34	438			
Total	154772.8	37				

F > F crit, therefore we reject the null hypothesis that the means of the brood sizes of the above genotypes are all equal, and perform post-hoc t-tests. The P values are shown below:

P(T<=t) two-tail	N2	*wrn-1(gk99)*	*wrn-1(tm764)*	*mut-7(pk204)*
N2	x	0.7985	1.73E-09	2.22E-11
wrn-1(gk99)	0.7985	x	6.20E-09	6.74E-11
wrn-1(tm764)	0.0000	0.0000	x	1.45E-01
mut-7(pk204)	0.0000	0.0000	1.45E-01	x

11 Statistical analysis for Figure 3.10 – does CPT alter the brood size of *wrn-1* and *mut-7* single mutants?

Anova: Two-Factor With Replication

Summary

No CPT	N2	*wrn-1(gk99)*	*wrn-1(tm764)*	*mut-7(pk204)*	Total
Average	231	283.5	179	130.5	206
Variance	862	4527	657.3	2453.7	5182.8
CPT					
Average	168.75	205	189.25	33.5	149.125
Variance	199.6	3981.3	394.3	473.0	5939.3
Total					
Average	199.9	244.3	184.1	82	
Variance	1562.1	5407.1	480.7	3942.6	

ANOVA

Source of Variation	*SS*	*df*	*MS*	*F*	*P-value*	*F crit*
CPT +/-	25878.1	1	25878.1	15.2807	0.0007	4.2597
genotype	112962.6	3	37654.2	22.2343	0.0000	3.0088
Interaction	13224.6	3	4408.2	2.6030	0.0753	3.0088
Within	40644.5	24	1693.5			
Total	192709.9	31				

F > F crit, for genotype and CPT treatment, therefore we reject the null hypothesis and perform post-hoc t-tests. The P values are shown below.

Genotype	P(T<=t) two-tail +/- CPT
N2	0.008
wrn-1(gk99)	0.030
wrn-1(tm764)	0.712
mut-7(pk204)	0.003

Since two-way ANOVA requires the n number for each genotype/treatment to be there same, and the n value for N2 in this experiment was lower than the n values for the other 3 strains, a second two-way ANOVA was performed in order to test whether there was interaction between genotype and the presence of CPT.

ANOVA:

no CPT	*wrn-1(gk99)*	*wrn-1(tm764)*	*mut-7(pk204)*	Total
Average	291.83	175.67	130.83	199.44
Variance	3230.97	427.47	1921.37	6514.73
CPT				
Average	200.67	188.83	40.17	143.22
Variance	2793.87	352.57	866.57	6827.59
Total				
Average	246.25	182.25	85.5	
Variance	5005.30	401.84	3509.18	

ANOVA:

Source of Variation	*SS*	*df*	*MS*	*F*	*P-value*	*F crit*
Sample	28448.44	1	28448.44	17.794	0.000	4.171
Columns	157188.50	2	78594.25	49.158	0.000	3.316
Interaction	21667.06	2	10833.53	6.776	0.004	3.316
Within	47964	30	1598.8			
Total	255268	35				

F > F crit, for genotype , CPT treatment, AND interaction - therefore we reject the null hypothesis. Note that Sample = CPT +/- and Columns = genotype.

12 Statistical analysis for Figure 3.12 – brood size of *wrn-1* and *mut-7* single and double mutants.

Single Factor/One-way ANOVA

Summary:

Groups	*Count*	*Sum*	*Average*	*Variance*
N2	10	2389	239	556
wrn-1(gk99)	9	2125	236	538
wrn-1(tm764)	10	1226	123	540
mut-7(pk204)	9	989	110	88
mut-7(pk204);wrn-1(gk99)	10	1430	143	480
mut-7(pk204);wrn-1(tm64,	10	1404	140	698

ANOVA:

Source of Variation	*SS*	*df*	*MS*	*F*	*P-value*	*F crit*
Between Groups	156326.7	5	31265.34	63.7981	5.59E-21	2.392953
Within Groups	25483.48	52	490.0669			
Total	181810.2	57				

F > F crit, therefore we reject the null hypothesis that the means of the brood sizes of the above genotypes are all equal, and perform post-hoc t-tests:

P(T<=t) two-tail	N2	*wrn-1(gk99)*	*wrn-1(tm764)*	*mut-7(pk204)*	*mut-7(pk204); wrn-1(gk99)*	*mut-7(pk204); wrn-1(tm764)*
N2	x	0.7985	1.73E-09	2.22E-11	2.22747E-08	6.18E-08
wrn-1(gk99)	0.7985	x	6.20E-09	6.74E-11	5.92681E-06	2.03451E-07
wrn-1(tm764)	0.0000	0.0000	x	1.45E-01	0.058588452	0.127001489
mut-7(pk204)	0.0000	0.0000	1.45E-01	x	0.00061595	0.00445562
mut-7(pk204); wrn-1(gk99)	2.22747E-08	5.92681E-06	0.058588452	0.00061595	x	0.813387249
mut-7(pk204); wrn-1(tm764)	6.18E-08	2.03451E-07	0.127001489	0.00445562	0.813387249	x

13 Statistical analysis for Figure 3.14 – the effect of CPT on the brood size of *wrn-1* and *mut-7* single and double mutants.

Anova: Two-Factor With Replication

Summary

No CPT	N2	*wrn-1(gk99)*	*wrn-1(tm764)*	*mut-7(pk204)*	*wrn-1(gk99); mut-7(pk204)*	*wrn-1(tm764); mut-7(pk204)*	Total
Average	231	283.5	179	130.5	110.5	105.25	173.3
Variance	862	4527	657.3	2453.7	629.7	534.9	5767.1
CPT							
Average	168.75	205	189.25	33.5	116.5	106	136.5
Variance	199.6	3981.3	394.3	473.0	549.7	354.0	4333.6
Total							
Average	199.875	244.25	184.125	82	113.5	105.625	
Variance	1562.13	5407.07	480.70	3942.57	515.71	381.13	

ANOVA:

Source of Variation	*SS*	*df*	*MS*	*F*	*P-value*	*F crit*
Sample	16243.52	1	16243.52	12.48188	0.001148	4.113165
Columns	162533.4	5	32506.67	24.97884	8.78E-11	2.477169
Interaction	22932.35	5	4586.471	3.524346	0.010744	2.477169
Within	46849.25	36	1301.368			
Total	248558.5	47				

F > F crit, for genotype and CPT treatment, therefore we reject the null hypothesis and perform post-hoc t-tests. Furthermore, F> F crit for interaction between genotype and CPT treatment.

14 Statistical analysis for Figure 4.10 – brood size of *wrn-1* and *cep-1* single and double mutants, across generations.

Two-way ANOVA

Summary:

F1	N2	*cep-1(gk138)*	*wrn-1(gk99)*	*wrn-1(tm764)*	*cep-1(gk138); wrn-1(tm764)*	*cep-1(gk138); wrn-1(tm764)*	Total
Count	42	42	42	42	42	42	252
Sum	9946	11491	11816	11657	8537	11149	64596
Average	236.8	273.6	281.3	277.5	203.3	265.5	256.3333
Variance	2016.1	8460.5	716.7	1108.4	915.2	3460.9	3503.012
F10							
Count	42	42	42	42	42	42	252
Sum	9408	10364	10599	9943	10721	13269	64304
Average	224	246.76	252.36	236.74	255.26	315.93	255.1746
Variance	1195.707	2026.48	704.48	750.59	1771.47	27736.65	6434.36
F32							
Count	42	42	42	42	42	42	252
Sum	9483	6307	10590	10296	8850	12224	57750
Average	225.7857	150.17	252.14	245.14	210.71	291.05	229.1667
Variance	637.4895	2113.65	1856.27	1173.44	1135.18	1402.49	3233.797
Total							
Count	126	126	126	126	126	126	
Sum	28837	28162	33005	31896	28108	36642	
Average	228.8651	223.51	261.94	253.14	223.08	290.81	
Variance	1294.918	6964.97	1264.47	1306.68	1784.91	11120.88	

ANOVA:

Source of Variation	*SS*	*df*	*MS*	*F*	*P-value*	*F crit*
Generation	118925.8	2	59462.89	18.09	2.14771E-08	3.01
Genotype	457786.2	5	91557.25	27.85	6.95683E-26	2.23
Interaction	421726.3	10	42172.63	12.83	8.47536E-21	1.84
Within	2426451	738	3287.87			
Total	3424889	755				

F > F crit, for genotype and generation treatment, therefore we reject the null hypothesis and perform post-hoc t-tests. Furthermore, F> F crit for interaction between genotype and generation.

F1 P(T<=t) two-tail	N2	*cep-1(gk138)*	*wrn-1(gk99)*	*wrn-1(tm764)*	*cep-1(gk138); wrn-1(gk99)*	*cep-1(gk138); wrn-1(tm764)*
N2	x	0.027191293	2.11446E-06	3.26536E-07	2.1959E-05	0.001300411
cep-1(gk138)	0.027191	x	0.390623608	0.279652399	1.10523E-05	0.719463853
wrn-1(gk99)	2.11E-06	0.390623608	x	0.636258783	6.43776E-17	0.571363011
wrn-1(tm764)	3.27E-07	0.279652399	0.636258783	x	1.26455E-18	0.370431958
cep-1(gk138); wrn-1(gk99)	2.2E-05	1.10523E-05	6.43776E-17	1.26455E-18	x	2.219E-09
cep-1(gk138); wrn-1(tm764)	0.0013	0.719463853	0.571363011	0.370431958	2.219E-09	x

F10 P(T<=t) two-tail	N2	*cep-1(gk138)*	*wrn-1(gk99)*	*wrn-1(tm764)*	*cep-1(gk138); wrn-1(gk99)*	*cep-1(gk138); wrn-1(tm764)*
N2	x	0.000541808	2.96599E-05	0.101912299	6.482E-06	1.27445E-05
cep-1(gk138)	0.000542	x	0.901789252	0.022094721	0.380138586	0.001127419
wrn-1(gk99)	2.97E-05	0.901789252	x	0.004480029	0.233589251	0.000807985
wrn-1(tm764)	0.101912	0.022094721	0.004480029	x	0.000670215	8.97591E-05
cep-1(gk138); wrn-1(gk99)	6.48E-06	0.380138586	0.233589251	0.000670215	x	0.003132234
cep-1(gk138); wrn-1(tm764)	1.27E-05	0.001127419	0.000807985	8.97591E-05	0.003132234	x

F32 P(T<=t) two-tail	N2	*cep-1(gk138)*	*wrn-1(gk99)*	*wrn-1(tm764)*	*cep-1(gk138); wrn-1(gk99)*	*cep-1(gk138); wrn-1(tm764)*
N2	x	1.27524E-15	0.002119166	4.60486E-05	0.01691628	3.61E-19
cep-1(gk138)	1.28E-15	x	3.90E-18	9.49437E-24	7.19601E-09	1.36581E-36
wrn-1(gk99)	0.002119	3.90E-18	x	0.891158078	3.5626E-06	4.75984E-07
wrn-1(tm764)	4.6E-05	9.49437E-24	0.891158078	x	1.15075E-08	2.415E-09
cep-1(gk138); wrn-1(gk99)	0.016916	7.19601E-09	3.5626E-06	1.15075E-08	x	2.60271E-22
cep-1(gk138); wrn-1(tm764)	3.61E-19	1.36581E-36	4.75984E-07	2.415E-09	2.60271E-22	x

P(T<=t) two-tail	F1 vs F10	F1 vs F32	F10 vs F32
N2	0.115855	0.00132	0.0515341
cep-1(gk138)	0.203739	2.17E-16	1.545E-25
wrn-1(gk99)	2.36E-05	3.81E-05	3.81E-05
wrn-1(tm764)	3.55E-11	4.36E-08	4.362E-08
cep-1(gk138); wrn-1(gk99)	8.74E-12	0.566088	1.308E-13
cep-1(gk138); wrn-1(tm764)	0.053903	0.053903	0.137306

15 Statistical analysis for Figure 4.19 – embryonic and larval survival of *wrn-1* and *cep-1* after IR exposure.

Single Factor/One-way ANOVA for untreated worms – larval survival

Summary:

Groups	*Count*	*Sum*	*Average*	*Variance*
N2 larvae	8	2582	322.75	254.2143
cep-1 larvae	7	2159	308.4286	289.619
gk99 larvae	8	2501	312.625	507.6964
tm764 larvae	8	2780	347.5	1400
CG larvae	8	2739	342.375	791.9821
CT larvae	8	2923	365.375	492.5536

ANOVA:

Source of Variation	*SS*	*df*	*MS*	*F*	*P-value*	*F crit*
Between Groups	19134.99	5	3826.998	6.066887	0.000272	2.443429
Within Groups	25862.84	41	630.801			
Total	44997.83	46				

F > F crit, therefore we reject the null hypothesis and perform post-hoc t-tests.

Post-hoc t-tests:

larval surival P(T<=t) two-tail	N2	*cep-1(gk138)*	*wrn-1(gk99)*	*wrn-1(tm764)*	*cep-1(gk138); wrn-1(gk99)*	*cep-1(gk138); wrn-1(tm764)*
N2	x	0.116357081	0.317091362	0.107232391	0.10817429	0.000591229
cep-1(gk138)	0.116357	x	0.694294395	0.02493219	0.015874655	0.000100566
wrn-1(gk99)	0.317091	0.694294395	x	0.040406991	0.035009573	0.00033008
wrn-1(tm764)	0.107232	0.02493219	0.040406991	x	0.761415003	0.264598874
cep-1(gk138); wrn-1(gk99)	0.108174	0.015874655	0.035009573	0.761415003	x	0.362492668
cep-1(gk138); wrn-1(tm764)	0.000591	0.000100566	0.00033008	0.264598874	0.362492668	x

Single Factor/One-way ANOVA for untreated worms – dead eggs

Summary:

Groups	*Count*	*Sum*	*Average*	*Variance*
N2 dead eggs	8	11	1.375	0.553571
cep-1 dead eggs	8	16	2	2
gk99 dead eggs	8	22	2.75	5.357143
tm764 dead eggs	8	7	0.875	1.267857
CG dead eggs	8	38	4.75	32.78571
CT dead eggs	8	21	2.625	7.982143

ANOVA:

Source of Variation	*SS*	*df*	*MS*	*F*	*P-value*	*F crit*
Between Groups	73.85417	5	14.77083	1.774401	0.13906	2.437693
Within Groups	349.625	42	8.324405			
Total	423.4792	47				

F < F crit, therefore we accept the null hypothesis. There is no significant difference in embryonic lethality when worms are left untreated.

Single Factor/One-way ANOVA for irradiated worms – dead eggs

Summary:

Groups	*Count*	*Sum*	*Average*	*Variance*
N2 dead eggs +60 Gy	8	646	80.75	468.21
cep-1 dead eggs +60 Gy	8	793	99.125	427.55
gk99 dead eggs +60 Gy	8	907	113.375	681.70
tm764 dead eggs +60 Gy	8	857	107.125	702.13
CG dead eggs +60 Gy	8	1072	134	640.29
CT dead eggs +60 Gy	8	991	123.875	1018.13

ANOVA:

Source of Variation	*SS*	*df*	*MS*	*F*	*P-value*	*F crit*
Between Groups	14091.92	5	2818.383	4.294134	0.003033	2.437693
Within Groups	27566	42	656.3333			
Total	41657.92	47				

F > F crit, therefore we reject the null hypothesis and perform post-hoc t-tests.

embryonic lethality after IR(T<=t) two-tail	N2	*cep-1(gk138)*	*wrn-1(gk99)*	*wrn-1(tm764)*	*cep-1(gk138); wrn-1(gk99)*	*cep-1(gk138); wrn-1(tm764)*
N2	x	0.104417997	0.016553884	0.046766006	0.000477041	0.006899129
cep-1(gk138)	0.104418	x	0.246251805	0.51176785	0.009205625	0.086889456
wrn-1(gk99)	0.016554	0.246251805	x	0.641966454	0.130929084	0.483175083
wrn-1(tm764)	0.046766	0.51176785	0.641966454	x	0.056934284	0.272506914
cep-1(gk138); wrn-1(gk99)	0.000477	0.009205625	0.130929084	0.056934284	x	0.493445432
cep-1(gk138); wrn-1(tm764)	0.006899	0.086889456	0.483175083	0.272506914	0.493445432	x

larval survival after IR P(T<=t) two-tail	N2	*cep-1(gk138)*	*wrn-1(gk99)*	*wrn-1(tm764)*	*cep-1(gk138); wrn-1(gk99)*	*cep-1(gk138); wrn-1(tm764)*
N2	x	0.001437685	0.000193938	0.066001344	0.248730196	0.006705963
cep-1(gk138)	0.001438	x	1.53396E-06	0.00019197	0.029764175	0.788261676
wrn-1(gk99)	0.000194	1.53396E-06	x	0.062828165	0.00010076	9.15709E-06
wrn-1(tm764)	0.066001	0.00019197	0.062828165	x	0.015554994	0.000709734
cep-1(gk138); wrn-1(gk99)	0.24873	0.029764175	0.00010076	0.015554994	x	0.076201445
cep-1(gk138); wrn-1(tm764)	0.006706	0.788261676	9.15709E-06	0.000709734	0.076201445	x

Single Factor/One-way ANOVA for irradiated worms – surviving embryos

Summary:

Groups	*Count*	*Sum*	*Average*	*Variance*
N2 surving embryos +60 Gy	8	1117	139.63	264.55
cep-1 surving embryos +60 Gy	8	1434	179.25	538.50
gk99 surving embryos +60 Gy	8	767	95.88	347.55
tm764 surving embryos +60 Gy	8	947	118.38	643.98
CG surving embryos +60 Gy	8	1212	151.50	514.29
CT surving embryos +60Gy	8	1406	175.75	769.07

ANOVA:

Source of Variation	*SS*	*df*	*MS*	*F*	*P-value*	*F crit*
Between Groups	42371.85	5	8474.371	16.51953	5.33E-09	2.437693
Within Groups	21545.63	42	512.9911			
Total	63917.48	47				

F > F crit, therefore we reject the null hypothesis and perform post-hoc t-tests.

16 Statistical analysis of indicators of health

17 Statistical analysis of thrashing rates of *wrn-1* and *cep-1* single and double mutants at 20°C.

Two-way ANOVA:

Summary:

day 6	N2	*wrn-1(gk99)*	*wrn-1(tm764)*	*cep-1(gk138)*	*cep-1(gk138); wrn-1(gk99)*	*cep-1(gk138); wrn-1(tm764)*	Total
Count	10	10	10	10	10	10	60
Sum	534	226	369	345	389	581	2444
Average	53.4	22.6	36.9	34.5	38.9	58.1	40.73333
Variance	208.0444	117.3777778	137.4333333	151.6111111	66.54444444	25.21111111	251.4192
day 9							
Count	10	10	10	10	10	10	60
Sum	345	243	348	228	375	573	2112
Average	34.5	24.3	34.8	22.8	37.5	57.3	35.2
Variance	455.1667	307.1222222	174.8444444	204.1777778	124.5	14.45555556	325.2814
day 13							
Count	10	10	10	10	10	10	60
Sum	214	109	148	182	194	485	1332
Average	21.4	10.9	14.8	18.2	19.4	48.5	22.2
Variance	295.6	174.1	169.9555556	211.7333333	292.4888889	110.7222222	343.6881
Total							
Count	30	30	30	30	30	30	
Sum	1093	578	865	755	958	1639	
Average	36.43333	19.26666667	28.83333333	25.16666667	31.93333333	54.63333333	
Variance	476.0471	222.4781609	252.2816092	224.8333333	231.6505747	66.24022989	

ANOVA:

Source of Variation	*SS*	*df*	*MS*	*F*	*P-value*	*F crit*
Days post L4	10862.04	2	5431.02	30.16	0.00000	3.05
Genotype	22432.58	5	4486.52	24.92	0.00000	2.27
Interaction	2700.56	10	270.06	1.50	0.14365	1.89
Within	29169.8	162	180.06			
Total	65164.98	179				

F > F crit, for genotype and age, therefore we reject the null hypothesis and perform post-hoc t-tests. The P values are shown below.

Post-hoc analysis

P values indicating whether there is a statistically significant difference between trashing rates of different strains 6 days post-L4:

6 days post L4 P(T<=t) two-tail	N2	*wrn-1(gk99)*	*wrn-1(tm764)*	*cep-1(gk138)*	*cep-1(gk138); wrn-1(gk99)*	*cep-1(gk138); wrn-1(tm764)*
N2	x	3.94583E-05	0.011655363	0.005520048	0.012699783	0.343373641
wrn-1(gk99)	3.95E-05	x	0.011030595	0.034007416	0.00130917	2.28974E-08
wrn-1(tm764)	0.011655	0.011030595	x	0.660628716	0.663163363	5.34421E-05
cep-1(gk138)	0.00552	0.034007416	0.660628716	x	0.358644532	2.51691E-05
cep-1(gk138); wrn-1(gk99)	0.0127	0.00130917	0.663163363	0.358644532	x	5.67698E-06
cep-1(gk138); wrn-1(tm764)	0.343374	2.28974E-08	5.34421E-05	2.51691E-05	5.67698E-06	x

P values indicating whether there is a statistically significant difference between trashing rates of different strains 9 days post-L4:

9 days post L4 P(T<=t) two-tail	N2	*wrn-1(gk99)*	*wrn-1(tm764)*	*cep-1(gk138)*	*cep-1(gk138); wrn-1(gk99)*	*cep-1(gk138); wrn-1(tm764)*
N2	x	0.257942156	0.970266276	0.166786712	0.698186003	0.003750359
wrn-1(gk99)	0.257942	x	0.147778719	0.836199469	0.059754681	1.63513E-05
wrn-1(tm764)	0.970266	0.147778719	x	0.067033526	0.62763369	6.41636E-05
cep-1(gk138)	0.166787	0.836199469	0.067033526	x	0.019516089	7.60317E-07
cep-1(gk138); wrn-1(gk99)	0.698186	0.059754681	0.62763369	0.019516089	x	4.75335E-05
cep-1(gk138); wrn-1(tm764)	0.00375	1.63513E-05	6.41636E-05	7.60317E-07	4.75335E-05	x

P values indicating whether there is a statistically significant difference between trashing rates of different strains 13 days post-L4:

13 days post L4 P(T<=t) two-tail	N2	*wrn-1(gk99)*	*wrn-1(tm764)*	*cep-1(gk138)*	*cep-1(gk138); wrn-1(gk99)*	*cep-1(gk138); wrn-1(tm764)*
N2	x	0.142891794	0.346215464	0.658602482	0.797206669	0.000230714
wrn-1(gk99)	0.142892	x	0.514549536	0.255214816	0.229321322	4.63384E-07
wrn-1(tm764)	0.346215	0.514549536	x	0.588857293	0.50736233	1.91132E-06
cep-1(gk138)	0.658602	0.255214816	0.588857293	x	0.867686258	1.82548E-05
cep-1(gk138); wrn-1(gk99)	0.797207	0.229321322	0.50736233	0.867686258	x	0.000105277
cep-1(gk138); wrn-1(tm764)	0.000231	4.63384E-07	1.91132E-06	1.82548E-05	0.000105277	x

The table below shows P values indicating whether there is a statistically significant difference between trashing rates of different strains 20 days post-L4 (only performed between N2 and the five other strains as ANOVA suggested no significant difference. The test below simply verifies that. Note, the only difference at 20 day was between cep-1(gk138);wrn-1(tm764) and all other strains (P values not shown but all >0.001):

20 days post L4 P(T<=t) two-tail	*wrn-1(gk99)*	*wrn-1(tm764)*	*cep-1(gk138)*	*cep-1(gk138); wrn-1(gk99)*	*cep-1(gk138); wrn-1(tm764)*
N2	0.425002254	0.974836937	0.571674107	0.339579164	6.20713E-06

Post-hoc t-tests between days for a given strain:

P values between ages	6 vs 9 days post-L4	9 vs 13 days post-L4	13 vs 20 days post-L4
N2	0.032	0.148	0.116
wrn-1(gk99)	0.797	0.069	0.160
wrn-1(tm764)	0.711	0.003	0.219
cep-1(gk138)	0.065	0.485	0.053
cep-1(gk138); wrn-1(gk99)	0.752	0.012	0.021
cep-1(gk138); wrn-1(tm764)	0.693	0.023	0.149

Table shows P values calculated for post-hoc t-tests. These establish whether there is a statistically significant difference in thrashing between days for a given strain at 20°C.

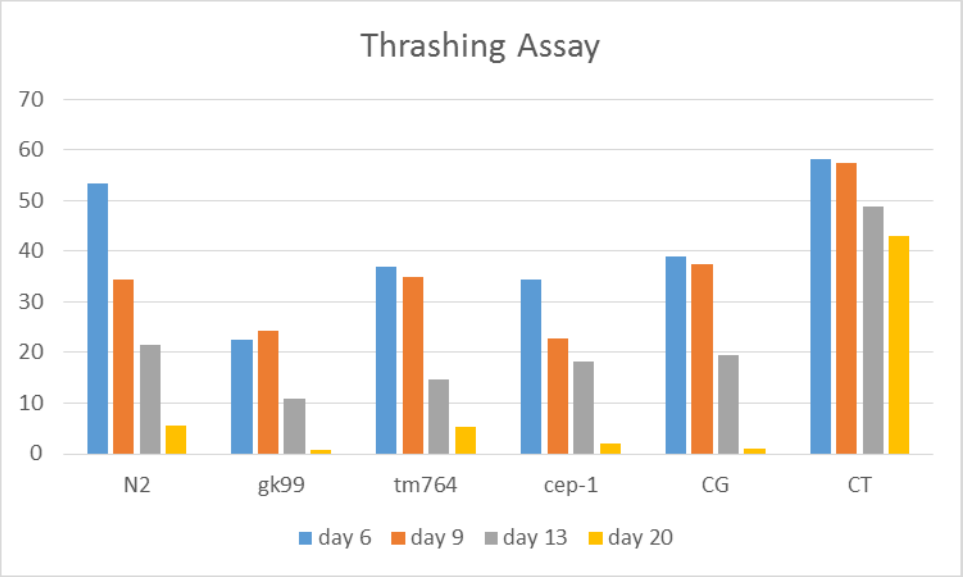

Graph 1: Mean thrash rate of *wrn-1* and *cep-1* single and double mutants at 20°C, at different ages.

18 Statistical analysis of thrashing rates of *wrn-1* and *cep-1* single and double mutants at 25°C.

One-way ANOVA

Summary:

Groups	*Count*	*Sum*	*Average*	*Variance*
N2	20	480	24	120.21
gk99	20	271	13.55	262.26
tm764	20	298	14.9	262.62
cep-1	20	510	25.5	204.26
CG	20	807	40.35	225.19
CT	20	1112	55.6	76.46

ANOVA:

Source of Variation	*SS*	*df*	*MS*	*F*	*P-value*	*F crit*
Between Groups	26222.87	5	5244.57	27.34	4.27E-18	2.29
Within Groups	21869.1	114	191.83			
Total	48091.97	119				

F > F crit, therefore we reject the null hypothesis and perform post-hoc t-tests. The P values are shown below.

5 days post L4 at 25°C P(T<=t) two-tail	N2	*wrn-1(gk99)*	*wrn-1(tm764)*	*cep-1(gk138)*	*cep-1(gk138); wrn-1(gk99)*	*cep-1(gk138); wrn-1(tm764)*
N2	x	0.021931007	0.044326428	0.71165968	0.000342944	2.75783E-12
wrn-1(gk99)	0.021931	x	0.793571472	0.017931021	3.45819E-06	1.86939E-12
wrn-1(tm764)	0.044326	0.793571472	x	0.034429689	8.21904E-06	4.71026E-12
cep-1(gk138)	0.71166	0.017931021	0.034429689	x	0.002738365	1.02763E-09
cep-1(gk138); wrn-1(gk99)	0.000343	3.45819E-06	8.21904E-06	0.002738365	x	0.000350724
cep-1(gk138); wrn-1(tm764)	2.76E-12	1.86939E-12	4.71026E-12	1.02763E-09	0.000350724	x

Table shows P values calculated for post-hoc t-tests. These establish whether there is a statistically

significant difference in thrashing between strains 5 days post-L4, at 25°C.

19 Statistical analysis of DAF-16::GFP localisation at 20°C, in *wrn-1* and *cep-1* single and double mutants.

For each strain, the number of DAF-16::GFP positive nuclei per worm was recorded. From this data, frequencies of GFP positive nuclei per worm was tabulated and plotted on to a histogram (see below).

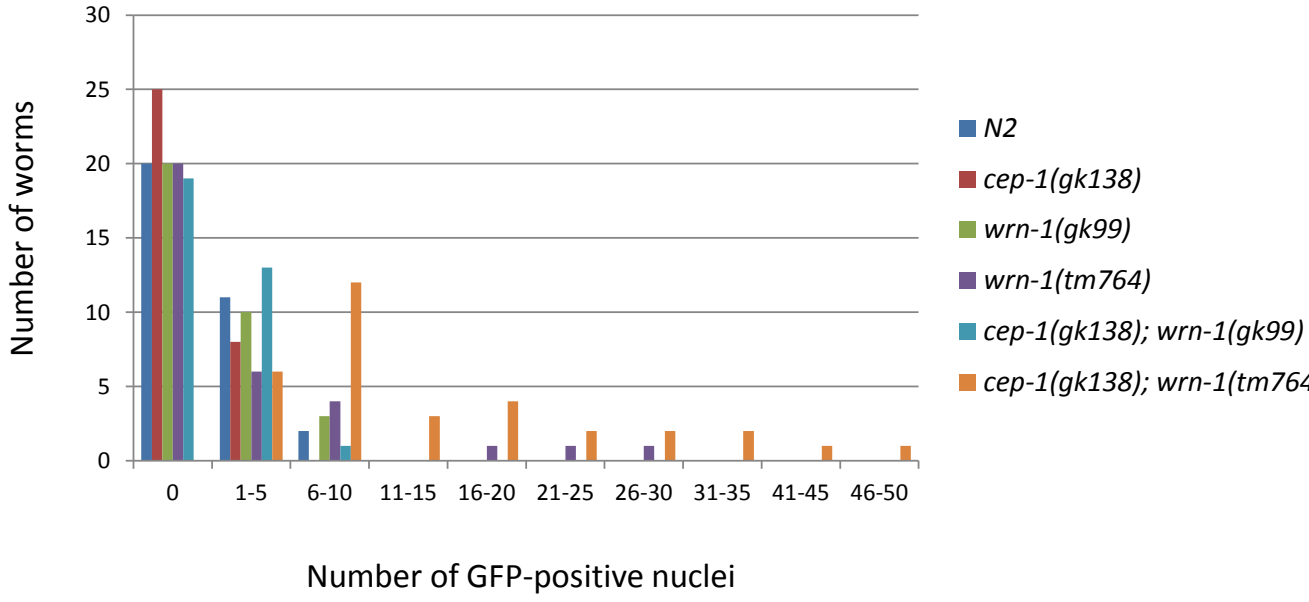

The table below shows the raw data for the previous histogram:

Number of GFP +ve nuclei	N2	*cep-1(gk138)*	*wrn-1(gk99)*	*wrn-1(tm764)*	*cep-1(gk138); wrn-1(gk99)*	*cep-1(gk138); wrn-1(tm764)*
0	20	25	20	20	19	0
1-5	11	8	10	6	13	6
6-10	2		3	4	1	12
11-15				0		3
16-20				1		4
21-25				1		2
26-30				1		2
31-35						2
41-45						1
46-50						1
total worms	33	33	33	33	33	33

The table below represents the same data as above but represented as percentages of worms:

Number of GFP +ve nuclei	N2	*cep-1(gk138)*	*wrn-1(gk99)*	*wrn-1(tm764)*	*cep-1(gk138); wrn-1(gk99)*	*cep-1(gk138); wrn-1(tm764)*
0	60.61%	75.76%	60.61%	60.61%	57.58%	0.00%
1-5	33.33%	24.24%	30.30%	18.18%	39.39%	18.18%
6-10	6.06%	0.00%	9.09%	12.12%	3.03%	36.36%
11-15	0.00%	0.00%	0.00%	0.00%	0.00%	9.09%
16-20	0.00%	0.00%	0.00%	3.03%	0.00%	12.12%
21-25	0.00%	0.00%	0.00%	3.03%	0.00%	6.06%
26-30	0.00%	0.00%	0.00%	3.03%	0.00%	6.06%
31-35	0.00%	0.00%	0.00%	0.00%	0.00%	6.06%
41-45	0.00%	0.00%	0.00%	0.00%	0.00%	3.03%
46-50	0.00%	0.00%	0.00%	0.00%	0.00%	3.03%
total %	100	100	100	100	100	100

It should be noted that the majority of nuclei are not intestinal (however, *wrn-1(tm764)* did show more intestinal nuclear GFP than other strains). Furthermore, although *cep-1(gk138);wrn-1(tm764)* show a statistically significant difference in the number of GFP-positive nuclei compared to all other strains (see table above), this number is much lower than that observed for the long lived *daf-2* strains, where nuclear GFP is in almost all nuclei, including the intestine, in almost all worms, and also at a much brighter level.

The average number of GFP positive nuclei was also calculated and plotted on the chart below:

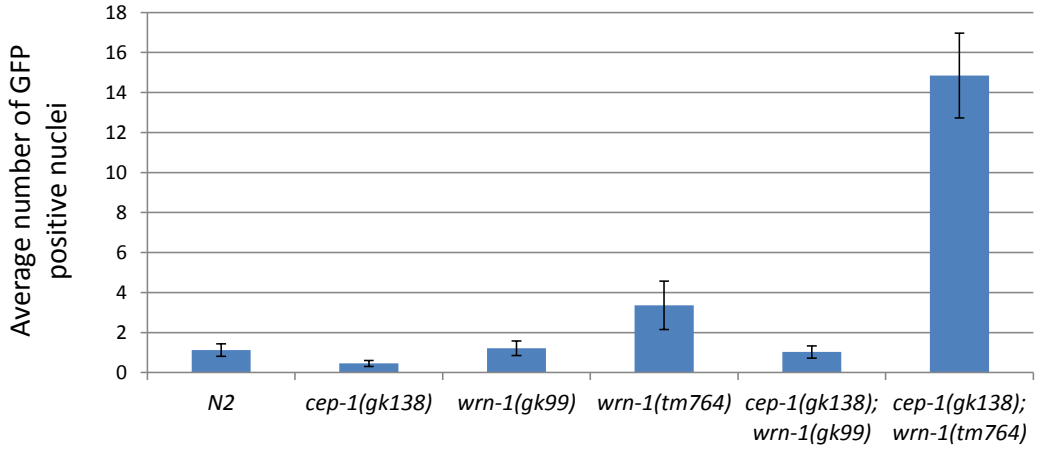

	N2	*cep-1(gk138)*	*wrn-1(gk99)*	*wrn-1(tm764)*	*cep-1(gk138); wrn-1(gk99)*	*cep-1(gk138); wrn-1(tm764)*
number	33	33	33	33	33	33
sqrt (n)	5.745	5.745	5.745	5.745	5.745	5.745
average	1.121	0.455	1.212	3.364	1.030	14.848
St Dev	1.781	0.869	2.088	6.963	1.759	12.158
SEM	0.310	0.151	0.363	1.212	0.306	2.116

In order to determine whether there was any statistically significant difference between strains, ANOVA was performed:

One-way ANOVA

Summary:

Groups	*Count*	*Sum*	*Average*	*Variance*
N2	33	37	1.12	3.17
cep-1(gk138)	33	15	0.45	0.76
wrn-1(gk99)	33	40	1.21	4.36
wrn-1(tm764)	33	111	3.36	48.49
cep-1(gk138); wrn-1(gk99)	33	34	1.03	3.09
cep-1(gk138); wrn-1(tm764)	33	490	14.85	147.82

ANOVA:

Source of Variation	*SS*	*df*	*MS*	*F*	*P-value*	*F crit*
Between Groups	5111.60	5	1022.32	29.53	0.00	2.26
Within Groups	6646.06	192	34.61			
Total	11757.66	197				

F > F crit, therefore we reject the null hypothesis and perform post-hoc t-tests. The P values are shown in the next table.

GFP +ve nuclei at 20°C P(T<=t) two-tail	N2	*cep-1(gk138)*	*wrn-1(gk99)*	*wrn-1(tm764)*	*cep-1(gk138); wrn-1(gk99)*	*cep-1(gk138); wrn-1(tm764)*
N2	x	0.057748924	0.849688469	0.07782305	0.835391548	1.93397E-08
cep-1(gk138)	0.057749	x	0.058785324	0.020231154	0.096669969	4.45295E-09
wrn-1(gk99)	0.849688	0.058785324	x	0.093959618	0.703288033	2.53079E-08
wrn-1(tm764)	0.077823	0.020231154	0.093959618	x	0.066579063	1.38196E-05
cep-1(gk138); wrn-1(gk99)	0.835392	0.096669969	0.703288033	0.066579063	x	1.62088E-08
cep-1(gk138); wrn-1(tm764)	1.93E-08	4.45295E-09	2.53079E-08	1.38196E-05	1.62088E-08	x

Table shows P values calculated for post-hoc t-tests. These establish whether there is a statistically

significant difference in DAF-16::GFP nuclear localisation between strains at 20°C (7 days post-L4).

20 Statistical analysis of DAF-16::GFP localisation at 25°C, in *wrn-1* and *cep-1* single and double mutants.

Single factor/one-way ANOVA

Summary:

SUMMARY				
Groups	*Count*	*Sum*	*Average*	*Variance*
N2	30	57	1.9	8.99
cep-1(gk138)	30	339	11.3	72.08
wrn-1(gk99)	27	52	1.93	7.69
wrn-1(tm764)	28	59	2.11	6.10
cep-1(gk138); wrn-1(gk99)	28	585	20.89	631.65
cep-1(gk138); wrn-1(tm764)	33	807	24.45	366.01

ANOVA:

Source of Variation	*SS*	*df*	*MS*	*F*	*P-value*	*F crit*
Between Groups	15630.83	5	3126.17	16.88	0.00	2.27
Within Groups	31482.39	170	185.19			
Total	47113.22	175				

Since F > F crit (from the ANOVA above), we reject the null hypothesis and perform post-hoc t-tests. The P values are shown in the next table.

GFP +ve nuclei at 20°C P(T<=t) two-tail	N2	*cep-1(gk138)*	*wrn-1(gk99)*	*wrn-1(tm764)*	*cep-1(gk138); wrn-1(gk99)*	*cep-1(gk138); wrn-1(tm764)*
N2	x	3.953E-07	0.973179709	0.775915495	0.000130264	2.04857E-08
cep-1(gk138)	3.95E-07	x	1.11026E-06	9.27909E-07	0.053272985	0.000292411
wrn-1(gk99)	0.97318	1.11026E-06	x	0.798801726	0.000275107	8.73075E-08
wrn-1(tm764)	0.775915	9.27909E-07	0.798801726	x	0.000238708	6.15763E-08
cep-1(gk138); wrn-1(gk99)	0.00013	0.053272985	0.000275107	0.000238708	x	0.277496037
cep-1(gk138); wrn-1(tm764)	2.05E-08	0.000292411	8.73075E-08	6.15763E-08	0.277496037	x

Table shows P values calculated for post-hoc t-tests. These establish whether there is a statistically

significant difference in DAF-16::GFP nuclear localisation between strains at 25°C.

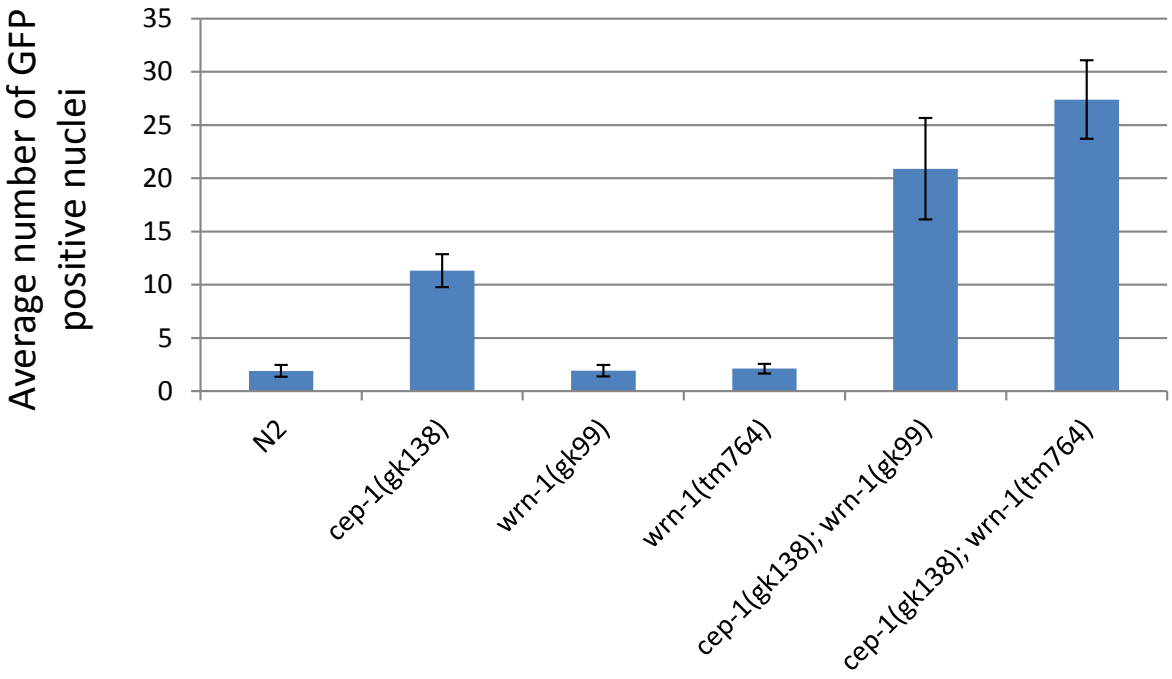

	N2	*cep-1(gk138)*	*wrn-1(gk99)*	*wrn-1(tm764)*	*cep-1(gk138); wrn-1(gk99)*	*cep-1(gk138); wrn-1(tm764)*
number	30	30	27	28	28	34
sqrt (n)	5.48	5.48	5.20	5.29	5.29	5.83
average	1.90	11.30	1.93	2.11	20.89	26.26
St Dev	3.00	8.49	2.77	2.47	25.13	21.59
SEM	0.55	1.55	0.53	0.47	4.75	3.70

For each strain, the number of DAF-16::GFP positive nuclei per worm was recorded. From this data, frequencies of GFP positive nuclei per worm was tabulated and plotted on to a histogram (see below).

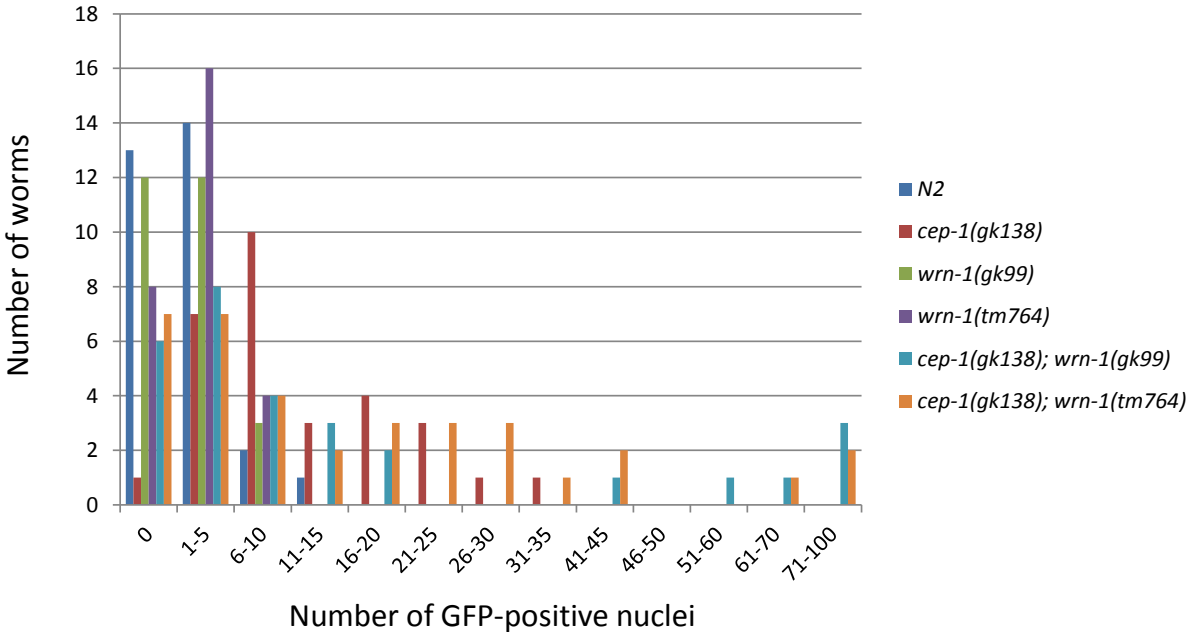

The table below shows the raw data for the previous histogram:

Number of GFP +ve nuclei	N2	*cep-1(gk138)*	*wrn-1(gk99)*	*wrn-1(tm764)*	*cep-1(gk138); wrn-1(gk99)*	*cep-1(gk138); wrn-1(tm764)*
0	13	1	12	8	6	7
1-5	14	7	12	16	8	7
6-10	2	10	3	4	4	4
11-15	1	3			3	2
16-20		4			2	3
21-25		3				3
26-30		1				3
31-35		1				1
41-45					1	2
46-50					0	0
51-60					1	0
61-70					1	1
71-100					3	2
total	30	30	27	28	29	35

% Frequency	N2	*cep-1(gk138)*	*wrn-1(gk99)*	*wrn-1(tm764)*	*cep-1(gk138); wrn-1(gk99)*	*cep-1(gk138); wrn-1(tm764)*
0	43.33%	3.33%	44.44%	28.57%	20.69%	20.00%
1-5	46.67%	23.33%	44.44%	57.14%	27.59%	20.00%
6-10	6.67%	33.33%	11.11%	14.29%	13.79%	11.43%
11-15	3.33%	10.00%	0.00%	0.00%	10.34%	5.71%
16-20	0.00%	13.33%	0.00%	0.00%	6.90%	8.57%
21-25	0.00%	10.00%	0.00%	0.00%	0.00%	8.57%
26-30	0.00%	3.33%	0.00%	0.00%	0.00%	8.57%
31-35	0.00%	3.33%	0.00%	0.00%	0.00%	2.86%
41-45	0.00%	0.00%	0.00%	0.00%	3.45%	5.71%
46-50	0.00%	0.00%	0.00%	0.00%	0.00%	0.00%
51-60	0.00%	0.00%	0.00%	0.00%	3.45%	0.00%
61-70	0.00%	0.00%	0.00%	0.00%	3.45%	2.86%
71-100	0.00%	0.00%	0.00%	0.00%	10.34%	5.71%

Although *cep-1(gk138);wrn-1(tm764), cep-1(gk138);wrn-1(gk99),*and *cep-1(gk138)* show a statistically significant difference in the number of GFP-positive nuclei compared to all other strains (see tables above), this number is much lower than that observed for the long lived *daf-2* strains, where nuclear GFP is in almost all nuclei, including the intestine, in almost all worms, and also at a much brighter level.

21 Statistical analysis of DAF-16::GFP localisation after heat shock of WT and *cep-1(gk138)* worms.

Heat shock causes DAF-16::GFP to localise in the nucleus. From performing my own experiments on this, I noted that nuclear localisation first occurs (after ~30 minutes) in cells in the anterior half of the worm, particularly the head, and the majority of these appear to be neuronal cells. After an hour of heat shock, the nuclear localisation of DAF-16 appears to be propagated to the rest of the worm, with intestinal nuclear GFP being evident. Therefore, GFP-positive nuclei were not just counted across the entire worm, but also with respect to whether they were present in the anterior half of the worm (head region) or the posterior (tail region).

Two-way ANOVA for counts of GFP-positive nuclei in the head and tail (counted separately).

Summary:

30 minutes	N2 head	N2 tail	*cep-1(gk138)* head	*cep-1(gk138)* tail	Total
Count	23	23	23	23	92
Sum	402	45	558	65	1070
Average	17.48	1.96	24.26	2.83	11.63
Variance	113.53	4.77	161.57	6.60	161.47
60 minutes					
Count	23	23	23	23	92
Sum	510	251	1672	986	3419
Average	22.17	10.91	72.70	42.87	37.16
Variance	191.97	52.45	1840.95	539.94	1192.97
Total					
Count	46	46	46	46	
Sum	912	296	2230	1051	
Average	19.83	6.43	48.48	22.85	
Variance	154.99	48.47	1578.52	676.98	

ANOVA:

Source of Variation	*SS*	*df*	*MS*	*F*	*P-value*	*F crit*
Length of heat shock	29988.05	1	29988.05	82.39	2.22E-16	3.89
Genotype - head and	42588.71	3	14196.24	39.00	2.24E-19	2.66
Interaction	16606.23	3	5535.41	15.21	7.64E-09	2.66
Within	64059.04	176	363.97			
Total	153242	183				

F > F crit, for genotype and length of heat shock, therefore we reject the null hypothesis and perform post-hoc t-tests. Furthermore, F> F crit for interaction between genotype and length of heat shock. Below is the results of the post-hoc tests (two-tailed T-test):

	P(T<=t) two-tail
N2 vs *cep-1* at 30 minutes - head count	0.0562
N2 vs *cep-1* at 60 minutes - head count	6.68E-06
N2 vs *cep-1* at 30 minutes - tail count	0.223
N2 vs *cep-1* at 60 minutes - tail count	1.59E-07
N2 vs *cep-1* at 30 minutes total nuclei	0.055
N2 vs *cep-1* at 60 minutes total nuclei	5.78E-07
N2 total at 30 min vs N2 total at 60 min	5.78E-07
cep-1 total at 30 min vs *cep-1* total at 60 min	5.78E-07

Two-way ANOVA was also performed on counts of the total number of GFP-positive nuclei (head + tail nuclei). The results of this statistical analysis is shown below.

Summary:

30 minutes	N2	*cep-1(gk138)*	Total
Count	23	23	46
Sum	447	623	1070
Average	19.43478	27.08695652	23.26087
Variance	137.3478	210.083004	184.8193
60 minutes			
Count	23	23	46
Sum	761	2658	3419
Average	33.08696	115.5652174	74.32609
Variance	402.2648	3813.438735	3799.469
Total			
Count	46	46	
Sum	1208	3281	
Average	26.26087	71.32608696	
Variance	311.4415	3967.64686	

ANOVA:

Source of Variation	*SS*	*df*	*MS*	*F*	*P-value*	*F crit*
Length of heat shock	59976.1	1	59976.1	52.57447	1.53E-10	3.949321
Genotype	46710.1	1	46710.1	40.94563	7.36E-09	3.949321
Interaction	32193.92	1	32193.92	28.22089	8.07E-07	3.949321
Within	100389	88	1140.784			
Total	239269.1	91				

F > F crit, for genotype and length of heatshock, therefore we reject the null hypothesis and perform post-hoc t-tests. Furthermore, F> F crit for interaction between genotype and length of heat shock.

The same data was converted into a frequency table (below) and plotted in a histogram (below the table).

Number of GFP +ve nuclei	N2 30 min	*cep-1(gk138) 30 min*	N2 60 min	*cep-1(gk138) 60 min*
0	0	0	1	0
1-20	15	11	6	1
21-40	8	7	7	1
41-60	0	5	9	5
61-80	0	0	0	2
81-100	0	0	0	4
101-120	0	0	0	3
121-140	0	0	0	1
141-160	0	0	0	2
161-180	0	0	0	3
181-200	0	0	0	1
201-220	0	0	0	1
221-240	0	0	0	2
total	23	23	23	26

Table of the frequency of the number of GFP-positive nuclei (in groups of 20) in a given worm. This data was used to create the histogram below.

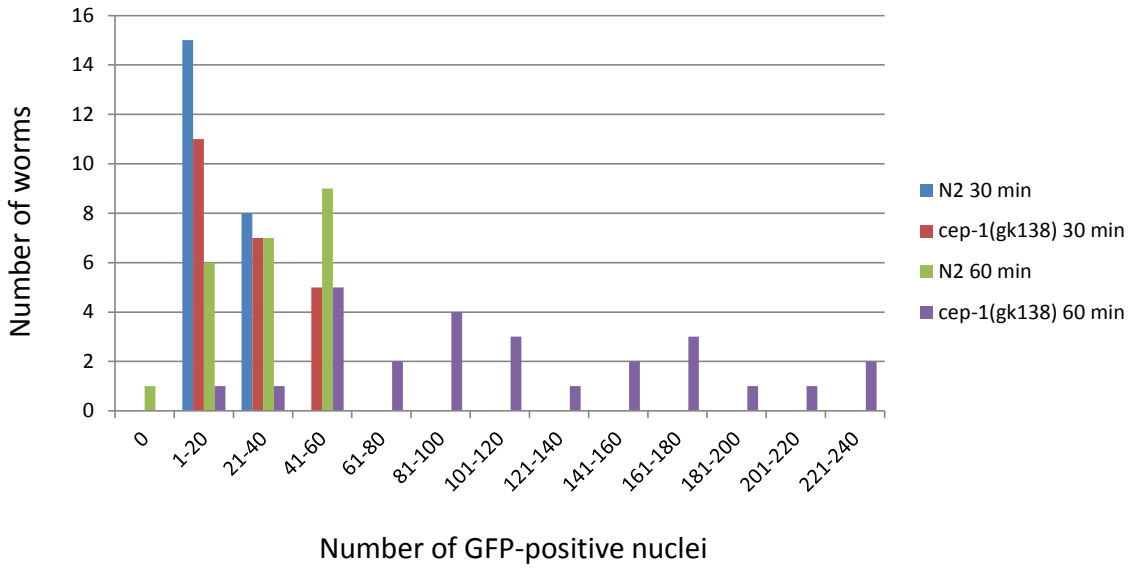

Histogram showing the relative number of GFP-positive nuclei per worm after 30 minutes or 60 minutes of heat shock. This experiment was performed using WT worms and *cep-1(gk138)* mutants crossed into the DAF-16::GFP background.

22 Statistical analysis for figure 3.5 – lipofuscin/auto fluorescence accumulation with age in *wrn-1* and *mut-7* mutants.

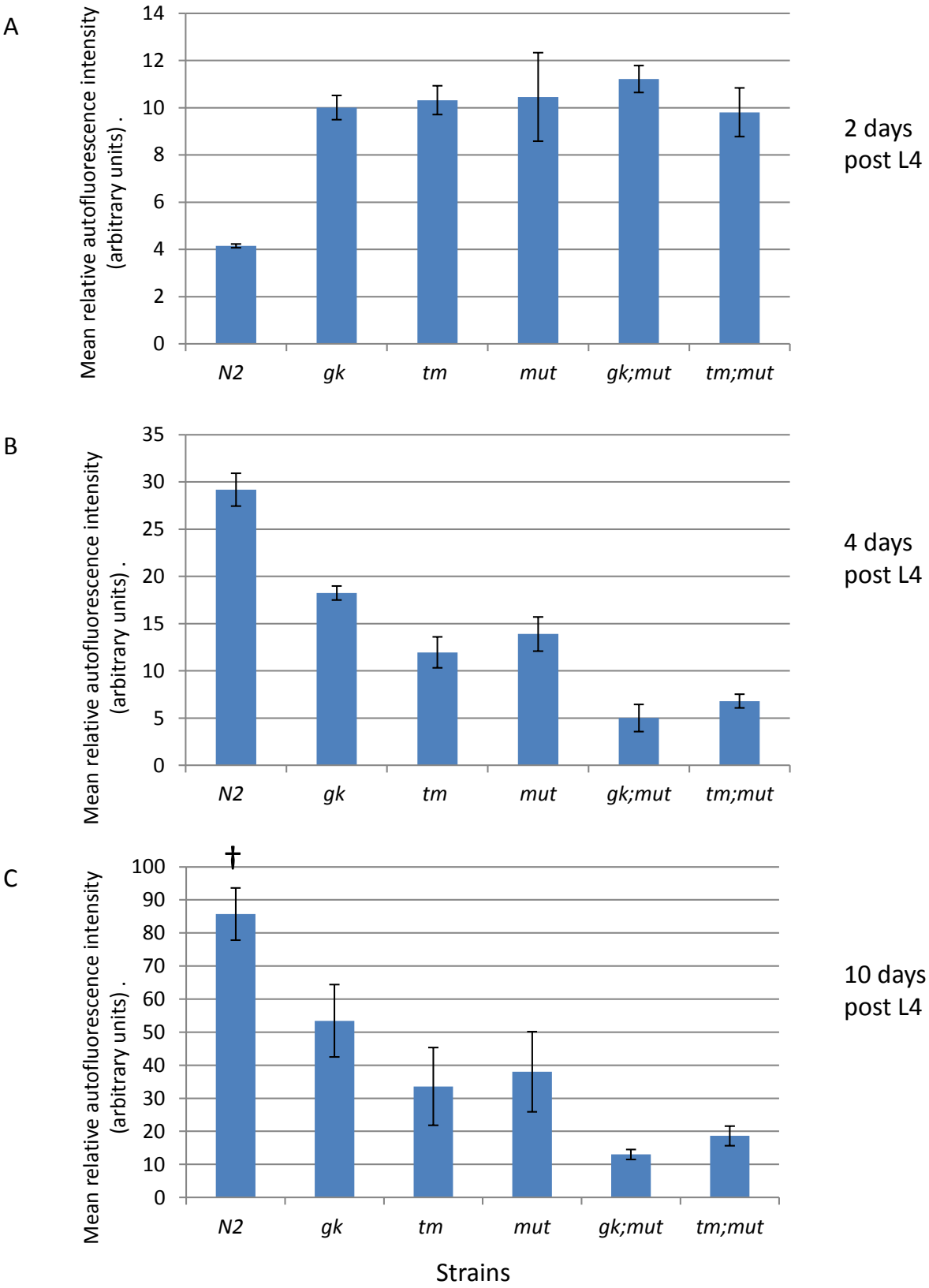

Figure 3.5: Quantification of lipofuscin accumulation with age in various strains. Leica LAS AF® software was used to quantify lipofuscin autofluorescence in photomicrographs of worms 2, 4 and 10 day post-L4. Charts A, B and C correspond to worms 2, 4 days and 10 days post-L4 respectively. For each strain and age, n = 5. N2 WT worms showed negligible lipofuscin/autofluorescence 2 days or 4 days post-L4 relative to background autofluorescence

(p = 0.94), whereas all five mutant strains showed significantly higher autofluorescence at both ages ($p < 0.01$), with no difference between mutant worms at any age with the exception of 10 day post-L4 *wrn-1 (gk99)* single mutants compared to both double mutants ($p<0.05$). Importantly, lipofscin accumulates in mutant worms at a younger chronological age than WT. † note – high levels of autofluorescence does not appear to be characteristic of lipofuscin and may be a result of exposure of the animals to phenoxypropanol in this experiment. A subjective estimate at the mean relative autofluorescence intensity for 10 day post-L4 N2 worms, based by analysing photomicrographs by eye, would be at around the level seen in *wrn-1 (gk99)* single mutants 10 days post-L4. P-values were calculated using student t-test (two tailed). *gk = wrn-1(gk99)*; *tm = wrn-1(tm764); mut = mut-7(pk204); gk;mut = wrn-1(gk99); mut-7(pk204);* and *tm;mut = wrn-1(tm764); mut-7(pk204).*

The data shown in the charts above (A,B and C) is tabulated below:

Strain	2 days post L4		4 days post L4		10 days post L4	
	average	SEM	average	SEM	average	SEM
N2	4.2	0.1	29.2	1.7	85.7	7.9
wrn-1(gk99)	10.0	0.5	18.2	0.7	53.4	11.0
wrn-1(tm764)	10.3	0.6	11.9	1.6	33.6	11.8
mut-7(pk204)	10.5	1.9	13.9	1.8	38.0	12.1
wrn-1(gk99);mut-7(pk204)	11.2	0.6	5.0	1.4	13.0	1.5
wrn-1(tm764);mut-7(pk204)	9.8	1.0	6.8	0.7	18.6	3.0

Statistical analysis was undertaken by conducting two-way ANOVA on this data – the results of this analysis are shown in the table below.

SUMMARY	N2	wrn-1(gk99)	wrn-1(tm764)	mut-7(pk204)	gk99;mut-7	tm764;mut-7	Total
2 days post L4							
Count	5	5	5	5	5	5	30
Sum	20.75	50.04	51.59	52.26	56.08	49.02	279.74
Average	4.15	10.008	10.318	10.452	11.216	9.804	9.324667
Variance	0.02835	1.31287	1.88052	17.57437	1.61563	5.32568	9.568715
4 days post L4							
Count	5	5	5	5	5	5	30
Sum	34.13	63.27	87.11	68.24	69.26	62	384.01
Average	6.826	12.654	17.422	13.648	13.852	12.4	12.80033
Variance	15.23983	2.74758	23.26772	16.33412	10.33227	2.7187	19.92601
10 days post L4							
Count	5	5	5	5	5	5	30
Sum	428.6	267.15	167.95	189.99	66.08	93.13	1212.9
Average	85.72	53.43	33.59	37.998	13.216	18.626	40.43
Variance	314.3958	600.86265	691.31555	735.14937	6.89068	44.28113	931.5891
Total							
Count	15	15	15	15	15	15	
Sum	483.48	380.46	306.65	310.49	191.42	204.15	
Average	32.232	25.364	20.44333333	20.69933333	12.761333	13.61	
Variance	1628.129	596.06774	306.3059667	381.8640352	6.7339981	29.63228571	
ANOVA							
Source of Variation	*SS*	*df*	*MS*	*F*	*P-value*	*F crit*	
Sample	17430.21	2	8715.102503	62.96855445	1.545E-16	3.123907449	
Columns	4019.375	5	803.87493	5.808175208	0.0001465	2.341827531	
Interaction	13886.96	10	1388.696451	10.03364081	2.57E-10	1.964941901	
Within	9965.091	72	138.4040428				
Total	45301.64	89					

Note that 'Sample' = days post L4, and 'Columns' = genotype. F > F crit for days post L4, genotype, AND for the interaction between them. Therefore, we reject the null hypothesis. The means of the three populations are not all equal.

Two way ANOVA

Summary:

7 days post L4	N2	*cep-1(gk138)*	*wrn-1(gk99)*	*wrn-1(tm764)*	*cep-1(gk138); wrn-1(gk99)*	*cep-1(gk138); wrn-1(tm764)*	Total
Count	15	15	15	15	15	15	90
Sum	40	43	60	45	56	22	266
Average	2.67	2.87	4.00	3.00	3.73	1.47	2.96
Variance	0.52	0.84	0.86	0.86	0.78	0.41	1.35
14 days post L4							
Count	15	15	15	15	15	15	90
Sum	59	58	66	59	63	27	332
Average	3.93	3.87	4.40	3.93	4.20	1.80	3.69
Variance	0.50	0.41	0.54	0.50	0.46	0.46	1.21
Total							
Count	30	30	30	30	30	30	
Sum	99	101	126	104	119	49	
Average	3.30	3.37	4.20	3.47	3.97	1.63	
Variance	0.91	0.86	0.72	0.88	0.65	0.45	

ANOVA:

Source of Variation	*SS*	*df*	*MS*	*F*	*P-value*	*F crit*
days post L4	24.2	1	24.20	40.76	1.61491E-09	3.90
Genotype	121.84	5	24.37	41.05	1.85125E-27	2.27
Interaction	5.53	5	1.11	1.86	0.103	2.27
Within	99.73	168	0.59			
Total	251.3111	179				

F > F crit, for genotype and length of heat shock, therefore we reject the null hypothesis and perform post-hoc t-tests. However, since F< F crit for interaction between genotype and days post L4 (age), there is no interaction between the two. The results of the post-hoc tests (two-tailed T-test) are shown in the next two tables.

Results from the post-hoc t-tests:

7 days post L4 P(T<=t) two-tail	N2	*cep-1(gk138)*	*wrn-1(gk99)*	*wrn-1(tm764)*	*cep-1(gk138); wrn-1(gk99)*	*cep-1(gk138); wrn-1(tm764)*
N2	x	0.512281242	0.000144833	0.28130475	0.001162348	4.65349E-05
cep-1(gk138)	0.512281	x	0.002199664	0.6946582	0.01346373	4.1299E-05
wrn-1(gk99)	0.000145	0.002199664	x	0.006230192	0.426498949	1.81614E-09
wrn-1(tm764)	0.281305	0.6946582	0.006230192	x	0.034756346	1.30255E-05
cep-1(gk138); wrn-1(gk99)	0.001162	0.01346373	0.426498949	0.034756346	x	9.2301E-09
cep-1(gk138); wrn-1(tm764)	4.65E-05	4.1299E-05	1.81614E-09	1.30255E-05	9.2301E-09	x

14 days post L4 P(T<=t) two-tail	N2	*cep-1(gk138)*	*wrn-1(gk99)*	*wrn-1(tm764)*	*cep-1(gk138); wrn-1(gk99)*	*cep-1(gk138); wrn-1(tm764)*
N2	x	0.788037575	0.086953482	1	0.298963515	3.31357E-09
cep-1(gk138)	0.788038	x	0.043313069	0.788037575	0.176460282	2.41711E-09
wrn-1(gk99)	0.086953	0.043313069	x	0.086953482	0.445070221	8.25371E-11
wrn-1(tm764)	1	0.788037575	0.086953482	x	0.298963515	3.31357E-09
cep-1(gk138); wrn-1(gk99)	0.298964	0.176460282	0.445070221	0.298963515	x	1.79039E-10
cep-1(gk138); wrn-1(tm764)	3.31E-09	2.41711E-09	8.25371E-11	3.31357E-09	1.79039E-10	x

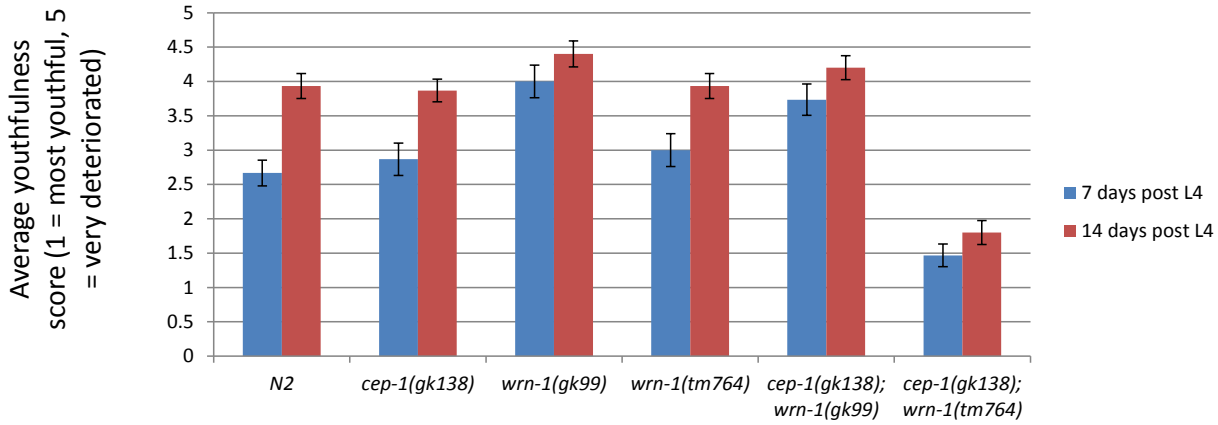

Chart showing the average score at 7 and 14 days post L4 that each strain received when scored blind for 'youthfulness'. The table below shows the same data in numerical form.

average score (1-5)	N2	*cep-1(gk138)*	*wrn-1(gk99)*	*wrn-1(tm764)*	*cep-1(gk138); wrn-1(gk99)*	*cep-1(gk138); wrn-1(tm764)*
7 days post L4	2.67	2.87	4.00	3.00	3.73	1.47
14 days post L4	3.93	3.87	4.40	3.93	4.20	1.80

24 Statistical analysis of germline phenotypes

25 Statistical analysis for Figures 3.9 and 3.13 - germline apoptosis, as detected by TUNEL staining.

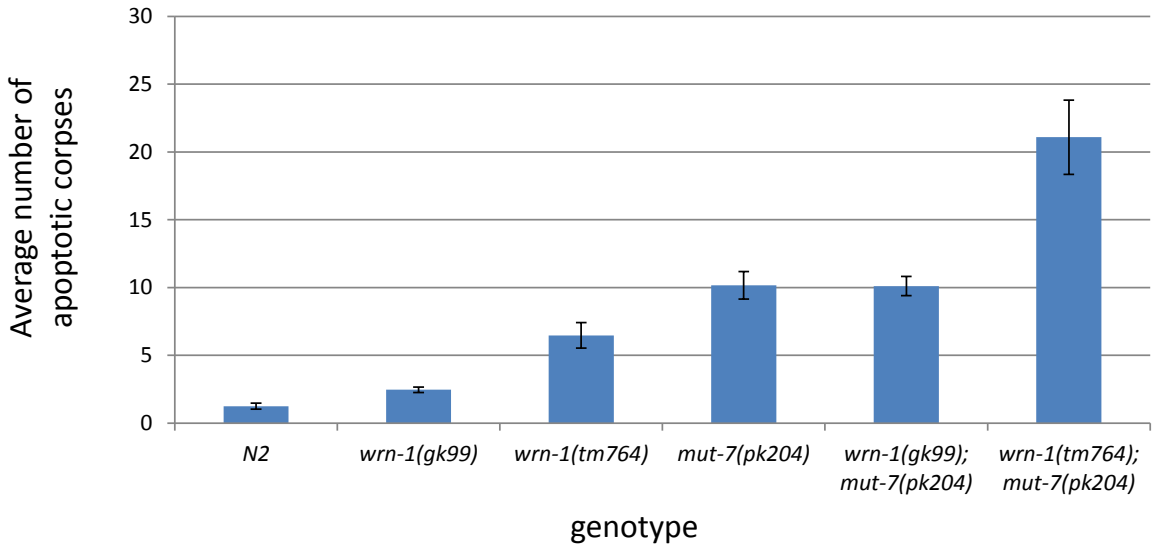

	N2	*wrn-1(gk99)*	*wrn-1(tm764)*	*mut-7(pk204)*	*wrn-1(gk99); mut-7(pk204)*	*wrn-1(tm764); mut-7(pk204)*
average	1.241379	2.454545455	6.470588235	10.15384615	10.1	21.08333333
SEM	0.220027	0.207304623	0.930949336	1.011765111	0.70632067	2.73988037

Single factor/one-way ANOVA

Summary:

Groups	*Count*	*Sum*	*Average*	*Variance*
N2	29	36	1.24	1.40
wrn-1(gk99)	11	27	2.45	0.47
wrn-1(tm764)	17	110	6.47	15.14
mut-7(pk204)	13	132	10.15	13.31
wrn-1(gk99);mut-7(pk204)	10	101	10.10	4.99
wrn-1(tm764);mut-7(pk204)	12	253	21.08	90.08

ANOVA:

Source of Variation	*SS*	*df*	*MS*	*F*	*P-value*	*F crit*
Between Groups	3796.77	5	759.35	44.07	0.0000	2.32
Within Groups	1481.78	86	17.23			
Total	5278.55	91				

F > F crit, therefore we reject the null hypothesis and perform post-hoc t-tests. The P values are shown in the next table.

P(T<=t) two-tail	N2	*wrn-1(gk99)*	*wrn-1(tm764)*	*mut-7(pk204)*	*wrn-1(gk99); mut-7(pk204)*	*wrn-1(tm764); mut-7(pk204)*
N2	x	0.002909024	2.50715E-08	8.43506E-15	3.21044E-18	8.27725E-14
wrn-1(gk99)	0.002909	x	0.002370974	6.6379E-07	1.44195E-09	2.0153E-06
wrn-1(tm764)	2.51E-08	0.002370974	x	0.013443593	0.012625532	4.26673E-06
mut-7(pk204)	8.44E-15	6.6379E-07	0.013443593	x	0.967672528	0.000795861
wrn-1(gk99); mut-7(pk204)	3.21E-18	1.44195E-09	0.012625532	0.967672528	x	0.001942403
wrn-1(tm764); mut-7(pk204)	8.28E-14	2.0153E-06	4.26673E-06	0.000795861	0.001942403	x

26 Statistical analysis of Figure 4.7 – the dependency of DNA-damaged induced apoptosis on cep-1.

The chart below shows the average number of CED-1::GFP labelled germline nuclei in WT worms (carrying integrated CED-1::GFP), and *wrn-1(gk99)** and *wrn-1(tm764)** mutants (*=in the CED-1::GFP background). Additional counts (including those on *cep-1(gk138)* single and double mutants) were performed using the TUNEL method

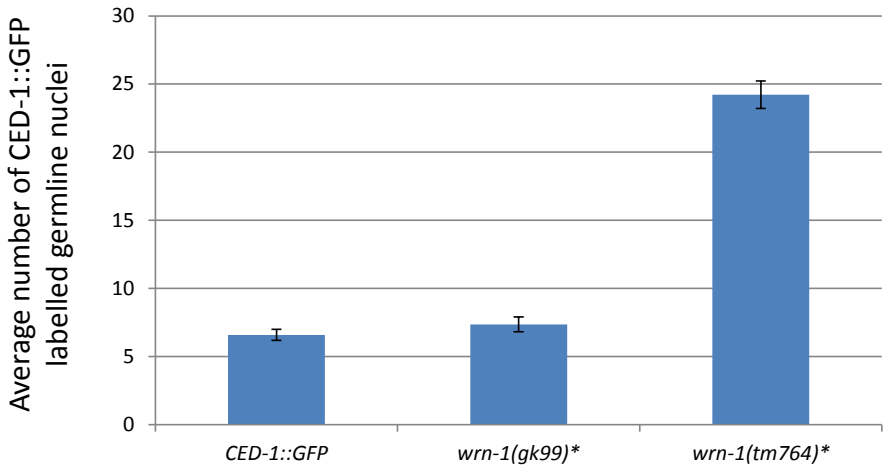

Single factor/one-way ANOVA:

Summary:

Groups	*Count*	*Sum*	*Average*	*Variance*
CED-1::GFP	27	178	6.59	4.33
*wrn-1(gk99)**	11	81	7.36	3.25
*wrn-1(tm764)**	36	872	24.22	36.58

ANOVA:

Source of Variation	*SS*	*df*	*MS*	*F*	*P-value*	*F crit*
Between Groups	5605.754	2	2802.877	139.624	2.48E-25	3.126
Within Groups	1425.286	71	20.074			
Total	7031.041	73				

F > F crit, therefore we reject the null hypothesis and perform post-hoc t-tests. The P values are shown in the table below:

Genotype	P(T<=t) two-tail
CED-1::GFP vs *wrn-1(gk99)**	0.290
CED-1::GFP vs *wrn-1(tm764)**	2.026E-21
*wrn-1(gk99)** vs *wrn-1(tm764)**	1.042E-11

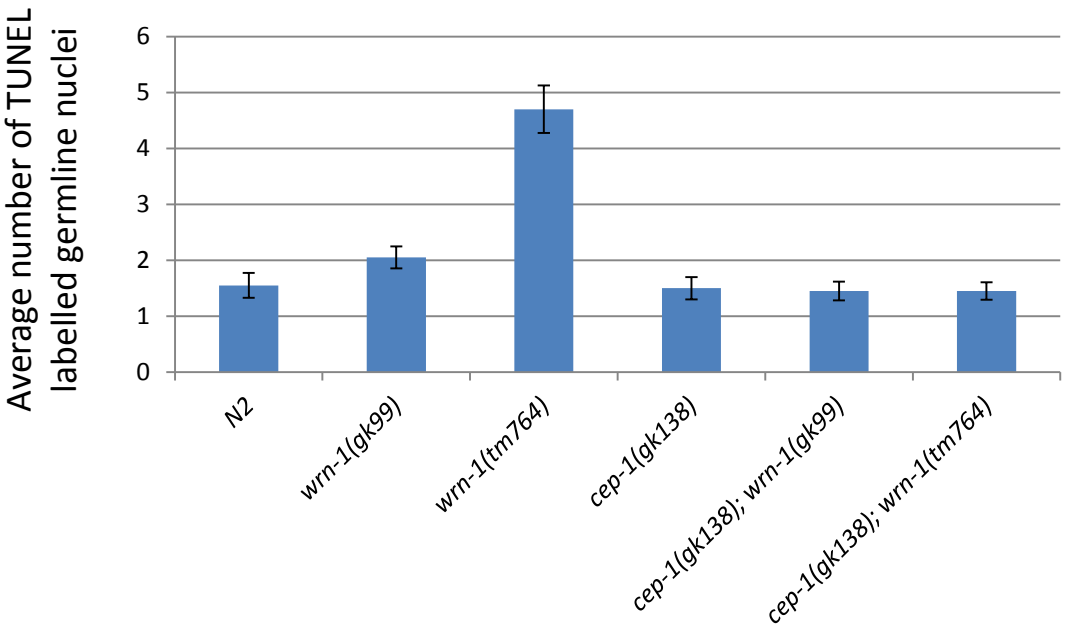

	N2	*wrn-1(gk99)*	*wrn-1(tm764)*	*cep-1(gk138)*	*cep-1(gk138); wrn-1(gk99)*	*cep-1(gk138); wrn-1(tm764)*
number	20	20	20	20	20	20
Sqrt(n)	4.47	4.47	4.47	4.47	4.47	4.47
average	1.55	2.05	4.70	1.50	1.45	1.45
STDEV	1.00	0.89	1.89	0.89	0.76	0.69
SEM	0.22	0.20	0.42	0.20	0.17	0.15

Single factor/one-way ANOVA

Summary:

Groups	*Count*	*Sum*	*Average*	*Variance*
N2	20	31	1.55	0.997
wrn-1(gk99)	20	41	2.05	0.787
wrn-1(tm764)	20	94	4.7	3.589
cep-1(gk138)	20	30	1.5	0.789
cep-1(gk138); wrn-1(gk99)	20	29	1.45	0.576
cep-1(gk138); wrn-1(tm764)	20	29	1.45	0.471

ANOVA:

Source of Variation	*SS*	*df*	*MS*	*F*	*P-value*	*F crit*
Between Groups	165.367	5	33.073	27.521	3.49E-18	2.294
Within Groups	137	114	1.202			
Total	302.367	119				

F > F crit, therefore we reject the null hypothesis and perform post-hoc t-tests. The P values are shown in the next table.

P(T<=t) two-tail	N2	*wrn-1(gk99)*	*wrn-1(tm764)*	*cep-1(gk138)*	*cep-1(gk138); wrn-1(gk99)*	*cep-1(gk138); wrn-1(tm764)*
N2	x	0.102338689	9.21944E-08	0.868037417	0.723440112	0.714136071
wrn-1(gk99)	0.102338689	x	1.63987E-06	0.057468695	0.027143463	0.02178569
wrn-1(tm764)	9.21944E-08	1.63987E-06	x	4.06686E-08	1.68722E-08	1.26945E-08
cep-1(gk138)	0.868037417	0.057468695	4.06686E-08	x	0.849282277	0.843196966
cep-1(gk138); wrn-1(gk99)	0.723440112	0.027143463	1.68722E-08	0.849282277	x	1
cep-1(gk138); wrn-1(tm764)	0.714136071	0.02178569	1.26945E-08	0.843196966	1	x

27 Occurrence of spontaneous mutants and males.

Single factor/one-way ANOVA for the percentage occurrence of spontaneous visible mutants:

Summary:

Groups	*Count*	*Sum*	*Average*	*Variance*
N2	55	0	0	0
cep-1(gk138)	49	1.8573	0.0379	0.0136
wrn-1(gk99)	58	4.1848	0.0722	0.0568
wrn-1(tm764)	55	2.9516	0.0537	0.0218
cep-1(gk138);wrn-1(gk99)	42	4.3314	0.1031	0.0491
cep-1(gk138);wrn-1(tm764)	52	5.0590	0.0973	0.0397

ANOVA:

Source of Variation	*SS*	*df*	*MS*	*F*	*P-value*	*F crit*
Between Groups	0.3829	5	0.0766	2.5661	0.0271	2.2436
Within Groups	9.1015	305	0.0298			
Total	9.4844	310				

F > F crit, therefore we reject the null hypothesis and perform post-hoc t-tests. The P values are shown in the next table.

Mutants P(T<=t) two-tail	N2	*cep-1(gk138)*	*wrn-1(gk99)*	*wrn-1(tm764)*	*cep-1(gk138); wrn-1(gk99)*	*cep-1(gk138); wrn-1(tm764)*
N2	x	0.017836185	0.026737715	0.00810042	0.000817863	0.000448465
cep-1(gk138)	0.017836185	x	0.361284315	0.550490419	0.076600437	0.072733476
wrn-1(gk99)	0.026737715	0.361284315	x	0.623180042	0.510414561	0.552114676
wrn-1(tm764)	0.00810042	0.550490419	0.623180042	x	0.190790835	0.199057839
cep-1(gk138); wrn-1(gk99)	0.000817863	0.076600437	0.510414561	0.190790835	x	0.893336512
cep-1(gk138); wrn-1(tm764)	0.000448465	0.072733476	0.552114676	0.199057839	0.893336512	x

Single factor/one-way ANOVA for the percentage occurrence of males:

Summary:

Groups	*Count*	*Sum*	*Average*	*Variance*
N2	55	1.1306	0.0206	0.0115
cep-1(gk138)	49	15.4287	0.3149	0.1054
wrn-1(gk99)	58	9.3241	0.1608	0.1165
wrn-1(tm764)	55	8.1558	0.1483	0.0758
cep-1(gk138);wrn-1(gk99)	42	16.0126	0.3813	0.1863
cep-1(gk138);wrn-1(tm764)	52	20.4061	0.3924	0.2710

ANOVA:

Source of Variation	*SS*	*df*	*MS*	*F*	*P-value*	*F crit*
Between Groups	5.740	5	1.148	9.245	3.29E-08	2.244
Within Groups	37.875	305	0.124			
Total	43.615	310				

F > F crit, therefore we reject the null hypothesis and perform post-hoc t-tests. The P values are shown in the next table.

Males P(T<=t) two-tail	N2	*cep-1(gk138)*	*wrn-1(gk99)*	*wrn-1(tm764)*	*cep-1(gk138); wrn-1(gk99)*	*cep-1(gk138); wrn-1(tm764)*
N2	x	6.09038E-09	0.004333498	0.001766418	4.08514E-08	1.06E-06
cep-1(gk138)	6.09E-09	x	0.019155794	0.005592634	0.405579047	0.374605901
wrn-1(gk99)	0.004333	0.019155794	x	0.831625419	0.00531612	0.006290135
wrn-1(tm764)	0.001766	0.005592634	0.831625419	x	0.001673359	0.002846636
cep-1(gk138); wrn-1(gk99)	4.09E-08	0.405579047	0.00531612	0.001673359	x	0.911454909
cep-1(gk138); wrn-1(tm764)	1.06E-06	0.374605901	0.006290135	0.002846636	0.911454909	x

28 Statistical analysis of mitotic abnormalities in all strains (wrn-1, cep-1 and mut-7 single and double mutants).

average number per germline	N2	*wrn-1(gk99)*	*wrn-1(tm764)*	*mut-7(pk204)*	*wrn-1(gk99); mut-7(pk204)*	*wrn-1(tm764); mut-7(pk204)*	*cep-1(gk138)*	*cep-1(gk138); wrn-1(gk99)*	*cep-1(gk138); wrn-1(tm764)*
enlarged nuclei	0.067	0.400	0.267	5.800	5.467	5.667	0.200	0.467	0.600
Anapase bridges	0.000	0.333	0.267	0.333	0.400	0.467	0.000	0.533	0.600
Gaps between nuclei	0.000	0.267	0.333	0.467	0.600	0.400	0.133	0.200	0.333
abnormal mitotic bodies	0.000	0.933	0.800	0.933	1.067	0.933	2.067	1.867	2.000

SEM	N2	*wrn-1(gk99)*	*wrn-1(tm764)*	*mut-7(pk204)*	*wrn-1(gk99); mut-7(pk204)*	*wrn-1(tm764); mut-7(pk204)*	*cep-1(gk138)*	*cep-1(gk138); wrn-1(gk99)*	*cep-1(gk138); wrn-1(tm764)*
enlarged nuclei	0.067	0.163	0.118	0.962	0.970	0.969	0.145	0.165	0.190
Anapase bridges	0.000	0.211	0.153	0.159	0.163	0.215	0.000	0.236	0.254
Gaps between nuclei	0.000	0.153	0.159	0.236	0.349	0.190	0.091	0.145	0.159
abnormal mitotic bodies	0.000	0.441	0.327	0.330	0.267	0.371	0.384	0.435	0.436

Note that abnormal mitotic bodies include: apparent chromosome fragmentation, >3 mitotic bodies, and odd shaped mitotic-bodies.

The chart for this data is on the next page.

Chart showing the average number of germline phenotypes per germline.

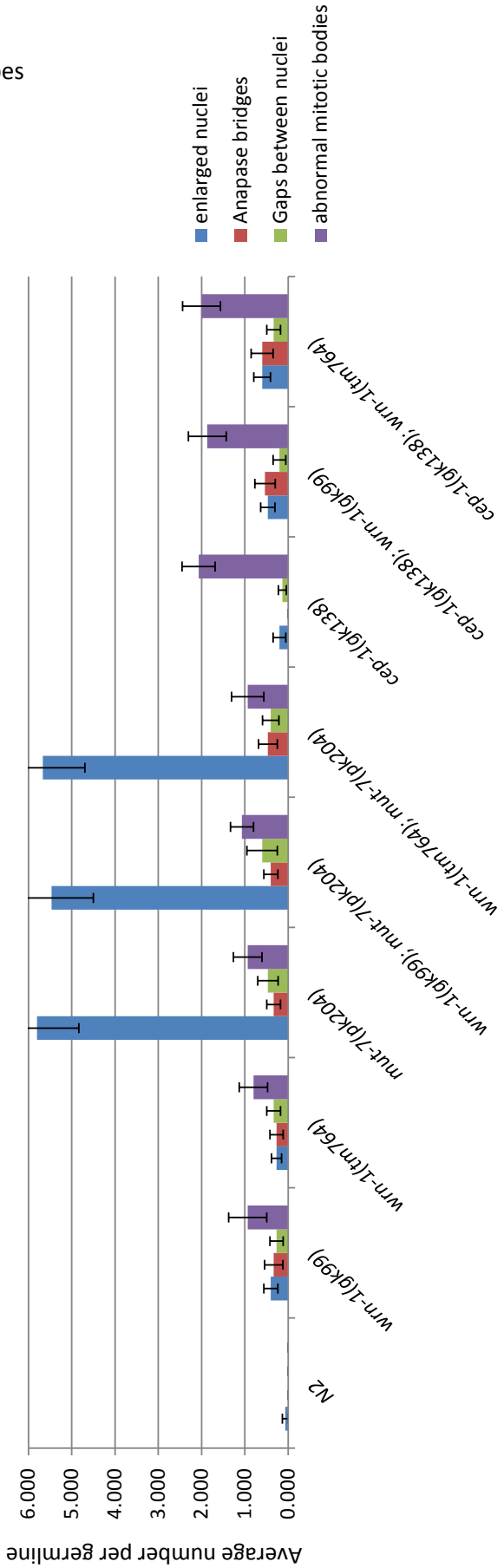

Single Factor/one-way ANOVA for germline phenotypes:

SUMMARY: enlarged nuclei				
Groups	*Count*	*Sum*	*Average*	*Variance*
N2	15	1	0.067	0.067
wrn-1(gk99)	15	6	0.400	0.400
wrn-1(tm764)	15	4	0.267	0.210
mut-7(pk204)	15	87	5.800	13.886
wrn-1(gk99); mut-7(pk204)	15	82	5.467	14.124
wrn-1(tm764); mut-7(pk204)	15	85	5.667	14.095
cep-1(gk138)	15	3	0.200	0.314
cep-1(gk138); wrn-1(gk99)	15	7	0.467	0.410
cep-1(gk138); wrn-1(tm764)	15	9	0.600	0.543

ANOVA: enlarged nuclei						
Source of Variation	*SS*	*df*	*MS*	*F*	*P-value*	*F crit*
Between Groups	849.881	8.000	106.235	21.706	0.000	2.013
Within Groups	616.667	126.000	4.894			
Total	1466.548	134.000				

SUMMARY: Anapase bridges				
Groups	*Count*	*Sum*	*Average*	*Variance*
N2	15	0	0	0
wrn-1(gk99)	15	5	0.333	0.667
wrn-1(tm764)	15	4	0.267	0.352
mut-7(pk204)	15	5	0.333	0.381
wrn-1(gk99); mut-7(pk204)	15	6	0.400	0.400
wrn-1(tm764); mut-7(pk204)	15	7	0.467	0.695
cep-1(gk138)	15	0	0.000	0.000
cep-1(gk138); wrn-1(gk99)	15	8	0.533	0.838
cep-1(gk138); wrn-1(tm764)	15	9	0.600	0.971

ANOVA: Anapase bridges						
Source of Variation	*SS*	*df*	*MS*	*F*	*P-value*	*F crit*
Between Groups	5.393	8	0.674	1.409	0.199	2.013
Within Groups	60.267	126	0.478			
Total	65.659	134				

SUMMARY: Gaps between nuclei				
Groups	*Count*	*Sum*	*Average*	*Variance*
N2	15	0	0	0
wrn-1(gk99)	15	4	0.267	0.352
wrn-1(tm764)	15	5	0.333	0.381
mut-7(pk204)	15	7	0.467	0.838
wrn-1(gk99); mut-7(pk204)	15	9	0.600	1.829
wrn-1(tm764); mut-7(pk204)	15	6	0.400	0.543
cep-1(gk138)	15	2	0.133	0.124
cep-1(gk138); wrn-1(gk99)	15	3	0.200	0.314
cep-1(gk138); wrn-1(tm764)	15	5	0.333	0.381

ANOVA: Gaps between nuclei						
Source of Variation	*SS*	*df*	*MS*	*F*	*P-value*	*F crit*
Between Groups	3.881481481	8	0.485185185	0.917	0.504821303	2.012654388
Within Groups	66.66666667	126	0.529100529			
Total	70.54814815	134				

SUMMARY: abnormal mitotic bodies				
Groups	*Count*	*Sum*	*Average*	*Variance*
N2	15	0	0	0
wrn-1(gk99)	15	14	0.933	2.924
wrn-1(tm764)	15	12	0.800	1.600
mut-7(pk204)	15	14	0.933	1.638
wrn-1(gk99); mut-7(pk204)	15	16	1.067	1.067
wrn-1(tm764); mut-7(pk204)	15	14	0.933	2.067
cep-1(gk138)	15	31	2.067	2.210
cep-1(gk138); wrn-1(gk99)	15	28	1.867	2.838
cep-1(gk138); wrn-1(tm764)	15	30	2.000	2.857

ANOVA: abnormal mitotic bodies						
Source of Variation	*SS*	*df*	*MS*	*F*	*P-value*	*F crit*
Between Groups	54.933	8	6.867	3.593	0.001	2.013
Within Groups	240.800	126	1.911			
Total	295.733	134				

29 Statistical analysis of Figure 4.12 – HU-induced germ cell proliferation arrest.

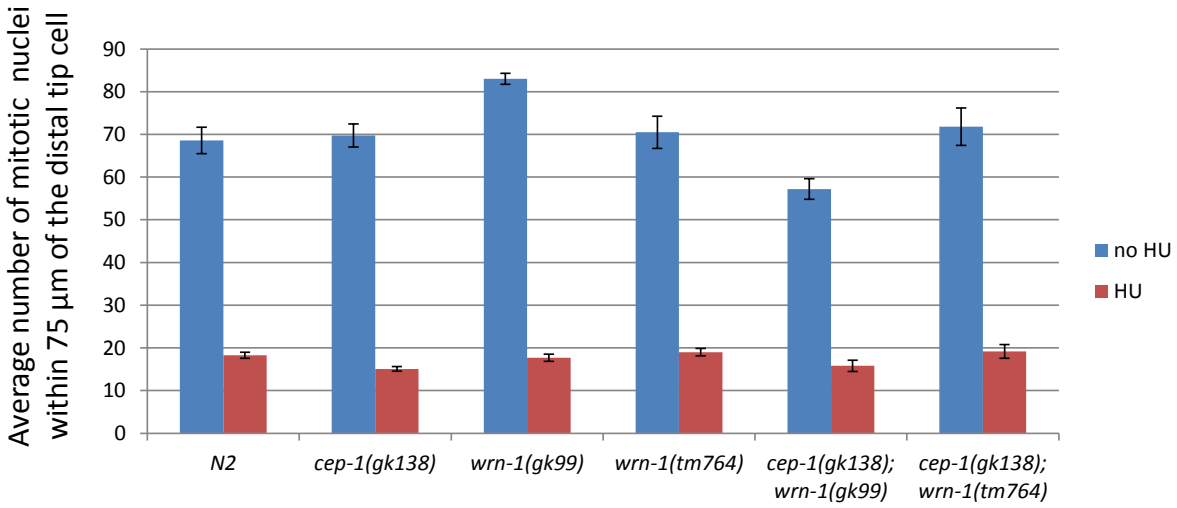

	N2	*cep-1(gk138)*	*wrn-1(gk99)*	*wrn-1(tm764)*	*cep-1(gk138); wrn-1(gk99)*	*cep-1(gk138); wrn-1(tm764)*
no HU	69	70	83	71	57	72
HU	18	15	18	19	16	19

Single factor/one-way ANOVA for untreated worms (48 hours post L4)

Summary:

Groups	*Count*	*Sum*	*Average*	*Variance*
N2 no HU	5	343	68.6	47.8
cep-1(gk138) no HU	4	279	69.8	28.9
wrn-1(gk99) no HU	4	332	83	6.7
wrn-1(tm764) no HU	4	282	70.5	57
cep-1(gk138);wrn-1(gk99) no HU	5	286	57.2	29.2
cep-1(gk138);wrn-1(tm764) no HU	5	359	71.8	96.7

ANOVA:

Source of Variation	*SS*	*df*	*MS*	*F*	*P-value*	*F crit*
Between Groups	1519.45	5	303.89	6.56	0.000801	2.68
Within Groups	972.55	21	46.31			
Total	2492	26				

F > F crit, therefore we reject the null hypothesis and perform post-hoc t-tests. The P values are shown in the next table.

no HU P(T<=t) two-tail	N2	*cep-1(gk138)*	*wrn-1(gk99)*	*wrn-1(tm764)*	*cep-1(gk138); wrn-1(gk99)*	*cep-1(gk138); wrn-1(tm764)*
N2	x	0.793429099	0.005838185	0.705483216	0.019740135	0.568126748
cep-1(gk138)	0.793429	x	0.004364348	0.876753646	0.010414717	0.721221289
wrn-1(gk99)	0.005838	0.004364348	x	0.020242852	5.3152E-05	0.06466616
wrn-1(tm764)	0.705483	0.876753646	0.020242852	x	0.017516093	0.834327282
cep-1(gk138); wrn-1(gk99)	0.01974	0.010414717	5.3152E-05	0.017516093	x	0.019602784
cep-1(gk138); wrn-1(tm764)	0.568127	0.721221289	0.06466616	0.834327282	0.019602784	x

Single factor/one-way ANOVA for worms treated with HU (48 hours post L4)

Summary:

Groups	*Count*	*Sum*	*Average*	*Variance*
N2 + HU	11	201	18.27	5.42
cep-1(gk138) + HU	14	211	15.07	4.53
wrn-1(gk99) + HU	13	230	17.69	8.73
wrn-1(tm764) + HU	11	209	19	8
cep-1(gk138);wrn-1(gk99) + HU	10	158	15.80	17.51
cep-1(gk138);wrn-1(tm764) + HU	11	211	19.18	28.76

ANOVA:

Source of Variation	*SS*	*df*	*MS*	*F*	*P-value*	*F crit*
Between Groups	174.03	5	34.81	3.00	0.017113	2.36
Within Groups	743.12	64	11.61			
Total	917.14	69				

F > F crit, therefore we reject the null hypothesis and perform post-hoc t-tests. The P values are shown in the next table.

HU P(T<=t) two-tail	N2	*cep-1(gk138)*	*wrn-1(gk99)*	*wrn-1(tm764)*	*cep-1(gk138); wrn-1(gk99)*	*cep-1(gk138); wrn-1(tm764)*
N2	x	0.001574797	0.603406771	0.517734979	0.106383285	0.611710691
cep-1(gk138)	0.001575	x	0.013468984	0.000610136	0.580535232	0.015031324
wrn-1(gk99)	0.603407	0.013468984	x	0.282606356	0.217008158	0.398582087
wrn-1(tm764)	0.517735	0.000610136	0.282606356	x	0.052216531	0.921767548
cep-1(gk138); wrn-1(gk99)	0.106383	0.580535232	0.217008158	0.052216531	x	0.12634238
cep-1(gk138); wrn-1(tm764)	0.611711	0.015031324	0.398582087	0.921767548	0.12634238	x

30 Statistical analysis of Figure 4.15 – IR- induced germ cell proliferation arrest.

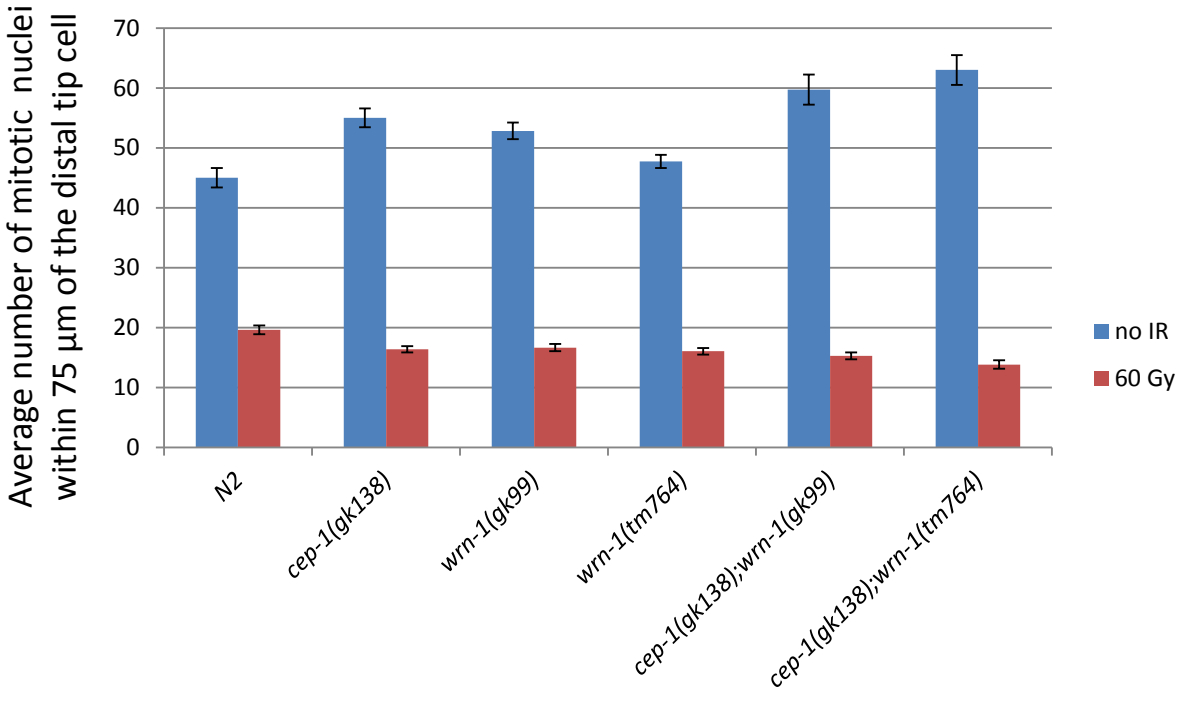

	N2	*cep-1(gk138)*	*wrn-1(gk99)*	*wrn-1(tm764)*	*cep-1(gk138); wrn-1(gk99)*	*cep-1(gk138); wrn-1(tm764)*
no IR	45	55	53	48	60	63
60 Gy	20	16	17	16	15	14

Single factor/one-way ANOVA for untreated worms (12 hours post L4):

Summary:

Groups	*Count*	*Sum*	*Average*	*Variance*
N2 no IR	10	450	45	27
cep-1(gk138) no IR	14	770	55	35
wrn-1(gk99) no IR	12	634	53	24
wrn-1(tm764) no IR	15	716	48	19
cep-1(gk138);wrn-1(gk99) no IR	14	836	60	89
cep-1(gk138);wrn-1(tm764) no IR	10	630	63	61

ANOVA:

Source of Variation	*SS*	*df*	*MS*	*F*	*P-value*	*F crit*
Between Groups	2694	5	539	12.73395	8.96E-09	2.348
Within Groups	2919	69	42			
Total	5613	74				

F > F crit, therefore we reject the null hypothesis and perform post-hoc t-tests. The P values are shown in the next table.

no IR P(T<=t) two-tail	N2	*cep-1(gk138)*	*wrn-1(gk99)*	*wrn-1(tm764)*	*cep-1(gk138); wrn-1(gk99)*	*cep-1(gk138); wrn-1(tm764)*
N2	x	0.000285434	0.001581558	0.165656333	0.000191585	9.8118E-06
cep-1(gk138)	0.000285	x	0.322573954	0.000749223	0.124247247	0.009098595
wrn-1(gk99)	0.001582	0.322573954	x	0.008143547	0.031788841	0.001344454
wrn-1(tm764)	0.165656	0.000749223	0.008143547	x	0.000131491	2.07127E-06
cep-1(gk138); wrn-1(gk99)	0.000192	0.124247247	0.031788841	0.000131491	x	0.376822409
cep-1(gk138); wrn-1(tm764)	9.81E-06	0.009098595	0.001344454	2.07127E-06	0.376822409	x

Single factor/one-way ANOVA for irradiated worms (12 hours post L4):

Summary:

Groups	*Count*	*Sum*	*Average*	*Variance*
N2 + 60 Gy	18	353	20	10
cep-1(gk138) + 60 Gy	13	213	16	3
wrn-1(gk99) + 60 Gy	15	250	17	5
wrn-1(tm764) + 60 Gy	20	321	16	6
cep-1(gk138);wrn-1(gk99) + 60 Gy	7	107	15	2
cep-1(gk138);wrn-1(tm764) + 60 Gy	6	83	14	3

ANOVA:

Source of Variation	*SS*	*df*	*MS*	*F*	*P-value*	*F crit*
Between Groups	225	5	45	7.745	6.88E-06	2.340
Within Groups	424	73	6			
Total	649	78				

F > F crit, therefore we reject the null hypothesis and perform post-hoc t-tests. The P values are shown in the next table.

60 Gy P(T<=t) two-tail	N2	*cep-1(gk138)*	*wrn-1(gk99)*	*wrn-1(tm764)*	*cep-1(gk138); wrn-1(gk99)*	*cep-1(gk138); wrn-1(tm764)*
N2	x	0.002468549	0.004751848	0.000394259	0.002054363	0.000310672
cep-1(gk138)	0.002469	x	0.723253564	0.680277614	0.194682557	0.0110646
wrn-1(gk99)	0.004752	0.723253564	x	0.455108734	0.158338351	0.012615867
wrn-1(tm764)	0.000394	0.680277614	0.455108734	x	0.453138219	0.053335907
cep-1(gk138); wrn-1(gk99)	0.002054	0.194682557	0.158338351	0.453138219	x	0.131662354
cep-1(gk138); wrn-1(tm764)	0.000311	0.0110646	0.012615867	0.053335907	0.131662354	x

31 Statistical analysis of Figure 4.17 - germline apoptosis after IR treatment.

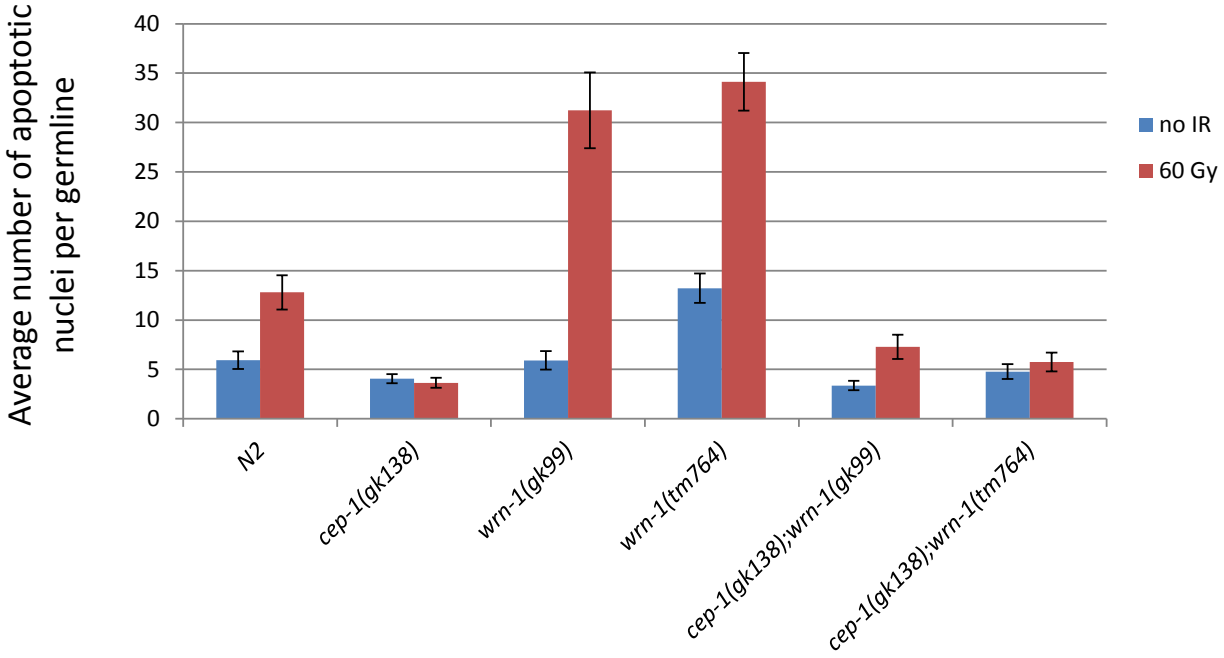

	N2	*cep-1(gk138)*	*wrn-1(gk99)*	*wrn-1(tm764)*	*cep-1(gk138); wrn-1(gk99)*	*cep-1(gk138); wrn-1(tm764)*
no IR	6	4	6	13	3	5
60 Gy	13	4	31	34	7	6

Single factor/one-way ANOVA for untreated worms

Summary:

Groups	*Count*	*Sum*	*Average*	*Variance*
N2 no IR	14	83	6	11
cep-1(gk138) no IR	15	61	4	3
wrn-1(gk99) no IR	12	71	6	10
wrn-1(tm764) no IR	9	119	13	20
cep-1(gk138);wrn-1(gk99) no IR	11	37	3	2
cep-1(gk138);wrn-1(tm764) no IR	13	62	5	7

ANOVA:

Source of Variation	*SS*	*df*	*MS*	*F*	*P-value*	*F crit*
Between Groups	620	5	124	14.6	1.09E-09	2.3
Within Groups	579	68	9			
Total	1199	73				

F > F crit, therefore we reject the null hypothesis and perform post-hoc t-tests. The P values are shown in the next table.

no IR P(T<=t) two-tail	N2	*cep-1(gk138)*	*wrn-1(gk99)*	*wrn-1(tm764)*	*cep-1(gk138); wrn-1(gk99)*	*cep-1(gk138); wrn-1(tm764)*
N2	x	0.071001382	0.992738138	0.000219398	0.028850283	0.335867395
cep-1(gk138)	0.071001	x	0.068894912	4.14364E-07	0.30829508	0.420221921
wrn-1(gk99)	0.992738	0.068894912	x	0.000337833	0.026271517	0.342602983
wrn-1(tm764)	0.000219	4.14364E-07	0.000337833	x	2.19107E-06	2.12858E-05
cep-1(gk138); wrn-1(gk99)	0.02885	0.30829508	0.026271517	2.19107E-06	x	0.144040388
cep-1(gk138); wrn-1(tm764)	0.335867	0.420221921	0.342602983	2.12858E-05	0.144040388	x

Single factor/one-way ANOVA for irradiated worms

Summary:

Groups	*Count*	*Sum*	*Average*	*Variance*
N2 + 60 Gy	10	128	13	30
cep-1(gk138) + 60 Gy	14	51	4	3
wrn-1(gk99) + 60 Gy	13	406	31	191
wrn-1(tm764) + 60 Gy	9	307	34	77
cep-1(gk138);wrn-1(gk99) + 60 Gy	14	102	7	21
cep-1(gk138);wrn-1(tm764) + 60 Gy	8	46	6	7

ANOVA:

Source of Variation	*SS*	*df*	*MS*	*F*	*P-value*	*F crit*
Between Groups	10078	5	2015.5	35.3	6.58E-17	2.4
Within Groups	3542	62	57.1			
Total	13620	67				

F > F crit, therefore we reject the null hypothesis and perform post-hoc t-tests. The P values are shown in the next table.

60 Gy P(T<=t) two-tail	N2	*cep-1(gk138)*	*wrn-1(gk99)*	*wrn-1(tm764)*	*cep-1(gk138); wrn-1(gk99)*	*cep-1(gk138); wrn-1(tm764)*
N2	x	7.28743E-06	0.000700148	6.30583E-06	0.013613787	0.004449204
cep-1(gk138)	7.29E-06	x	9.14316E-08	2.46947E-11	0.010345918	0.042913301
wrn-1(gk99)	0.0007	9.14316E-08	x	0.587522693	2.00657E-06	6.22442E-05
wrn-1(tm764)	6.31E-06	2.46947E-11	0.587522693	x	3.48975E-09	2.78056E-07
cep-1(gk138); wrn-1(gk99)	0.013614	0.010345918	2.00657E-06	3.48975E-09	x	0.398321885
cep-1(gk138); wrn-1(tm764)	0.004449	0.042913301	6.22442E-05	2.78056E-07	0.398321885	x

	0 Gy vs 60 Gy: P(T<=t) two-tail
N2	0.000969
cep-1(gk138)	0.537770
wrn-1(gk99)	0.000003
wrn-1(tm764)	0.000009
cep-1(gk138); wrn-1(gk99)	0.012317
cep-1(gk138); wrn-1(tm764)	0.430999

32 Statistical analysis of Figure 4.21 – germline apoptosis 48 hours post CPT treatment.

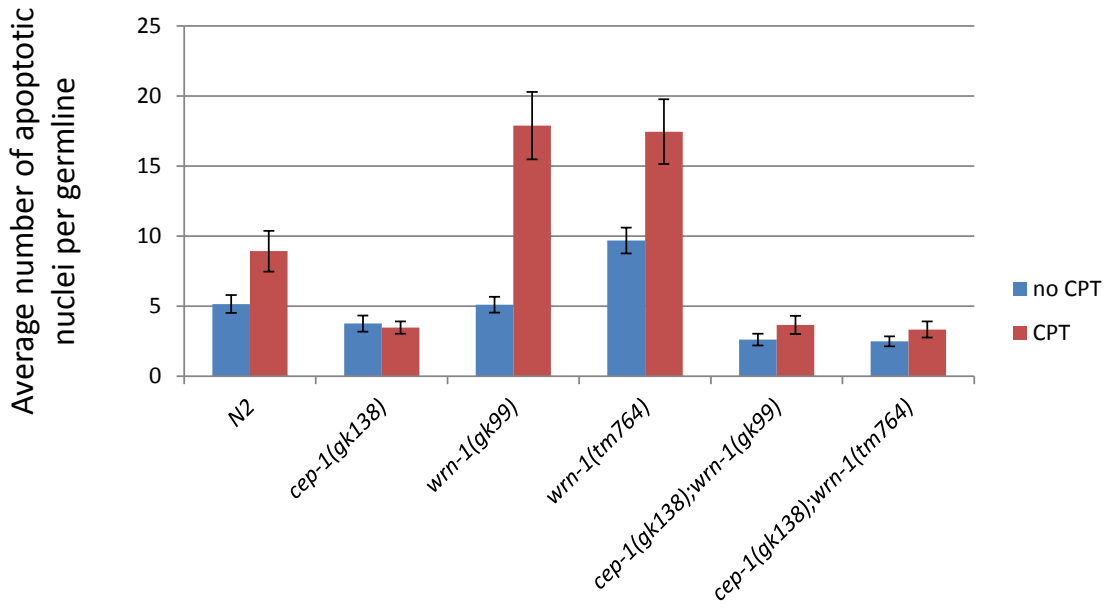

	N2	*cep-1(gk138)*	*wrn-1(gk99)*	*wrn-1(tm764)*	*cep-1(gk138); wrn-1(gk99)*	*cep-1(gk138); wrn-1(tm764)*
no CPT	5.2	3.8	5.1	9.7	2.6	2.5
CPT	8.9	3.5	17.9	17.4	3.7	3.3

Single factor/one-way ANOVA for untreated worms

Summary:

Groups	*Count*	*Sum*	*Average*	*Variance*
N2 no CPT	19	98	5.2	7.8
cep-1(gk138) no CPT	17	64	3.8	5.7
wrn-1(gk99) no CPT	19	97	5.1	6.1
wrn-1(tm764) no CPT	19	184	9.7	16.0
cep-1(gk138);wrn-1(gk99) no CPT	13	34	2.6	2.3
cep-1(gk138);wrn-1(tm764) no CPT	14	35	2.5	1.8

ANOVA:

Source of Variation	*SS*	*df*	*MS*	*F*	*P-value*	*F crit*
Between Groups	604.5	5.0	120.9	16.9	6.5E-12	2.3
Within Groups	680.1	95.0	7.2			
Total	1284.5	100.0				

F > F crit, therefore we reject the null hypothesis and perform post-hoc t-tests. The P values are shown in the next table.

no CPT P(T<=t) two-tail	N2	*cep-1(gk138)*	*wrn-1(gk99)*	*wrn-1(tm764)*	*cep-1(gk138); wrn-1(gk99)*	*cep-1(gk138); wrn-1(tm764)*
N2	x	0.119077141	0.951285486	0.000265786	0.005547814	0.00256467
cep-1(gk138)	0.119077	x	0.107717841	6.80685E-06	0.140055706	0.088416425
wrn-1(gk99)	0.951285	0.107717841	x	0.000146523	0.002930939	0.001196431
wrn-1(tm764)	0.000266	6.80685E-06	0.000146523	x	1.18245E-06	3.59726E-07
cep-1(gk138); wrn-1(gk99)	0.005548	0.140055706	0.002930939	1.18245E-06	x	0.834892617
cep-1(gk138); wrn-1(tm764)	0.002565	0.088416425	0.001196431	3.59726E-07	0.834892617	x

Single factor/one-way ANOVA for CPT treated worms

Summary:

Groups	*Count*	*Sum*	*Average*	*Variance*
N2 + CPT	13	116	8.9	27.6
cep-1(gk138) + CPT	19	66	3.5	3.6
wrn-1(gk99) + CPT	8	143	17.9	46.1
wrn-1(tm764) + CPT	9	157	17.4	48.0
cep-1(gk138);wrn-1(gk99) + CPT	9	33	3.7	3.8
cep-1(gk138);wrn-1(tm764) + CPT	9	30	3.3	3.0

ANOVA:

Source of Variation	*SS*	*df*	*MS*	*F*	*P-value*	*F crit*
Between Groups	2347.0	5	469.4	24.8	1.58E-13	2.4
Within Groups	1156.8	61	19.0			
Total	3503.8	66				

F > F crit, therefore we reject the null hypothesis and perform post-hoc t-tests. The P values are shown in the next two tables.

CPT P(T<=t) two-tail	N2	*cep-1(gk138)*	*wrn-1(gk99)*	*wrn-1(tm764)*	*cep-1(gk138); wrn-1(gk99)*	*cep-1(gk138); wrn-1(tm764)*
N2	x	0.000239582	0.003031199	0.00369048	0.009820224	0.006180054
cep-1(gk138)	0.00024	x	5.16853E-09	8.63808E-09	0.804673617	0.852533937
wrn-1(gk99)	0.003031	5.16853E-09	x	0.89902817	2.31009E-05	1.63102E-05
wrn-1(tm764)	0.00369	8.63808E-09	0.89902817	x	3.01699E-05	2.13007E-05
cep-1(gk138); wrn-1(gk99)	0.00982	0.804673617	2.31009E-05	3.01699E-05	x	0.705379657
cep-1(gk138); wrn-1(tm764)	0.00618	0.852533937	1.63102E-05	2.13007E-05	0.705379657	x

	P(T<=t) two-tail for no CPT vs CPT
N2	0.013
cep-1(gk138)	0.686
wrn-1(gk99)	0.000
wrn-1(tm764)	0.001
cep-1(gk138);wrn-1(gk99)	0.167
cep-1(gk138);wrn-1(tm764)	0.209

References

(1998) Genome sequence of the nematode C. elegans: a platform for investigating biology. *Science* **282**(5396)**:** 2012-2018

Abraham RT, Wiederrecht GJ (1996) Immunopharmacology of rapamycin. *Annu Rev Immunol* **14:** 483-510

Adachi H, Fujiwara Y, Ishii N (1998) Effects of oxygen on protein carbonyl and aging in Caenorhabditis elegans mutants with long (age-1) and short (mev-1) life spans. *J Gerontol A Biol Sci Med Sci* **53**(4)**:** B240-244

Ahmed S, Hodgkin J (2000) MRT-2 checkpoint protein is required for germline immortality and telomere replication in C. elegans. *Nature* **403**(6766)**:** 159-164

Aitlhadj L, Sturzenbaum SR (2010) The use of FUdR can cause prolonged longevity in mutant nematodes. *Mech Ageing Dev* **131**(5)**:** 364-365

Alcedo J, Kenyon C (2004) Regulation of C. elegans longevity by specific gustatory and olfactory neurons. *Neuron* **41**(1)**:** 45-55

Alers S, Loffler AS, Wesselborg S, Stork B (2012) Role of AMPK-mTOR-Ulk1/2 in the regulation of autophagy: cross talk, shortcuts, and feedbacks. *Mol Cell Biol* **32**(1)**:** 2-11

An JH, Blackwell TK (2003) SKN-1 links C. elegans mesendodermal specification to a conserved oxidative stress response. *Genes Dev* **17**(15)**:** 1882-1893

Anderson RM, Weindruch R (2010) Metabolic reprogramming, caloric restriction and aging. *Trends Endocrinol Metab* **21**(3)**:** 134-141

Angeli S, Klang I, Sivapatham R, Mark K, Zucker D, Bhaumik D, Lithgow GJ, Andersen JK (2013) A DNA synthesis inhibitor is protective against proteotoxic stressors via modulation of fertility pathways in Caenorhabditis elegans. *Aging (Albany NY)* **5**(10)**:** 759-769

Anisimov VN, Berstein LM, Popovich IG, Zabezhinski MA, Egormin PA, Piskunova TS, Semenchenko AV, Tyndyk ML, Yurova MN, Kovalenko IG, Poroshina TE (2011) If started early in life, metformin treatment increases life span and postpones tumors in female SHR mice. *Aging (Albany NY)* **3**(2)**:** 148-157

Apfeld J, Kenyon C (1999) Regulation of lifespan by sensory perception in Caenorhabditis elegans. *Nature* **402**(6763)**:** 804-809

Apfeld J, O'Connor G, McDonagh T, DiStefano PS, Curtis R (2004) The AMP-activated protein kinase AAK-2 links energy levels and insulin-like signals to lifespan in C. elegans. *Genes Dev* **18**(24)**:** 3004-3009

Arantes-Oliveira N, Apfeld J, Dillin A, Kenyon C (2002) Regulation of life-span by germ-line stem cells in Caenorhabditis elegans. *Science* **295**(5554)**:** 502-505

Ariyoshi K, Suzuki K, Goto M, Watanabe M, Kodama S (2007) Increased chromosome instability and accumulation of DNA double-strand breaks in Werner syndrome cells. *J Radiat Res* **48**(3)**:** 219-231

Armata HL, Garlick DS, Sluss HK (2007) The ataxia telangiectasia-mutated target site Ser18 is required for p53-mediated tumor suppression. *Cancer Res* **67**(24)**:** 11696-11703

Arum O, Johnson TE (2007) Reduced expression of the Caenorhabditis elegans p53 ortholog cep-1 results in increased longevity. *J Gerontol A Biol Sci Med Sci* **62**(9)**:** 951-959

Attardi LD, Jacks T (1999) The role of p53 in tumour suppression: lessons from mouse models. *Cell Mol Life Sci* **55**(1)**:** 48-63

Augustin M, Bamberger C, Paul D, Schmale H (1998) Cloning and chromosomal mapping of the human p53-related KET gene to chromosome 3q27 and its murine homolog Ket to mouse chromosome 16. *Mamm Genome* **9**(11)**:** 899-902

Babar P, Adamson C, Walker GA, Walker DW, Lithgow GJ (1999) P13-kinase inhibition induces dauer formation, thermotolerance and longevity in C. elegans. *Neurobiol Aging* **20**(5)**:** 513-519

Baker DJ, Wijshake T, Tchkonia T, LeBrasseur NK, Childs BG, van de Sluis B, Kirkland JL, van Deursen JM (2011) Clearance of p16Ink4a-positive senescent cells delays ageing-associated disorders. *Nature* **479**(7372)**:** 232-236

Balajee AS, Machwe A, May A, Gray MD, Oshima J, Martin GM, Nehlin JO, Brosh R, Orren DK, Bohr VA (1999) The Werner syndrome protein is involved in RNA polymerase II transcription. *Mol Biol Cell* **10**(8)**:** 2655-2668

Barbieri M, Bonafe M, Franceschi C, Paolisso G (2003) Insulin/IGF-I-signaling pathway: an evolutionarily conserved mechanism of longevity from yeast to humans. *Am J Physiol Endocrinol Metab* **285**(5)**:** E1064-1071

Barsyte D, Lovejoy DA, Lithgow GJ (2001) Longevity and heavy metal resistance in daf-2 and age-1 long-lived mutants of Caenorhabditis elegans. *FASEB J* **15**(3)**:** 627-634

Bartke A (2008) Impact of reduced insulin-like growth factor-1/insulin signaling on aging in mammals: novel findings. *Aging Cell* **7**(3)**:** 285-290

Baruah A, Chang H, Hall M, Yuan J, Gordon S, Johnson E, Shtessel LL, Yee C, Hekimi S, Derry WB, Lee SS (2014) CEP-1, the Caenorhabditis elegans p53 homolog, mediates opposing longevity outcomes in mitochondrial electron transport chain mutants. *PLoS Genet* **10**(2)**:** e1004097

Barzilai N, Huffman DM, Muzumdar RH, Bartke A (2012) The critical role of metabolic pathways in aging. *Diabetes* **61**(6)**:** 1315-1322

Bensaad K, Tsuruta A, Selak MA, Vidal MN, Nakano K, Bartrons R, Gottlieb E, Vousden KH (2006) TIGAR, a p53-inducible regulator of glycolysis and apoptosis. *Cell* **126**(1)**:** 107-120

Benson EK, Zhao B, Sassoon DA, Lee SW, Aaronson SA (2009) Effects of p21 deletion in mouse models of premature aging. *Cell Cycle* **8**(13)**:** 2002-2004

Bird JL, Jennert-Burston KC, Bachler MA, Mason PA, Lowe JE, Heo SJ, Campisi J, Faragher RG, Cox LS (2013) Recapitulation of Werner syndrome sensitivity to camptothecin by limited knockdown of the WRN helicase/exonuclease. *Biogerontology* **13**(1)**:** 49-62

Bishop NA, Guarente L (2007) Two neurons mediate diet-restriction-induced longevity in C. elegans. *Nature* **447**(7144)**:** 545-549

Blander G, Kipnis J, Leal JF, Yu CE, Schellenberg GD, Oren M (1999) Physical and functional interaction between p53 and the Werner's syndrome protein. *J Biol Chem* **274**(41)**:** 29463-29469

Blander G, Zalle N, Leal JF, Bar-Or RL, Yu CE, Oren M (2000) The Werner syndrome protein contributes to induction of p53 by DNA damage. *FASEB J* **14**(14)**:** 2138-2140

Blasco MA (2007) Telomere length, stem cells and aging. *Nat Chem Biol* **3**(10)**:** 640-649

Bluher M, Kahn BB, Kahn CR (2003) Extended longevity in mice lacking the insulin receptor in adipose tissue. *Science* **299**(5606)**:** 572-574

Boubriak I, Mason PA, Clancy DJ, Dockray J, Saunders RD, Cox LS (2009) DmWRNexo is a 3'-5' exonuclease: phenotypic and biochemical characterization of mutants of the Drosophila orthologue of human WRN exonuclease. *Biogerontology* **10**(3)**:** 267-277

Bouwman P, Aly A, Escandell JM, Pieterse M, Bartkova J, van der Gulden H, Hiddingh S, Thanasoula M, Kulkarni A, Yang Q, Haffty BG, Tommiska J, Blomqvist C, Drapkin R, Adams DJ, Nevanlinna H, Bartek J, Tarsounas M, Ganesan S, Jonkers J (2010) 53BP1 loss rescues BRCA1 deficiency and is associated with triple-negative and BRCA-mutated breast cancers. *Nat Struct Mol Biol* **17**(6)**:** 688-695

Brenner S (1974) The genetics of Caenorhabditis elegans. *Genetics* **77**(1)**:** 71-94

Brosh RM, Jr., Karmakar P, Sommers JA, Yang Q, Wang XW, Spillare EA, Harris CC, Bohr VA (2001) p53 Modulates the exonuclease activity of Werner syndrome protein. *J Biol Chem* **276**(37)**:** 35093-35102

Broue F, Liere P, Kenyon C, Baulieu EE (2007) A steroid hormone that extends the lifespan of Caenorhabditis elegans. *Aging Cell* **6**(1)**:** 87-94

Brown WT, Kieras FJ, Houck GE, Jr., Dutkowski R, Jenkins EC (1985) A comparison of adult and childhood progerias: Werner syndrome and Hutchinson-Gilford progeria syndrome. *Adv Exp Med Biol* **190:** 229-244

Butler AA, LeRoith D (2001) Minireview: tissue-specific versus generalized gene targeting of the igf1 and igf1r genes and their roles in insulin-like growth factor physiology. *Endocrinology* **142**(5)**:** 1685-1688

Byerly L, Cassada RC, Russell RL (1976) The life cycle of the nematode Caenorhabditis elegans. I. Wild-type growth and reproduction. *Dev Biol* **51**(1)**:** 23-33

Calabrese EJ, Baldwin LA (1999) Chemical hormesis: its historical foundations as a biological hypothesis. *Toxicol Pathol* **27**(2)**:** 195-216

Calabrese EJ, Baldwin LA, Holland CD (1999) Hormesis: a highly generalizable and reproducible phenomenon with important implications for risk assessment. *Risk Anal* **19**(2)**:** 261-281

Calabreseci EJ (1999) Evidence that hormesis represents an "overcompensation" response to a disruption in homeostasis. *Ecotoxicol Environ Saf* **42**(2)**:** 135-137

Campisi J (1996) Replicative senescence: an old lives' tale? *Cell* **84**(4)**:** 497-500

Campisi J (2005) Senescent cells, tumor suppression, and organismal aging: good citizens, bad neighbors. *Cell* **120**(4)**:** 513-522

Campisi J, Dimri GP, Nehlin JO, Testori A, Yoshimoto K (1996) Coming of age in culture. *Exp Gerontol* **31**(1-2)**:** 7-12

Cao H, Hegele RA (2003) LMNA is mutated in Hutchinson-Gilford progeria (MIM 176670) but not in Wiedemann-Rautenstrauch progeroid syndrome (MIM 264090). *J Hum Genet* **48**(5)**:** 271-274

Cargill SL, Carey JR, Muller HG, Anderson G (2003) Age of ovary determines remaining life expectancy in old ovariectomized mice. *Aging Cell* **2**(3)**:** 185-190

Chang S (2005) A mouse model of Werner Syndrome: what can it tell us about aging and cancer? *Int J Biochem Cell Biol* **37**(5)**:** 991-999

Chang S, Multani AS, Cabrera NG, Naylor ML, Laud P, Lombard D, Pathak S, Guarente L, DePinho RA (2004) Essential role of limiting telomeres in the pathogenesis of Werner syndrome. *Nat Genet* **36**(8)**:** 877-882

Chen D, Thomas EL, Kapahi P (2009) HIF-1 modulates dietary restriction-mediated lifespan extension via IRE-1 in Caenorhabditis elegans. *PLoS Genet* **5**(5)**:** e1000486

Chen Q, Fischer A, Reagan JD, Yan LJ, Ames BN (1995) Oxidative DNA damage and senescence of human diploid fibroblast cells. *Proc Natl Acad Sci U S A* **92**(10)**:** 4337-4341

Cheng WH, Muftuoglu M, Bohr VA (2007) Werner syndrome protein: functions in the response to DNA damage and replication stress in S-phase. *Exp Gerontol* **42**(9)**:** 871-878

Cheng WH, von Kobbe C, Opresko PL, Arthur LM, Komatsu K, Seidman MM, Carney JP, Bohr VA (2004) Linkage between Werner syndrome protein and the Mre11 complex via Nbs1. *J Biol Chem* **279**(20)**:** 21169-21176

Chi SW, Ayed A, Arrowsmith CH (1999) Solution structure of a conserved C-terminal domain of p73 with structural homology to the SAM domain. *EMBO J* **18**(16)**:** 4438-4445

Chu WK, Hickson ID (2009) RecQ helicases: multifunctional genome caretakers. *Nat Rev Cancer* **9**(9)**:** 644-654

Clancy DJ, Gems D, Harshman LG, Oldham S, Stocker H, Hafen E, Leevers SJ, Partridge L (2001) Extension of life-span by loss of CHICO, a Drosophila insulin receptor substrate protein. *Science* **292**(5514)**:** 104-106

Collado M, Blasco MA, Serrano M (2007) Cellular senescence in cancer and aging. *Cell* **130**(2)**:** 223-233

Collins J, Saari B, Anderson P (1987) Activation of a transposable element in the germ line but not the soma of Caenorhabditis elegans. *Nature* **328**(6132)**:** 726-728

Colman RJ, Anderson RM, Johnson SC, Kastman EK, Kosmatka KJ, Beasley TM, Allison DB, Cruzen C, Simmons HA, Kemnitz JW, Weindruch R (2009) Caloric restriction delays disease onset and mortality in rhesus monkeys. *Science* **325**(5937)**:** 201-204

Copeland JM, Cho J, Lo T, Jr., Hur JH, Bahadorani S, Arabyan T, Rabie J, Soh J, Walker DW (2009) Extension of Drosophila life span by RNAi of the mitochondrial respiratory chain. *Curr Biol* **19**(19)**:** 1591-1598

Coppede F, Migliore L (2010) DNA repair in premature aging disorders and neurodegeneration. *Curr Aging Sci* **3**(1)**:** 3-19

Corcoran CA, Huang Y, Sheikh MS (2006) The regulation of energy generating metabolic pathways by p53. *Cancer Biol Ther* **5**(12)**:** 1610-1613

Cox LS (2009) Live fast, die young: new lessons in mammalian longevity. *Rejuvenation Res* **12**(4)**:** 283-288

Cox LS, Clancy DJ, Boubriak I, Saunders RD (2007) Modeling Werner Syndrome in Drosophila melanogaster: hyper-recombination in flies lacking WRN-like exonuclease. *Ann N Y Acad Sci* **1119:** 274-288

Cox LS, Faragher RG (2007) From old organisms to new molecules: integrative biology and therapeutic targets in accelerated human ageing. *Cell Mol Life Sci* **64**(19-20)**:** 2620-2641

Cox LS, Mattison JA (2009) Increasing longevity through caloric restriction or rapamycin feeding in mammals: common mechanisms for common outcomes? *Aging Cell* **8**(5)**:** 607-613

Crabbe L, Jauch A, Naeger CM, Holtgreve-Grez H, Karlseder J (2007) Telomere dysfunction as a cause of genomic instability in Werner syndrome. *Proc Natl Acad Sci U S A* **104**(7)**:** 2205-2210

Crabbe L, Verdun RE, Haggblom CI, Karlseder J (2004) Defective telomere lagging strand synthesis in cells lacking WRN helicase activity. *Science* **306**(5703)**:** 1951-1953

Craig AL, Moser SC, Bailly AP, Gartner A (2012) Methods for studying the DNA damage response in the Caenorhabdatis elegans germ line. *Methods Cell Biol* **107:** 321-352

Culmsee C, Zhu X, Yu QS, Chan SL, Camandola S, Guo Z, Greig NH, Mattson MP (2001) A synthetic inhibitor of p53 protects neurons against death induced by ischemic and excitotoxic insults, and amyloid beta-peptide. *J Neurochem* **77**(1)**:** 220-228

Cypser JR, Johnson TE (2002) Multiple stressors in Caenorhabditis elegans induce stress hormesis and extended longevity. *J Gerontol A Biol Sci Med Sci* **57**(3)**:** B109-114

Cypser JR, Johnson TE (2003) Hormesis in Caenorhabditis elegans dauer-defective mutants. *Biogerontology* **4**(4)**:** 203-214

Cypser JR, Tedesco P, Johnson TE (2006) Hormesis and aging in Caenorhabditis elegans. *Exp Gerontol* **41**(10)**:** 935-939

Dallaire A, Garand C, Paquel ER, Mitchell SJ, de Cabo R, Simard MJ, Lebel M (2012) Down regulation of miR-124 in both Werner syndrome DNA helicase mutant mice and mutant Caenorhabditis elegans wrn-1 reveals the importance of this microRNA in accelerated aging. *Aging (Albany NY)* **4**(9)**:** 636-647

Damerla RR, Knickelbein KE, Strutt S, Liu FJ, Wang H, Opresko PL (2012) Werner syndrome protein suppresses the formation of large deletions during the replication of human telomeric sequences. *Cell Cycle* **11**(16)**:** 3036-3044

Davis T, Haughton MF, Jones CJ, Kipling D (2006) Prevention of accelerated cell aging in the Werner syndrome. *Ann N Y Acad Sci* **1067:** 243-247

Davis T, Singhrao SK, Wyllie FS, Haughton MF, Smith PJ, Wiltshire M, Wynford-Thomas D, Jones CJ, Faragher RG, Kipling D (2003) Telomere-based proliferative lifespan barriers in Werner-syndrome fibroblasts involve both p53-dependent and p53-independent mechanisms. *J Cell Sci* **116**(Pt 7)**:** 1349-1357

Dell'agnello C, Leo S, Agostino A, Szabadkai G, Tiveron C, Zulian A, Prelle A, Roubertoux P, Rizzuto R, Zeviani M (2007) Increased longevity and refractoriness to Ca(2+)-dependent neurodegeneration in Surf1 knockout mice. *Hum Mol Genet* **16**(4)**:** 431-444

Derry WB, Bierings R, van Iersel M, Satkunendran T, Reinke V, Rothman JH (2007) Regulation of developmental rate and germ cell proliferation in Caenorhabditis elegans by the p53 gene network. *Cell Death Differ* **14**(4)**:** 662-670

Derry WB, Putzke AP, Rothman JH (2001) Caenorhabditis elegans p53: role in apoptosis, meiosis, and stress resistance. *Science* **294**(5542)**:** 591-595

Dhillon KK, Sidorova J, Saintigny Y, Poot M, Gollahon K, Rabinovitch PS, Monnat RJ, Jr. (2007) Functional role of the Werner syndrome RecQ helicase in human fibroblasts. *Aging Cell* **6**(1)**:** 53-61

Di Leonardo A, Linke SP, Clarkin K, Wahl GM (1994) DNA damage triggers a prolonged p53-dependent G1 arrest and long-term induction of Cip1 in normal human fibroblasts. *Genes Dev* **8**(21)**:** 2540-2551

Dillin A, Hsu AL, Arantes-Oliveira N, Lehrer-Graiwer J, Hsin H, Fraser AG, Kamath RS, Ahringer J, Kenyon C (2002) Rates of behavior and aging specified by mitochondrial function during development. *Science* **298**(5602)**:** 2398-2401

Dimri GP, Itahana K, Acosta M, Campisi J (2000) Regulation of a senescence checkpoint response by the E2F1 transcription factor and p14(ARF) tumor suppressor. *Mol Cell Biol* **20**(1)**:** 273-285

Dimri GP, Lee X, Basile G, Acosta M, Scott G, Roskelley C, Medrano EE, Linskens M, Rubelj I, Pereira-Smith O, et al. (1995) A biomarker that identifies senescent human cells in culture and in aging skin in vivo. *Proc Natl Acad Sci U S A* **92**(20)**:** 9363-9367

Donehower LA, Harvey M, Slagle BL, McArthur MJ, Montgomery CA, Jr., Butel JS, Bradley A (1992) Mice deficient for p53 are developmentally normal but susceptible to spontaneous tumours. *Nature* **356**(6366)**:** 215-221

Doonan R, McElwee JJ, Matthijssens F, Walker GA, Houthoofd K, Back P, Matscheski A, Vanfleteren JR, Gems D (2008) Against the oxidative damage theory of aging: superoxide dismutases protect against oxidative stress but have little or no effect on life span in Caenorhabditis elegans. *Genes Dev* **22**(23)**:** 3236-3241

Dorman JB, Albinder B, Shroyer T, Kenyon C (1995) The age-1 and daf-2 genes function in a common pathway to control the lifespan of Caenorhabditis elegans. *Genetics* **141**(4)**:** 1399-1406

Dotsch V, Bernassola F, Coutandin D, Candi E, Melino G (2010) p63 and p73, the ancestors of p53. *Cold Spring Harb Perspect Biol* **2**(9)**:** a004887

Du X, Shen J, Kugan N, Furth EE, Lombard DB, Cheung C, Pak S, Luo G, Pignolo RJ, DePinho RA, Guarente L, Johnson FB (2004) Telomere shortening exposes functions for the mouse Werner and Bloom syndrome genes. *Mol Cell Biol* **24**(19)**:** 8437-8446

Durieux J, Wolff S, Dillin A (2011) The cell-non-autonomous nature of electron transport chain-mediated longevity. *Cell* **144**(1)**:** 79-91

Epstein CJ, Martin GM, Schultz AL, Motulsky AG (1966) Werner's syndrome a review of its symptomatology, natural history, pathologic features, genetics and relationship to the natural aging process. *Medicine (Baltimore)* **45**(3)**:** 177-221

Epstein J, Himmelhoch S, Gershon D (1972) Studies on aging in nematodes. *Mechanisms of Ageing and Development*

Eriksson M, Brown WT, Gordon LB, Glynn MW, Singer J, Scott L, Erdos MR, Robbins CM, Moses TY, Berglund P, Dutra A, Pak E, Durkin S, Csoka AB, Boehnke M, Glover TW, Collins FS (2003) Recurrent de novo point mutations in lamin A cause Hutchinson-Gilford progeria syndrome. *Nature* **423**(6937)**:** 293-298

Ermolaeva MA, Segref A, Dakhovnik A, Ou HL, Schneider JI, Utermohlen O, Hoppe T, Schumacher B (2013) DNA damage in germ cells induces an innate immune response that triggers systemic stress resistance. *Nature* **501**(7467)**:** 416-420

Evans RJ, Wyllie FS, Wynford-Thomas D, Kipling D, Jones CJ (2003) A P53-dependent, telomere-independent proliferative life span barrier in human astrocytes consistent with the molecular genetics of glioma development. *Cancer Res* **63**(16)**:** 4854-4861

Feldman N, Kosolapov L, Ben-Zvi A (2014) Fluorodeoxyuridine improves Caenorhabditis elegans proteostasis independent of reproduction onset. *PLoS One* **9**(1)**:** e85964

Feng J, Bussiere F, Hekimi S (2001) Mitochondrial electron transport is a key determinant of life span in Caenorhabditis elegans. *Dev Cell* **1**(5)**:** 633-644

Ferbeyre G, de Stanchina E, Querido E, Baptiste N, Prives C, Lowe SW (2000) PML is induced by oncogenic ras and promotes premature senescence. *Genes Dev* **14**(16)**:** 2015-2027

Fire AZ (2007) Gene silencing by double-stranded RNA. *Cell Death Differ* **14**(12)**:** 1998-2012

Flores ER, Tsai KY, Crowley D, Sengupta S, Yang A, McKeon F, Jacks T (2002) p63 and p73 are required for p53-dependent apoptosis in response to DNA damage. *Nature* **416**(6880)**:** 560-564

Fontana L, Partridge L, Longo VD (2010) Extending healthy life span--from yeast to humans. *Science* **328**(5976)**:** 321-326

Francis R, Barton MK, Kimble J, Schedl T (1995a) gld-1, a tumor suppressor gene required for oocyte development in Caenorhabditis elegans. *Genetics* **139**(2)**:** 579-606

Francis R, Maine E, Schedl T (1995b) Analysis of the multiple roles of gld-1 in germline development: interactions with the sex determination cascade and the glp-1 signaling pathway. *Genetics* **139**(2)**:** 607-630

Friedman DB, Johnson TE (1988a) A mutation in the age-1 gene in Caenorhabditis elegans lengthens life and reduces hermaphrodite fertility. *Genetics* **118**(1)**:** 75-86

Friedman DB, Johnson TE (1988b) Three mutants that extend both mean and maximum life span of the nematode, Caenorhabditis elegans, define the age-1 gene. *J Gerontol* **43**(4)**:** B102-109

Fries JF (1992) Strategies for reduction of morbidity. *Am J Clin Nutr* **55**(6 Suppl)**:** 1257S-1262S

Fries JF (2005) The compression of morbidity. *Milbank Q* **83**(4)**:** 801-823

Fukuchi K, Martin GM, Monnat RJ, Jr. (1989) Mutator phenotype of Werner syndrome is characterized by extensive deletions. *Proc Natl Acad Sci U S A* **86**(15)**:** 5893-5897

Gabel CV, Antoine F, Chuang CF, Samuel AD, Chang C (2008) Distinct cellular and molecular mechanisms mediate initial axon development and adult-stage axon regeneration in C. elegans. *Development* **135**(6)**:** 1129-1136

Gandhi S, Santelli J, Mitchell DH, Stiles JW, Sanadi DR (1980) A simple method for maintaining large, aging populations of Caenorhabditis elegans. *Mech Ageing Dev* **12**(2)**:** 137-150

Garcia-Cao I, Garcia-Cao M, Martin-Caballero J, Criado LM, Klatt P, Flores JM, Weill JC, Blasco MA, Serrano M (2002) "Super p53" mice exhibit enhanced DNA damage response, are tumor resistant and age normally. *EMBO J* **21**(22)**:** 6225-6235

Garigan D, Hsu AL, Fraser AG, Kamath RS, Ahringer J, Kenyon C (2002) Genetic analysis of tissue aging in Caenorhabditis elegans: a role for heat-shock factor and bacterial proliferation. *Genetics* **161**(3)**:** 1101-1112

Garinis GA, van der Horst GT, Vijg J, Hoeijmakers JH (2008) DNA damage and ageing: new-age ideas for an age-old problem. *Nat Cell Biol* **10**(11)**:** 1241-1247

Garsin DA, Villanueva JM, Begun J, Kim DH, Sifri CD, Calderwood SB, Ruvkun G, Ausubel FM (2003) Long-lived C. elegans daf-2 mutants are resistant to bacterial pathogens. *Science* **300**(5627)**:** 1921

Gartner A, Boag PR, Blackwell TK (2008) Germline survival and apoptosis. *WormBook***:** 1-20

Gartner A, MacQueen AJ, Villeneuve AM (2004) Methods for analyzing checkpoint responses in Caenorhabditis elegans. *Methods Mol Biol* **280:** 257-274

Gartner A, Milstein S, Ahmed S, Hodgkin J, Hengartner MO (2000) A conserved checkpoint pathway mediates DNA damage--induced apoptosis and cell cycle arrest in C. elegans. *Mol Cell* **5**(3)**:** 435-443

Gems D, Partridge L (2001) Insulin/IGF signalling and ageing: seeing the bigger picture. *Curr Opin Genet Dev* **11**(3)**:** 287-292

Gems D, Partridge L (2008) Stress-response hormesis and aging: "that which does not kill us makes us stronger". *Cell Metab* **7**(3)**:** 200-203

Gems D, Partridge L (2013) Genetics of longevity in model organisms: debates and paradigm shifts. *Annu Rev Physiol* **75:** 621-644

Ghosh S, Zhou Z (2014) Genetics of aging, progeria and lamin disorders. *Curr Opin Genet Dev* **26C:** 41-46

Glazov E, Phillips K, Budziszewski GJ, Schob H, Meins F, Jr., Levin JZ (2003) A gene encoding an RNase D exonuclease-like protein is required for post-transcriptional silencing in Arabidopsis. *Plant J* **35**(3)**:** 342-349

Golden TR, Melov S (2004) Microarray analysis of gene expression with age in individual nematodes. *Aging Cell* **3**(3)**:** 111-124

Gomes NM, Ryder OA, Houck ML, Charter SJ, Walker W, Forsyth NR, Austad SN, Venditti C, Pagel M, Shay JW, Wright WE (2011) Comparative biology of mammalian telomeres: hypotheses on ancestral states and the roles of telomeres in longevity determination. *Aging Cell* **10**(5)**:** 761-768

Goto M (1997) Hierarchical deterioration of body systems in Werner's syndrome: implications for normal ageing. *Mech Ageing Dev* **98**(3)**:** 239-254

Goto M, Miller R (2001) From Premature Gray Hair to Helicase - Werner Syndrome: Implications for Aging and Cancer. *Tokyo, Japan Scientific Societies Press*

Goto M, Miller RW, Ishikawa Y, Sugano H (1996) Excess of rare cancers in Werner syndrome (adult progeria). *Cancer Epidemiol Biomarkers Prev* **5**(4)**:** 239-246

Goudeau J, Aguilaniu H (2010) Carbonylated proteins are eliminated during reproduction in C. elegans. *Aging Cell* **9**(6)**:** 991-1003

Grabowski MM, Svrzikapa N, Tissenbaum HA (2005) Bloom syndrome ortholog HIM-6 maintains genomic stability in C. elegans. *Mech Ageing Dev* **126**(12)**:** 1314-1321

Gravato-Nobre MJ, Nicholas HR, Nijland R, O'Rourke D, Whittington DE, Yook KJ, Hodgkin J (2005) Multiple genes affect sensitivity of Caenorhabditis elegans to the bacterial pathogen Microbacterium nematophilum. *Genetics* **171**(3)**:** 1033-1045

Gray MD, Shen JC, Kamath-Loeb AS, Blank A, Sopher BL, Martin GM, Oshima J, Loeb LA (1997) The Werner syndrome protein is a DNA helicase. *Nat Genet* **17**(1)**:** 100-103

Gray MD, Wang L, Youssoufian H, Martin GM, Oshima J (1998) Werner helicase is localized to transcriptionally active nucleoli of cycling cells. *Exp Cell Res* **242**(2)**:** 487-494

Greer EL, Brunet A (2009) Different dietary restriction regimens extend lifespan by both independent and overlapping genetic pathways in C. elegans. *Aging Cell* **8**(2)**:** 113-127

Greiss S, Schumacher B, Grandien K, Rothblatt J, Gartner A (2008) Transcriptional profiling in C. elegans suggests DNA damage dependent apoptosis as an ancient function of the p53 family. *BMC Genomics* **9:** 334

Guarente L, Kenyon C (2000) Genetic pathways that regulate ageing in model organisms. *Nature* **408**(6809)**:** 255-262

Gumienny TL, Lambie E, Hartwieg E, Horvitz HR, Hengartner MO (1999) Genetic control of programmed cell death in the Caenorhabditis elegans hermaphrodite germline. *Development* **126**(5)**:** 1011-1022

Hamilton B, Dong Y, Shindo M, Liu W, Odell I, Ruvkun G, Lee SS (2005) A systematic RNAi screen for longevity genes in C. elegans. *Genes Dev* **19**(13)**:** 1544-1555

Hammarlund M, Nix P, Hauth L, Jorgensen EM, Bastiani M (2009) Axon regeneration requires a conserved MAP kinase pathway. *Science* **323**(5915)**:** 802-806

Hansen M, Taubert S, Crawford D, Libina N, Lee SJ, Kenyon C (2007) Lifespan extension by conditions that inhibit translation in Caenorhabditis elegans. *Aging Cell* **6**(1)**:** 95-110

Hardie DG (2007) AMP-activated/SNF1 protein kinases: conserved guardians of cellular energy. *Nat Rev Mol Cell Biol* **8**(10)**:** 774-785

Harley CB, Futcher AB, Greider CW (1990) Telomeres shorten during ageing of human fibroblasts. *Nature* **345**(6274)**:** 458-460

Harrigan JA, Wilson DM, 3rd, Prasad R, Opresko PL, Beck G, May A, Wilson SH, Bohr VA (2006) The Werner syndrome protein operates in base excision repair and cooperates with DNA polymerase beta. *Nucleic Acids Res* **34**(2)**:** 745-754

Harrison DE, Strong R, Sharp ZD, Nelson JF, Astle CM, Flurkey K, Nadon NL, Wilkinson JE, Frenkel K, Carter CS, Pahor M, Javors MA, Fernandez E, Miller RA (2009) Rapamycin fed late in life extends lifespan in genetically heterogeneous mice. *Nature* **460**(7253)**:** 392-395

Hartung F, Plchova H, Puchta H (2000) Molecular characterisation of RecQ homologues in Arabidopsis thaliana. *Nucleic Acids Res* **28**(21)**:** 4275-4282

Hayflick L (1965) The Limited in Vitro Lifetime of Human Diploid Cell Strains. *Exp Cell Res* **37:** 614-636

Hayflick L, Moorhead PS (1961) The serial cultivation of human diploid cell strains. *Exp Cell Res* **25:** 585-621

Heidler T, Hartwig K, Daniel H, Wenzel U (2009) Caenorhabditis elegans lifespan extension caused by treatment with an orally active ROS-generator is dependent on DAF-16 and SIR-2.1. *Biogerontology* **11**(2)**:** 183-195

Heitman J, Movva NR, Hall MN (1991) Targets for cell cycle arrest by the immunosuppressant rapamycin in yeast. *Science* **253**(5022)**:** 905-909

Hekimi S, Burgess J, Bussiere F, Meng Y, Benard C (2001) Genetics of lifespan in C. elegans: molecular diversity, physiological complexity, mechanistic simplicity. *Trends Genet* **17**(12)**:** 712-718

Henderson ST, Johnson TE (2001) daf-16 integrates developmental and environmental inputs to mediate aging in the nematode Caenorhabditis elegans. *Curr Biol* **11**(24)**:** 1975-1980

Herbig U, Jobling WA, Chen BP, Chen DJ, Sedivy JM (2004) Telomere shortening triggers senescence of human cells through a pathway involving ATM, p53, and p21(CIP1), but not p16(INK4a). *Mol Cell* **14**(4)**:** 501-513

Hercus MJ, Loeschcke V, Rattan SI (2003) Lifespan extension of Drosophila melanogaster through hormesis by repeated mild heat stress. *Biogerontology* **4**(3)**:** 149-156

Herndon LA, Schmeissner PJ, Dudaronek JM, Brown PA, Listner KM, Sakano Y, Paupard MC, Hall DH, Driscoll M (2002) Stochastic and genetic factors influence tissue-specific decline in ageing C. elegans. *Nature* **419**(6909)**:** 808-814

Hertweck M, Gobel C, Baumeister R (2004) C. elegans SGK-1 is the critical component in the Akt/PKB kinase complex to control stress response and life span. *Dev Cell* **6**(4)**:** 577-588

Hickson ID (2003) RecQ helicases: caretakers of the genome. *Nat Rev Cancer* **3**(3)**:** 169-178

Hietakangas V, Cohen SM (2009) Regulation of tissue growth through nutrient sensing. *Annu Rev Genet* **43:** 389-410

Hill AA, Hunter CP, Tsung BT, Tucker-Kellogg G, Brown EL (2000) Genomic analysis of gene expression in C. elegans. *Science* **290**(5492)**:** 809-812

Hoffman S, Martin D, Melendez A, Bargonetti J (2014) C. elegans CEP-1/p53 and BEC-1 are involved in DNA repair. *PLoS One* **9**(2)**:** e88828

Hollstein M, Hergenhahn M, Yang Q, Bartsch H, Wang ZQ, Hainaut P (1999) New approaches to understanding p53 gene tumor mutation spectra. *Mutat Res* **431**(2)**:** 199-209

Holzenberger M, Dupont J, Ducos B, Leneuve P, Geloen A, Even PC, Cervera P, Le Bouc Y (2003) IGF-1 receptor regulates lifespan and resistance to oxidative stress in mice. *Nature* **421**(6919)**:** 182-187

Honda Y, Honda S (1999) The daf-2 gene network for longevity regulates oxidative stress resistance and Mn-superoxide dismutase gene expression in Caenorhabditis elegans. *FASEB J* **13**(11)**:** 1385-1393

Hosokawa H, Ishii N, Ishida H, Ichimori K, Nakazawa H, Suzuki K (1994) Rapid accumulation of fluorescent material with aging in an oxygen-sensitive mutant mev-1 of Caenorhabditis elegans. *Mech Ageing Dev* **74**(3)**:** 161-170

Hosono R, Mitsui Y, Sato Y, Aizawa S, Miwa J (1982) Life span of the wild and mutant nematode Caenorhabditis elegans. Effects of sex, sterilization, and temperature. *Exp Gerontol* **17**(2)**:** 163-172

Houthoofd K, Braeckman BP, Lenaerts I, Brys K, De Vreese A, Van Eygen S, Vanfleteren JR (2002) Axenic growth up-regulates mass-specific metabolic rate, stress resistance, and extends life span in Caenorhabditis elegans. *Exp Gerontol* **37**(12)**:** 1371-1378

Houtkooper RH, Canto C, Wanders RJ, Auwerx J (2010a) The secret life of NAD+: an old metabolite controlling new metabolic signaling pathways. *Endocr Rev* **31**(2)**:** 194-223

Houtkooper RH, Williams RW, Auwerx J (2010b) Metabolic networks of longevity. *Cell* **142**(1)**:** 9-14

Hsin H, Kenyon C (1999) Signals from the reproductive system regulate the lifespan of C. elegans. *Nature* **399**(6734)**:** 362-366

Hsu AL, Murphy CT, Kenyon C (2003) Regulation of aging and age-related disease by DAF-16 and heat-shock factor. *Science* **300**(5622)**:** 1142-1145

Hu PJ, Xu J, Ruvkun G (2006) Two membrane-associated tyrosine phosphatase homologs potentiate C. elegans AKT-1/PKB signaling. *PLoS Genet* **2**(7)**:** e99

Huang S, Li B, Gray MD, Oshima J, Mian IS, Campisi J (1998) The premature ageing syndrome protein, WRN, is a 3'-->5' exonuclease. *Nat Genet* **20**(2)**:** 114-116

Huyen Y, Jeffrey PD, Derry WB, Rothman JH, Pavletich NP, Stavridi ES, Halazonetis TD (2004) Structural differences in the DNA binding domains of human p53 and its C. elegans ortholog Cep-1. *Structure* **12**(7)**:** 1237-1243

Hyun M, Bohr VA, Ahn B (2008a) Biochemical characterization of the WRN-1 RecQ helicase of Caenorhabditis elegans. *Biochemistry* **47**(28)**:** 7583-7593

Hyun M, Lee J, Lee K, May A, Bohr VA, Ahn B (2008b) Longevity and resistance to stress correlate with DNA repair capacity in Caenorhabditis elegans. *Nucleic Acids Res* **36**(4)**:** 1380-1389

Hyun M, Park S, Kim E, Kim DH, Lee SJ, Koo HS, Seo YS, Ahn B (2012) Physical and functional interactions of Caenorhabditis elegans WRN-1 helicase with RPA-1. *Biochemistry* **51**(7)**:** 1336-1345

Ishikawa N, Nakamura K, Izumiyama-Shimomura N, Aida J, Ishii A, Goto M, Ishikawa Y, Asaka R, Matsuura M, Hatamochi A, Kuroiwa M, Takubo K (2011) Accelerated in vivo epidermal telomere loss in Werner syndrome. *Aging (Albany NY)* **3**(4)**:** 417-429

Jakobsen H, Bojer MS, Marinus MG, Xu T, Struve C, Krogfelt KA, Lobner-Olesen A (2013) The alkaloid compound harmane increases the lifespan of Caenorhabditis elegans during bacterial infection, by modulating the nematode's innate immune response. *PLoS One* **8**(3)**:** e60519

Jia K, Chen D, Riddle DL (2004) The TOR pathway interacts with the insulin signaling pathway to regulate C. elegans larval development, metabolism and life span. *Development* **131**(16)**:** 3897-3906

Johnson SC, Rabinovitch PS, Kaeberlein M (2013) mTOR is a key modulator of ageing and age-related disease. *Nature* **493**(7432)**:** 338-345

Johnson TE, Cypser J, de Castro E, de Castro S, Henderson S, Murakami S, Rikke B, Tedesco P, Link C (2000) Gerontogenes mediate health and longevity in nematodes through increasing resistance to environmental toxins and stressors. *Exp Gerontol* **35**(6-7)**:** 687-694

Johnson TE, Henderson S, Murakami S, de Castro E, de Castro SH, Cypser J, Rikke B, Tedesco P, Link C (2002) Longevity genes in the nematode Caenorhabditis elegans also mediate increased resistance to stress and prevent disease. *J Inherit Metab Dis* **25**(3)**:** 197-206

Jolliffe AK, Derry WB (2013) The TP53 signaling network in mammals and worms. *Brief Funct Genomics* **12**(2)**:** 129-141

Jost CA, Marin MC, Kaelin WG, Jr. (1997) p73 is a simian [correction of human] p53-related protein that can induce apoptosis. *Nature* **389**(6647)**:** 191-194

Kaeberlein M, Kapahi P (2009) The hypoxic response and aging. *Cell Cycle* **8**(15)**:** 2324

Kaeberlein M, Powers RW, 3rd, Steffen KK, Westman EA, Hu D, Dang N, Kerr EO, Kirkland KT, Fields S, Kennedy BK (2005) Regulation of yeast replicative life span by TOR and Sch9 in response to nutrients. *Science* **310**(5751)**:** 1193-1196

Kaghad M, Bonnet H, Yang A, Creancier L, Biscan JC, Valent A, Minty A, Chalon P, Lelias JM, Dumont X, Ferrara P, McKeon F, Caput D (1997) Monoallelically expressed gene related to p53 at 1p36, a region frequently deleted in neuroblastoma and other human cancers. *Cell* **90**(4)**:** 809-819

Kaletsky R, Murphy CT (2010) The role of insulin/IGF-like signaling in C. elegans longevity and aging. *Dis Model Mech* **3**(7-8)**:** 415-419

Kamath-Loeb AS, Welcsh P, Waite M, Adman ET, Loeb LA (2004) The enzymatic activities of the Werner syndrome protein are disabled by the amino acid polymorphism R834C. *J Biol Chem* **279**(53)**:** 55499-55505

Kamath RS, Ahringer J (2003) Genome-wide RNAi screening in Caenorhabditis elegans. *Methods (San Diego, Calif* **30**(4)**:** 313-321

Kapahi P, Zid BM, Harper T, Koslover D, Sapin V, Benzer S (2004) Regulation of lifespan in Drosophila by modulation of genes in the TOR signaling pathway. *Curr Biol* **14**(10)**:** 885-890

Kashino G, Kodama S, Nakayama Y, Suzuki K, Fukase K, Goto M, Watanabe M (2003) Relief of oxidative stress by ascorbic acid delays cellular senescence of normal human and Werner syndrome fibroblast cells. *Free Radic Biol Med* **35**(4)**:** 438-443

Kashino G, Kodama S, Suzuki K, Matsumoto T, Watanabe M (2005) Exogenous expression of exonuclease domain-deleted WRN interferes with the repair of radiation-induced DNA damages. *J Radiat Res* **46**(4)**:** 407-414

Kelly WG, Xu S, Montgomery MK, Fire A (1997) Distinct requirements for somatic and germline expression of a generally expressed Caernorhabditis elegans gene. *Genetics* **146**(1)**:** 227-238

Kennedy BK, Steffen KK, Kaeberlein M (2007) Ruminations on dietary restriction and aging. *Cell Mol Life Sci* **64**(11)**:** 1323-1328

Kenyon C (2005) The plasticity of aging: insights from long-lived mutants. *Cell* **120**(4)**:** 449-460

Kenyon C (2010a) A pathway that links reproductive status to lifespan in Caenorhabditis elegans. *Ann N Y Acad Sci* **1204:** 156-162

Kenyon C, Chang J, Gensch E, Rudner A, Tabtiang R (1993) A C. elegans mutant that lives twice as long as wild type. *Nature* **366**(6454)**:** 461-464

Kenyon CJ (2010b) The genetics of ageing. *Nature* **464**(7288)**:** 504-512

Ketting RF, Haverkamp TH, van Luenen HG, Plasterk RH (1999) Mut-7 of C. elegans, required for transposon silencing and RNA interference, is a homolog of Werner syndrome helicase and RNaseD. *Cell* **99**(2)**:** 133-141

Ketting RF, Plasterk RH (2000) A genetic link between co-suppression and RNA interference in C. elegans. *Nature* **404**(6775)**:** 296-298

Kimura KD, Tissenbaum HA, Liu Y, Ruvkun G (1997) daf-2, an insulin receptor-like gene that regulates longevity and diapause in Caenorhabditis elegans. *Science* **277**(5328)**:** 942-946

Kinzler KW, Vogelstein B (1997) Cancer-susceptibility genes. Gatekeepers and caretakers. *Nature* **386**(6627)**:** 761, 763

Kipling D, Davis T, Ostler EL, Faragher RG (2004) What can progeroid syndromes tell us about human aging? *Science* **305**(5689)**:** 1426-1431

Kipling D, Faragher RG (1997) Progeroid syndromes: probing the molecular basis of aging? *Mol Pathol* **50**(5)**:** 234-241

Kirkwood TB (1998) Biological theories of aging: an overview. *Aging (Milano)* **10**(2)**:** 144-146

Kirkwood TB (2002) Molecular gerontology. *J Inherit Metab Dis* **25**(3)**:** 189-196

Kirkwood TB (2005) Understanding the odd science of aging. *Cell* **120**(4)**:** 437-447

Kirkwood TB, Holliday R (1979) The evolution of ageing and longevity. *Proc R Soc Lond B Biol Sci* **205**(1161)**:** 531-546

Kirkwood TB, Kowald A (1997) Network theory of aging. *Exp Gerontol* **32**(4-5)**:** 395-399

Kitano K, Yoshihara N, Hakoshima T (2007) Crystal structure of the HRDC domain of human Werner syndrome protein, WRN. *J Biol Chem* **282**(4)**:** 2717-2728

Klass MR (1977) Aging in the nematode Caenorhabditis elegans: major biological and environmental factors influencing life span. *Mech Ageing Dev* **6**(6)**:** 413-429

Klass MR (1983) A method for the isolation of longevity mutants in the nematode Caenorhabditis elegans and initial results. *Mech Ageing Dev* **22**(3-4)**:** 279-286

Komarov PG, Komarova EA, Kondratov RV, Christov-Tselkov K, Coon JS, Chernov MV, Gudkov AV (1999) A chemical inhibitor of p53 that protects mice from the side effects of cancer therapy. *Science* **285**(5434)**:** 1733-1737

Kowald A, Kirkwood TB (1996) A network theory of ageing: the interactions of defective mitochondria, aberrant proteins, free radicals and scavengers in the ageing process. *Mutat Res* **316**(5-6)**:** 209-236

Kuilman T, Michaloglou C, Mooi WJ, Peeper DS (2010) The essence of senescence. *Genes Dev* **24**(22)**:** 2463-2479

Kunz J, Henriquez R, Schneider U, Deuter-Reinhard M, Movva NR, Hall MN (1993) Target of rapamycin in yeast, TOR2, is an essential phosphatidylinositol kinase homolog required for G1 progression. *Cell* **73**(3)**:** 585-596

Kyng KJ, May A, Kolvraa S, Bohr VA (2003) Gene expression profiling in Werner syndrome closely resembles that of normal aging. *Proc Natl Acad Sci U S A* **100**(21)**:** 12259-12264

Lakowski B, Hekimi S (1996) Determination of life-span in Caenorhabditis elegans by four clock genes. *Science* **272**(5264)**:** 1010-1013

Landis JN, Murphy CT (2010) Integration of diverse inputs in the regulation of Caenorhabditis elegans DAF-16/FOXO. *Dev Dyn* **239**(5)**:** 1405-1412

Lane D, Levine A (2010) p53 Research: the past thirty years and the next thirty years. *Cold Spring Harb Perspect Biol* **2**(12)**:** a000893

Lans H, Lindvall JM, Thijssen K, Karambelas AE, Cupac D, Fensgard O, Jansen G, Hoeijmakers JH, Nilsen H, Vermeulen W (2013) DNA damage leads to progressive replicative decline but extends the life span of long-lived mutant animals. *Cell Death Differ* **20**(12)**:** 1709-1718

Laplante M, Sabatini DM (2012) mTOR signaling in growth control and disease. *Cell* **149**(2)**:** 274-293

Larrieu D, Britton S, Demir M, Rodriguez R, Jackson SP (2014) Chemical inhibition of NAT10 corrects defects of laminopathic cells. *Science* **344**(6183)**:** 527-532

Larsen PL (1993) Aging and resistance to oxidative damage in Caenorhabditis elegans. *Proc Natl Acad Sci U S A* **90**(19)**:** 8905-8909

Larsen PL, Albert PS, Riddle DL (1995) Genes that regulate both development and longevity in Caenorhabditis elegans. *Genetics* **139**(4)**:** 1567-1583

Lebel M (2002) Increased frequency of DNA deletions in pink-eyed unstable mice carrying a mutation in the Werner syndrome gene homologue. *Carcinogenesis* **23**(1)**:** 213-216

Lebel M, Spillare EA, Harris CC, Leder P (1999) The Werner syndrome gene product co-purifies with the DNA replication complex and interacts with PCNA and topoisomerase I. *J Biol Chem* **274**(53)**:** 37795-37799

Lee JW, Harrigan J, Opresko PL, Bohr VA (2005) Pathways and functions of the Werner syndrome protein. *Mech Ageing Dev* **126**(1)**:** 79-86

Lee RY, Hench J, Ruvkun G (2001) Regulation of C. elegans DAF-16 and its human ortholog FKHRL1 by the daf-2 insulin-like signaling pathway. *Curr Biol* **11**(24)**:** 1950-1957

Lee SJ, Gartner A, Hyun M, Ahn B, Koo HS (2010a) The Caenorhabditis elegans Werner syndrome protein functions upstream of ATR and ATM in response to DNA replication inhibition and double-strand DNA breaks. *PLoS Genet* **6**(1)**:** e1000801

Lee SJ, Hwang AB, Kenyon C (2010b) Inhibition of respiration extends C. elegans life span via reactive oxygen species that increase HIF-1 activity. *Curr Biol* **20**(23)**:** 2131-2136

Lee SJ, Kenyon C (2009) Regulation of the longevity response to temperature by thermosensory neurons in Caenorhabditis elegans. *Curr Biol* **19**(9)**:** 715-722

Lee SJ, Murphy CT, Kenyon C (2009) Glucose shortens the life span of C. elegans by downregulating DAF-16/FOXO activity and aquaporin gene expression. *Cell Metab* **10**(5)**:** 379-391

Lee SJ, Yook JS, Han SM, Koo HS (2004) A Werner syndrome protein homolog affects C. elegans development, growth rate, life span and sensitivity to DNA damage by acting at a DNA damage checkpoint. *Development* **131**(11)**:** 2565-2575

Lee SS, Kennedy S, Tolonen AC, Ruvkun G (2003a) DAF-16 target genes that control C. elegans life-span and metabolism. *Science* **300**(5619)**:** 644-647

Lee SS, Lee RY, Fraser AG, Kamath RS, Ahringer J, Ruvkun G (2003b) A systematic RNAi screen identifies a critical role for mitochondria in C. elegans longevity. *Nat Genet* **33**(1)**:** 40-48

Leiser SF, Begun A, Kaeberlein M (2011) HIF-1 modulates longevity and healthspan in a temperature-dependent manner. *Aging Cell* **10**(2)**:** 318-326

Leiser SF, Kaeberlein M (2010) The hypoxia-inducible factor HIF-1 functions as both a positive and negative modulator of aging. *Biol Chem* **391**(10)**:** 1131-1137

Lettre G, Hengartner MO (2006) Developmental apoptosis in C. elegans: a complex CEDnario. *Nat Rev Mol Cell Biol* **7**(2)**:** 97-108

Levine AJ (1997) p53, the cellular gatekeeper for growth and division. *Cell* **88**(3)**:** 323-331

Levine AJ, Tomasini R, McKeon FD, Mak TW, Melino G (2011) The p53 family: guardians of maternal reproduction. *Nat Rev Mol Cell Biol* **12**(4)**:** 259-265

Levy MZ, Allsopp RC, Futcher AB, Greider CW, Harley CB (1992) Telomere end-replication problem and cell aging. *J Mol Biol* **225**(4)**:** 951-960

Li B, Iglesias-Pedraz JM, Chen LY, Yin F, Cadenas E, Reddy S, Comai L (2014) Downregulation of the Werner syndrome protein induces a metabolic shift that compromises redox homeostasis and limits proliferation of cancer cells. *Aging Cell* **13**(2)**:** 367-378

Li W, Kennedy SG, Ruvkun G (2003) daf-28 encodes a C. elegans insulin superfamily member that is regulated by environmental cues and acts in the DAF-2 signaling pathway. *Genes Dev* **17**(7)**:** 844-858

Libina N, Berman JR, Kenyon C (2003) Tissue-specific activities of C. elegans DAF-16 in the regulation of lifespan. *Cell* **115**(4)**:** 489-502

Lin AW, Barradas M, Stone JC, van Aelst L, Serrano M, Lowe SW (1998) Premature senescence involving p53 and p16 is activated in response to constitutive MEK/MAPK mitogenic signaling. *Genes Dev* **12**(19)**:** 3008-3019

Lin K, Dorman JB, Rodan A, Kenyon C (1997) daf-16: An HNF-3/forkhead family member that can function to double the life-span of Caenorhabditis elegans. *Science* **278**(5341)**:** 1319-1322

Lin K, Hsin H, Libina N, Kenyon C (2001) Regulation of the Caenorhabditis elegans longevity protein DAF-16 by insulin/IGF-1 and germline signaling. *Nat Genet* **28**(2)**:** 139-145

Linskens MH, Feng J, Andrews WH, Enlow BE, Saati SM, Tonkin LA, Funk WD, Villeponteau B (1995) Cataloging altered gene expression in young and senescent cells using enhanced differential display. *Nucleic Acids Res* **23**(16)**:** 3244-3251

Lithgow GJ (2000) Stress response and aging in Caenorhabditis elegans. *Results Probl Cell Differ* **29:** 131-148

Lithgow GJ, Walker GA (2002) Stress resistance as a determinate of C. elegans lifespan. *Mech Ageing Dev* **123**(7)**:** 765-771

Lithgow GJ, White TM, Melov S, Johnson TE (1995) Thermotolerance and extended life-span conferred by single-gene mutations and induced by thermal stress. *Proc Natl Acad Sci U S A* **92**(16)**:** 7540-7544

Liu D, Ou L, Clemenson GD, Jr., Chao C, Lutske ME, Zambetti GP, Gage FH, Xu Y (2010) Puma is required for p53-induced depletion of adult stem cells. *Nat Cell Biol* **12**(10)**:** 993-998

Lombard DB, Beard C, Johnson B, Marciniak RA, Dausman J, Bronson R, Buhlmann JE, Lipman R, Curry R, Sharpe A, Jaenisch R, Guarente L (2000) Mutations in the WRN gene in mice accelerate mortality in a p53-null background. *Mol Cell Biol* **20**(9)**:** 3286-3291

Lopez-Otin C, Blasco MA, Partridge L, Serrano M, Kroemer G (2013) The hallmarks of aging. *Cell* **153**(6)**:** 1194-1217

Lowe J, Sheerin A, Jennert-Burston K, Burton D, Ostler EL, Bird J, Green MH, Faragher RG (2004) Camptothecin sensitivity in Werner syndrome fibroblasts as assessed by the COMET technique. *Ann N Y Acad Sci* **1019:** 256-259

Lu WJ, Abrams JM (2006) Lessons from p53 in non-mammalian models. *Cell Death Differ* **13**(6)**:** 909-912

Lund J, Tedesco P, Duke K, Wang J, Kim SK, Johnson TE (2002) Transcriptional profile of aging in C. elegans. *Curr Biol* **12**(18)**:** 1566-1573

Machwe A, Xiao L, Lloyd RG, Bolt E, Orren DK (2007) Replication fork regression in vitro by the Werner syndrome protein (WRN): holliday junction formation, the effect of leading arm structure and a potential role for WRN exonuclease activity. *Nucleic Acids Res* **35**(17)**:** 5729-5747

Madan E, Gogna R, Bhatt M, Pati U, Kuppusamy P, Mahdi AA (2012) Regulation of glucose metabolism by p53: emerging new roles for the tumor suppressor. *Oncotarget* **2**(12)**:** 948-957

Maier B, Gluba W, Bernier B, Turner T, Mohammad K, Guise T, Sutherland A, Thorner M, Scrable H (2004) Modulation of mammalian life span by the short isoform of p53. *Genes Dev* **18**(3)**:** 306-319

Maier W, Adilov B, Regenass M, Alcedo J (2010) A neuromedin U receptor acts with the sensory system to modulate food type-dependent effects on C. elegans lifespan. *PLoS Biol* **8**(5)**:** e1000376

Mair W, Morantte I, Rodrigues AP, Manning G, Montminy M, Shaw RJ, Dillin A (2011) Lifespan extension induced by AMPK and calcineurin is mediated by CRTC-1 and CREB. *Nature* **470**(7334)**:** 404-408

Mair W, Panowski SH, Shaw RJ, Dillin A (2009) Optimizing dietary restriction for genetic epistasis analysis and gene discovery in C. elegans. *PLoS One* **4**(2)**:** e4535

Marciniak RA, Lombard DB, Johnson FB, Guarente L (1998) Nucleolar localization of the Werner syndrome protein in human cells. *Proc Natl Acad Sci U S A* **95**(12)**:** 6887-6892

Marino G, Fernandez AF, Lopez-Otin C (2010) Autophagy and aging: lessons from progeria models. *Adv Exp Med Biol* **694:** 61-68

Martin GM (1982) Syndromes of accelerated aging. *Natl Cancer Inst Monogr* **60:** 241-247

Martin GM (1985) Genetics and aging; the Werner syndrome as a segmental progeroid syndrome. *Adv Exp Med Biol* **190:** 161-170

Martin GM, Oshima J (2000) Lessons from human progeroid syndromes. *Nature* **408**(6809)**:** 263-266

Martin GM, Oshima J, Gray MD, Poot M (1999) What geriatricians should know about the Werner syndrome. *J Am Geriatr Soc* **47**(9)**:** 1136-1144

Martin GM, Sprague CA, Epstein CJ (1970) Replicative life-span of cultivated human cells. Effects of donor's age, tissue, and genotype. *Lab Invest* **23**(1)**:** 86-92

Mason JB, Cargill SL, Anderson GB, Carey JR (2009) Transplantation of young ovaries to old mice increased life span in transplant recipients. *J Gerontol A Biol Sci Med Sci* **64**(12)**:** 1207-1211

Masoro EJ (2005) Overview of caloric restriction and ageing. *Mech Ageing Dev* **126**(9)**:** 913-922

Masse I, Molin L, Mouchiroud L, Vanhems P, Palladino F, Billaud M, Solari F (2008) A novel role for the SMG-1 kinase in lifespan and oxidative stress resistance in Caenorhabditis elegans. *PLoS One* **3**(10)**:** e3354

Massip L, Garand C, Paquet ER, Cogger VC, O'Reilly JN, Tworek L, Hatherell A, Taylor CG, Thorin E, Zahradka P, Le Couteur DG, Lebel M (2009) Vitamin C restores healthy aging in a mouse model for Werner syndrome. *FASEB J* **24**(1)**:** 158-172

Massip L, Garand C, Turaga RV, Deschenes F, Thorin E, Lebel M (2006) Increased insulin, triglycerides, reactive oxygen species, and cardiac fibrosis in mice with a mutation in the helicase domain of the Werner syndrome gene homologue. *Exp Gerontol* **41**(2)**:** 157-168

Matheu A, Maraver A, Klatt P, Flores I, Garcia-Cao I, Borras C, Flores JM, Vina J, Blasco MA, Serrano M (2007) Delayed ageing through damage protection by the Arf/p53 pathway. *Nature* **448**(7151)**:** 375-379

Mattison JA, Roth GS, Beasley TM, Tilmont EM, Handy AM, Herbert RL, Longo DL, Allison DB, Young JE, Bryant M, Barnard D, Ward WF, Qi W, Ingram DK, de Cabo R (2012) Impact of caloric restriction on health and survival in rhesus monkeys from the NIA study. *Nature* **489**(7415)**:** 318-321

Mattison JA, Roth GS, Lane MA, Ingram DK (2007) Dietary restriction in aging nonhuman primates. *Interdiscip Top Gerontol* **35:** 137-158

McConnell BB, Starborg M, Brookes S, Peters G (1998) Inhibitors of cyclin-dependent kinases induce features of replicative senescence in early passage human diploid fibroblasts. *Curr Biol* **8**(6)**:** 351-354

McElwee JJ, Schuster E, Blanc E, Thomas JH, Gems D (2004) Shared transcriptional signature in Caenorhabditis elegans Dauer larvae and long-lived daf-2 mutants implicates detoxification system in longevity assurance. *J Biol Chem* **279**(43)**:** 44533-44543

McGee MD, Day N, Graham J, Melov S (2012) cep-1/p53-dependent dysplastic pathology of the aging C. elegans gonad. *Aging (Albany NY)* **4**(4)**:** 256-269

Melendez A, Talloczy Z, Seaman M, Eskelinen EL, Hall DH, Levine B (2003) Autophagy genes are essential for dauer development and life-span extension in C. elegans. *Science* **301**(5638)**:** 1387-1391

Mendrysa SM, O'Leary KA, McElwee MK, Michalowski J, Eisenman RN, Powell DA, Perry ME (2006) Tumor suppression and normal aging in mice with constitutively high p53 activity. *Genes Dev* **20**(1)**:** 16-21

Mendrysa SM, Perry ME (2006) Tumor suppression by p53 without accelerated aging: just enough of a good thing? *Cell Cycle* **5**(7)**:** 714-717

Mihaylova VT, Borland CZ, Manjarrez L, Stern MJ, Sun H (1999) The PTEN tumor suppressor homolog in Caenorhabditis elegans regulates longevity and dauer formation in an insulin receptor-like signaling pathway. *Proc Natl Acad Sci U S A* **96**(13)**:** 7427-7432

Mitchell DH, Stiles JW, Santelli J, Sanadi DR (1979) Synchronous growth and aging of Caenorhabditis elegans in the presence of fluorodeoxyuridine. *J Gerontol* **34**(1)**:** 28-36

Moser MJ, Oshima J, Monnat RJ, Jr. (1999) WRN mutations in Werner syndrome. *Hum Mutat* **13**(4)**:** 271-279

Murakami S, Johnson TE (1998) Life extension and stress resistance in Caenorhabditis elegans modulated by the tkr-1 gene. *Curr Biol* **8**(19)**:** 1091-1094

Murphy CT, Lee SJ, Kenyon C (2007) Tissue entrainment by feedback regulation of insulin gene expression in the endoderm of Caenorhabditis elegans. *Proc Natl Acad Sci U S A* **104**(48)**:** 19046-19050

Murphy CT, McCarroll SA, Bargmann CI, Fraser A, Kamath RS, Ahringer J, Li H, Kenyon C (2003) Genes that act downstream of DAF-16 to influence the lifespan of Caenorhabditis elegans. *Nature* **424**(6946)**:** 277-283

Nakamura M, Ando R, Nakazawa T, Yudazono T, Tsutsumi N, Hatanaka N, Ohgake T, Hanaoka F, Eki T (2007) Dicer-related drh-3 gene functions in germ-line development by maintenance of chromosomal integrity in Caenorhabditis elegans. *Genes Cells* **12**(9)**:** 997-1010

Nehlin JO, Skovgaard GL, Bohr VA (2000) The Werner syndrome. A model for the study of human aging. *Ann N Y Acad Sci* **908:** 167-179

Nelson G, Wordsworth J, Wang C, Jurk D, Lawless C, Martin-Ruiz C, von Zglinicki T (2012) A senescent cell bystander effect: senescence-induced senescence. *Aging Cell* **11**(2)**:** 345-349

Niccoli T, Partridge L (2012) Ageing as a risk factor for disease. *Curr Biol* **22**(17)**:** R741-752

Nix P, Hisamoto N, Matsumoto K, Bastiani M (2011) Axon regeneration requires coordinate activation of p38 and JNK MAPK pathways. *Proc Natl Acad Sci U S A* **108**(26)**:** 10738-10743

Oda E, Ohki R, Murasawa H, Nemoto J, Shibue T, Yamashita T, Tokino T, Taniguchi T, Tanaka N (2000) Noxa, a BH3-only member of the Bcl-2 family and candidate mediator of p53-induced apoptosis. *Science* **288**(5468)**:** 1053-1058

Ogg S, Paradis S, Gottlieb S, Patterson GI, Lee L, Tissenbaum HA, Ruvkun G (1997) The Fork head transcription factor DAF-16 transduces insulin-like metabolic and longevity signals in C. elegans. *Nature* **389**(6654)**:** 994-999

Ogg S, Ruvkun G (1998) The C. elegans PTEN homolog, DAF-18, acts in the insulin receptor-like metabolic signaling pathway. *Mol Cell* **2**(6)**:** 887-893

Ogryzko VV, Hirai TH, Russanova VR, Barbie DA, Howard BH (1996) Human fibroblast commitment to a senescence-like state in response to histone deacetylase inhibitors is cell cycle dependent. *Mol Cell Biol* **16**(9)**:** 5210-5218

Olovnikov AM (1973) A theory of marginotomy. The incomplete copying of template margin in enzymic synthesis of polynucleotides and biological significance of the phenomenon. *J Theor Biol* **41**(1)**:** 181-190

Olsen A, Vantipalli MC, Lithgow GJ (2006) Lifespan extension of Caenorhabditis elegans following repeated mild hormetic heat treatments. *Biogerontology* **7**(4)**:** 221-230

Olshansky SJ, Perry D, Miller RA, Butler RN (2007) Pursuing the longevity dividend: scientific goals for an aging world. *Ann N Y Acad Sci* **1114:** 11-13

Onken B, Driscoll M (2010) Metformin induces a dietary restriction-like state and the oxidative stress response to extend C. elegans Healthspan via AMPK, LKB1, and SKN-1. *PLoS One* **5**(1)**:** e8758

Opresko PL, Cheng WH, von Kobbe C, Harrigan JA, Bohr VA (2003) Werner syndrome and the function of the Werner protein; what they can teach us about the molecular aging process. *Carcinogenesis* **24**(5)**:** 791-802

Opresko PL, Laine JP, Brosh RM, Jr., Seidman MM, Bohr VA (2001) Coordinate action of the helicase and 3' to 5' exonuclease of Werner syndrome protein. *J Biol Chem* **276**(48)**:** 44677-44687

Opresko PL, Otterlei M, Graakjaer J, Bruheim P, Dawut L, Kolvraa S, May A, Seidman MM, Bohr VA (2004) The Werner syndrome helicase and exonuclease cooperate to resolve telomeric D loops in a manner regulated by TRF1 and TRF2. *Mol Cell* **14**(6)**:** 763-774

Osada M, Ohba M, Kawahara C, Ishioka C, Kanamaru R, Katoh I, Ikawa Y, Nimura Y, Nakagawara A, Obinata M, Ikawa S (1998) Cloning and functional analysis of human p51, which structurally and functionally resembles p53. *Nat Med* **4**(7)**:** 839-843

Oshima J, Huang S, Pae C, Campisi J, Schiestl RH (2002) Lack of WRN results in extensive deletion at nonhomologous joining ends. *Cancer Res* **62**(2)**:** 547-551

Ou HD, Lohr F, Vogel V, Mantele W, Dotsch V (2007) Structural evolution of C-terminal domains in the p53 family. *EMBO J* **26**(14)**:** 3463-3473

Pagano G, Zatterale A, Degan P, d'Ischia M, Kelly FJ, Pallardo FV, Kodama S (2005) Multiple involvement of oxidative stress in Werner syndrome phenotype. *Biogerontology* **6**(4)**:** 233-243

Pallardo FV, Lloret A, Lebel M, d'Ischia M, Cogger VC, Le Couteur DG, Gadaleta MN, Castello G, Pagano G (2010) Mitochondrial dysfunction in some oxidative stress-related genetic diseases: Ataxia-Telangiectasia, Down Syndrome, Fanconi Anaemia and Werner Syndrome. *Biogerontology* **11**(4)**:** 401-419

Pan KZ, Palter JE, Rogers AN, Olsen A, Chen D, Lithgow GJ, Kapahi P (2007) Inhibition of mRNA translation extends lifespan in Caenorhabditis elegans. *Aging Cell* **6**(1)**:** 111-119

Paradis S, Ailion M, Toker A, Thomas JH, Ruvkun G (1999) A PDK1 homolog is necessary and sufficient to transduce AGE-1 PI3 kinase signals that regulate diapause in Caenorhabditis elegans. *Genes Dev* **13**(11)**:** 1438-1452

Paradis S, Ruvkun G (1998) Caenorhabditis elegans Akt/PKB transduces insulin receptor-like signals from AGE-1 PI3 kinase to the DAF-16 transcription factor. *Genes Dev* **12**(16)**:** 2488-2498

Partridge L (2010) Some highlights of research on aging with invertebrates, 2010. *Aging Cell* **10**(1)**:** 5-9

Partridge L, Slack C (2013) Genes, pathways and metabolism in ageing.

Pearson M, Carbone R, Sebastiani C, Cioce M, Fagioli M, Saito S, Higashimoto Y, Appella E, Minucci S, Pandolfi PP, Pelicci PG (2000) PML regulates p53 acetylation and premature senescence induced by oncogenic Ras. *Nature* **406**(6792)**:** 207-210

Pehar M, O'Riordan KJ, Burns-Cusato M, Andrzejewski ME, del Alcazar CG, Burger C, Scrable H, Puglielli L (2010) Altered longevity-assurance activity of p53:p44 in the mouse causes memory loss, neurodegeneration and premature death. *Aging Cell* **9**(2)**:** 174-190

Pereira S, Bourgeois P, Navarro C, Esteves-Vieira V, Cau P, De Sandre-Giovannoli A, Levy N (2008) HGPS and related premature aging disorders: from genomic identification to the first therapeutic approaches. *Mech Ageing Dev* **129**(7-8)**:** 449-459

Perry JJ, Yannone SM, Holden LG, Hitomi C, Asaithamby A, Han S, Cooper PK, Chen DJ, Tainer JA (2006) WRN exonuclease structure and molecular mechanism imply an editing role in DNA end processing. *Nat Struct Mol Biol* **13**(5)**:** 414-422

Pichierri P, Franchitto A, Mosesso P, Palitti F (2000) Werner's syndrome cell lines are hypersensitive to camptothecin-induced chromosomal damage. *Mutat Res* **456**(1-2)**:** 45-57

Pichierri P, Nicolai S, Cignolo L, Bignami M, Franchitto A (2012) The RAD9-RAD1-HUS1 (9.1.1) complex interacts with WRN and is crucial to regulate its response to replication fork stalling. *Oncogene* **31**(23)**:** 2809-2823

Pierce SB, Costa M, Wisotzkey R, Devadhar S, Homburger SA, Buchman AR, Ferguson KC, Heller J, Platt DM, Pasquinelli AA, Liu LX, Doberstein SK, Ruvkun G (2001) Regulation of DAF-2

receptor signaling by human insulin and ins-1, a member of the unusually large and diverse C. elegans insulin gene family. *Genes Dev* **15**(6)**:** 672-686

Pinkston JM, Garigan D, Hansen M, Kenyon C (2006) Mutations that increase the life span of C. elegans inhibit tumor growth. *Science* **313**(5789)**:** 971-975

Plchova H, Hartung F, Puchta H (2003) Biochemical characterization of an exonuclease from Arabidopsis thaliana reveals similarities to the DNA exonuclease of the human Werner syndrome protein. *J Biol Chem* **278**(45)**:** 44128-44138

Pollex RL, Hegele RA (2004) Hutchinson-Gilford progeria syndrome. *Clin Genet* **66**(5)**:** 375-381

Poot M, Gollahon KA, Rabinovitch PS (1999) Werner syndrome lymphoblastoid cells are sensitive to camptothecin-induced apoptosis in S-phase. *Hum Genet* **104**(1)**:** 10-14

Poot M, Yom JS, Whang SH, Kato JT, Gollahon KA, Rabinovitch PS (2001) Werner syndrome cells are sensitive to DNA cross-linking drugs. *FASEB J* **15**(7)**:** 1224-1226

Price NL, Gomes AP, Ling AJ, Duarte FV, Martin-Montalvo A, North BJ, Agarwal B, Ye L, Ramadori G, Teodoro JS, Hubbard BP, Varela AT, Davis JG, Varamini B, Hafner A, Moaddel R, Rolo AP, Coppari R, Palmeira CM, de Cabo R, Baur JA, Sinclair DA (2012) SIRT1 is required for AMPK activation and the beneficial effects of resveratrol on mitochondrial function. *Cell Metab* **15**(5)**:** 675-690

Prince PR, Ogburn CE, Moser MJ, Emond MJ, Martin GM, Monnat RJ, Jr. (1999) Cell fusion corrects the 4-nitroquinoline 1-oxide sensitivity of Werner syndrome fibroblast cell lines. *Hum Genet* **105**(1-2)**:** 132-138

Rizzon C, Martin E, Marais G, Duret L, Segalat L, Biemont C (2003) Patterns of selection against transposons inferred from the distribution of Tc1, Tc3 and Tc5 insertions in the mut-7 line of the nematode Caenorhabditis elegans. *Genetics* **165**(3)**:** 1127-1135

Robida-Stubbs S, Glover-Cutter K, Lamming DW, Mizunuma M, Narasimhan SD, Neumann-Haefelin E, Sabatini DM, Blackwell TK (2012) TOR signaling and rapamycin influence longevity by regulating SKN-1/Nrf and DAF-16/FoxO. *Cell Metab* **15**(5)**:** 713-724

Robles SJ, Adami GR (1998) Agents that cause DNA double strand breaks lead to p16INK4a enrichment and the premature senescence of normal fibroblasts. *Oncogene* **16**(9)**:** 1113-1123

Rodier F, Campisi J (2011) Four faces of cellular senescence. *J Cell Biol* **192**(4)**:** 547-556

Rodier F, Campisi J, Bhaumik D (2007) Two faces of p53: aging and tumor suppression. *Nucleic Acids Res* **35**(22)**:** 7475-7484

Rodriguez-Lopez AM, Jackson DA, Iborra F, Cox LS (2002) Asymmetry of DNA replication fork progression in Werner's syndrome. *Aging Cell* **1**(1)**:** 30-39

Rodriguez-Lopez AM, Jackson DA, Nehlin JO, Iborra F, Warren AV, Cox LS (2003) Characterisation of the interaction between WRN, the helicase/exonuclease defective in progeroid Werner's syndrome, and an essential replication factor, PCNA. *Mech Ageing Dev* **124**(2)**:** 167-174

Rodriguez-Lopez AM, Whitby MC, Borer CM, Bachler MA, Cox LS (2007) Correction of proliferation and drug sensitivity defects in the progeroid Werner's Syndrome by Holliday junction resolution. *Rejuvenation Res* **10**(1)**:** 27-40

Rouault JP, Kuwabara PE, Sinilnikova OM, Duret L, Thierry-Mieg D, Billaud M (1999) Regulation of dauer larva development in Caenorhabditis elegans by daf-18, a homologue of the tumour suppressor PTEN. *Curr Biol* **9**(6)**:** 329-332

Rubin GM, Yandell MD, Wortman JR, Gabor Miklos GL, Nelson CR, Hariharan IK, Fortini ME, Li PW, Apweiler R, Fleischmann W, Cherry JM, Henikoff S, Skupski MP, Misra S, Ashburner M, Birney E, Boguski MS, Brody T, Brokstein P, Celniker SE, Chervitz SA, Coates D, Cravchik A, Gabrielian A, Galle RF, Gelbart WM, George RA, Goldstein LS, Gong F, Guan P, Harris NL, Hay BA, Hoskins RA, Li J, Li Z, Hynes RO, Jones SJ, Kuehl PM, Lemaitre B, Littleton JT, Morrison DK, Mungall C, O'Farrell PH, Pickeral OK, Shue C, Vosshall LB, Zhang J, Zhao Q, Zheng XH, Lewis S (2000) Comparative genomics of the eukaryotes. *Science* **287**(5461)**:** 2204-2215

Russell RL, Seppa RI (1987) Genetic and environmental manipulation of aging in Caenorhabditis elegans. *Basic Life Sci* **42:** 35-48

Saintigny Y, Makienko K, Swanson C, Emond MJ, Monnat RJ, Jr. (2002) Homologous recombination resolution defect in werner syndrome. *Mol Cell Biol* **22**(20)**:** 6971-6978

Sakashita T, Takanami T, Yanase S, Hamada N, Suzuki M, Kimura T, Kobayashi Y, Ishii N, Higashitani A (2010) Radiation biology of Caenorhabditis elegans: germ cell response, aging and behavior. *J Radiat Res* **51**(2)**:** 107-121

Salk D (1982) Werner's syndrome: a review of recent research with an analysis of connective tissue metabolism, growth control of cultured cells, and chromosomal aberrations. *Hum Genet* **62**(1)**:** 1-5

Salk D, Au K, Hoehn H, Martin GM (1981) Cytogenetics of Werner's syndrome cultured skin fibroblasts: variegated translocation mosaicism. *Cytogenet Cell Genet* **30**(2)**:** 92-107

Salminen A, Kauppinen A, Kaarniranta K (2012) Emerging role of NF-kappaB signaling in the induction of senescence-associated secretory phenotype (SASP). *Cell Signal* **24**(4)**:** 835-845

Saunders RD, Boubriak I, Clancy DJ, Cox LS (2008) Identification and characterization of a Drosophila ortholog of WRN exonuclease that is required to maintain genome integrity. *Aging Cell* **7**(3)**:** 418-425

Scappaticci S, Cerimele D, Fraccaro M (1982) Clonal structural chromosomal rearrangements in primary fibroblast cultures and in lymphocytes of patients with Werner's Syndrome. *Hum Genet* **62**(1)**:** 16-24

Schmale H, Bamberger C (1997) A novel protein with strong homology to the tumor suppressor p53. *Oncogene* **15**(11)**:** 1363-1367

Schumacher B, Garinis GA, Hoeijmakers JH (2008a) Age to survive: DNA damage and aging. *Trends Genet* **24**(2)**:** 77-85

Schumacher B, Hofmann K, Boulton S, Gartner A (2001) The C. elegans homolog of the p53 tumor suppressor is required for DNA damage-induced apoptosis. *Curr Biol* **11**(21)**:** 1722-1727

Schumacher B, Schertel C, Wittenburg N, Tuck S, Mitani S, Gartner A, Conradt B, Shaham S (2005) C. elegans ced-13 can promote apoptosis and is induced in response to DNA damage. *Cell Death Differ* **12**(2)**:** 153-161

Schumacher B, van der Pluijm I, Moorhouse MJ, Kosteas T, Robinson AR, Suh Y, Breit TM, van Steeg H, Niedernhofer LJ, van Ijcken W, Bartke A, Spindler SR, Hoeijmakers JH, van der Horst GT, Garinis GA (2008b) Delayed and accelerated aging share common longevity assurance mechanisms. *PLoS Genet* **4**(8)**:** e1000161

Sedensky MM, Morgan PG (2006) Mitochondrial respiration and reactive oxygen species in C. elegans. *Exp Gerontol* **41**(10)**:** 957-967

Selman C, Tullet JM, Wieser D, Irvine E, Lingard SJ, Choudhury AI, Claret M, Al-Qassab H, Carmignac D, Ramadani F, Woods A, Robinson IC, Schuster E, Batterham RL, Kozma SC, Thomas G, Carling D, Okkenhaug K, Thornton JM, Partridge L, Gems D, Withers DJ (2009) Ribosomal protein S6 kinase 1 signaling regulates mammalian life span. *Science* **326**(5949)**:** 140-144

Senoo M, Seki N, Ohira M, Sugano S, Watanabe M, Inuzuka S, Okamoto T, Tachibana M, Tanaka T, Shinkai Y, Kato H (1998) A second p53-related protein, p73L, with high homology to p73. *Biochem Biophys Res Commun* **248**(3)**:** 603-607

Serrano M, Lin AW, McCurrach ME, Beach D, Lowe SW (1997) Oncogenic ras provokes premature cell senescence associated with accumulation of p53 and p16INK4a. *Cell* **88**(5)**:** 593-602

Sgro CM, Partridge L (1999) A delayed wave of death from reproduction in Drosophila. *Science* **286**(5449)**:** 2521-2524

Shama S, Lai CY, Antoniazzi JM, Jiang JC, Jazwinski SM (1998) Heat stress-induced life span extension in yeast. *Exp Cell Res* **245**(2)**:** 379-388

Shelton DN, Chang E, Whittier PS, Choi D, Funk WD (1999) Microarray analysis of replicative senescence. *Curr Biol* **9**(17)**:** 939-945

Shen J, Tower J (2009) Programmed cell death and apoptosis in aging and life span regulation. *Discov Med* **8**(43)**:** 223-226

Shen JC, Gray MD, Oshima J, Kamath-Loeb AS, Fry M, Loeb LA (1998a) Werner syndrome protein. I. DNA helicase and dna exonuclease reside on the same polypeptide. *J Biol Chem* **273**(51)**:** 34139-34144

Shen JC, Gray MD, Oshima J, Loeb LA (1998b) Characterization of Werner syndrome protein DNA helicase activity: directionality, substrate dependence and stimulation by replication protein A. *Nucleic Acids Res* **26**(12)**:** 2879-2885

Shen JC, Loeb LA (2000) The Werner syndrome gene: the molecular basis of RecQ helicase-deficiency diseases. *Trends Genet* **16**(5)**:** 213-220

Shieh SY, Ikeda M, Taya Y, Prives C (1997) DNA damage-induced phosphorylation of p53 alleviates inhibition by MDM2. *Cell* **91**(3)**:** 325-334

Sidorova JM (2008) Roles of the Werner syndrome RecQ helicase in DNA replication. *DNA Repair (Amst)* **7**(11)**:** 1776-1786

Sidorova JM, Kehrli K, Mao F, Monnat R, Jr. (2013) Distinct functions of human RECQ helicases WRN and BLM in replication fork recovery and progression after hydroxyurea-induced stalling. *DNA Repair (Amst)* **12**(2)**:** 128-139

Sidorova JM, Li N, Folch A, Monnat RJ, Jr. (2008) The RecQ helicase WRN is required for normal replication fork progression after DNA damage or replication fork arrest. *Cell Cycle* **7**(6)**:** 796-807

Sijen T, Plasterk RH (2003) Transposon silencing in the Caenorhabditis elegans germ line by natural RNAi. *Nature* **426**(6964)**:** 310-314

Singh V, Aballay A (2006) Heat-shock transcription factor (HSF)-1 pathway required for Caenorhabditis elegans immunity. *Proc Natl Acad Sci U S A* **103**(35)**:** 13092-13097

Sitte N, Saretzki G, von Zglinicki T (1998) Accelerated telomere shortening in fibroblasts after extended periods of confluency. *Free Radic Biol Med* **24**(6)**:** 885-893

Slack C, Giannakou ME, Foley A, Goss M, Partridge L (2011) dFOXO-independent effects of reduced insulin-like signaling in Drosophila. *Aging Cell* **10**(5)**:** 735-748

Smith ED, Kaeberlein TL, Lydum BT, Sager J, Welton KL, Kennedy BK, Kaeberlein M (2008a) Age- and calorie-independent life span extension from dietary restriction by bacterial deprivation in Caenorhabditis elegans. *BMC Dev Biol* **8:** 49

Smith ED, Tsuchiya M, Fox LA, Dang N, Hu D, Kerr EO, Johnston ED, Tchao BN, Pak DN, Welton KL, Promislow DE, Thomas JH, Kaeberlein M, Kennedy BK (2008b) Quantitative evidence for conserved longevity pathways between divergent eukaryotic species. *Genome Res* **18**(4)**:** 564-570

Smith SK, Kipling D (2004) The role of replicative senescence in cancer and human ageing: utility (or otherwise) of murine models. *Cytogenet Genome Res* **105**(2-4)**:** 455-463

Sommers JA, Sharma S, Doherty KM, Karmakar P, Yang Q, Kenny MK, Harris CC, Brosh RM, Jr. (2005) p53 modulates RPA-dependent and RPA-independent WRN helicase activity. *Cancer Res* **65**(4)**:** 1223-1233

Spillare EA, Robles AI, Wang XW, Shen JC, Yu CE, Schellenberg GD, Harris CC (1999) p53-mediated apoptosis is attenuated in Werner syndrome cells. *Genes Dev* **13**(11)**:** 1355-1360

Squires S, Ryan AJ, Strutt HL, Smith PJ, Johnson RT (1991) Deoxyguanosine enhances the cytotoxicity of the topoisomerase I inhibitor camptothecin by reducing the repair of double-strand breaks induced in replicating DNA. *J Cell Sci* **100 (Pt 4):** 883-893

Stanfel MN, Shamieh LS, Kaeberlein M, Kennedy BK (2009) The TOR pathway comes of age. *Biochim Biophys Acta* **1790**(10)**:** 1067-1074

Stanulis-Praeger BM (1987) Cellular senescence revisited: a review. *Mech Ageing Dev* **38**(1)**:** 1-48

Statistics OfN (2012) Mortality Statistics: Deaths Registered in England and Wales (Series DR), 2012. *wwwonsgovuk*

Stergiou L, Doukoumetzidis K, Sendoel A, Hengartner MO (2007) The nucleotide excision repair pathway is required for UV-C-induced apoptosis in Caenorhabditis elegans. *Cell Death Differ* **14**(6)**:** 1129-1138

Strom E, Sathe S, Komarov PG, Chernova OB, Pavlovska I, Shyshynova I, Bosykh DA, Burdelya LG, Macklis RM, Skaliter R, Komarova EA, Gudkov AV (2006) Small-molecule inhibitor of p53 binding to mitochondria protects mice from gamma radiation. *Nat Chem Biol* **2**(9)**:** 474-479

Suh EK, Yang A, Kettenbach A, Bamberger C, Michaelis AH, Zhu Z, Elvin JA, Bronson RT, Crum CP, McKeon F (2006) p63 protects the female germ line during meiotic arrest. *Nature* **444**(7119)**:** 624-628

Sulston JE, Hodgkin J (1988) METHODS APPENDIX IN THE NEMATODE CAENORHABDITIS ELEGANS. *Cold Spring Harbor Laboratory Press, New York*

Sulston JE, Horvitz HR (1977) Post-embryonic cell lineages of the nematode, Caenorhabditis elegans. *Dev Biol* **56**(1)**:** 110-156

Sutphin GL, Kaeberlein M (2009) Measuring Caenorhabditis elegans life span on solid media. *J Vis Exp*(27)

Tabara H, Sarkissian M, Kelly WG, Fleenor J, Grishok A, Timmons L, Fire A, Mello CC (1999) The rde-1 gene, RNA interference, and transposon silencing in C. elegans. *Cell* **99**(2)**:** 123-132

Tadokoro T, Kulikowicz T, Dawut L, Croteau DL, Bohr VA (2012) DNA binding residues in the RQC domain of Werner protein are critical for its catalytic activities. *Aging (Albany NY)* **4**(6)**:** 417-429

Tatar M, Bartke A, Antebi A (2003) The endocrine regulation of aging by insulin-like signals. *Science* **299**(5611)**:** 1346-1351

TeKippe M, Aballay A C. elegans germline-deficient mutants respond to pathogen infection using shared and distinct mechanisms. *PLoS One* **5**(7)**:** e11777

Thoms KM, Kuschal C, Emmert S (2007) Lessons learned from DNA repair defective syndromes. *Exp Dermatol* **16**(6)**:** 532-544

Tissenbaum HA, Guarente L (2002) Model organisms as a guide to mammalian aging. *Dev Cell* **2**(1)**:** 9-19

Tollefsbol TO, Cohen HJ (1984) Werner's syndrome: An underdiagnosed disorder resembling premature aging. *Age*

Tops BB, Tabara H, Sijen T, Simmer F, Mello CC, Plasterk RH, Ketting RF (2005) RDE-2 interacts with MUT-7 to mediate RNA interference in Caenorhabditis elegans. *Nucleic Acids Res* **33**(1)**:** 347-355

Toth ML, Melentijevic I, Shah L, Bhatia A, Lu K, Talwar A, Naji H, Ibanez-Ventoso C, Ghose P, Jevince A, Xue J, Herndon LA, Bhanot G, Rongo C, Hall DH, Driscoll M (2012) Neurite sprouting and synapse deterioration in the aging Caenorhabditis elegans nervous system. *J Neurosci* **32**(26)**:** 8778-8790

Trink B, Okami K, Wu L, Sriuranpong V, Jen J, Sidransky D (1998) A new human p53 homologue. *Nat Med* **4**(7)**:** 747-748

Tyner SD, Venkatachalam S, Choi J, Jones S, Ghebranious N, Igelmann H, Lu X, Soron G, Cooper B, Brayton C, Park SH, Thompson T, Karsenty G, Bradley A, Donehower LA (2002) p53 mutant mice that display early ageing-associated phenotypes. *Nature* **415**(6867)**:** 45-53

Van Raamsdonk JM, Hekimi S (2009) Deletion of the mitochondrial superoxide dismutase sod-2 extends lifespan in Caenorhabditis elegans. *PLoS Genet* **5**(2)**:** e1000361

Van Raamsdonk JM, Hekimi S (2011) FUdR causes a twofold increase in the lifespan of the mitochondrial mutant gas-1. *Mech Ageing Dev* **132**(10)**:** 519-521

Vellai T, Takacs-Vellai K, Zhang Y, Kovacs AL, Orosz L, Muller F (2003) Genetics: influence of TOR kinase on lifespan in C. elegans. *Nature* **426**(6967)**:** 620

Ventura N, Rea SL, Schiavi A, Torgovnick A, Testi R, Johnson TE (2009) p53/CEP-1 increases or decreases lifespan, depending on level of mitochondrial bioenergetic stress. *Aging Cell* **8**(4)**:** 380-393

Vogelstein B, Lane D, Levine AJ (2000) Surfing the p53 network. *Nature* **408**(6810)**:** 307-310

Vousden KH, Lane DP (2007) p53 in health and disease. *Nat Rev Mol Cell Biol* **8**(4)**:** 275-283

Walker GA, Thompson FJ, Brawley A, Scanlon T, Devaney E (2003) Heat shock factor functions at the convergence of the stress response and developmental pathways in Caenorhabditis elegans. *FASEB J* **17**(13)**:** 1960-1962

Wang Y, Tissenbaum HA (2006) Overlapping and distinct functions for a Caenorhabditis elegans SIR2 and DAF-16/FOXO. *Mech Ageing Dev* **127**(1)**:** 48-56

Wright WE, Shay JW (2000) Telomere dynamics in cancer progression and prevention: fundamental differences in human and mouse telomere biology. *Nat Med* **6**(8)**:** 849-851

Wu Z, Ghosh-Roy A, Yanik MF, Zhang JZ, Jin Y, Chisholm AD (2007) Caenorhabditis elegans neuronal regeneration is influenced by life stage, ephrin signaling, and synaptic branching. *Proc Natl Acad Sci U S A* **104**(38)**:** 15132-15137

Yamabe Y, Shimamoto A, Goto M, Yokota J, Sugawara M, Furuichi Y (1998) Sp1-mediated transcription of the Werner helicase gene is modulated by Rb and p53. *Mol Cell Biol* **18**(11)**:** 6191-6200

Yamagata K, Kato J, Shimamoto A, Goto M, Furuichi Y, Ikeda H (1998) Bloom's and Werner's syndrome genes suppress hyperrecombination in yeast sgs1 mutant: implication for genomic instability in human diseases. *Proc Natl Acad Sci U S A* **95**(15)**:** 8733-8738

Yamawaki TM, Arantes-Oliveira N, Berman JR, Zhang P, Kenyon C (2008) Distinct activities of the germline and somatic reproductive tissues in the regulation of Caenorhabditis elegans' longevity. *Genetics* **178**(1)**:** 513-526

Yamawaki TM, Berman JR, Suchanek-Kavipurapu M, McCormick M, Gaglia MM, Lee SJ, Kenyon C (2010) The somatic reproductive tissues of C. elegans promote longevity through steroid hormone signaling. *PLoS Biol* **8**(8)

Yanase S, Yasuda K, Ishii N (2002) Adaptive responses to oxidative damage in three mutants of Caenorhabditis elegans (age-1, mev-1 and daf-16) that affect life span. *Mech Ageing Dev* **123**(12)**:** 1579-1587

Yang A, Kaghad M, Caput D, McKeon F (2002) On the shoulders of giants: p63, p73 and the rise of p53. *Trends Genet* **18**(2)**:** 90-95

Yang A, Kaghad M, Wang Y, Gillett E, Fleming MD, Dotsch V, Andrews NC, Caput D, McKeon F (1998) p63, a p53 homolog at 3q27-29, encodes multiple products with transactivating, death-inducing, and dominant-negative activities. *Mol Cell* **2**(3)**:** 305-316

Yang A, McKeon F (2000) P63 and P73: P53 mimics, menaces and more. *Nat Rev Mol Cell Biol* **1**(3)**:** 199-207

Yang W, Li J, Hekimi S (2007) A Measurable increase in oxidative damage due to reduction in superoxide detoxification fails to shorten the life span of long-lived mitochondrial mutants of Caenorhabditis elegans. *Genetics* **177**(4)**:** 2063-2074

Ye S, Dhillon S, Ke X, Collins AR, Day IN (2001) An efficient procedure for genotyping single nucleotide polymorphisms. *Nucleic Acids Res* **29**(17)**:** E88-88

Yoneda T, Benedetti C, Urano F, Clark SG, Harding HP, Ron D (2004) Compartment-specific perturbation of protein handling activates genes encoding mitochondrial chaperones. *J Cell Sci* **117**(Pt 18)**:** 4055-4066

Yu CE, Oshima J, Fu YH, Wijsman EM, Hisama F, Alisch R, Matthews S, Nakura J, Miki T, Ouais S, Martin GM, Mulligan J, Schellenberg GD (1996) Positional cloning of the Werner's syndrome gene. *Science* **272**(5259)**:** 258-262

Yu J, Zhang L, Hwang PM, Kinzler KW, Vogelstein B (2001) PUMA induces the rapid apoptosis of colorectal cancer cells. *Mol Cell* **7**(3)**:** 673-682

Zhang M, Poplawski M, Yen K, Cheng H, Bloss E, Zhu X, Patel H, Mobbs CV (2009) Role of CBP and SATB-1 in aging, dietary restriction, and insulin-like signaling. *PLoS Biol* **7**(11)**:** e1000245

Zhang Y, Xu J, Puscau C, Kim Y, Wang X, Alam H, Hu PJ (2008) Caenorhabditis elegans EAK-3 inhibits dauer arrest via nonautonomous regulation of nuclear DAF-16/FoxO activity. *Dev Biol* **315**(2)**:** 290-302

Zhu J, Woods D, McMahon M, Bishop JM (1998) Senescence of human fibroblasts induced by oncogenic Raf. *Genes Dev* **12**(19)**:** 2997-3007